S O R P T I O N C O M P L E X E S

O F Z E O L I T E S

by

Andreas George Kanellopoulos

A Thesis submitted for the
Degree of Doctor of Philosophy
in the University of London

Chemistry Department,
Imperial College,
London, S.W.7.

September 1968

ABSTRACT

The sorption of the gases, hydrogen chloride and ammonia, and their mixture resulting from the dissociation of vapourized ammonium chloride, at temperatures between 200-350°C, has been studied in molecular sieve zeolites such as H-Zeolon, NaY and KL.

The sorption of hydrogen chloride in an ion-exchanged zeolite is accompanied by an exchange reaction of part of its cations by protons while the chloride salt of the cation is formed. Depending upon the silica content of the zeolite, this can cause decomposition of its crystal structure. The salt produced from the exchange reaction can either remain molecularly dispersed in the crystal cavities or migrate outside the crystals. In hydrogen zeolites a reaction of hydrogen chloride with the aluminium of the zeolitic framework takes place. Due to these reactions, the sorption isotherms of hydrogen chloride were irreversible.

Reversible isotherms of ammonia were obtained in most zeolites. The affinity of hydrogen zeolites for ammonia was higher than that of ion-exchanged zeolites because of the formation of the ammonium-zeolite.

The sorption of the mixture is governed by the recombination reaction of ammonia and hydrogen chloride to form ammonium chloride and the sorption of the pure gases. If one of the gases is sorbed more strongly than the other, a disproportionation arises in the gas and sorbed phases, which decreases with increasing pressure. In an ion-exchanged zeolite an exchange reaction of its cations by ammonium ions also takes place. All the isotherms showed strong interaction between ammonia and hydrogen chloride. The partial isotherms of ammonia and hydrogen chloride were calculated from the isotherms of the mixture in most cases. The sorption from the mixture was several

times higher than from the pure gases. In view of these findings, a mechanism was suggested for the Clark-Steiger preparation of ammonium zeolites.

ACKNOWLEDGEMENTS

I wish to express my gratitude to Professor R.M. Barrer, F.R.S., for suggesting this topic of research, for his unfailing interest and encouragement, and for many useful discussions.

I am also very grateful to my wife Clare for typing this thesis and for her invaluable help during its preparation.

I thank the State Scholarship Foundation of Greece for financial support.

INDEX

page

ABSTRACT 2

ACKNOWLEDGEMENTS 4

PART I

1. INTRODUCTION

1.1 General introduction 10

1.2 The structure and properties of the sorbents

Chemical composition and crystal structure 12

The structure of mordenite 15

The structure of sodalite 17

The structure of Linde A 18

The structure of Linde X and Y 19

The structure of chabazite 21

The structure of clinoptilolite 22

The structure of Molecular Sieve L 22

Ion-exchanged and decationated zeolites 25

1.3 The properties of the sorbates 27

1.4 Literature survey on sorption of ammonia, hydrogen chloride and ammonium chloride in zeolites 28

2. THEORETICAL

2.1 The adsorption isotherm 33

2.2 Thermodynamics of adsorption 35

Isosteric heat of sorption 37

Entropy of adsorption 38

Half standard entropy of sorption 39

Integral thermodynamic quantities 39

Thermodynamic properties of the sorbent 39

2.3	Physical models of the sorbed phase	41
	Localized sorption without interaction	41
	Localized sorption with interaction	42
	Mobile sorption, sorbate obeys Volmer equation of state	43
	Mobile sorption, sorbate obeys van der Waals equation of state	43
2.4	General isotherm equations	
	Van't Hoff isotherm	43
	Osmotic pressure and empirical isotherm equations	44
2.5	Physical adsorption forces	47
2.6	Sorption hysteresis	49
3.	EXPERIMENTAL	
3.1	Introduction	51
3.2	The sorbents	52
3.3	The sorbates	53
3.4	Sorption system 1	57
3.5	Sorption system 2	62
3.6	Apparatus for hydrogen chloride - silicate stability experiments	64
3.7	The vacuum system	66
3.8	Calibration of the measuring devices	
	Thermocouples	68
	Silica springs	69
	Spiral gauge	70
	Volume of the balance case in sorption system 1	71
3.9	Analytical methods	71
3.10	X-ray techniques	72
3.11	Accuracy of the sorption measurements	73

PART II

1. HYDROGEN CHLORIDE - SILICATE STABILITY, SORPTION AND ION-EXCHANGE EXPERIMENTS

1.1 Study of hydrogen chloride - silicate stability 77

1.2 Hydrogen chloride - zeolite sorption and ion-exchange experiments 84

Hydrogen chloride - hydrogen zeolite complexes 84

Ion-exchanged zeolite - hydrogen chloride complexes 88

2. ION-EXCHANGE AND DECATIONATION EXPERIMENTS

2.1 Introduction 103

2.2 Decationated products from NaY 103

2.3 Preparation of decationated zeolites from Linde L 108

3. AMMONIA-ZEOLITE SORPTION COMPLEXES

3.1 Experimental isotherms 115

3.2 Thermodynamic properties of the sorbed phase

Isosteric heat of sorption 119

Integral heats of sorption 123

Differential entropy of the sorbate and half standard entropy of sorption 124

3.3 Selectivity and affinity 129

3.4 Empirical isotherm equations 132

Evaluation of virial coefficients 132

Calculation of thermodynamic properties in the standard state 133

3.5 Activity coefficients and correspondence with isotherm models 138

3.6 The sorption of ammonia in HY 140

4. AMMONIUM CHLORIDE - ZEOLITE SORPTION COMPLEXES

4.1 H-Zeolon - ammonium chloride

Experimental isotherms 145

Some theoretical considerations 147

Calculation of the partial isotherms from the isotherm of the mixture 155

Description of the sorbed phase by a virial equation 164

4.2 HY - ammonium chloride 166

4.3 KL - ammonium chloride 172

Calculation of the partial isotherms 177

4.4 NaY - ammonium chloride 178

4.5 Comparison of the sorption of ammonium chloride in different zeolites 186

5. SUMMARY OF RESULTS AND CONCLUSIONS 188

REFERENCES 192

PART III

APPENDIX 196

P A R T I

INTRODUCTION,

THEORETICAL,

EXPERIMENTAL

1. INTRODUCTION

1.1 General Introduction

When a gas or a vapour is allowed to come to equilibrium with a solid surface the concentration of the gas molecules is greater in the immediate vicinity of the surface than in the gas phase. This is due to unbalanced forces to which the atoms at the surface of the solid are subject and it is called adsorption. It is also possible that a bulk penetration of the gas into the structure of the solid may take place; this is governed by a process of diffusion and is called absorption. In cases where both the above processes take place simultaneously the term sorption is applied.

The porous solids present a large surface area on which a considerable amount of gas may be sorbed. In porous crystals the host lattices are often quite rigid and the pores have diameters of molecular dimensions. They therefore introduce a selectivity factor in the sorption of gases by acting towards mixtures of appropriate molecules as perfect molecular sieves[1]. When gases or vapours are sorbed by porous crystals, they may be regarded as included in them. The term "inclusion complex" or "sorption complex" is applied to the sorbate-sorbent system.

Many natural and synthetic zeolites act as molecular sieves and form sorption complexes with gases and vapours. Their structure and sorption properties have recently been extensively studied in these laboratories and elsewhere. The present research extends this study to the sorption studies of condensable vapours like ammonium chloride. Ammonium chloride in the vapour phase has been used for the exchange of sodium ions by ammonium ions in zeolites. This method was originated by Clark and Steiger[2]. The exact mechanism of this exchange is not known. The ammonium forms of the zeolites are used as intermediates for the preparation of "decationated"

or "decationized" zeolites. Decationated zeolites have received great attention lately because of their catalytic activities for certain acid catalyzed reactions[5,22]. The study of the system ammonium chloride-zeolite gives useful information regarding the mechanism of Clark-Steiger reaction and adds to the understanding of the mechanism of decationation and the properties of decationated zeolites.

Another interesting point in the study of the system ammonium chloride-zeolite arises from the dissociation of ammonium chloride in vapour phase into ammonia and hydrogen chloride. Ammonium chloride then, in the vapour phase, behaves as the equimolar mixture of ammonia and hydrogen chloride. Therefore, a complete study of the system necessitates the study of the systems hydrogen chloride-zeolite and ammonia-zeolite.

Several silicates, covering a wide SiO_2:Al_2O_3 range (2-12.8) were used in the study of the system hydrogen chloride-zeolite. Useful information about the stability of zeolites to hydrogen chloride and its sorption were obtained. The sorption of ammonia on different zeolites gave useful information about the nature of the surface of the sorbents. The results of both systems were used as a guide to choose the proper zeolites for the system ammonium chloride-zeolite. For the study of this system, hydrogen zeolites and ion-exchanged zeolites were employed. In a hydrogen zeolite, besides physical sorption, a reaction of ammonia with the zeolite to form the ammonium form of the zeolite is possible and in an ion-exchanged form an exchange of sodium ions by ammonium ions may take place. The ammonium forms of the zeolites, in which only sorption of ammonium chloride can take place, cannot be used because they are not stable at 350°C - the temperature at which the zeolites were outgassed.

From the study of the above or analogous systems, interesting information and conclusions can be obtained regarding the nature and

properties of salt-zeolite sorption complexes and the sorption of gas mixtures in which the components exhibit strong interaction, as ammonia and hydrogen chloride may be expected to do in the present case.

1.2 The structure and properties of the sorbents

Chemical composition and crystal structure[4,5]

All the sorbents used in this research are aluminosilicate minerals and belong to the classes of zeolites, feldspars and feldspathoids. A number of synthetic zeolites without natural counterparts were also used.

All zeolites have readily exchangeable cations and intracrystalline water which can be removed by heat and evacuation. They may be given the empirical oxide formula:

$$(M^{II},M^{I}_{2})O.Al_2O_3.nSiO_2.mH_2O$$

The values of n and m vary. M^{II} and M^{I} are respectively di- and monovalent cations, namely Ca,Sr,Ba,Na,K. The ratio $(M^{II},M^{I}_{2})O:Al_2O_3$ is usually unity. The structures are based on $(Al,Si)O_4$ tetrahedra linked to each of four other tetrahedra by sharing four apical oxygen atoms. The $(Al,Si)O_4$ tetrahedra form a three dimensional framework which carries a negative charge equal to the number of aluminium atoms in it. This negative charge is balanced by the positive charge of the cations which, together with the water molecules, are present in the interstices of the framework. According to an empirical rule by W. Löwenstein[6] AlO_4 can be joined to SiO_4 tetrahedra only and never to another AlO_4. This rules out the possibility of n being less than 2 in the oxide formula. In special circumstances discrete $NaAlO_2$ molecules can be trapped in some of the interstices of the framework and may cause apparent anomalies of the composition[7]. However, these molecules are not part of the framework.

In synthetic zeolites, the cations M^{II} and M^{I} may, in addition to those already referred to, be:

$$Rb^+ \text{ , } Cs^+ \text{ and } NH_4^+$$

or simple organic ions such as

$$(CH_3)NH_3^+ \text{ , } (CH_3)_2NH_2^+ \text{ , } (CH_3)_3NH^+ \text{ and } (CH_3)_4N^+ \text{ .}$$

Replacement of Al^{III} by Ga^{III} and Si^{IV} by Ge^{IV} in the ionic framework is also possible. In addition, H_3O^+ can replace Na^+ by ion-exchange.

In order to illustrate the relation between chemical composition and crystal structure, a structural formula of the form

$$(M^{II},M^{I}_2)_{x/n}\left[(AlO_2)_x(SiO_2)_y\right].mH_2O$$

is used where x,y,m and n are integers. This applies to one unit cell of the zeolite structure, the part in brackets representing the framework composition.

Zeolites are included in the framework silicates together with feldspars and feldspathoids. They differ from the feldspars and feldspathoids because their sponge-like frameworks have large cavities which are interconnected in one, two or three dimensions by apertures or "windows", which permit passage of small molecules from one cavity to another. They are, in general, more open than the feldspars and feldspathoids, being therefore the most important members of the family. Because of their greater openness they may exhibit to a greater extent the properties of ion-exchange and adsorption. Depending on the way of linking of $(Al,Si)O_4$ tetrahedra, the zeolites are classified as follows:

(a) Fibrous zeolites: Including natrolite, erionite and thomsonite. The linkages of tetrahedra are more numerous in one crystallographic direction than in the plane at right angles to it and the minerals have fibrous morphology and cleavage.

(b) Lamellar zeolites: Including heulandite and stilbite. They are characterized by cleavage in plates and their structure linkages are more numerous in one plane than the direction at right angles to it.

(c) Three-dimensional zeolites: Including philipsite mordenite, chabazite and faujasite. Their framework structures are of similar strength in every direction. The zeolites belonging to class (c) are often characterized by greater thermal stability.

A more recent attempt to classify the zeolites, based upon their framework structures, has been reported by Meier[8].

In the present work, chabazite and the synthetic zeolites Zeolon, Linde A, X, Y, L were used from class (c). From class (b) clinoptilolite was used.

The feldspars have compact structures in which the cations are in relatively small cavities and are completely surrounded by oxygens of the framework. The cations and the framework are strongly inter-dependent so that the cations cannot move easily unless framework bonds are broken[9] and replacement of Na or K by Ca necessarily involves a change in the Al:Si ratio. The simplest way of picturing their framework is to regard it as consisting of chains of tetrahedra parallel to the a-axis (100) cross-linked to adjacent parallel chains by shared oxygen atoms either on twofold axis or on reflection planes[9]. The chains are formed by the superposition of rings of four tetrahedra which share some of their vertices and form four-membered rings; the remaining vertices which project to right and left are available for cross-linking between the chains. The distinction between orthoclase and plagioclase groups arises from the way in which this non-rigid framework is held extended by the large cations K^{+}, Ba^{++} or allowed to collapse around the small cations Na^{+}, Ca^{++}.

The feldspathoids have more open structures than the feldspars and the cations occupy their interconnected cavities. They may have, together with water, inorganic salts or hydroxides which can sometimes be extracted.

In the present work the synthetic felspathoids, basic cancrinite and sodalite and a mixture of feldspars containing 17% albite and 82% orthoclase were used.

The structure of mordenite

Na-Zeolon is a synthetic form of the natural zeolite mordenite. It contains only sodium ions in contrast to the natural mineral which contains sodium, potassium and calcium ions.

The crystal structure of the sodium form of the natural mordenite has been determined by Meier[10]. The sample he obtained after ion-exchange to the sodium form had a unit cell composition:

$$Na_8Al_8Si_{40}O_{96}\cdot 24H_2O \ .$$

The aluminosilicate framework consists of characteristic chains in which 5-membered rings of tetrahedra prevail. Each $(Al,Si)O_4$ tetrahedron is part of one or more 5-membered rings in the framework and the number of 4-, 5-, 6- and 8-membered loops of tetrahedra per unit cell are 4, 48, 16 and 16 respectively. It has been shown that the most stable loops in silicates are of 5 and 6 tetrahedra[11]. The prevailing number of 5-membered loops in the mordenite structure and its high silica content account for its extraordinary stability.

The mordenite structure contains wide non-intersecting channels, circumscribed by rings of 12 oxygen atoms of the aluminosilicate framework, running parallel to the axis (001) with free diameter of 6.6 Å. (By "free" diameter we mean not occupied even by the peripheries of the framework oxygen atoms.) They open in the (010) direction into smaller side channels circumscribed by 8-membered

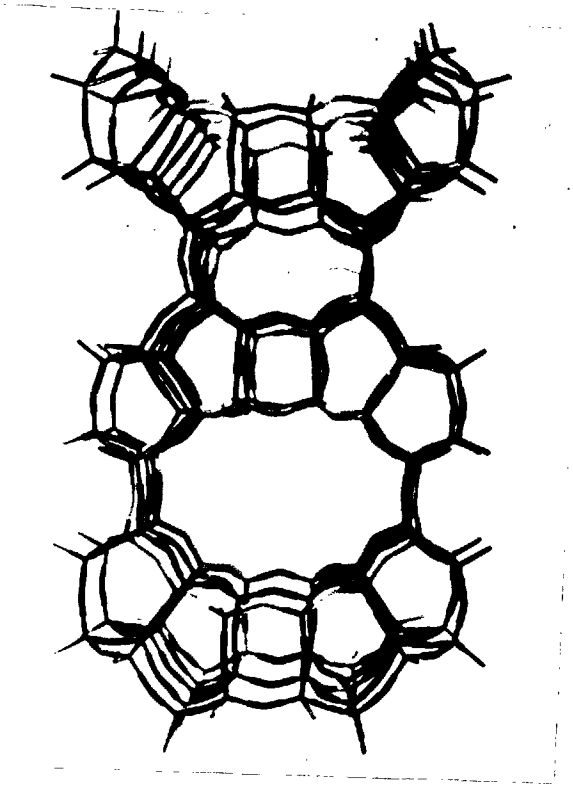


Fig. 1. The main channels in mordenite

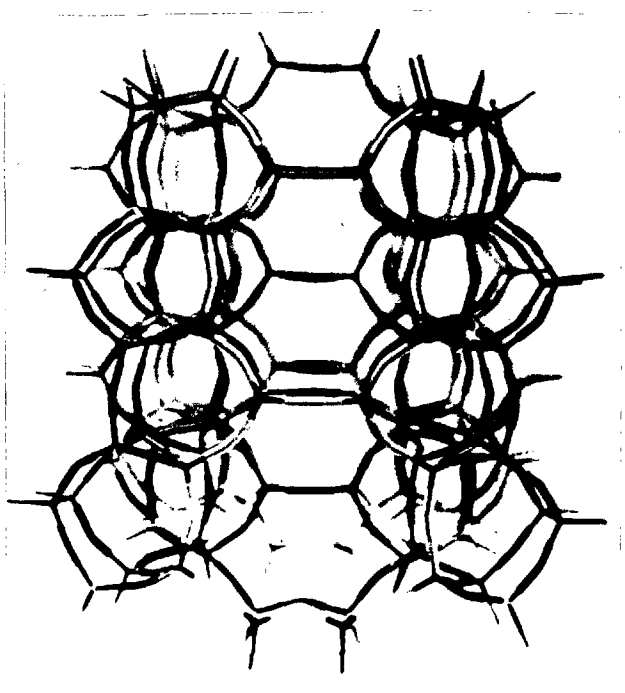


Fig. 2. The small channels in mordenite

rings having a minimum free diameter of 3.9 Å and leading towards the next main channel. However, halfway to the next main channel each side channel branches through two distorted 8-membered rings of 2.8 Å minimum free diameter into two similar side channels opening into the next main one. A sodium ion rests at the centre of each distorted 8-membered ring. These isolate the main channels from one another and leave each main channel lined with rows of side pockets. The main channels are shown in fig. 1 and the small ones in fig. 2. The positions of the sodium ions in the centre of the distorted 8-membered rings account for only half of the eight in the unit cell. Meier suggests that the remaining four occupy randomly some of the 8- and 12-fold positions available. The structure of hydrogen Zeolon is the same as that of Na-Zeolon. Na-Zeolon and H-Zeolon used in the present work gave identical X-ray diffraction patterns. The samples of Na-Zeolon and H-Zeolon used in this work were found by chemical analysis[12] to have the following composition:

Na-Zeolon : $0.9Na_2O.\ Al_2O_3.\ 9.5SiO_2.\ 6.2H_2O$

H-Zeolon : $0.085Na_2O.\ 0.9H_2O.\ Al_2O_3.\ 11.4SiO_2.\ 6.43H_2O$.

The structure of sodalite

Various zeolites such as Linde A, X and Y and the feldspathoid basic sodalite can be conveniently represented in terms of secondary building units of polyhedra, appropriately linked and stacked. For the above mentioned structures one such building unit is the truncated octahedron (cubo-octahedron) shown in fig. 4(a). The structure of sodalite can be visualized[4] by stacking the cubo-octahedra in 8-fold co-ordination so that a given central cubo-octahedron shares one of its 8-membered ring faces with one each of eight other cubo-octahedra (fig. 3). The cavities have an internal free diameter of 6.6 Å and are interconnected with 6-membered rings of aperture ca. 2Å. The sample of basic sodalite used had the

following composition:

$$6\,[NaAlSiO_4]\,.\,1.6NaOH.\,4.8H_2O\,.$$

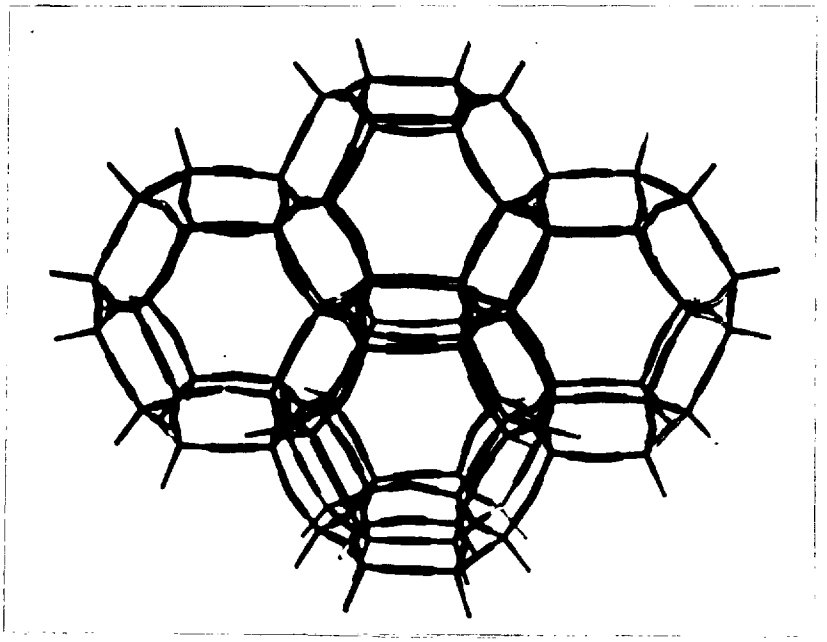


Fig. 3. Model structure of sodalite

The structure of Linde A [3]

NaA or Linde Sieve A is a synthetic zeolite without natural counterpart. Breck et al[13] gave its composition as

$$Na_2O.Al_2O_3.2SiO_2.nH_2O$$

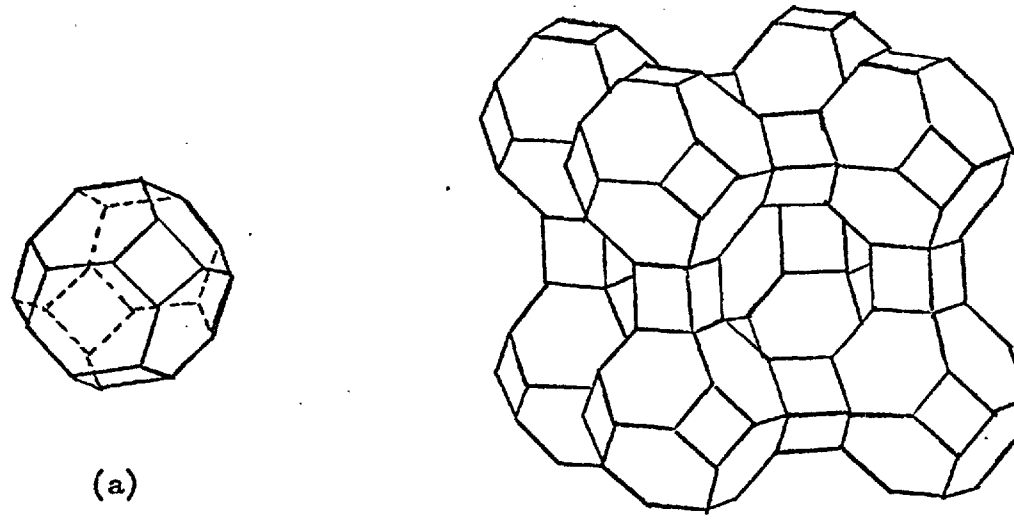
although the composition can vary slightly and their actual analysis figure for the SiO_2:Al_2O_3 was 1.92. Barrer and Meier[7] found for their sample 1.87 and showed that the excess aluminium in their sample was included in the framework as $NaAlO_2$.

In the structure of NaA the cubo-octahedra are linked in a cubic array by joining them with cubes on the square faces[13]. This produces a central truncated cubo-octahedron with an internal cavity of 11 Å in diameter (fig. 4(b)). Each central cavity (termed α-cage) is entered through six circular apertures formed by a nearly regular ring of eight atoms with a free diameter of 4.2 Å. The cavities are thus arranged in a continuous three-dimensional pattern forming a system of channels with a maximum diameter of 11 Å and a minimum of 4.2 Å. The truncated octahedra themselves enclose a second set of smaller cavities (β-cages or sodalite cages). A third type of cavity is the cube formed by joining the square faces of cubo-octahedra of practically no free volume. In each unit cell of zeolite A there are 12 monovalent cations. Eight of these lie in the centre of the 6-membered rings in the hexagonal faces (referred to as type I) and four occupy positions adjacent to the 8-membered rings (referred to as type II)[5].

The structure of Linde X and Y

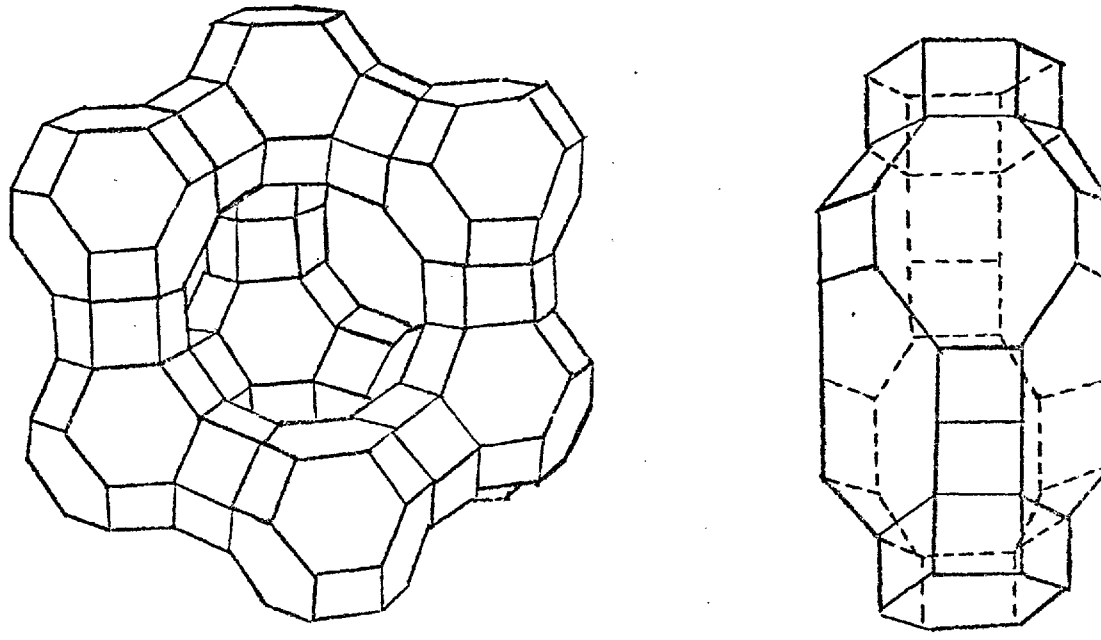
NaX and NaY or Linde X and Y are synthetic zeolites; their natural counterpart is the zeolite faujasite. The difference in chemical composition between X and Y is that Y is richer in silica.

The aluminosilicate framework in faujasite, X and Y consists of a tetrahedral arrangement of the truncated octahedra, i.e. the octahedra are joined at four of the eight octahedral faces by hexagonal prisms. The large cavities in this structure have an elliptical shape and a free diameter of 13 Å. They are entered by apertures of distorted, chair-shaped, 12-membered rings which have a free diameter of 8.0 Å. A second type of cavity is the sodalite cage (as in Molecular Sieve A) and a third, the hexagonal prisms formed from twelve $(Al,Si)O_4$ octahedra. A model of the structure of X and Y is shown in fig. 5(a).



(a) (b)

Fig. 4. (a) Truncated octahedron (cubo-octahedron).
(b) Framework structure of Linde A.



(a) (b)

Fig. 5. (a) Framework structure of faujasite.
(b) Cavity of chabazite.

N.B. The diagrams are drawn under different scales

The cations in zeolites X and Y occupy three types of positions[5]. These are:

type I, in the centre of the hexagonal prisms (16 sites per unit cell);

type II, on the 6-membered rings, the unjoined hexagonal faces (32 sites per unit cell);

type III, on the walls of the channels (48 sites per unit cell).

Type I and II sites are fully occupied in X and Y. In type III sites there are 38 and 8 cations in X and Y respectively. This non-occupancy of type III sites in Y is the major difference between X and Y. The positions of cations is not necessarily the same in hydrated and dehydrated zeolites.

NaX and NaY are synthesized from sodium hydroxide, silica and alumina in aqueous solutions. It is possible in the final product to have a deficiency of sodium ions and this is balanced by hydronium ions. Evidence for the existence of H_3O^+ in the hydrated form of NaX was obtained by the occurrence of certain bands in the IR spectrum[14].

The sample of zeolite X used had a SiO_2:Al_2O_3 ratio of 2.65. The composition of zeolite Y used was found by chemical analysis to be:

$$nNa_2O.\ Al_2O_3.\ 4.78SiO_2.\ 8.77H_2O$$

with $0.9 < n < 1$.

The structure of chabazite

In the natural zeolite chabazite one may recognize sheets containing hexagonal prism units in which two 6-membered rings are united by shared apical oxygen atoms to give the prisms[15]. The layer sequence is 123123... The cavities so formed are elongated

and have free dimensions of 6.6 Å and 11 Å. These cavities are shown in fig. 5(b). The sample of chabazite used was exchanged to the sodium form and had the following composition:

$$0.96Na_2O.\ 0.03CaO.\ Al_2O_3.\ 5.0SiO_2.\ 6.25H_2O$$

The structure of clinoptilolite

Clinoptilolite is a silica-rich zeolite related to heulandite[16,17]. Its structure has not yet been completely defined but it is believed to be like the structure of heulandite. According to Merkle and Slaughter[18] heulandite is monoclinic. Its crystal structure is characterized by large intersecting channels composed of 12-, 10- and 8-membered rings open across the mirrors and tied together by layers of 6-, 5- and 4-membered ring groups located at heights of about $\frac{1}{4}$ and $\frac{3}{4}$ along b. The bc crystallographic plane is composed of 8-membered rings held together by 4- and 6-membered ring groups. The ab crystallographic plane is composed of a combination of 8- and 12-membered rings held by a complex arrangement of 6-, 5- and 4-membered groups. The channels formed by the 8- and 12-membered rings are shown in fig. 6 and those by the 8-membered rings perpendicular to bc plane in fig. 7.

The sample of clinoptilolite used was exchanged to the sodium form and had the following composition:

$$0.91Na_2O.\ Al_2O_3.\ 9.3SiO_2.\ mH_2O$$

The structure of Molecular Sieve L

Molecular Sieve L is a synthetic zeolite without natural counterpart[19]. Its structure was resolved by Barrer and Villiger[20]. The zeolite was found to be hexagonal with unit cell dimensions

$$a = 18.40\ Å$$

$$c = 7.52\ Å$$

The building units of the aluminosilicate framework are the 11-hedral

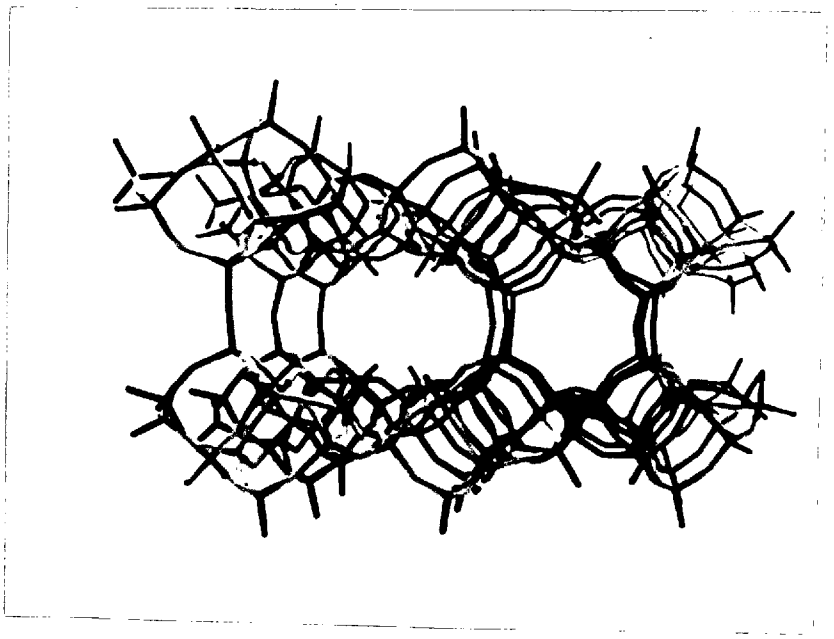


Fig. 6. The 8- and 12-membered channels in heulandite.

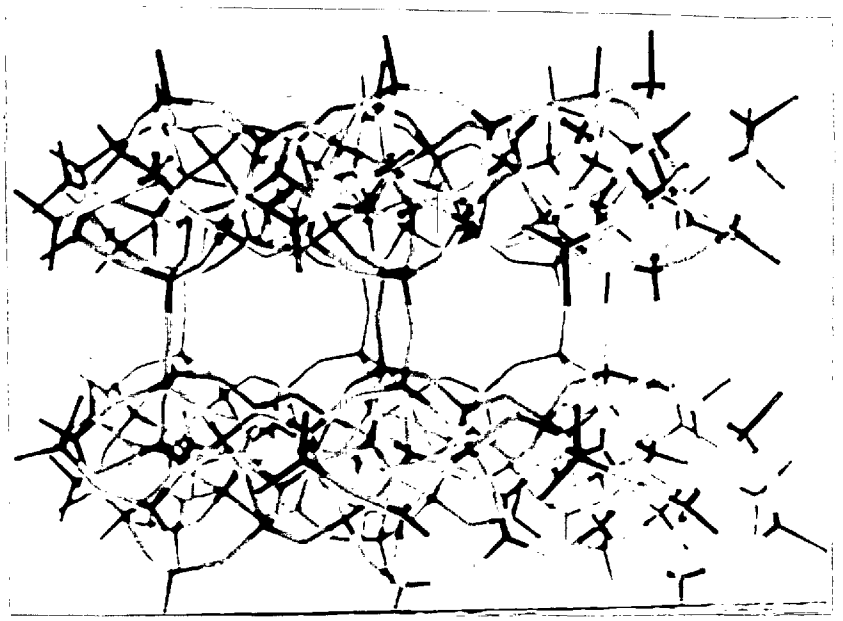


Fig. 7. The 8-membered channels in heulandite (perpendicular to bc plane)

cages found in cancrinite[21], erionite and offretite[23]. These cages are linked through their 6-membered rings, forming hexagonal prisms with the planes of the 6-membered rings normal to the c axis. The columns thereby formed are joined by single oxygen bridges which are part of the planar 12-membered rings that circumscribe the main channels running parallel to the c axis (fig. 8). The channels are made by the stacking of sections which are joined top and bottom to one another by shared 12-membered ring windows having minimum and maximum free diameters of 7.1 and 7.8 Å. The main channels are connected with each other by a less important two-dimensional channel system along the a_1 and a_2 axes as well as the enclosed mirror plane. The openings are formed by a non-planar 8-membered ring with a limiting aperture dimension of 1.5 Å.

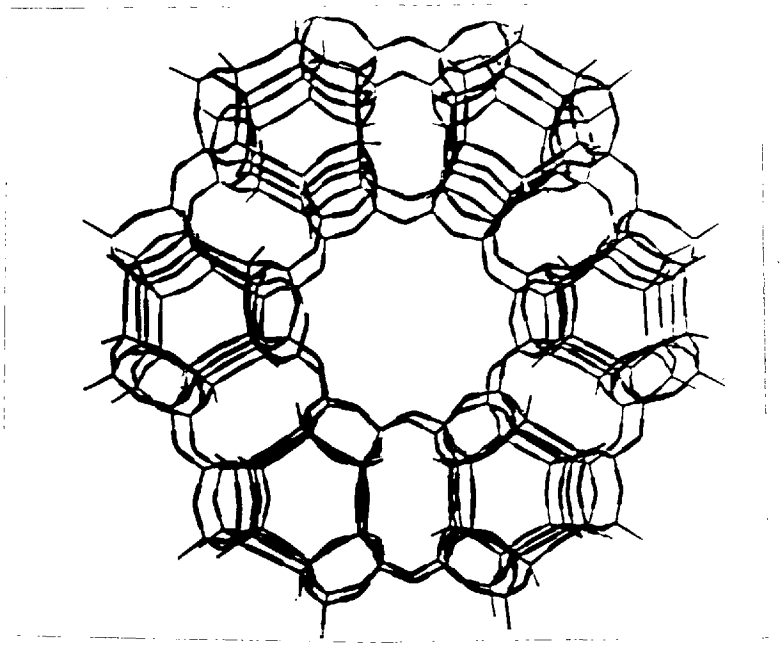


Fig. 8. The main channels in Linde L

Cations are present in at least four different sites denoted A, B, C and D. Site A is located in the middle of the hexagonal prism. Site B, in the centre of the cancrinite cavity, is fully occupied by K. Site C is located midway between the centres of the two adjacent cancrinite cavities and has a fractional occupancy of 0.9. Site D is the only cation position found in the main channel. The main channels in zeolite L are shown in section in fig. 8.

The sample of zeolite L used in the present work was found by chemical analysis to have the following composition:

$$0.94K_2O.\ 0.06Na_2O.\ Al_2O_3.\ 6.01SiO_2.\ 4.9H_2O\ .$$

Ion-exchanged and decationated zeolites

The sorptive and sieve properties of zeolites can be modified in different ways. Two of them, relevant to the present work, are ion-exchange and decationation.

A review on crystalline ion-exchangers including zeolites is given by Barrer[24]. Two different methods for exchange of the cations of a zeolite by ammonium ions which have previously been employed were used in the present work:

(a) by equilibration of the zeolite with a concentrated solution of ammonium chloride several times, at temperatures between 25°C and 100°C; and

(b) via the vapour phase, by heating the outgassed zeolite and ammonium chloride in a sealed glass tube.

The decationated zeolites have aroused special interest since their catalytic properties were reported[22]. Decationation of a zeolite consists of exchanging part or all its cations with ammonium ions and removal of the ammonia. The methods referred to

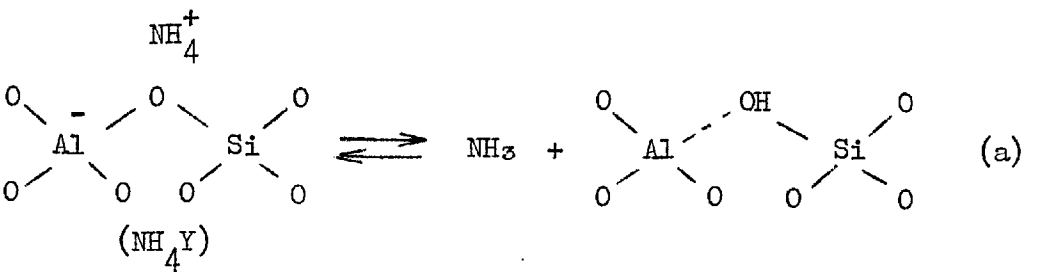
previously can be used for preparation of the ammonium forms. Ammonia can be removed by:

(a) heating the zeolite;
(b) heating the zeolite under vacuum; or
(c) heating the zeolite in a stream of oxygen[25].

In (a) and (b) temperatures between 300°C and 600°C are used. In (c) 300-350°C will usually suffice. Hall[26] in a review paper on decationated zeolites concluded that the decationation process is made up in two steps:

(a) the decationation step, in which one proton is left in the zeolite as an acidic hydroxyl group, for each ammonium ion which is decomposed;
(b) the dehydroxylation step in which water is formed.

These steps can be followed by IR spectroscopy[27]. Step (a) in the case of Y seems to be completed at around 300°C. At higher temperatures step (b) takes place. The following chemical equations[26] can describe steps (a) and (b).



Step (a) is reversible [28] which proves that the hydroxyl acts as a Brønsted acid to a base like ammonia. Step (b) is not reversible.

Another method for the creation of decationated sites in zeolites was described by Yates[29]. This consists of reduction of Cd cations by hydrogen. Cd^{o} moves out of the crystal, and hydrogen forms of zeolites are formed. In the place of Cd any other reducible cation can be used.

1.3 The properties of the sorbates

The study of sorption of ammonium chloride on zeolites is particularly important because of the Clark-Steiger reaction and because of the dissociation of ammonium chloride in the vapour phase into ammonia and hydrogen chloride. Hydrogen chloride is an interesting sorbate because of its reaction with silicates which is one of the main factors determining the nature of the system ammonium chloride-zeolite (Ch.1, Pt.II). Ammonia and hydrogen chloride are both dipole molecules. Their average molecular radii are 1.7 Å and 2.1 Å respectively. Therefore they can easily be sorbed by the zeolites used. Ammonium chloride is dimorphous and crystallizes in the cubic system. There is an upper transition point at 184.5°C below which the structure is that of CsCl (8:1) body-centred lattice while above this temperature it is that of the NaCl (6:1) face-centred lattice. The unit cell contains one molecule of ammonium chloride and has an edge length of 3.866 Å. Around each nitrogen atom the four hydrogen atoms are arranged tetrahedrally and the eight equidistant chlorine ions at the corners of a cube. The dissociation of ammonium chloride has been the study-subject of many investigators. The whole matter has been clarified by the work of Rodebush and Michalek[30] who showed that when ammonium chloride is intensively dried it evaporates very slowly. The methods of Dumas and V. Meyer employed by previous workers[31,32] for vapour density measurements cannot therefore be used for ammonium chloride. The method they employed was based on the use of a microbalance to

measure the buoyancy effect of the vapour on thin-walled tubes. The complete dissociation has also been confirmed by other methods[33]. The rates of evaporation and condensation of ammonium chloride have been studied by Spingler[34]. The vapour pressures of ammonium chloride at different temperatures[30] are plotted in fig. 9.

General information regarding the properties of the sorbates can be found in Mellor[35] or Landolt-Börnstein[36]. Reference will be made to the sources from which values for some of their properties were taken when discussing the experimental results.

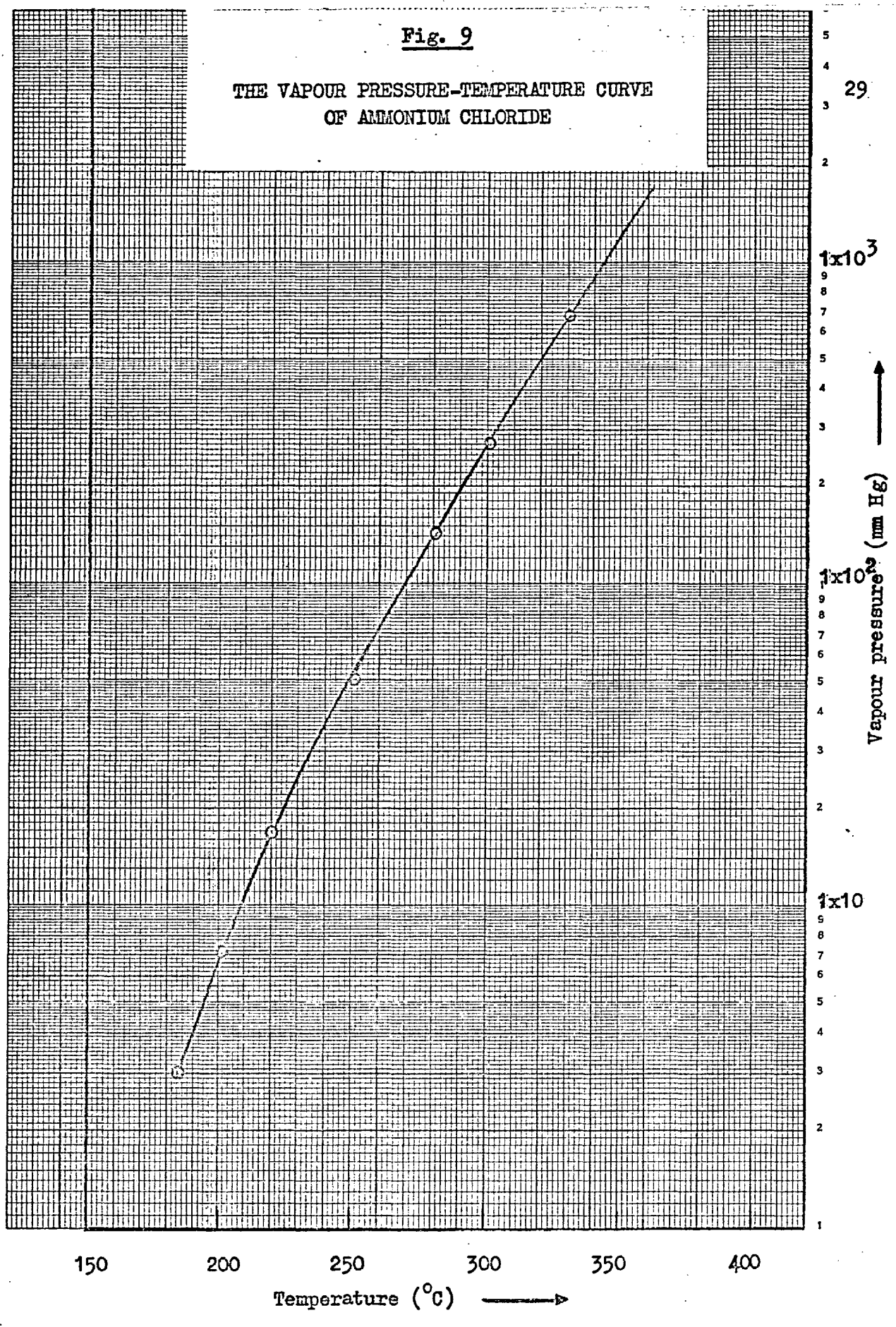
1.4 Literature survey on sorption of ammonia, hydrogen chloride and ammonium chloride on zeolites

Ammonia has been studied widely as a sorbate on different sorbents. It has not been used very much for sorption studies on zeolites. Barrer and co-workers have studied briefly the sorption of ammonia on chabazite and analcite[37] and on NaX. Barrer and Gibbons[38] have studied the sorption of ammonia on nine ion-exchanged forms of synthetic faujasite. Their study covered a wide range of temperatures. From the isotherms they obtained, the differential heats of sorption were calculated and plotted against amount sorbed. Their initial values were influenced by the type of cation, this influence being approximately proportional to the polarizing power of the cation. Kiselev et al[39] used inter alia IR techniques to study the sorption of NH_3 and ND_3 on NaX. IR techniques have also been used by other investigators[28,40] to study the sorption of ammonia on decationated forms of the synthetic zeolites X and Y.

Ammonia is a weak base. As such it has been used as a sorbate for the study of the surface acidity of certain adsorbents[41,42]. Pohl and Rebentish[43] developed a dynamic method for measurement of the surface acidity. By this method the Brønsted and Lewis acid

Fig. 9

THE VAPOUR PRESSURE-TEMPERATURE CURVE
OF AMMONIUM CHLORIDE



sites cannot be differentiated. Stone and Whalley[42] measured the heat of chemisorption of ammonia on various preparations of alumina and on the synthetic zeolite X. They did not find strong acid sites in CaX or NaX comparable to those on silica-alumina or pure alumina. Benson et al[44] measured sorption isotherms of ammonia on a decationated Y zeolite over a considerable range of temperatures (25-350°C) and for the pressure range between 10^{-6} and 100 Torr. From these isotherms they calculated isosteric heats and differential entropies at different uptakes. The initial heat of sorption was as high as 40 kcal/mole. A comparison of the isosteric heats of ammonia on decationated Y was made with the isosteric heats of ammonia on silica-alumina gel. They concluded that in the zeolite surface there were more acidic sites than on the gel surface.

Very little has been done on the sorption of hydrogen chloride on zeolites. Reyerson and Bemmels[45] studied the sorption of hydrogen chloride on silica gel. They obtained reversible and reproducible isotherms.

Solutions of hydrochloric acid react with zeolites[46]. Barrer and White[47] first reported ion-exchange reactions with dry hydrogen chloride gas in basic noseans, sodalites and cancrinites. They also reported partial decomposition of the silicate after heating it at 250°C and they suggested a possible reaction to explain it. Barrer and Brook[48] in their sorption and reactivity studies of different alkyl halides in chabazite have found that occluded fluoromethanes (CHF_3 and $CClF_2H$) underwent dehydrofluorination and produced a breakdown of the chabazite. Weak acids like H_2S do not seem to affect zeolites. Bering et al[49] studied the adsorption of H_2S and C_3H_8 mixtures on NaX. No reaction between H_2S and zeolite was observed.

The decationated zeolites have been studied to some extent since their catalytic properties were reported. Most of the work relevant to the present research concerns the mechanism of decationation and the nature of the surface of the decationated zeolites. Experimental techniques used in those studies comprise mainly IR spectroscopy [28,50,51] and ammonia adsorption [44,28]. Also NMR, ESR and electrical conductivity measurements were used [22,52].

"Ammonium chloride" vapour has not previously been used as a sorbate. Barrer [53] studied the ion-exchange properties of analcite, mordenite and chabazite by using different ion-exchange methods including that of Clark and Steiger.

The results of previous investigators, wherever relevant to the present research, will be referred to and compared to ours in the Discussion.

2. THEORETICAL

Summary of symbols

The following symbols and thermodynamic functions are used in this thesis:

P = pressure

T = temperature ^{o}K

V = volume

S = entropy

G = free energy

μ = chemical potential

E = energy

μ_{oA} = chemical potential of the pure sorbent

$\overline{X}$ = a partial molar derivative with respect to n

$\tilde{X}$ = integral quantity per mole

$\tilde{X}^{o}$ = integral quantity in a standard state

n = number of moles

"1" denotes sorbate, "A" sorbent and "g" gas

$\Gamma = \frac{n_1}{n_A}$

R = ideal gas constant

k = Boltzmann constant

H = enthalpy

2.1 The adsorption isotherm

Adsorption processes may be classified as physical or chemical, depending on the nature of the forces involved. Physical adsorption - also referred to as van der Waals adsorption - is caused by molecular interaction forces. In chemical adsorption or chemisorption a transfer of electrons between the sorbent and the sorbed molecule or atom occurs.

The amount of a gas adsorbed on a solid depends on the equilibrium pressure p, the temperature T, and also the nature of the gas and that of the solid. For a given solid at constant temperature:

$$x = f(p)_{T,\text{gas},\text{solid}} \qquad (1)$$

If the gas is below its critical temperature i.e. if it is a vapour, the alternative form

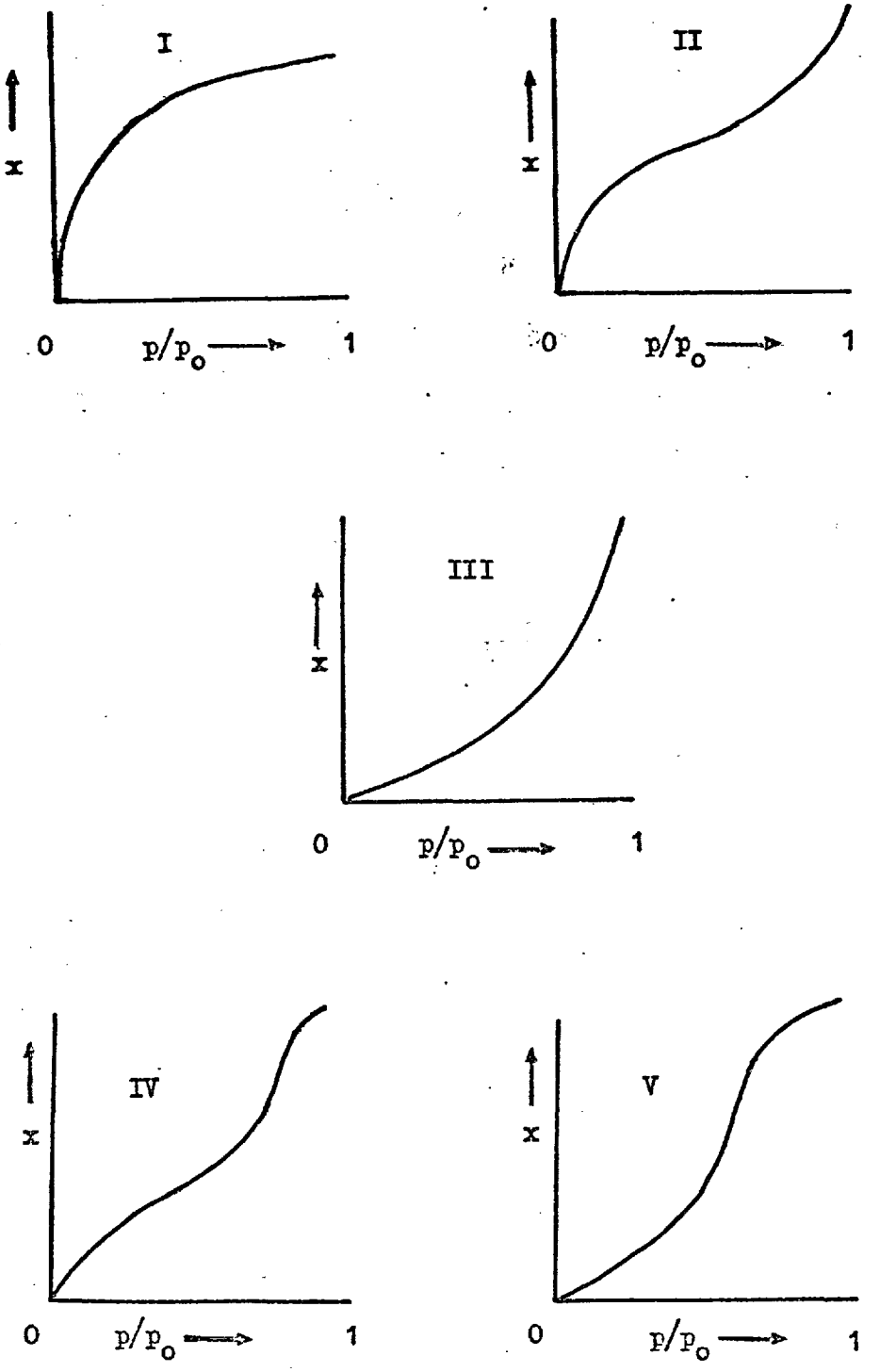
$$x = f(p/p_o)_{T,\text{gas},\text{solid}} \qquad (2)$$

is used where p_o is the saturation vapour pressure of the adsorbate. Equations (1) and (2) are expressions of the adsorption isotherm.

The majority of isotherms resulting from physical adsorption so far recorded in the literature belong to one of the five types of BET classification[54]. These types are shown in fig. 10. Besides the five classical types, there are borderline cases which are difficult to assign to one type. There is also a considerable number of isotherms which do not follow the classification at all as, for example, "stepped" isotherms[55]. One common characteristic of most isotherms is their linearity with pressure at very low pressures. This part of the isotherm is often referred to as Henry's law region, because of its similarity to the solubility of a gas in a liquid. Isotherms rectangular at low pressures indicate

Fig. 10

The five types of adsorption isotherm
in the BET classification



strong sorbate-sorbent interaction. Isotherms belonging to types III and V are indicative of strong sorbate-sorbate interaction in non-porous and porous sorbents respectively.

In the present work isotherms belonging to types I, IV and V were obtained.

Since the isotherms are comparisons of Gibb's free energy, they can be used for calculation of the thermodynamic properties of the sorbed phase and the sorbent as described in the following section.

2.2 Thermodynamics of adsorption

The present understanding of the thermodynamics of physical adsorption systems is largely due to the work of Hill[56-58] and Everett[59]. Reviews of the recent developments of the subject have been given by Hill[60] and Everett[61]. Thermodynamics may be applied to adsorption data using two different methods of approach.

(i) Solution thermodynamics. The adsorbent-adsorbate system is considered as a two-component system in equilibrium with the unadsorbed gas. This method of approach leads to partial molar thermodynamic quantities.

(ii) Adsorption thermodynamics. The adsorbed gas is considered as a single component system in equilibrium with the unadsorbed gas. This approach leads to molar thermodynamic quantities and involves the evaluation of an independent variable characteristic of the sorbent, the spreading pressure ϕ [56].

As some of the experimental results of this work were analyzed by the methods of solution thermodynamics (Ch. 3, Pt. II), a short outline of the approach will be given here. Using[60] the standard methods of solution thermodynamics we can write:

$$dE = TdS - PdV + \mu_1 dn_1 + \mu_A dn_A \tag{3}$$

$$dG = -SdT + VdP + \mu_1 dn_1 + \mu_A dn_A \tag{4}$$

where P is the hydrostatic pressure exerted by a hypothetical inert gas plus the sorbate gas pressure. Since

$$\mu_1 = \mu_1(T,P,\Gamma)$$

$$d\mu_1 = \left(\frac{\partial \mu_1}{\partial T}\right)_{P,\Gamma} dT + \left(\frac{\partial \mu_1}{\partial P}\right)_{T,\Gamma} dP + \left(\frac{\partial \mu_1}{\partial \Gamma}\right)_{T,P} d\Gamma \tag{5}$$

Also

$$\left(\frac{\partial \mu_1}{\partial T}\right)_{P,\Gamma} = -\overline{S}_1 \qquad \text{and} \qquad \left(\frac{\partial \mu_1}{\partial P}\right)_{T,\Gamma} = \overline{V}_1$$

Substitution of these quantities in equation (5) yields:

$$d\mu_1 = -\overline{S}_1 dT + \overline{V}_1 dP + \left(\frac{\partial \mu_1}{\partial \Gamma}\right)_{T,P} d\Gamma \tag{6}$$

For the gas we have the well-known expression:

$$d\mu_g = -\tilde{S}_g dT + \tilde{V}_g dp \tag{7}$$

At equilibrium between gas and the condensed phase

$$d\mu_1 = d\mu_g$$

so that

$$-\overline{S}_1 dT + \overline{V}_1 dP + \left(\frac{\partial \mu_1}{\partial \Gamma}\right)_{T,P} d\Gamma = -\tilde{S}_g dT + \tilde{V}_g dP \tag{8}$$

Under ordinary conditions P=p and we have for constant Γ

$$\left(\frac{\partial p}{\partial T}\right)_{\Gamma} = \frac{\tilde{S}_g - \bar{S}_1}{\tilde{V}_g - \bar{V}_1} \qquad (9)$$

Using the usual approximations of a perfect gas and $V_g \gg \bar{V}_1$ we obtain:

$$\left(\frac{\partial \ln p}{\partial T}\right)_{\Gamma} = \frac{\tilde{S}_g - \bar{S}_1}{RT} \doteq \frac{\tilde{H}_g - \bar{H}_1}{RT^2} = \frac{q_{st}}{RT^2} \qquad (10)$$

$\tilde{H}_g - \bar{H}_1 = -\Delta\bar{H}_1 = q_{st}$ is the isosteric heat of sorption.

Isosteric heat of sorption

The Clausius-Clapeyron equation (10) may be used in the following two ways to calculate isosteric heats from the experimental isotherm data.

(i) Plots of log p vs amount sorbed can be drawn for a number of isotherms. From these plots, $\log \frac{p_1}{p_2}$ corresponding to temperatures T_1 and T_2 for a given amount sorbed can be obtained. Isosteric heat is then calculated from the integrated form of equation (10).

$$q_{st} = -\Delta\bar{H}_1 = -2.303\,R\left(\frac{T_1 T_2}{T_1 - T_2}\right)\log\frac{p_2}{p_1}$$

In order to obtain reliable results, as many pairs of isotherms as possible must be used for evaluation of q_{st}, since q_{st} can be temperature dependent.

(ii) Equation (10) can be written in the form:

$$\left(\frac{\partial \ln p}{\partial \frac{1}{T}}\right)_{\Gamma} = \frac{\Delta\bar{H}_1}{R} \qquad (10a)$$

In this case, a plot of log p vs 1/T is necessary for every uptake for evaluation of q_{st}. The slope of this plot (if it is a straight line) or the tangent (if it is a curve) is equal to:

$$-\frac{q_{st}}{2.303R}$$

Entropy of adsorption

From equation (10) we obtain the entropy of sorption

$$\Delta S = \tilde{S}_g - \bar{S}_1 = -\frac{\Delta \bar{H}_1}{T} \qquad (11)$$

The molar entropy of the gas $\tilde{S}_g$ at pressure p referred to the standard entropy $\tilde{S}^o_g$ at a standard pressure p^o is given by

$$\tilde{S}_g = \tilde{S}^o_g + R\ln\frac{p^o}{p} \qquad (12)$$

From equations (11) and (12) we obtain

$$\bar{S}_1 = \tilde{S}^o_g + R\ln\frac{p^o}{p} + \frac{\Delta \bar{H}_1}{T} \qquad (13)$$

The standard pressure for a gas is usually taken to be 1 atm. If a correction for non-ideality of the gas is applied, a term ap is subtracted from the above expression for $\bar{S}_1$, where approximately $a = \frac{27RT_c^3}{32P_cT^3}$ and P_c and T_c are respectively the critical pressure and temperature of the gas. No correction was necessary for the values of entropies calculated in this work.

Half standard entropy of sorption

From equation (13) we obtain:

$$\Delta\bar{S}_1 = \tilde{S}^o_g - \bar{S}_1 = R\ln\frac{p}{p^o} - \frac{\Delta\bar{H}_1}{T} \qquad (14)$$

This entropy, referred to a standard state of the gaseous sorbate, was found by Barrer and Sutherland[62] to be independent of temperature. On differentiating equation (14) with respect to T and if $\Delta\bar{H}_1$ is independent of temperature we obtain:

$$\left(\frac{\partial\bar{S}_1}{\partial T}\right)_x = \frac{\partial\tilde{S}^o_g}{\partial T}$$

The temperature invariance of $\Delta\bar{S}_1$, also described as the half standard entropy of sorption, can be used for extrapolation purposes.

Integral thermodynamic quantities

Integral or molar thermodynamic quantities $\tilde{X}$ can be obtained by graphical integration of the corresponding differential quantities $\bar{X}$ vs amount adsorbed. Thus for the integral heat of sorption we have:

$$\Delta\tilde{H}_1 = \frac{1}{n_1}\int_0^{n_1}\Delta\bar{H}_1 dn_1$$

The other integral quantities can be obtained in a similar way.

Thermodynamic properties of the sorbent[63]

If we consider n_1 moles of sorbate and n_A moles of sorbent as a solution at constant temperature T, the Gibbs-Duhem relationship gives

$$n_1 d\mu_1 + n_A d\mu_A = Vdp \qquad (15)$$

If N_1 and N_A are the mole fractions of sorbate and sorbent respectively and V_x the volume of the mixed mole,

$$N_1 = \frac{n_1}{n_1+n_A}, \quad N_A = \frac{n_A}{n_1+n_A}, \quad V_x = \frac{V}{n_1+n_A}$$

On substituting these quantities in equation (15) we obtain:

$$N_1 d\mu_1 + (1-N_1) d\mu_A = V_x dp \tag{16}$$

and on rearrangement

$$d\mu_A = \frac{V_x dp}{1-N_1} - \frac{N_1 d\mu_1}{1-N_1} \tag{17}$$

At equilibrium

$$d\mu_1 = d\mu_g$$

and by assuming ideality

$$d\mu_g = RTd\ln p$$

If we substitute in equation (17) and integrate, assuming that there is no expansion of the zeolite lattice on sorption, we obtain:

$$\Delta\mu_A = \mu_A - \mu_{oA} = V_M p - \frac{MRT}{m}\int_o^p \frac{x}{p} dp \tag{18}$$

where x = amount sorbed in g/g of outgassed sorbent
m = molecular weight of sorbate
V_M = molecular volume of a lattice-forming unit of molecular weight M.

The first term of equation (18) is normally negligible; the second term is evaluated graphically from isotherm data (from a plot of $\frac{x}{p}$ vs p).

From the Gibbs-Helmholtz relationship we have

$$\frac{\partial (\mu_A - \mu_{oA})}{\partial T} = (\bar{S}_A - \bar{S}_{oA}) = -\Delta\bar{S}_A \qquad (19)$$

and

$$\left[\frac{\partial}{\partial T}\left(\frac{\Delta\mu_A}{T}\right)\right]_x = (\bar{H}_A - \bar{H}_{oA}) = -\frac{\Delta\bar{H}_A}{T^2} \qquad (20)$$

From equations (19) and (20) the entropy and enthalpy changes of the sorbent on sorption can be found.

2.3 Physical models of the sorbed phase

Numerous attempts have been made to fit mathematical expressions to experimentally determined isotherms. The earliest equations were entirely empirical. Later theories based upon physical pictures of sorption have been more successful. Everett[59,61] has shown that the fact that a particular physical theory of adsorption leads to an adsorption isotherm which is observed experimentally is no evidence for the correctness of the model. A complete theory must not only yield the correct form for the free energy (i.e. reproduce the isotherm) of the system, but must also account for the entropy and the energy of the adsorbed phase.

The experimental determination of the thermodynamic properties of the sorbent-sorbate system followed by attempts to interpret these properties in terms of limiting isotherm models has recently been the aim of several investigations (e.g. [64,65,101,66]). Some of the isotherm models will be described shortly in this section.

Localized sorption without interaction (Langmuir's isotherm)

In an ideal localized model of intracrystalline sorption, the molecules are assumed to be sorbed on a three-dimensional array

of energetically homogeneous sites with no interactions between neighbouring molecules. The equation describing localized sorption without interaction was originally derived by Langmuir[67] who was the first to develop a kinetic approach to sorption using models of sorption and desorption processes. The model he introduced was limited to an ideal localized monolayer, i.e. a single layer of non-interacting molecules on fixed sites of equal energy. In the original kinetic derivation the adsorbed layer is regarded as in dynamic equilibrium with the gas phase. If θ is the fraction of sites occupied at an equilibrium pressure p, the equilibrium constant K, is given by:

$$K = \frac{\theta}{p(1-\theta)}$$

The same relation has also been derived by thermodynamic considerations[68] and is independent of the kinetic mechanism originally assumed by Langmuir. Young and Crowell[69] review the analogues of Langmuir's equation.

Localized sorption with interaction

The model is that of the ideal localized monolayer with the further assumption that each molecule interacts with its nearest neighbouring molecules. The effect of interactions between nearest neighbouring molecules in a localized system has been considered by numerous workers. The equation obtained by Lacher[70] has the form:

$$K = \frac{\theta}{p(1-\theta)} \left[\frac{2(1-\theta)}{\beta + 1 - 2\theta} \right]^z$$

where z is the number of the nearest neighbours of any site and β is given by

$$\beta = \left[1 - 4\theta(1-\theta) \left[1 - \exp(-2w/zkT) \right] \right]^{\frac{1}{2}}$$

$2w/z$ is the interaction energy between two adjacent molecules and it is negative for attractive interactions.

Mobile sorption, sorbate obeys Volmer equation of state

Volmer[71] regarded the sorbed film as two-dimensional gas in which he introduced a finite "co-area" (analogous to the volume correction in the three-dimensional van der Waals equation) for each molecule. However, he neglected the possibility of mutual interaction between sorbed molecules. The equation that can be derived[59,72] from Volmer's equation of state has the form:

$$p = K \left(\frac{\theta}{1-\theta}\right) \exp \left(\frac{\theta}{1-\theta}\right)$$

Mobile sorption, sorbate obeys van der Waals equation of state

Hill[72] assumed that the adsorbed film obeys a two-dimensional van der Waals equation of state, i.e. the adsorbed molecules have a finite "co-area" and exhibit mutual interactions. The isotherm equation he derived from this equation of state was

$$p = K \frac{\theta}{1-\theta} \exp \left(\frac{\theta}{1-\theta} - \alpha\theta\right)$$

where α is a constant depending upon the temperature and the constants of the three-dimensional van der Waals equation (see p. 139).

2.4 General isotherm equations

Van't Hoff isotherm

The Van't Hoff isotherm is given by:

$$\Delta G = - RT\ln\left(\frac{a_s}{a_g}\right)_{eq} + RT\ln\frac{a_s}{a_g} \qquad (21)$$

where "a" denotes activity, "s" denotes the sorbed phase, "g" the gaseous phase and "eq" the equilibrium condition. a_s and a_g are arbitrary activities; ΔG is the free energy for isothermal and reversible transfer of a mole of gas from an infinite amount of gas

of activity a_g to an infinite amount of sorbent in which the activity of the sorbate is a_s.

If the sorbate is in its standard state in the gas phase and in the sorbent, then $a_g = 1$ and $a_s = 1$. Therefore

$$\Delta G = \Delta G_o = -RT\ln\left(\frac{a_s}{a_g}\right)_{eq} = -RT\ln K \qquad (22)$$

It follows that

$$-\frac{\partial(\Delta G_o)}{\partial T} = \Delta S_o = R\ln K + \frac{RT\,\partial \ln K}{\partial T} = -\frac{\Delta G_o}{T} + \frac{\Delta H_o}{T} \qquad (23)$$

and that

$$\frac{\partial}{\partial T}\left(\frac{\Delta G_o}{T}\right) = -\frac{\Delta H_o}{T^2} \qquad (24)$$

The equilibrium constant is given by

$$K = \left(\frac{a_s}{a_g}\right)_{eq} \qquad (25)$$

and for the gas phase $a_g = a_p$, so that the gaseous standard state is one where $p = 1$ (where p is measured in atms). In the sorbed phase

$$a_s = c_s \gamma_s \qquad (26)$$

where c_s denotes concentration and γ_s the activity coefficient. In the standard state $c_s \gamma_s = 1 = a_s$. c_s can be expressed as the number of moles of sorbate per 1 litre of sorbent-sorbate mixture.

Osmotic pressure and empirical isotherm equations

If the sorbent-sorbate system is regarded as a solution (solution thermodynamics) the change in the chemical potential of the sorbent during sorption is given by equation (18)

$$\Delta \mu_A = \int_0^p V_x dp - \frac{MRT}{m} \int_0^p \frac{x}{p} dp \qquad (27)$$

Also we can write[101]

$$\int_0^{-\pi} V dp = \Delta \mu_A \qquad (28)$$

where $-\pi$ is the tension that would have to be applied to the sorbate-free crystals to reduce their chemical potential to that of the host crystals when sorption has taken place, or π is the hydrostatic pressure which would need to be applied to the sorbent-sorbate solution to raise the chemical potential of the zeolite to that of the sorbate-free crystals. Thus π is the equivalent of the osmotic pressure. Since the first term of the right hand side of equation (27) is negligible (p. 40), combination of this equation with equation (28) yields:

$$\Delta \mu_A = \pi V = \frac{RTM}{m} \int_0^p \frac{x}{p} dp \qquad (29)$$

or

$$\frac{\pi}{RTc_s} = \frac{\rho}{mc_s} \int_0^p \frac{x}{p} dp \qquad (30)$$

where $\rho = \frac{M}{V}$ is the density of the outgassed zeolite.

The curves $\frac{\pi}{RTc_s}$ can be represented by the equation

$$\frac{\pi}{RTc_s} = 1 + A_1 c_s + A_2 c_s^2 + \ldots \qquad (31)$$

This equation can be used to derive the corresponding empirical

isotherm. From equations (31) and (30):

$$1 + A_1 c_s + A_2 c_s^2 + \ldots = \frac{\rho}{m c_s} \int_o^p \frac{x}{p}\, dp \qquad (32)$$

or

$$c_s + A_1 c_s^2 + A_2 c_s^3 + \ldots = \int_o^p \frac{c_s}{p}\, dp \qquad (33)$$

and the isotherm equation is:

$$p = K c_s \exp\,(2A_1 c_s + 3/2\ A_2 c_s^2 + \ldots) \qquad (34)$$

or

$$K = \frac{c_s}{p} \exp\,(2A_1 c_s + 3/2\ A_2 c_s^2 + \ldots) \qquad (35)$$

Equation (31) has been used[38,66] to calculate the coefficients A_1, A_2, ... Expressions for the osmotic ratio $\frac{\pi}{RTc_s}$ can be obtained from different isotherm models. The values obtained from these expressions can be compared with the experimental ones and the osmotic ratio can be used as a test for isotherm models.

From equations (25), (26) and (35) it follows that

$$\gamma_s = \exp\,(2A_1 c_s + 3/2\ A_2 c_s^2 + \ldots) \qquad (36)$$

and for small enough c_s $\gamma_s \longrightarrow 1$, $K = \frac{c_s}{p}$ and is the Henry's law constant. The state of unit activity, a_s, is one where

$$a_s = c_s \gamma_s = c_s \exp\,(2A_1 c_s + 3/2\ A_2 c_s^2 + \ldots) = 1 \qquad (37)$$

and cannot be determined from equation (37) without knowing A_1, A_2, ..., which in turn require the isotherm to be known outside the Henry's

law region (in which $\frac{\pi}{RTc_s} = 1$). According to this treatment, the standard state will vary from one sorbate to another, while for a given sorbate it will also vary with the temperature. In this scale of activities, just as in ordinary solutions, $\gamma_s \rightarrow 1$ as c_s becomes small, and in this range $c_s = a_s$. In Part II the above argument will be used to evaluate the coefficients A_1, A_2, ... and calculate the thermodynamic properties of the sorbed phase in the standard state. Activity coefficients will be calculated from the experimental results and compared with those calculated from different isotherm models (ch. 3). The argument will also be extended for sorption from a mixture of two gases and the coefficients A_{11} and A_{22} of the pure components and the cross-coefficient A_{12} will be evaluated (ch. 4).

2.5 Physical adsorption forces

Since physical adsorption results from interatomic or intermolecular interaction, the forces which contribute to the interaction of physically adsorbed molecules are the same as those involved in any other interatomic or intermolecular interaction phenomenon. The most frequently encountered physical interaction forces are:

(i) Dispersion forces.
(ii) Close-range repulsion forces.
(iii) Polarization forces.
(iv) Field-dipole interaction.
(v) Field-quadrupole interaction.

The forces that contribute most in the interaction of sorbed ammonia or hydrogen chloride with the zeolite are (i), (ii), (iii) and (iv).

Dispersion forces arise from the rapidly fluctuating electron density in one atom, which induces a corresponding electrical moment in a near neighbour and so leads to attraction between the atoms. The potential energy E_D of two isolated atoms separated by a distance r is

given by

$$E_D = -\frac{C}{r^6}$$

where C is a constant and the negative sign shows attraction.

When the electron clouds of two atoms overlap sufficiently, repulsion forces arise. The interaction due to repulsion forces can be described empirically by an equation of the form

$$E_R = Br^{-m}$$

where B is a constant and $9 < m < 14$. The value 12 for m is the most commonly used. Two important properties of dispersion and repulsion forces are that they are nearly additive and temperature independent.

Polarization forces arise when the sorbent is heteropolar (e.g. composed of positive and negative ions) so that there are local electrostatic fields F which polarize the sorbate of polarizability α. The energy of interaction then is:

$$E_p = -\tfrac{1}{2}\alpha F^2$$

The local field F also interacts with molecules possessing permanent dipole monents. The energy of interaction for a point dipole of dipole moment μ having its axis oriented at an angle θ to the local field direction is:

$$E_F = -F\mu\cos\theta$$

The local field F of a heteropolar or ionic surface will normally have an associated field gradient F which can interact powerfully with molecules possessing permanent quadrupole moments, e.g. CO_2. Dipole-quadrupole and quadrupole-quadrupole, although usually small, may also contribute a little to the bond energy.

Among the above-mentioned forces of physical interaction, dispersion and repulsion are found universally although their magnitudes may vary according to the local environment in the sorbent. The contribution of the other forces to the physical adsorption energy can vary depending upon the nature of the sorbent and sorbate. Barrer and co-workers[65,38,73] have calculated the energy of inclusion of certain gases in synthetic zeolites by summing the theoretical energy contributions due to the different interactions of the sorbed molecules with the atoms of the lattice. The values of the inclusion energies thus obtained were in fair agreement with the experimental values. The role of the different physical interactions in respect to the specificity in physical sorption has been discussed by Barrer[74].

2.6 Sorption hysteresis

The phenomenon of hysteresis in sorption is not rare. In many cases isotherms have been recorded possessing hysteresis loops, the lower branch of which represents measurements obtained by progressive addition of sorbate to the system and the upper branch by progressive removal.

Most of the theories of sorption hysteresis, especially in macroporous sorbents[75], are based on or related to capillary condensation. These theories in connection with the surface area and porosity of the sorbents have recently been reviewed by Gregg and Sing[76]. Since the zeolites are microporous sorbents, these theories cannot be considered in sorption in zeolites.

Barrer[77] proposed that hysteresis phenomena may be attributed to the need to nucleate a second phase of host crystal and guest molecules on or in a parent phase. When a germ-nucleus of the new phase forms on or in a matrix of the parent phase, then two additional positive free energy terms are involved associated with surface free

energy and with strain. The nucleus will not grow until the sorbate pressure is in excess of the pressure at the point of the true thermodynamic equilibrium. By similar considerations, the reversal to the original phase on desorption is delayed beyond the thermodynamic equilibrium point and so hysteresis results.

A more general theory attempting to correlate the behaviour of all systems exhibiting hysteresis was proposed by Everett and Whitton[78]. Hysteresis is attributed to a large number of independent domains each able to exist in at least two physical states. The expansion of the independent-domain theory together with theories on hysteresis has recently been given by Everett[79] in a review of the subject.

3. EXPERIMENTAL

3.1 Introduction

The study of sorption equilibria involving ammonia or hydrogen chloride at temperatures between 200°C and 350°C does not present significant practical problems and a conventional gravimetric sorption apparatus was used (sorption system 2). On the other hand, for the study of sorption of "ammonium chloride" vapour a number of practical problems is involved. The lower limit for isotherm measurement, set by the temperature at which 2.4 cm Hg of vapour pressure is attainable, is 230°C. This temperature prevents the measurement of pressure with a simple mercury manometer and the use of tap grease in the apparatus.

These problems were overcome by Barrer and Wasilewski[80] who designed an all-sealed gravimetric apparatus for the study of adsorption of reactive, condensable vapours at temperatures up to 350°C and in the pressure range 0.1 - 760 mm Hg. This apparatus (sorption system 1) was used with a few modifications for all ammonium chloride-zeolite isotherms.

At these high temperatures it is very difficult to maintain uniform temperature throughout a considerable volume. As no fluid stable for long periods at 350°C, and therefore suitable for a constant temperature bath, was available, electrically heated tubular furnaces were used. The errors arising from temperature gradients in the furnaces were eliminated as much as possible by calibrating all the measuring devices, i.e. silica springs and spiral gauges, under conditions as similar as possible to those used during isotherm measurements. The furnaces were of large heat capacity to assist thermal stability. In sorption system 1 at least 12 hours were required to re-establish thermal equilibrium after a considerable change in settings.

Silicone oil baths for temperatures up to 220°C were used wherever possible (e.g. in hydrogen chloride-silicate stability experiments).

Chemical analysis, thermogravimetric analysis and X-ray photography were used to obtain information concerning structural changes in the samples after sorption or ion-exchange experiments. After the run was completed, the samples were usually washed with distilled water and the tests for chlorides and aluminium were carried out on the filtrate. X-ray photographs were taken of starting materials at various stages during the experiments and, finally, after a series of experiments had been completed. Moreover, the amount of decomposition of crystalline zeolites in certain cases was estimated by using the powder method.

3.2 The sorbents

Two forms of silicates were used:

(i) Na^+ and K^+ exchanged forms.
(ii) Decationated zeolites.

All samples were washed with distilled water before they were used. Prolonged washing was avoided to minimize hydrolysis of the zeolite. Before samples were analyzed they were equilibrated with water vapour in a dessicator containing saturated aqueous ammonium chloride for at least a week.

The synthetic Molecular Sieves A, X, L and Y were supplied by Linde Air Products Ltd., as fine powders. A, X and Y were supplied and used in their Na^+ form. L was supplied in its mixed K^+ and Na^+ form. It was exchanged to the K^+ form by shaking it with a saturated solution of potassium chloride at room temperature for 12 hours. This treatment was repeated; the zeolite was filtered and washed free from chlorides. By this treatment a zeolite was obtained which contained 98% of its total cation capacity as K^+.

The synthetic zeolite mordenite was obtained from Norton Co.

The Na form of ferrierite was prepared by exchanging Sr^{++} with Na^{+} by treating the Sr form with a 20% solution of sodium chloride at 50°C for 4 hours, four times. The Sr form was synthesized and supplied by Dr J.A. Lee.

Na-clinoptilolite was kindly supplied by Dr B. Coughlan of these laboratories.

A mixture of feldspars containing 17% albite and 82% orthoclase was used, supplied by Dr D.E.W. Vaughan.

Na forms of basic synthetic sodalite and cancrinite were synthesized in these laboratories and were supplied by Mr J. Cole.

Na-chabazite was supplied by Dr J.A. Davies.

Hydrogen Zeolon - the hydrogen form of synthetic mordenite - was obtained from Norton Co. and it was used as supplied after washing with distilled water. Analysis showed that it contained Na^{+} to the extent of 8% of its total cation capacity.

Attempts were made to prepare stable hydrogen forms of the synthetic zeolites Y and L. Details of the methods used are given in Chapter 2 of Part II, where the experimental results are discussed.

The ammonium forms of the zeolites referred to are not stable at temperatures 300°C or 350°C. Some experiments carried out during the course of this research confirmed previous findings concerning their stability.

3.3 The sorbates

Anhydrous ammonia was supplied by I.C.I. in a 100 c.ft. cylinder. The ammonia cylinder was connected to the purification system by means of a polythene tube. The ends of the polythene tube were sealed to the cylinder and the apparatus with Araldite. The

main impurity of ammonia being water, the purification system consisted of two drying tubes containing ignited CaO and NaOH pellets respectively. A manometer attached between the cylinder and the drying tubes allowed the pressure of ammonia to be measured.

The storage system consisted of two cold traps and a buffer volume of 5 litres and was connected to the sorption system and the high vacuum line. The purification and storage system of ammonia is shown in fig.11.

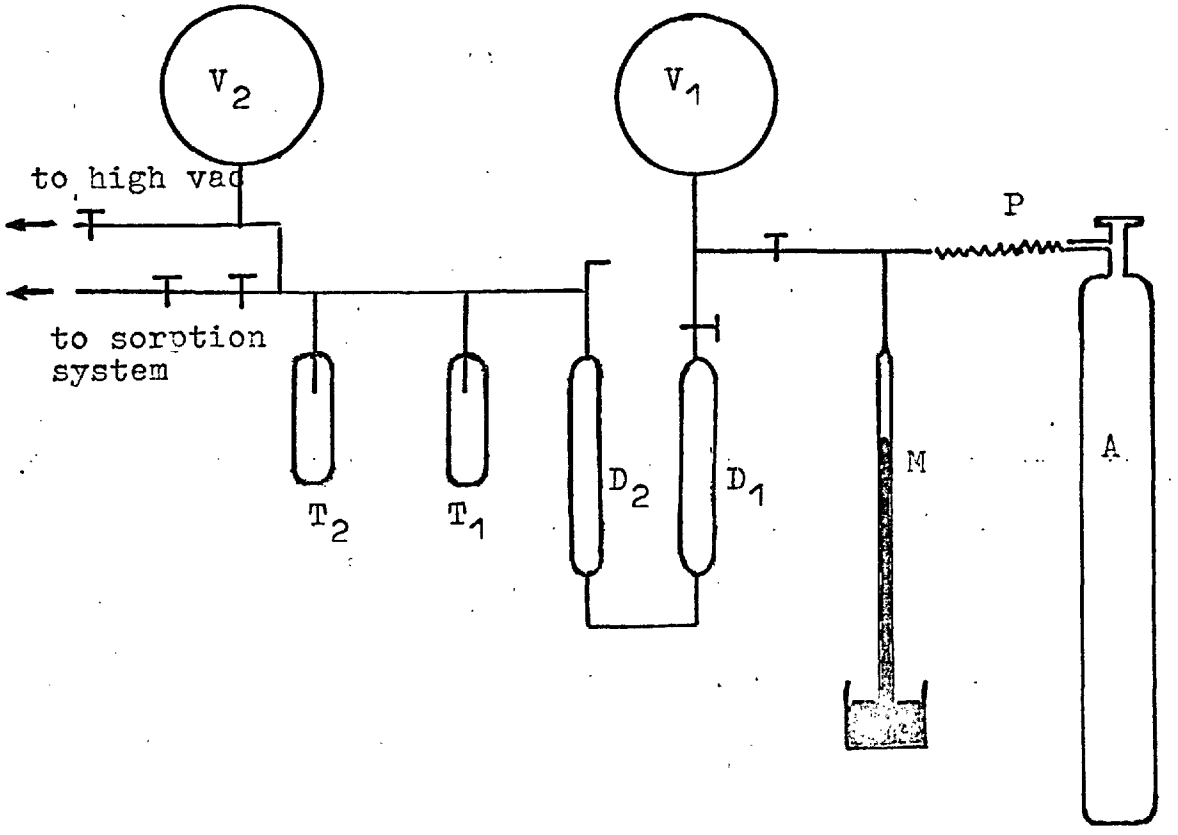
The apparatus was first outgassed as much as the polythene tube allowed, and ammonia was admitted slowly, its pressure being controlled by the mercury manometer. Then it was passed through the drying tubes D_1 and D_2 and frozen into the trap T_1 which was cooled with liquid nitrogen. It was further purified by three bulb to bulb distillations, the middle fractions being always kept.

Anhydrous hydrogen chloride was prepared by adding concentrated sulphuric acid to concentrated hydrochloric acid in an apparatus similar to the anhydrous hydrogen chloride generator described by Taniguchi and Janz[81]. This apparatus with the storage system is shown in fig.12 and consists of a dropping funnel, a reaction tube, a sulphuric acid trap and three drying tubes.

The required amount of concentrated hydrochloric acid was charged through the side arm A into the reaction tube E. Sulphuric acid was added by means of the dropping funnel B, its rate being controlled by a stopcock. The lower part of the dropper was a capillary so that small amounts of sulphuric acid came into contact with hydrochloric acid and hazard was avoided. The rate of hydrogen chloride production was indicated by the bubbler C containing concentrated sulphuric acid which serves for the preliminary drying of hydrogen chloride. The three drying tubes were filled with anhydrous phosphorus pentoxide, glass beads and glass wool. The first quantity

Fig. 11

Ammonia Purification and Storage System



A: Ammonia cylinder.

M: Mercury Manometer.

D_1: Tube containing ignited CaO.

D_2: Tube containing NaOH pellets.

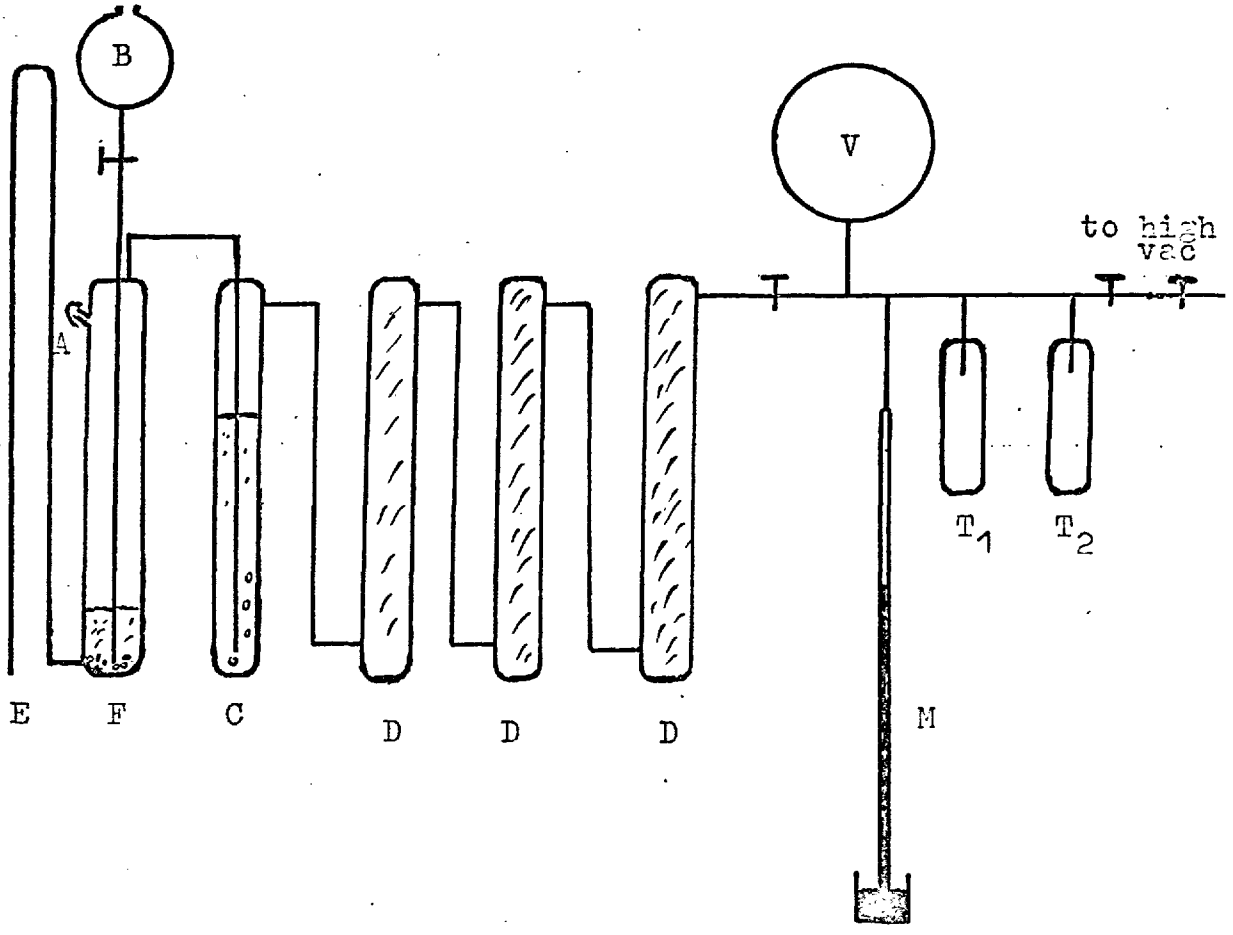
P: Polythene tube.

T_1, T_2: Cold traps.

V_1, V_2: Buffer Volumes.

Fig. 12

Apparatus for Preparation and Storage of Anhydrous HCl



A: Hydrochloric acid inlet.
B: Sulphuric acid reservoir.
C: Sulphuric acid bubbler.
D: P_2O_5 drying tubes.
E: Outlet.
F: Reaction tube.
M: Mercury manometer.
T_1, T_2 :Cold traps.
V: Buffer Volume.

of hydrogen chloride produced was pumped off in order to remove air from the apparatus. The next quantity was frozen in one of the traps T and further purified by three bulb to bulb distillations, the middle fractions being always kept. The spent reaction mixture could easily be siphoned from the reaction tube through outlet E by applying gentle suction. In order to be sure that no traces of water were present during the experiments, ammonia (or HCl) was introduced into the system by evaporation from the liquified gas.

Ammonium chloride, AnalaR, was supplied by Hopkins and Williams Ltd. and was used without any further purification. It was dried in the sorbate reservoir (see fig.13) under high vacuum at 90°C for ca 48 hours.

3.4 Sorption system 1

The sorption system 1 is shown in figs. 13 and 14. It consisted of a wholly enclosed glass balance case (fig. 13) containing a silica spring balance, a spiral gauge and a thermocouple. The system was surrounded by three electric furnaces.

A hook sealed into the top of the balance case supported the silica spring. On the lower end of the spring a pyrex bucket weighing ca 0.2 g was suspended. The sorbent was put in the bucket. A long hollow finger running along the balance case allowed the thermocouple to be moved.

Below the bucket containing the sorbent, a pyrex spiral gauge was sealed so that the inside of the spiral had direct contact with the vapour in the balance case. The outside surface of the spiral was in contact with nitrogen gas. The pressure of the nitrogen could be regulated by means of a reduction valve and was measured by a U-shaped mercury manometer from outside the system through a connecting tube. A mirror attached to the end of the spiral gauge

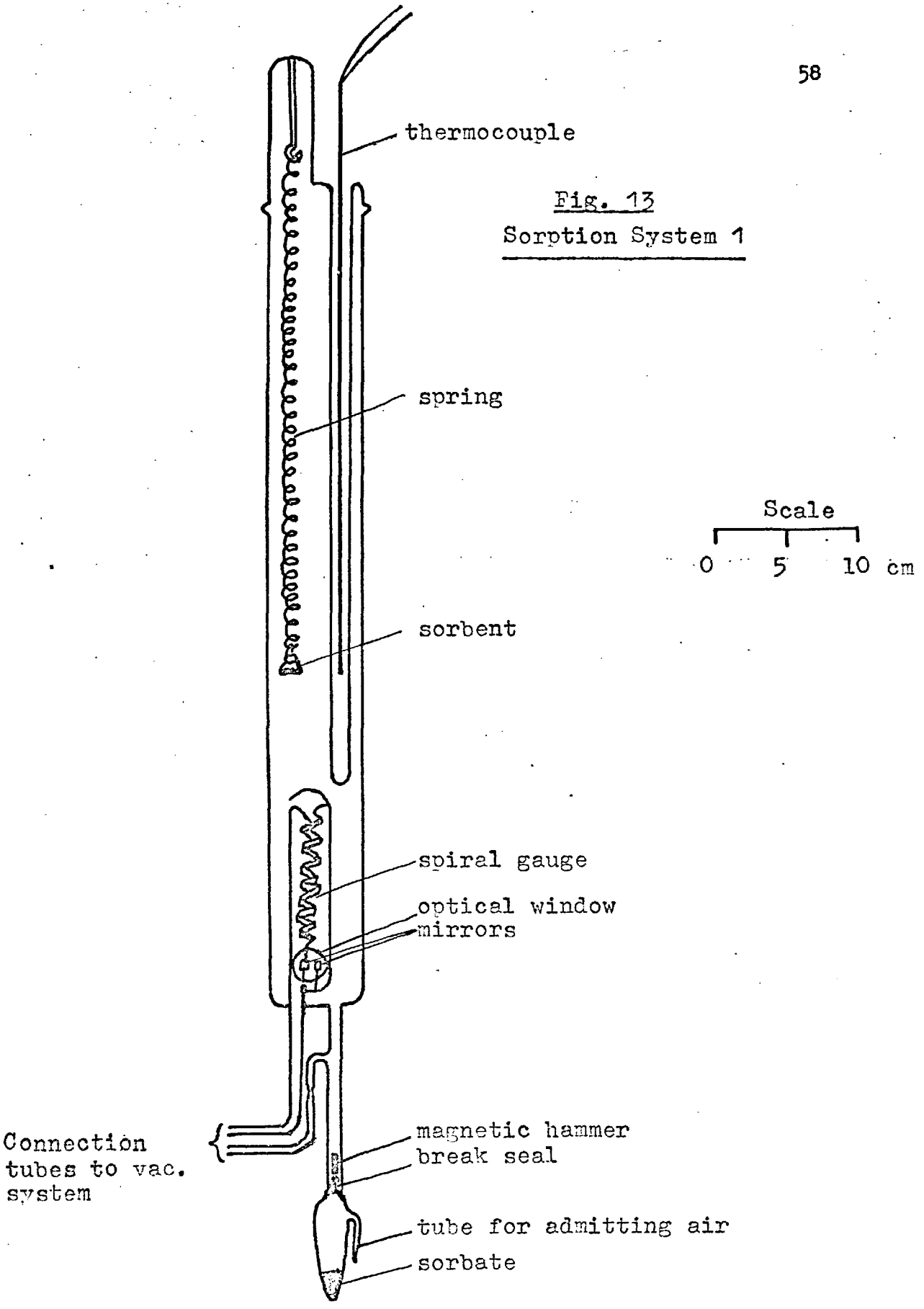


Fig. 13
Sorption System 1

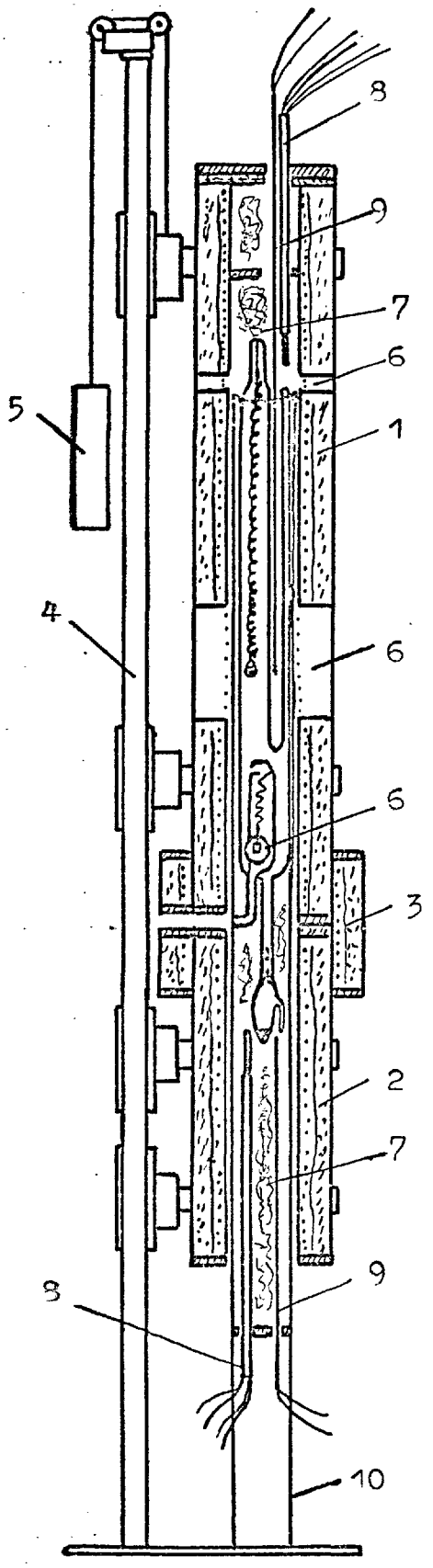


Fig. 14
The furnace system
(Sorption System 1)

Scale
0 10 20 cm

1: Main furnace
2: Small furnace
3: Junction furnace
4: Steel rails
5: Counterweight
6: Furnace windows
7: Asbestos wool
8: Pt resistance thermometers
9: Thermocouples
10: Steel tube supporting balance case

reflected a beam of light on to a scale and allowed any movement of the spring to be recorded. The reflection of another mirror fixed permanently on the balance case near that attached to the gauge was used as a reference point. Small pressure differences across the spiral applied for a short time (e.g. when the sorbate pressure is being changed) had no effect on the spiral gauge. But big differences applied for a long time caused deformation which was slow to recover. To avoid any deformation and so drifts of the zero pressure indication, the pressure on both sides of the spiral was kept as similar as possible. When the sample was outgassed, care was taken that both sides of the spiral were evacuated.

The sorbate was outgassed in a special reservoir under high vacuum. The reservoir was sealed to the bottom of the balance case. Sorbate vapour could be allowed to the balance case by breaking a break seal with a magnetic hammer.

The temperature was measured by means of a chromel-alumel thermocouple always placed opposite the bucket. This was found to record temperature more reliably than a platinum resistance thermometer several inches long[82].

The balance case was connected to the vacuum line through a side arm. A constriction made near the balance case helped to seal off the side arm and isolate the balance case when the sample was outgassed completely. When the run was finished, the system could be opened by breaking a small side arm attached to the sorbate reservoir. This small side arm was covered with a rubber tube closed by a screw clip and then broken. Air could be let into the system slowly.

Heat was supplied by three furnaces, the main furnace, the small furnace and the junction furnace. The main furnace heated the upper part of the balance case containing the sorbent. The small

furnace heated the sorbate reservoir. The temperature of the sorbate reservoir determined the vapour pressure of the sorbate. The temperature of the furnace necessary for a certain sorbate pressure was adjusted from the vapour pressure vs temperature curve of the sorbate.

Both the main and small furnaces were mounted on vertical steel rails. This preserved their alignment and allowed them to move easily to and from the balance case as required. Five quartz windows fitted on the main furnace allowed measurements of the spring length and observations of the mirror attached to the spiral gauge.

The junction furnace consisted of two semicircular segments fitting round the junction of the tubular furnaces. The tubes connecting the balance case to the vacuum system passed through a hole formed by slots cut in the main and small furnace and the two parts of the junction furnace.

Two insulated heating windings were in each of the tubular furnaces. Most of the heat was supplied by the outer winding while the inner one - the resistance of which was higher - allowed the sensitive control of heat input. The two parts of the junction furnace had only a single winding. Power was supplied to the furnace system via a constant voltage regulator and 2 kW variacs. The main windings (outer) were supplied directly by the variacs. The auxiliary (inner) windings were fed via an electronic controller. In each tubular furnace there was a platinum resistance thermometer used as a temperature controlling device. The controlling circuit was a Wheatstone bridge one arm of which was the platinum resistance thermometer. The other three arms were the compensating leads of the thermometer, a fixed resistance and a decade box. The out-of-balance current from the bridge was amplified in the controller and used to operate a switch. The switch closed or opened when the resistance of the Pt resistance thermometer was lower or higher than the resistance of the decade box, respectively. When the switch was open

current flowed through a resistance connected across the switch to the auxiliary winding and the power input was low. When the switch was closed, current flowed directly and the input was high. In this way the furnace temperature could be kept constant at a level determined by the resistance of the decade box. The settings of the decade boxes resistances necessary to maintain a certain temperature were determined by trial during a run.

The balance case was supported by a stainless steel tube mounted on a cast iron base. This tube was concentric with the furnaces and slots cut at appropriate positions allowed access to the balance case for observations and adjustments. The space between the balance case and the furnaces was filled with asbestos wool. Care was taken to avoid obscuring the windows. The same amount of asbestos wool was used in every run as it was found to be important for the temperature gradients in the furnace system.

3.5 Sorption system 2

The sorption system 2, which was simpler than the sorption system 1, is shown in fig. 15. It consisted of a glass balance case surrounded by an electric furnace and connected to a U-shaped mercury manometer, the gas storage reservoir, and a thermocouple.

A glass hook sealed into the top of the balance case supported the silica spring, at the lower end of which there was a pyrex bucket weighing ca 0.2 g and containing the sorbent. A glass hollow finger along the balance case allowed the thermocouple to be moved.

One end of the mercury manometer was connected to the high vacuum line and the other to the balance case and the gas reservoir. The sorbate pressure was measured as the difference in the height of mercury in the two limbs of the manometer. The two ends of the spring and the level of the mercury in the manometer were read by a cathetometer.

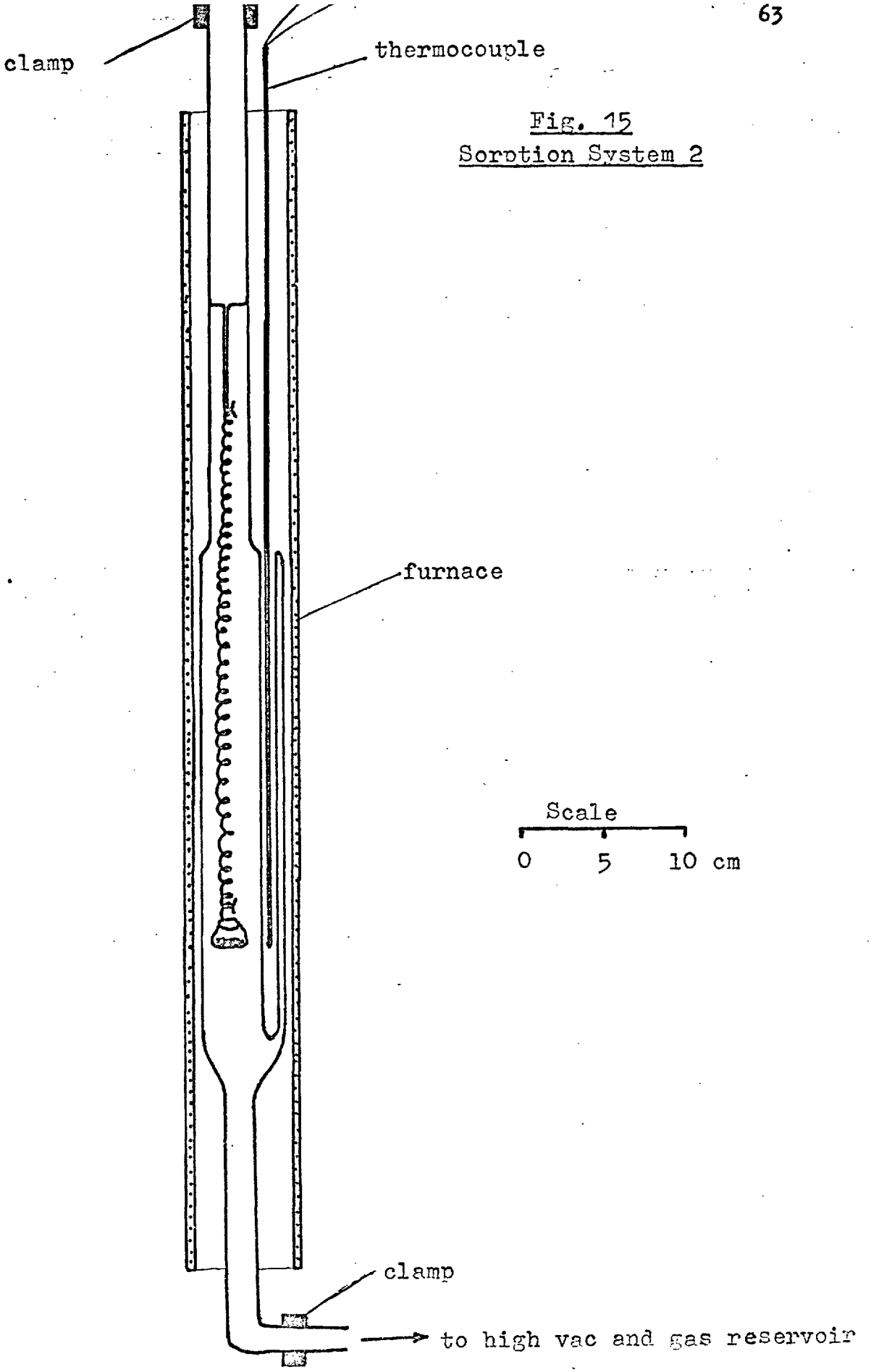


Fig. 15
Sorption System 2

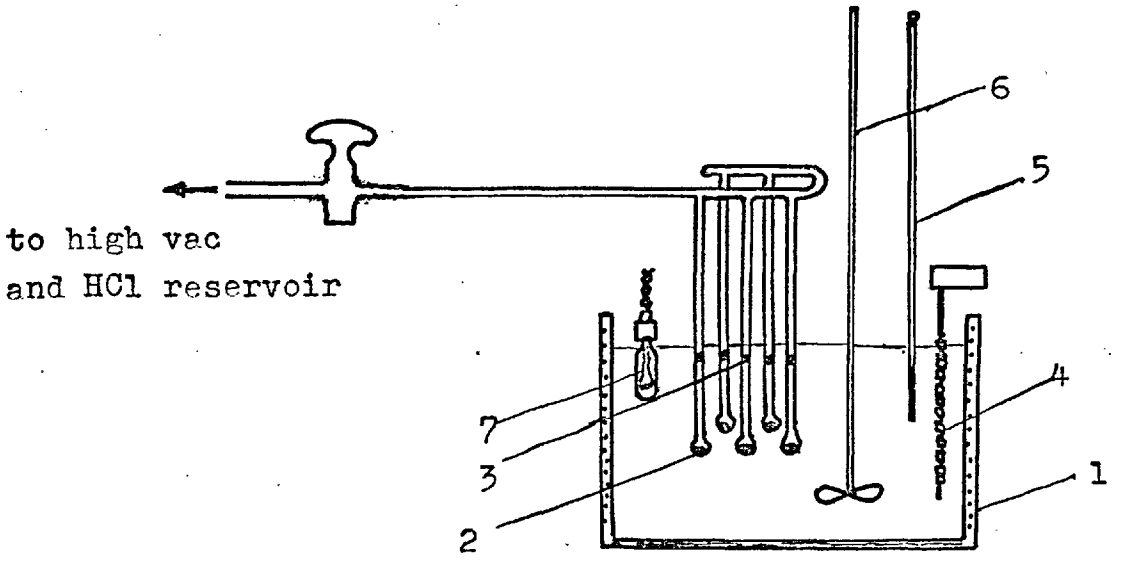
The heat was supplied by a round electric furnace of total resistance 80 Ohms at room temperature. It was made from a pyrex cylinder 5.8 cm in internal diameter and 70 cm long. The cylinder was covered with two layers of asbestos paper 0.1 cm thick and nichrome resistance wire of specific resistance 5.3 Ohms/m was wound on it, each coil being about 0.8 cm apart. It was then covered with eight layers of asbestos paper. Four windows cut on the asbestos paper allowed the two ends of the spring to be read. Power was supplied by a constant voltage regulator via a 2 kW variac which was manually controlled. The power input required for every temperature was found from the "furnace calibration" curve, i.e. temperature vs voltage. The furnace was constructed in such a way that maximum temperature (i.e. 350°C) was attained with maximum voltage (i.e. 260 volts) in order to minimize the effect of small voltage changes on the furnace temperature. Provided that the room temperature was constant, the furnace temperature could be held constant to 0.5-1.0°C depending on the temperature. The temperature was measured by means of a calibrated thermocouple.

3.6 Apparatus for hydrogen chloride-silicate stability experiments

The apparatus used for the study of the stability of silicates when exposed to anhydrous hydrogen chloride is shown in fig. 16. The zeolite was put in a small pyrex bulb. Five bulbs were sealed to a U-shaped pyrex tube closed at one end and connected to the vacuum line and HCl reservoir, through a mercury manometer, from the other. The samples were outgassed at 350°C under high vacuum for 30 hours. Hydrogen chloride was admitted, its pressure being measured by means of the mercury manometer, and left for 18 hours. The samples were outgassed at the experimental temperature for 24 hours. For temperatures up to 220°C a silicone oil bath was used. This was made from two pyrex beakers, the inner having a volume of 1 litre and the outer of 2 litres. The 1 litre beaker

Fig. 16

Apparatus used for HCl-Silicate stability experiments



1: Silicone oil bath

2: Zeolite.

3: glass wool.

4: Bimetallic spiral.

5: Thermometer.

6: Stirrer.

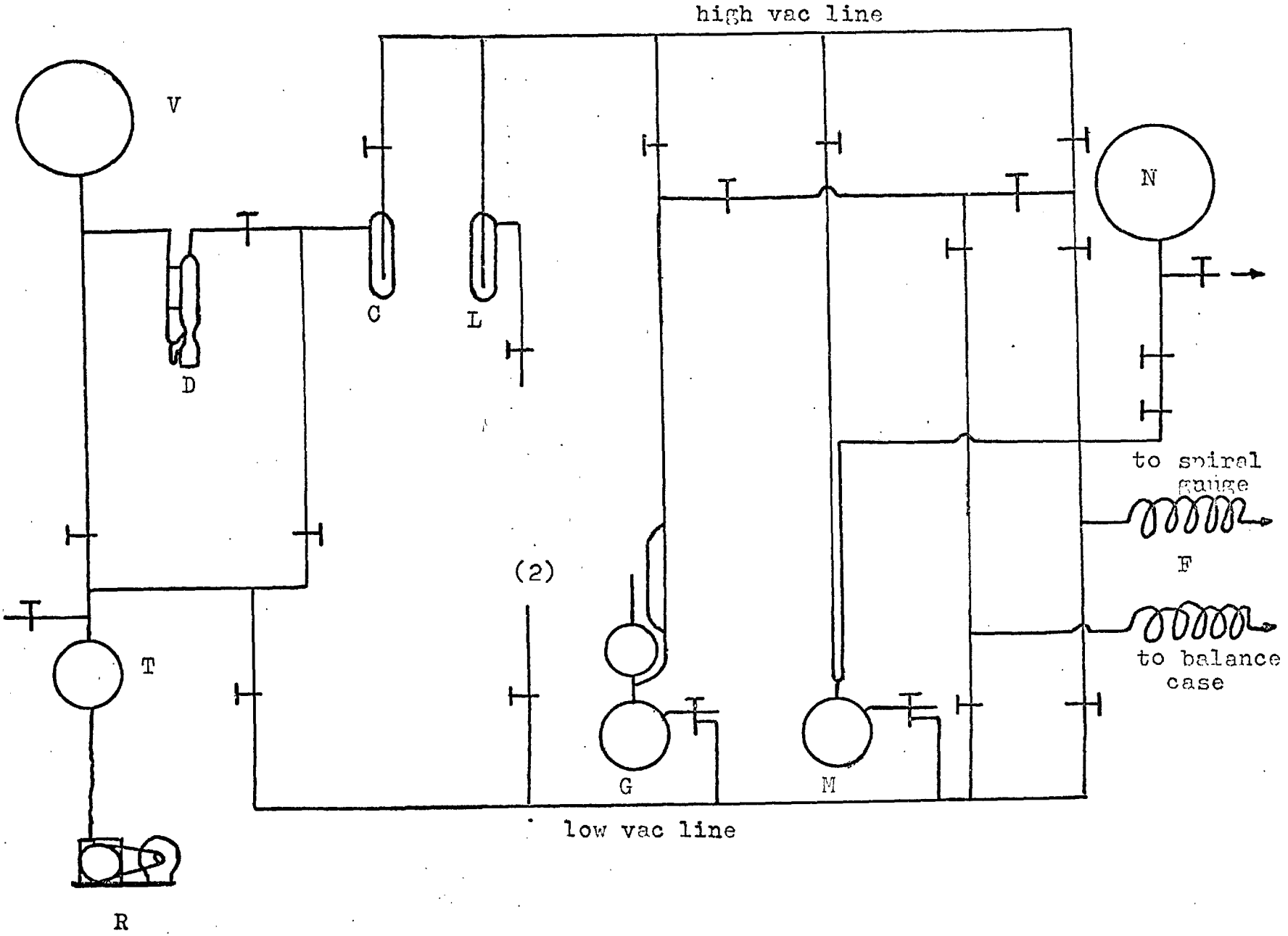
7: 15W lamp.

was covered with two layers of asbestos paper and resistance wire (24 Ohms/y) was wound round it. It was covered with asbestos paper again and put in the 2 litre beaker. Power was supplied from a constant voltage regulator through a variac. The temperature was controlled by means of a bimetallic spiral connected to a Sunvic relay and a 15 W lamp used as indicator and heater. For temperatures up to 150°C mercury thermometers accurate to 0.1°C were used for temperature measurement; for higher temperatures chromel-alumel thermocouples were used. For temperatures higher than 220°C a small round electric furnace was used. This was fed through a variac and was manually controlled. A quartz bulb was used for the experiments carried out at temperatures above 350°C.

3.7 The Vacuum System

The vacuum system is shown diagrammatically in fig. 17. Low vacuum was achieved by means of a rotary oil pump (R). The mercury diffusion pump (D) was used to produce high vacuum of about 10^{-6} mmHg. The oil trap (T) prevented oil from entering the diffusion pump in the event of power failure. The diffusion pump could be run for long periods without the backing of the oil pump because of the buffer volume (V), so pressure measuring devices could be operated without disturbing high vacuum. Condensable vapours were condensed in the cold trap (C). This trap also prevented mercury vapour from the diffusion pump from entering the system. A McLeod gauge (G) was used for low pressure measurements. The pressure of pure dry nitrogen gas supplied from the storage bulb was measured by means of the manometer (M). The two flexible glass spirals (F) connected the nitrogen line and the pumping system to the sorption system 1. These flexible connections allowed movement of the balance case due to expansion of its steel supporting tube when the furnace temperature was raised.

Fig. 17 The Vacuum System



Sorption system 2 was placed at (2) and connected to the high vacuum line through trap (L).

Apiezon grease N was used in the vacuum system and the rest of the apparatus. Silicone grease was used only where hydrogen chloride was used as it was found to attack Apiezon grease.

3.8 Calibration of the measuring devices

Thermocouples

All thermocouples used were chromel-alumel thermocouples. They were used for temperature measurements between 150-350°C and in a few cases at 800°C. They were calibrated for the temperature range 0°-450°C at fixed points[83], i.e. ice point, sulphur point and steam point; naphthalene point was also measured.

For ice point, the thermocouple was immersed in ice - prepared from distilled water - in a double walled glass tube which was also immersed in ordinary ice-water in a Dewar vessel ca 50 cm long[84].

For the steam, naphthalene and sulphur points, an apparatus consisting of two concentric pyrex tubes was used[85]. The thermocouple, in a pyrex protection tube, was placed in the inner tube which was open at the lower end and did not extend down the entire length of the outer tube. The material was put in the outer tube and heated with a Bunsen burner. The outer tube was also surrounded with a resistance wire, the voltage of which was adjusted so that the vapour of the material condensed just below a side arm near the outer tube. The atmospheric pressure at the moment of the measurement was measured by means of a barometer which was in the same building and a correction to the boiling point of the material was applied[86].

A correction chart was drawn, i.e. ΔEMF vs EMF_m where $\Delta EMF = EMF_{th} - EMF_m$; EMF_{th} = theoretical EMF; EMF_m = measured EMF. After the correction was applied to the measured EMF, the temperature could be read from calibration tables[87].

Silica springs

The silica springs were annealed several times before they were calibrated by heating them to 350°C and cooling them to room temperature slowly until their extension with a weight of 0.7 g remained constant. They were calibrated by measuring their extension to known weights at four different temperatures, covering the range 25-350°C.

Four different ring weights, weighing approximately 0.5, 0.6, 0.7 and 0.8 g and forming a chain were used, so that it was possible to reduce or increase the chain by one or more rings by raising or lowering a moveable platform. The temperature was always measured 1.5 cm below the end of the spring, corresponding to the centre of the sample during the sorption measurements. From the known weights and measured extensions the constants l_o and s of the equation:

$$l = l_o + \frac{w}{s} \qquad (38)$$

where l = spring length and w = weight, could be calculated and plotted against temperature. A decrease of l_o and increase of s with temperature was always found. From these plots the two constants l_o and s could be found for every temperature and by using equation (38) the weight could be calculated for every extension.

In sorption system 1 the calibrations were carried out in a glass tube resembling the balance case except that its lower part was open and there was no spiral gauge[82]. In sorption system 2 the balance case was used for the spring calibration. Appropriate

"cuts" allowed the spring to be placed in the case and the platform to be moved easily.

A correction called the "small furnace effect" was applied to the measured spring lengths in sorption system 1 when the small furnace was on. It was noticed that as the temperature of the small furnace increased, the length of the spring increased to a small extent. This effect was not important for high uptakes but it was considerable for low uptakes, e.g. in the low pressure part of the isotherms.

Additional calibration of the springs used in sorption system 1 involved measurements of their length at three or four different reservoir temperatures for a certain sample temperature. A table was made giving the increase in spring length at different sample and reservoir temperatures. From this table the correction for the "small furnace effect" was estimated. A more accurate treatment consisted in using these data in Lagrange's interpolation formula[88] to calculate this effect for every set of temperatures (sample and reservoir). The difference in the value of the correction found by this method and from the table was not considerable.

The silica spring and thermocouples were regularly checked during the period of three years and when any discrepancy from the calibration curves was noticed they were replaced.

Spiral gauge

The spiral gauge had a sensitivity of 1.0 mm Hg/cm. It was calibrated at the start of each isotherm by recording scale readings for different nitrogen pressures when the pressure inside the balance case was zero. The plot of the spot displacement against pressure was linear for pressures up to 3.0 cm Hg. The reciprocal of the slope was the sensitivity of the gauge. The zero pressure position of the spot and the sensitivity of the gauge were not

necessarily the same for every temperature. It should be stressed that any considerable pressure difference across the spiral was avoided and it was mainly used as a "null instrument".

Volume of the balance case in sorption system 1

The volume of the balance case in sorption system 1 was measured with the sample temperature at 230°C and different reservoir temperatures by allowing a known amount of Ar (B.O.C. grade X) to expand to a known volume. The volumes of certain parts of the apparatus necessary for the calibration were measured by filling these parts with water and measuring the volume of water in a graduated volumetric cylinder reading to 5 ml. A graph was drawn of the volume against reservoir temperature. This graph was used for calculation of the factor F (see Chapter 4 of Part II).

3.9 Analytical methods

Analysis of some zeolites was carried out to establish their composition. Other zeolites were analyzed for ammonia, sodium and potassium to estimate the amount of ion-exchange.

Standard gravimetric techniques were used for water, silica[89] and alumina[90] analysis.

For ammonia analysis the zeolite was digested in a platinum crucible with 1:9 sulphuric acid at steam bath temperature for a few hours. It was transferred to a distillation apparatus[91] and treated with 30% NaOH. The ammonia was collected in 2% solution of boric acid and titrated with N/20 HCl using a mixed indicator[7].

The amount of alkali metals in the zeolites was found by flame photometry. Their emission spectra were measured in a Unicam SP.90 atomic absorption spectrophotometer, Na at 589 mμ and K at 767 mμ[92]. The zeolite was first digested in 1:9 sulphuric acid and 40% HF and then 1:9 sulphuric acid. The remaining salts were dissolved

in concentrated hydrochloric acid and water and diluted to a known volume. A calibration of the instrument with a number (usually seven) of standard solutions was necessary every time it was used.

For aluminium the qualitative alizarin S test was used. To a small amount of the solution a few drops of 1N NaOH solution were added and a drop of 0.1% alizarin solution 1N acetic acid was added to discharge the violet colour and one drop in excess. A red precipitate or colour was formed if Al was present. A blank test was always carried out.

3.10 X-ray techniques

X-ray powder photography was used to observe any structural changes occurring during the sorption or ion-exchange experiments and also, in several zeolites, for quantitative study of the amount of decomposition.

The zeolite samples were mounted under Sellotape in a holder of a four unit Guinier camera using $Cu_{K\alpha}$ radiation. For the quantitative measurements, quartz and α-Al_2O_3 were used as internal standards[93]. Their absorbing coefficients are of the same order as those of zeolites and some of their strong reflection lines do not overlap the zeolite lines. The amount of the standard used was 20% per weight. The treated zeolite and standard were weighed with an analytical balance accurate to ± 0.1 mg and mixed in an agate mortar. An X-ray photograph of the mixture was taken. The intensities of a selected reflection of the zeolite (I_Z) and a selected reflection of the standard (I_S) were measured by means of a Joyce double-beam microdensitometer and the ratio $\frac{I_Z}{I_S}$ taken. The same procedure was repeated for the original zeolite. The amount of decomposition (%) was estimated from the formula:

$$100\left[1 - \frac{(I_Z/I_S)_t}{(I_Z/I_S)_o}\right]$$

where t and o stand for the treated and original zeolite respectively. Since many errors are involved in this procedure (e.g. in mixing of the zeolite with the standard, exposing and developing the film etc.), care was taken to ensure uniformity in each step. However, differences as high as 10% were observed in values obtained for the same sample. The procedure was repeated several times for each sample. The values of decomposition obtained are the average of at least three measurements and believed to be accurate to ± 5%.

3.11 Accuracy of the sorption measurements

Three variables are measured in gravimetric sorption studies: weight, pressure and temperature. In this study the weight was measured by means of silica springs, the pressure with the aid of mercury manometers or pyrex spiral gauges and the temperature with thermocouples.

The spring length was measured by a cathetometer, the scale of which could be read to 0.001 cm. Allowing this error for the height of each end of the spring, the error in its length was ± 0.002 cm, which corresponds to an average weight of ± 0.05 mg. The spring calibration was subject to the same uncertainty. The glass weights and the bucket were weighed by means of an analytical balance accurate to ± 0.1 mg. The weight of the outgassed zeolite was found by measuring the extension of the spring when the outgassing was completed. This gave the total weight of the zeolite and the bucket. By subtracting the weight of the bucket, the weight of the outgassed zeolite was found. So the sample weight was accurate to ± 0.14 mg, which for 0.4 g sample corresponds to ± 0.035%. The error was negligible for moderate or high uptakes but became significant for low uptakes. For isotherms in which the uptakes were very small, the inaccuracy was high as, for example, for the isotherm of ammonia on KL at 280°C, the maximum uptake measured was 8 mg/g and

thus the error was 3.5%. The inaccuracy in weight measurements was also high in the low pressure part of most isotherms because the uptakes were low.

In sorption system 1 another uncertainty was introduced by the "small furnace effect". Since this effect was measured by spring length changes, a further uncertainty of 0.002 cm to the measured extension was added. Since the uptakes of the isotherms taken in system 1 were moderate or high, this was significant for the low pressure part of the isotherms.

No correction of the measured uptakes was necessary for the buoyancy effect since it was within the limits of the experimental error.

In sorption system 2 the pressure was measured by a mercury manometer to ± 0.002 cm with the aid of a cathetometer. In sorption system 1 the nitrogen pressure was also measured with a mercury manometer to ± 0.002 cm with a cathetometer. The sensitivity of the spiral gauge was 1.0 cm on the scale for 1.0 mm Hg pressure change. The scale was read to ± 0.05 cm which corresponds to ± 0.05 mm Hg pressure. Calibration of the spiral gauge was subject to the same uncertainty giving a total uncertainty of ± 0.1 mm Hg. A fluctuation in the sorbate pressure was introduced at its highest pressures because of the thermostatic system. The temperature of each furnace could be held constant to within 0.2°C. For low temperatures this did not affect the sorbate pressure but at high temperatures this influence was significant, e.g. 0.2°C change in reservoir temperature produced a pressure change of 0.07 cm Hg in 10.4 cm Hg of "ammonium chloride" vapour .

The temperature was usually measured by thermocouples. The EMF was measured by means of a Cambridge portable potensiometer measuring to ± 0.005 mV corresponding to ± 0.125°C. Since the

calibration of the thermocouples was subject to the same error, the total error was $\pm$ 0.25°C.

The measurement of sample temperature by a thermocouple not placed in the sample cannot be very accurate. A hollow finger along the balance case allowed the thermocouple to be placed as near the sample as possible. It is believed that the differences between the isotherm temperatures and the actual sample temperatures in both systems were not higher than 0.5-2.0°C.

PART II

RESULTS AND DISCUSSION

1. HYDROGEN CHLORIDE-SILICATE STABILITY, SORPTION AND ION-EXCHANGE EXPERIMENTS

1.1 Study of hydrogen chloride-silicate stability

A number of silicates with different SiO_2:Al_2O_3 ratio, covering the range 2-12.8, were exposed to anhydrous hydrogen chloride gas at different temperatures as described on page 64. After treatment, the silicates were X-rayed and their X-ray photographs were compared to those of the untreated samples. The intensities of the reflection lines of the X-ray powder photographs in some silicates were weaker than the corresponding lines of the photographs of the untreated samples. This was attributed mainly to partial decomposition of these silicates. (Some alteration of the intensity of the reflection lines is expected because of the exchange of cations due to reaction (39)). Extra reflection lines were also observed in some cases. These extra lines were found to belong to sodium chloride by comparison to an X-ray powder photograph of pure sodium chloride. The results of this experiment are listed in Table 1 From these results a marked stability is shown by the silicates for which SiO_2:$Al_2O_3 > 5$. On the other hand, the silicates for which SiO_2:$Al_2O_3 < 5$ were found to be less stable. Since the SiO_2:Al_2O_3 ratio can vary considerably in certain silicates, the value 5 for this ratio is only an approximate borderline between the stable and the unstable silicates to hydrogen chloride. By "unstable" and "stable" silicates we mean the silicates that sorb hydrogen chloride with or without decomposing. Although the silica content seems to be the main factor affecting the stability of silicates when exposed to hydrogen chloride, it is not the only one. Other factors should include their crystal structure and their thermal stability when heated in the absence of hydrogen chloride. The stability of silicates having the same structure

Table 1

Stability of silicates exposed to anhydrous HCl at different temperatures. (p_{HCl} = 22.8 cm Hg).

Silicate	SiO_2:Al_2O_3	Al:Si	Temperature					
			200°C		310°C		610°C	
			stable	NaCl	stable	NaCl	stable	NaCl
Na-Ferrierite	12.8*	0.156	Yes	No	Yes	No	Yes	No
Na-Mordenite	9.5	0.211	Yes	Yes	Yes	Yes?	Yes	No
Na-Clinoptilolite	9.3	0.215	Yes	Yes	Yes	Yes	Yes	No
Linde L	6.01	0.332	Yes	No	Yes	No	Yes	No
Orthoclase/Albite	6.0	0.333	Yes	No	Yes	No	Yes	No
Na-Chabazite	5.0	0.400	No	Yes?				
NaY	4.78	0.418	Yes	No	Yes	No	Yes	No
NaX	2.65	0.753	No	Yes				
Na-Sodalite	2.00	1.000	No	Yes				
Na-Cancrinite	2.00	1.000	No	Yes				
NaA	2.00	1.000	No	Yes				

*This synthetic product was ~80% crystalline, and may contain some uncrystallized silica gel.

column "stable" : Yes = No change in the reflection lines was observed.

No = Reflection lines weaker than those of the original sample.

column "NaCl" : Yes = NaCl lines were observed.

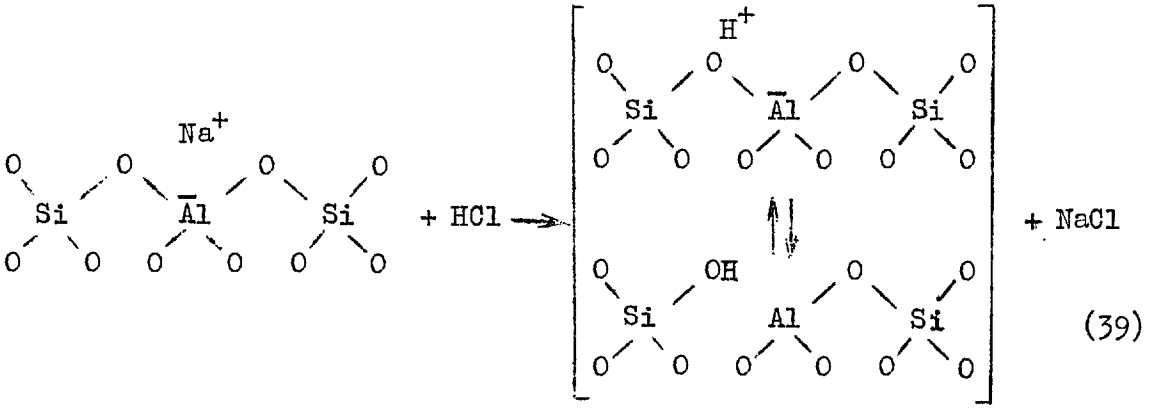
No = No NaCl lines were observed.

Yes? = Very weak lines were observed.

seems to depend mainly on their silica content. A typical example from Table 1 is NaX and NaY. These two synthetic zeolites have the same crystal structure and different silica contents (p. 19). NaY, which is rich in silica, is stable but NaX, the silica content of which is low, is not stable. Thus, the behaviour of silicates when treated with anhydrous hydrogen chloride gas appears to be similar to their behaviour when treated with acid solutions (94,46).

Possible reactions taking place during the sorption of anhydrous hydrogen chloride on zeolites include:

(a) An ion-exchange reaction of the cations by protons. This reaction could be represented schematically:



(39)

and (b) A reaction of hydrogen chloride with the aluminium atoms of the framework similar to that taking place in hydrogen zeolites (see p. 86).

In basic sodalite and cancrinite a reaction of hydrogen chloride with the sodium hydroxide of the interstices can also take place(47), i.e.

$$HCl + NaOH \longrightarrow NaCl + H_2O \quad . \qquad (40)$$

Reaction (39) occurs in all the silicates examined except orthoclase-albite in which there is no intracrystalline penetration of hydrogen chloride. Evidence for this reaction was obtained by the following

observations:

(i) Sodium chloride reflection lines were observed in some of the X-ray photographs.

(ii) The isotherms of hydrogen chloride on certain stable zeolites (see p.88) were irreversible. A residual uptake was found which could not be removed by prolonged evacuation. The treated samples were washed with distilled water and filtered. The amounts of Na^+ and Cl^- measured in the filtrate were found to be in good agreement with the residual uptake. In the case of orthoclase-albite no chlorides or cations were found in the filtrate.

Reaction (b) can be thought of as an analogous reaction to that taking place in zeolites when they are treated with aqueous solutions of acids[73]. No direct evidence for this reaction was obtained in this series of experiments. However, when H-Zeolon and HY were treated with anhydrous hydrogen chloride and washed with distilled water, aluminium was found in the filtrate (Alizarin S test). When the same experiment was carried out in Na-zeolites no aluminium was found in the filtrate. This means that reaction (b) either does not take place in ion-exchanged zeolites or it takes place to a very limited extent only.

Sodium chloride reflection lines were not observed in some of the X-ray photographs taken after treatment of Na-zeolites with HCl. Two possible reasons for this were considered:

(a) Not enough sodium chloride was formed (i.e. less than the detectable amount).

(b) The sodium chloride formed remained molecularly dispersed in the crystal cavities.

More detailed study of the decomposition showed that the amount of decomposition depends upon the ratio $SiO_2:Al_2O_3$. Silicates covering the $SiO_2:Al_2O_3$ range 2-5 were first treated with anhydrous hydrogen chloride, then mixed with 20% α-Al_2O_3 as internal standard and X-rayed. The amount of decomposition was calculated as described on p. 72. Since, by using this method, the assumption is made that any change in the reflection lines is due to decomposition of the zeolite only, an additional uncertainty is added. The results are plotted in fig. 18. The amount of decomposition usually increased with increasing temperature and decreasing $SiO_2:Al_2O_3$, except for NaA for which the amount of decomposition was almost constant at ca 70% for the temperature range 50-210°C. The increase of decomposition with increase of aluminium content is believed to be due to the ion-exchange reaction (39) when the hydrogen form of the zeolite is formed. A dehydration reaction may then take place which possibly involves formation of $-\overset{|}{\underset{|}{Si}}-O-\overset{|}{\underset{|}{Si}}-$ bonds and is accompanied by partial collapse of the structure. Increase of temperature facilitates this dehydration although the decomposition of NaA seems to be independent of temperature. No satisfactory explanation was found for this exceptional behaviour.

From the graphs of fig. 18 it can be seen that other factors influence the stability of silicates besides their $SiO_2:Al_2O_3$ ratio. For example, NaA, Na-cancrinite and Na-sodalite have the same $SiO_2:Al_2O_3$ ratio but their decomposition curves are different. In fig. 19 the amount of decomposition of the silicates at 209°C is plotted against their Al:Si ratio. (The ratio Al:Si is more convenient for a plot of this form than the $SiO_2:Al_2O_3$). A hypothetical curve is drawn to show the effect of silica content upon their stability. Since other factors besides the Al:Si ratio affect the stability, the shape of this curve will change with the particular silicates examined. The curve does, however, show qualitatively the dependence of the stability of some porous silicates on their Al:Si ratio.

Fig. 18

Decomposition of Silicates by anhydrous HCl

(p_{HCl} = 22.8 cm Hg)

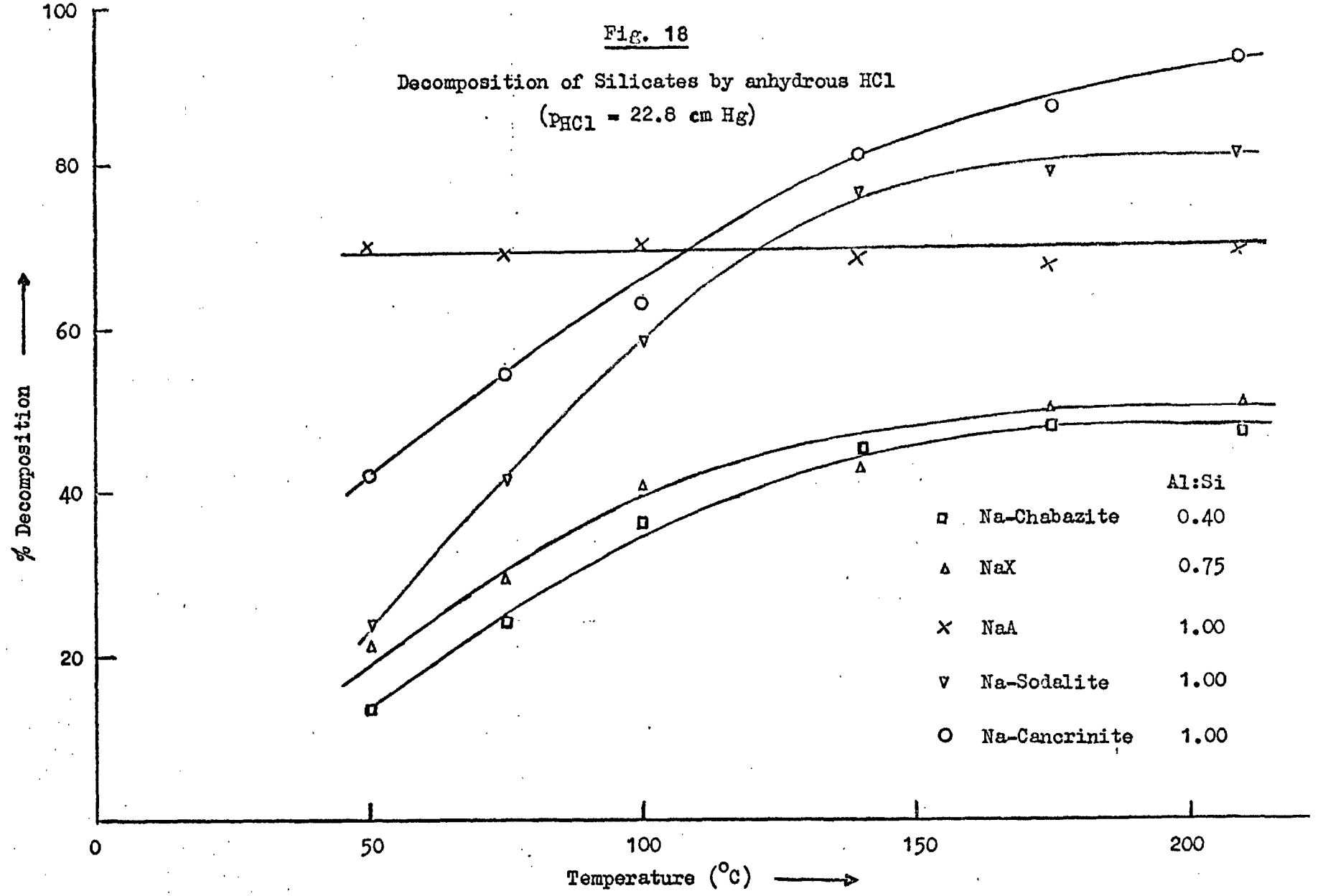
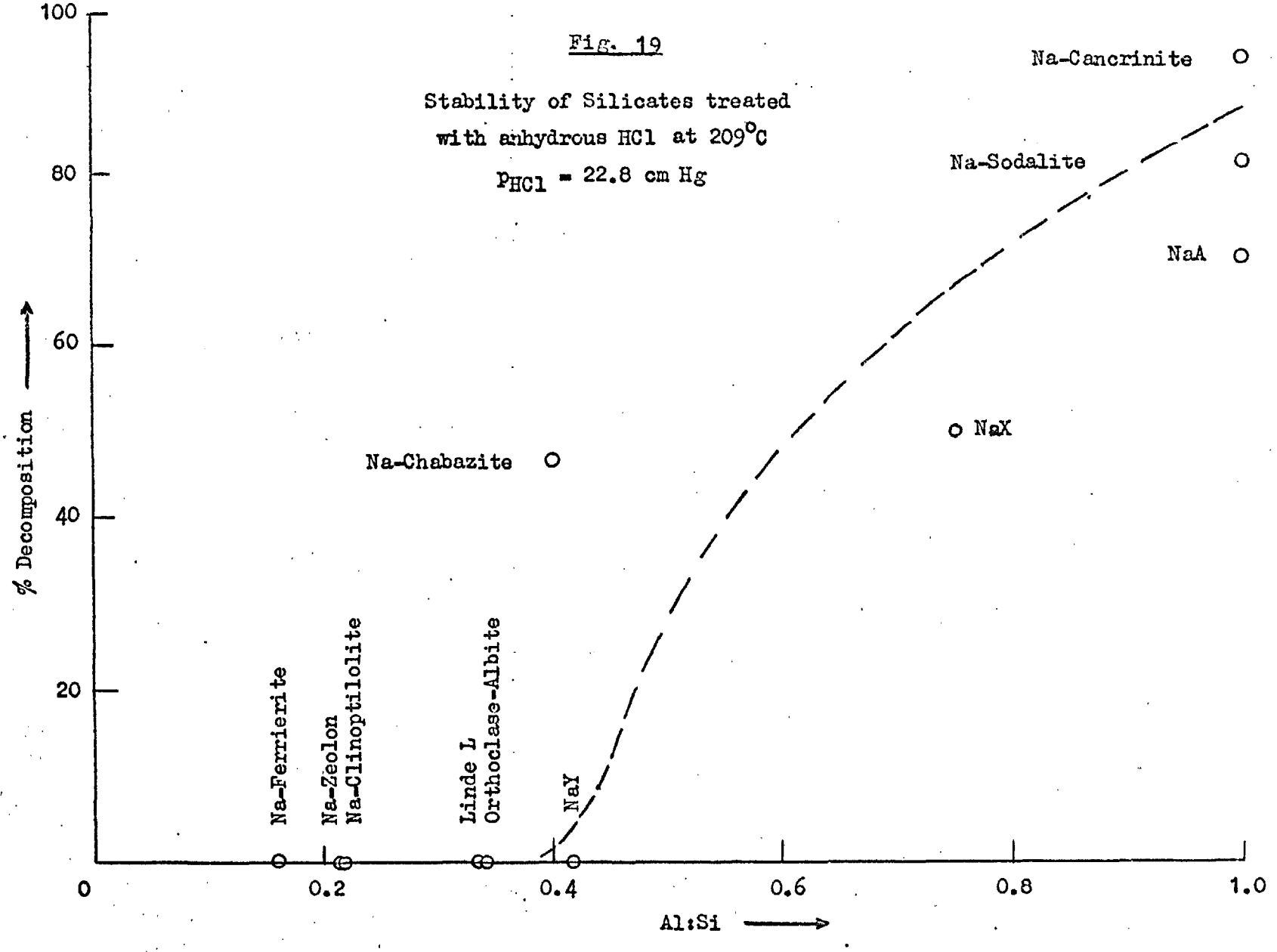


Fig. 19

Stability of Silicates treated with anhydrous HCl at 209°C

P_{HCl} = 22.8 cm Hg



The results of Table 1 and the diagram fig.19 set a limit on the number of zeolites that can be used in the study of the system ammonium chloride-zeolite. Only zeolites for which $SiO_2:Al_2O_3 > 5$ can be used because these zeolites can sorb hydrogen chloride without decomposing.

1.2 Hydrogen chloride - zeolite sorption and ion-exchange experiments

Sorption isotherms of hydrogen chloride were measured on the following zeolites: Na-clinoptilolite, Na-Zeolon, H-Zeolon, HY, NaY and KL. The isotherms were taken between 200°C and 350°C and all were found to be irreversible. Since the behaviour of hydrogen chloride sorbed on hydrogen and ion-exchanged zeolites was different, the experimental results obtained for these two classes of zeolites will be given and discussed separately.

Hydrogen chloride - hydrogen zeolite complexes

Two hydrogen zeolites were used, H-Zeolon and HY. Two sorption isotherms of hydrogen chloride were taken in H-Zeolon at 230°C and 294°C and one in HY at 245.5°C. The sample of HY used was prepared by method 1 (p.103) and it was found to be ca 80% crystalline. Equilibrium in sorption and desorption was established in ca 2 hours. However, two to three hours was allowed between readings. The measured isotherms are shown in figs. 20 and 21. The irreversible isotherms showed a residual uptake of sorbate which could not be removed by evacuation at the isotherm temperature. This uptake was 12.50 mg/g for HY at 245.5°C and 9.6 mg/g for H-Zeolon at 230°C. Evacuation at higher temperatures up to 350°C for prolonged periods resulted in a decrease of this uptake to ca 4 mg/g but it could not be removed completely.

Two reactions were considered to explain the observed hysteresis. First, a reaction is possible between the sorbed hydrogen chloride

Fig. 20

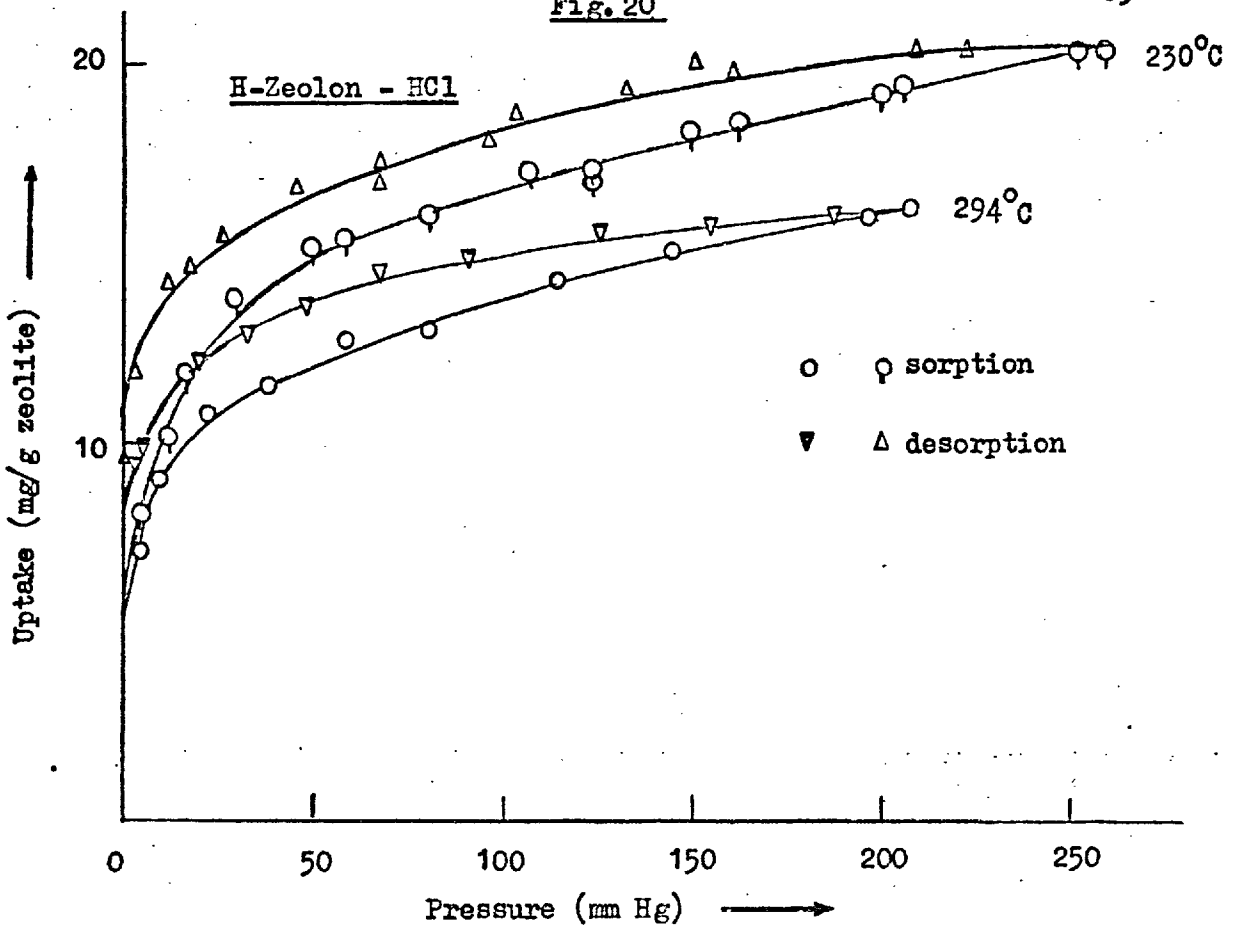
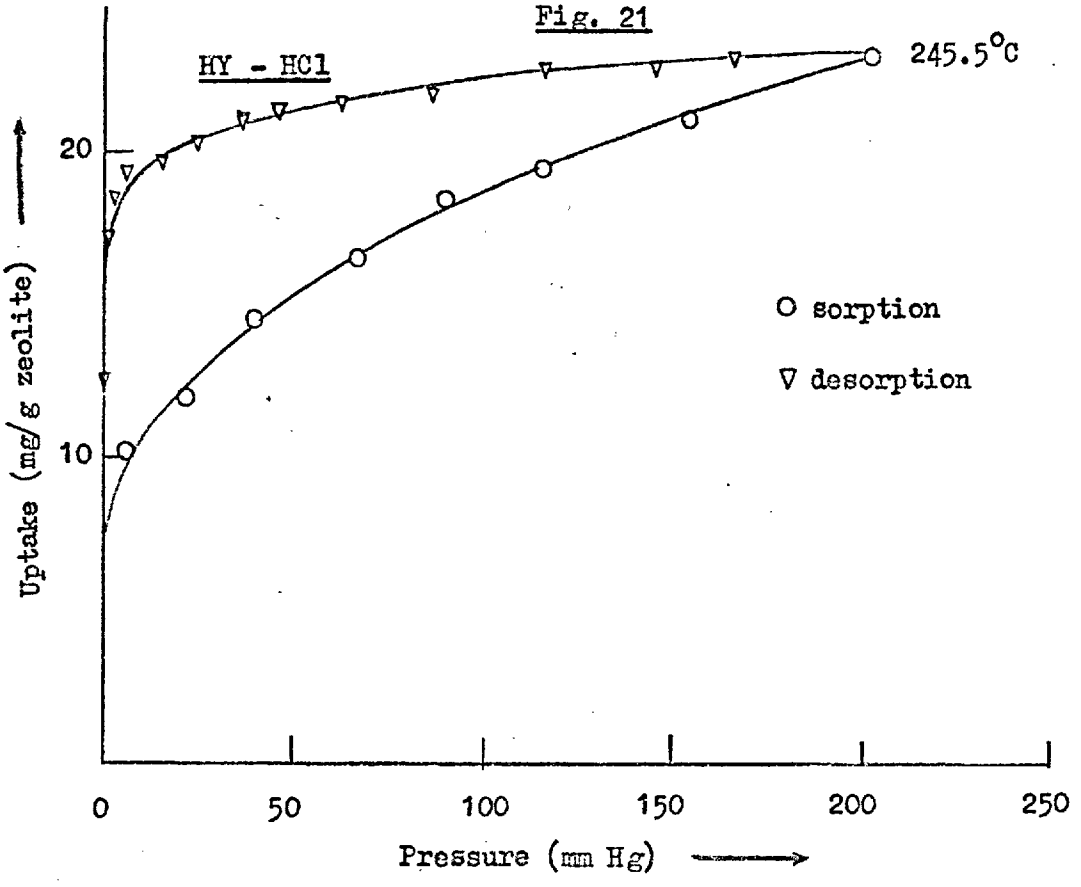
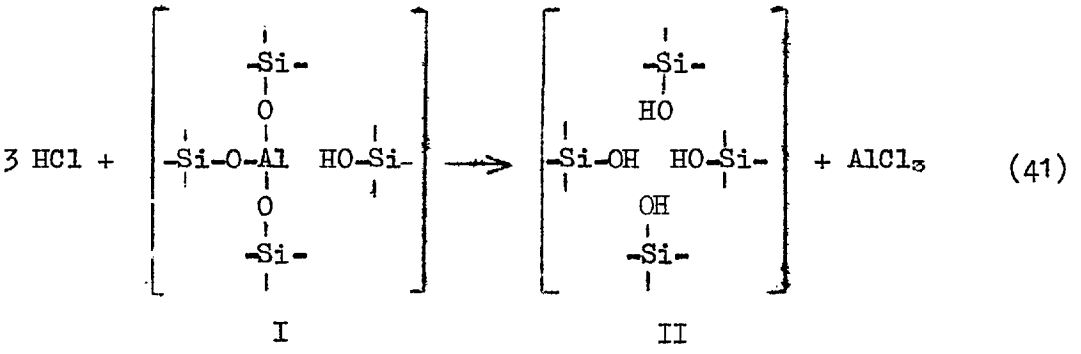

H-Zeolon - HCl
230°C
294°C
o ♀ sorption
▼ △ desorption
Uptake (mg/g zeolite)
20
10
0
50
100
150
200
250
Pressure (mm Hg)

Fig. 21

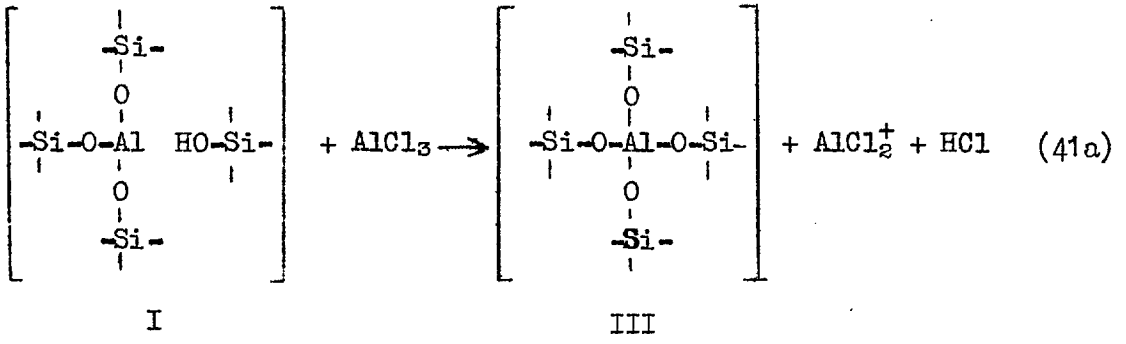

HY - HCl
245.5°C
O sorption
∇ desorption
Uptake (mg/g zeolite)
20
10
0
50
100
150
200
250
Pressure (mm Hg)

and the aluminium of the zeolitic framework according to the following scheme:



I II (41)

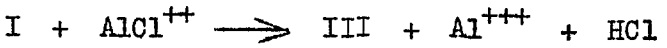
Further reaction of $AlCl_3$ with the zeolite, similar to that proposed by Kerr[95] to explain the intracrystalline rearrangement of constitutive water in hydrogen zeolite Y at temperatures around 800°C, is possible. This reaction should involve the following steps:



I III (41a)



(41b)



(41c)

The overall reaction could be represented by the following scheme:



(42)

Reaction (42) shows that in the presence of hydrogen chloride an intracrystalline rearrangement of aluminium takes place. According to this scheme, the hydrogen chloride can be removed from the zeolite and the original weight should be obtained. Since a residual uptake was found, either reactions (41a-c) did not take place or this chain of reactions was interrupted at some stage before completion.

The reactions (41a-c) imply that hydrogen chloride gas may be used for the preparation of stabilized decationated zeolites. However, if such a preparation is possible and considering the differences in structure and reactivity between water and hydrogen chloride, it would be expected that the experimental conditions for removing framework Al with hydrogen chloride would be different to those for water. Evidence for reaction (41) was obtained by washing the zeolites, after the sorption experiments, with distilled water. Aluminium was found in the filtrate, but no structural change of the zeolites was observed by X-ray photography.

The second reaction considered was an exchange reaction of the sorbed hydrogen chloride with the sodium ions of the zeolites (reaction (39) p.79). Chemical analysis of H-Zeolon and HY showed that they contained sodium ions equivalent respectively to 9% and 2% of their original total cation capacity. Therefore it is likely that an exchange reaction identical with that taking place in Na-zeolites occurs. These two reactions can account for the residual uptake. Exchange of the total residual amount of sodium corresponds to uptakes of 8.4 mg/g in H-Zeolon and 3.7 mg/g in HY. Since aluminium and sodium were detected in the filtrate, after washing the zeolites with distilled water, both reactions must take place. However, quantitative estimation of the amount of sodium in the filtrate showed that the exchange reaction was of minor importance as compared with reaction (41). Stoicheiometric calculation based on the residual uptakes and the amount of sodium in the filtrate

showed that reaction (41) took place to a degree of 2.0% in HY and 2.5% in H-Zeolon. This explains why no structural change of the zeolite was observed since a dealumination of 2-3% (of total aluminium) would not account for any structural change in silica rich zeolites like Y and Zeolon. The residual uptake also suggests that the aluminium chloride formed because of reaction (41) is not desorbed. Reaction (41) with subsequent removal of the aluminium chloride produced should result in a decrease of the original weight. Barrer and Wasilewski (96) found that aluminium chloride sorbed on certain zeolites could not be desorbed easily. Our attempts to remove aluminium chloride formed by reaction (41) by heating H-Zeolon with anhydrous hydrogen chloride at 700°C were not successful. No aluminium chloride was collected in a trap joined to the sorption bulb and cooled with liquid nitrogen.

It is then concluded that these two reactions of hydrogen chloride in the zeolite are responsible for the observed hysteresis and the residual uptake. The residual uptake shows that a considerable part of the sorbed hydrogen chloride has reacted with the zeolite.

Comparison of the isotherms of hydrogen chloride in H-Zeolon and HY with those of ammonia in the same sorbents shows that twice as much ammonia is sorbed as hydrogen chloride. This special affinity of hydrogen zeolites for ammonia is discussed in Chapter 3 of Part II.

Ion-exchanged zeolite - hydrogen chloride sorption complexes

Sorption isotherms were taken of hydrogen chloride on NaY, KL, Na-Zeolon and Na-clinoptilolite. All isotherms were irreversible. A considerable residual uptake, which could not be removed by prolonged evacuation, was found after every run. This was due to formation of sodium chloride (or potassium chloride in the case of KL), as explained in Section 1 of this chapter, because of an exchange reaction of hydrogen chloride with the cations of the zeolite. Therefore, when

hydrogen chloride is sorbed on an ion-exchanged zeolite, part of it reacts with the zeolite (i.e. it is chemisorbed) and the rest is physically adsorbed. This can be represented by the following scheme:

$$xHCl_{(g)} + MZ \rightleftarrows MZ.xHCl_{(a)} \rightleftharpoons (M_{1-y}H_y)Z.(x-y)HCl_{(a)} + yMCl_{(i,o)} \quad (43)$$

where Z denotes zeolite, M monovalent cation, a adsorbed and i or o inside or outside the crystal respectively and $y \ll 1$.

The salt MCl, produced because of reaction (43), can either remain molecularly dispersed in the crystal cavities or migrate out of the crystals and form, in the case of a sodium-zeolite, rock-salt. It is also possible that part of MCl remains in the crystals and the rest migrates out of the crystals. All three possibilities are examined in discussing the experimental results in this section.

If the salt MCl is formed outside the crystals, one would expect that complete exchange of the cations by protons should occur. However, in all cases studied, the amount of exchange was much less than 100% (Table 2). Evacuation of the system should result in removing the hydrogen chloride which is physically sorbed, i.e.

$$(M_{1-y}H_y)Z.(x-y)HCl_{(a)} \xrightarrow[\text{evacuation}]{-(x-y)HCl} (M_{1-y}H_y)Z \quad (44)$$

The value of y can be obtained from the residual uptake.

If MCl or part of it remains in the crystal cavities an equilibrium should be established:

$$MZ + HCl_{(a)} \rightleftharpoons (M,H)Z + MCl_{(i)} \quad (45)$$

Therefore, removal of the physically sorbed hydrogen chloride will shift the equilibrium to the left. Provided that all the MCl remains in the crystals and the zeolite has been outgassed for sufficient time, the original weight of the zeolite should be obtained. In all cases

examined, the original uptake could not be obtained by evacuation at the experimental temperature for ca three days (fig. 22). A constant residual uptake was obtained after 24 hours. This can be explained in terms of (a) or (b) below:

(a) Part of MCl remains in the crystals and is completely removed (because of the removal of hydrogen chloride, reaction (45)), by evacuation. Thus the residual uptake represents the amount of salt formed outside the crystals.

(b) The salt MCl or part of it remains in the crystals, but because the removal of hydrogen chloride is very slow and cannot be followed by the experimental method used (i.e. change in spring length, p. 62), the constant uptake represents the sum of MCl formed outside the crystals - if any - and that remaining in the crystals. Thus, it is not an equilibrium uptake in a thermodynamic sense.

By increasing the temperature and outgassing the zeolite at a higher temperature for ca two days a further decrease of the residual uptake was observed and a new "constant" residual uptake was obtained. Therefore (b) is more likely to occur than (a).

Assuming that

(i) the removal of hydrogen chloride generated from reaction (45) is extremely slow, and

(ii) the amount of hydrogen chloride removed in the first 24 hours of outgassing is approximately equal to the amount of physically sorbed hydrogen chloride when the zeolite is in equilibrium with hydrogen chloride at an initial pressure p,

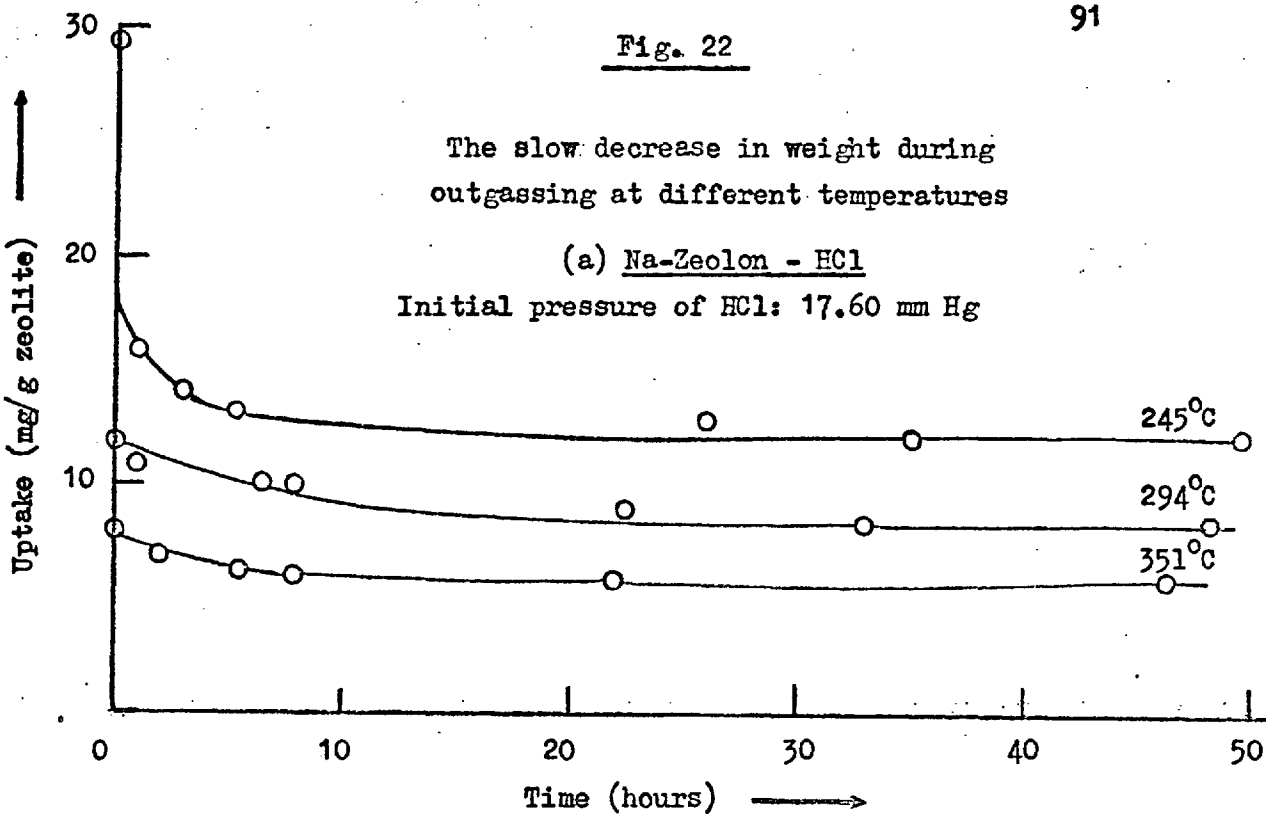
it is possible to analyze the sorption part of the isotherms and obtain values of y for different initial hydrogen chloride pressures.

Fig. 22

The slow decrease in weight during outgassing at different temperatures

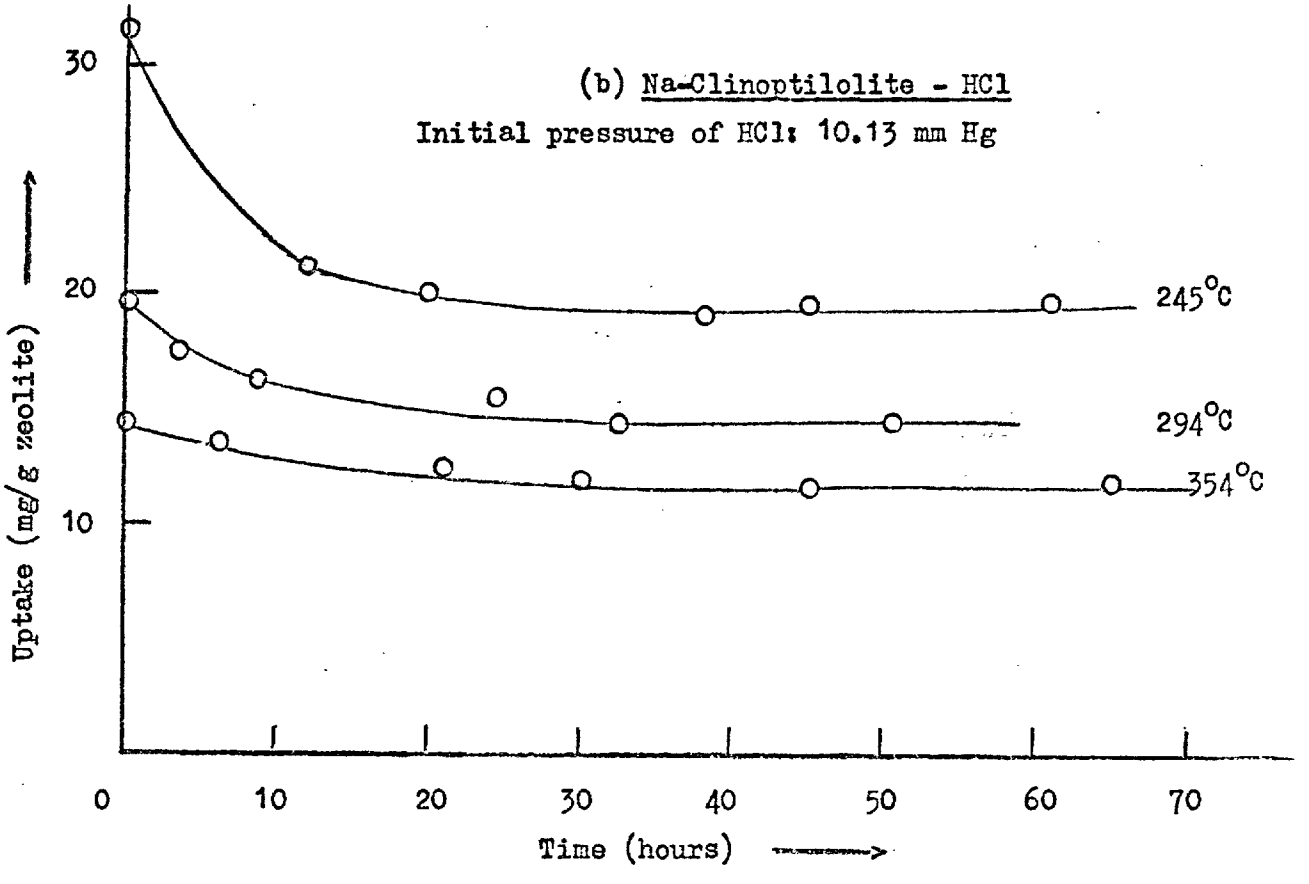
(a) Na-Zeolon - HCl

Initial pressure of HCl: 17.60 mm Hg



(b) Na-Clinoptilolite - HCl

Initial pressure of HCl: 10.13 mm Hg



The experimental method used for this analysis was the following.

A certain amount of hydrogen chloride was allowed into the sorption balance case. After the end-point was reached, pressure and uptake were recorded. The points thus measured gave the values of x (reaction (43)) at this pressure and were used to plot the "total" isotherms. The system was then outgassed at the experimental temperature to "constant" weight for at least 24 hours. The irreversible weight increase gave y for the initial pressure of hydrogen chloride and will be called "exchange" uptake. The difference of the "exchange" uptake from the "total" gave the "reversible" uptake (which is taken to represent the amount of hydrogen chloride physically sorbed). The plots of the "exchange" and "reversible" uptakes vs the initial hydrogen chloride pressure gave the "exchange" and "reversible" isotherms. Because of the assumptions made for calculation of the "exchange" uptake, the plots of "exchange" and "reversible" uptake vs pressure are not real isotherms in the sense this term has been used throughout this thesis (see p. 33). Although the word isotherm will be used in this section to describe these curves, there is no connection with the thermodynamic implications of the term.

Sorption of hydrogen chloride was rapid provided small amounts of hydrogen chloride were admitted to the system, especially at low pressures. In the case of NaY, when the first dose of hydrogen chloride allowed in the system was large (corresponding to a pressure of 26.00 mmHg), the uptake increased to a certain value in the first hour, and then it decreased with time as the pressure increased from 26.00 mm Hg to 31.00 mmHg. Equilibrium was attained in five days. This is explained in terms of reaction (43). If a large quantity of hydrogen chloride is admitted to the system, since the exchange isotherm for NaY (fig. 31) is rectangular, most of the sodium cations are exchanged, i.e. at hydrogen chloride pressure 26.00 mm Hg, 75% of

Fig. 23

The rate of establishment of equilibrium in the sorption of HCl in NaY at 245.5°C

(Initial pressure of HCl 26.00 mm Hg)

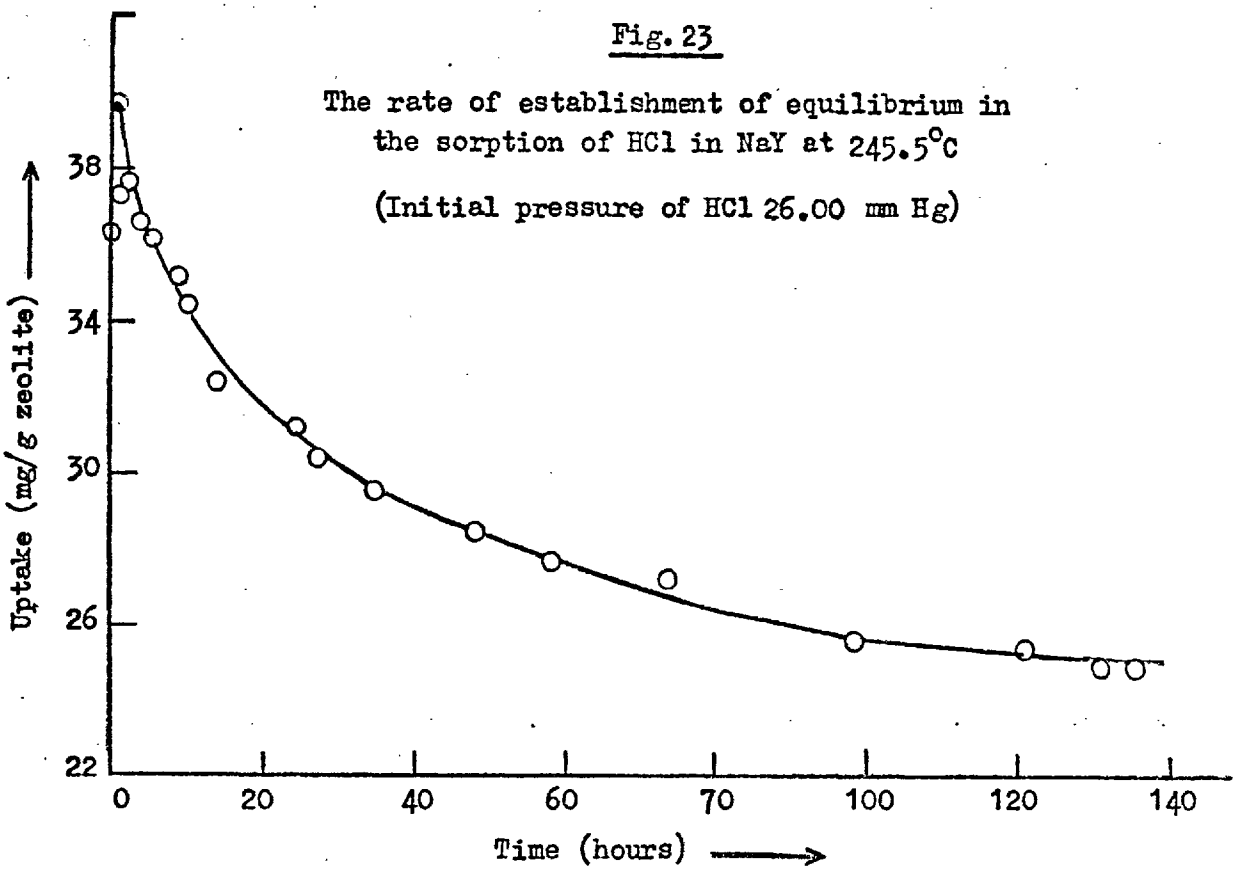
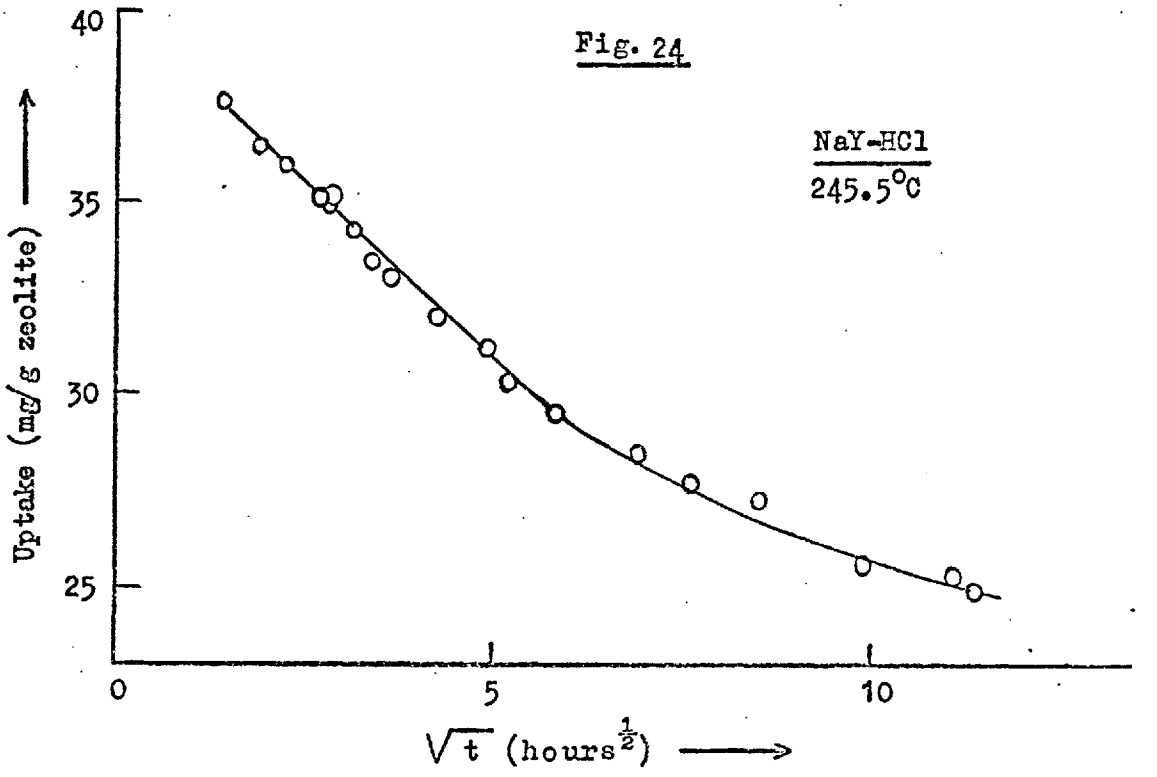


Fig. 24

NaY-HCl

245.5°C



the attainable exchange takes place. This results in a modification of the internal surface of the sorbent. Since hydrogen chloride is a polar molecule, exchange of sodium ions by protons in the zeolite results in a decrease of dipole-field interaction and consequently a decrease in sorption. If small amounts of hydrogen chloride are admitted to the system, the amount of exchange and therefore the decrease in sorption due to the decrease in dipole-field interaction is much less. The rate of establishment of equilibrium during the sorption of hydrogen chloride on NaY for an initial pressure of 26.00 mm Hg at 245.5°C is shown in fig. 23. The plot of the uptake against the square root of time (fig. 24) shows that at its early stage the change of uptake is governed by some process of diffusion.

In figs. 25-28 typical sets of "total", "exchange" and "reversible" isotherms are shown for all the systems examined. Inspection of these graphs shows that the zeolites studied exhibit different sorptive behaviour to hydrogen chloride. In Na-clinoptilolite and NaY most of the sorbed hydrogen chloride reacts with the zeolite. The amount of "exchange" uptake is at least twice higher than the "reversible" for the pressure range examined. On the other hand, the "reversible" uptakes in Na-zeolon and KL are slightly higher than the "exchange" uptakes. This results in a different shape of the "reversible" isotherm at low pressures for every system. In Na-clinoptilolite and NaY the "reversible" isotherms show a maximum at ca 7-9 mm Hg pressure and a minimum at ca 30 mm Hg pressure. At 30 mm Hg pressure most of the attainable exchange has taken place. For higher pressures the "reversible" uptake increases with increasing hydrogen chloride pressure. The occurrence of this minimum in the "reversible" isotherms of Na-clinoptilolite and NaY can be explained by considering the reaction (43) that takes place during the sorption of hydrogen chloride. Two factors are affecting the "reversible" uptake: pressure of hydrogen chloride and amount of exchange. These

Fig. 25

Na-Zeolon - HCl
245°C

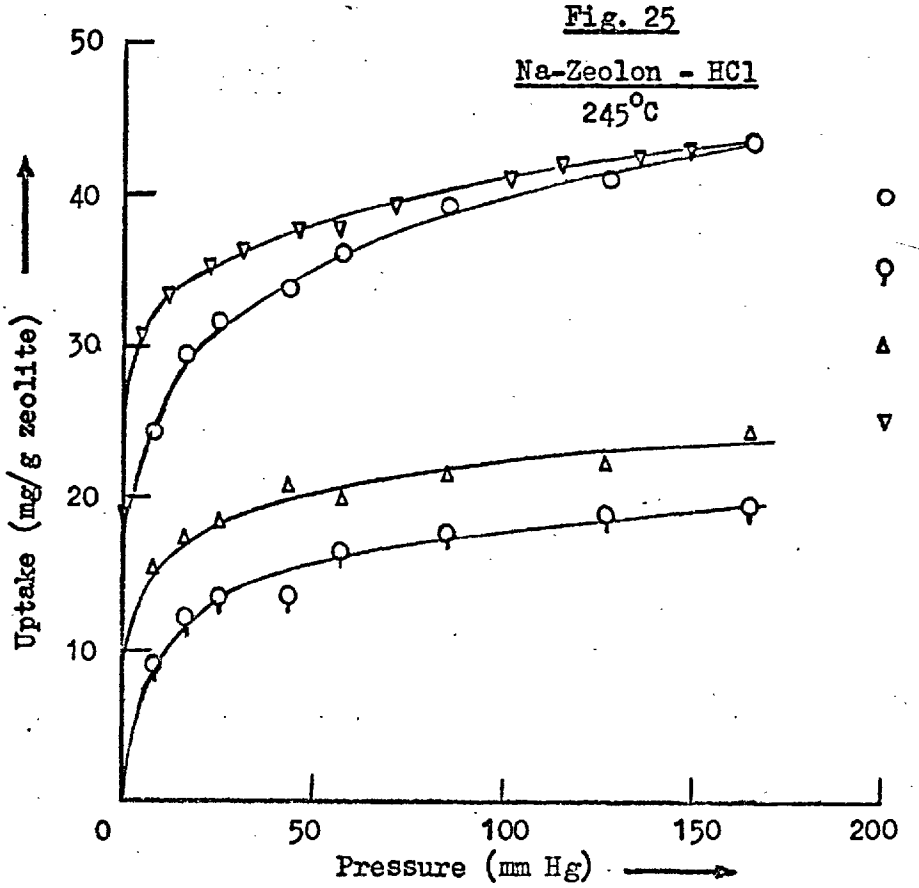


Fig. 26

Na-Clinoptilolite - HCl
245°C

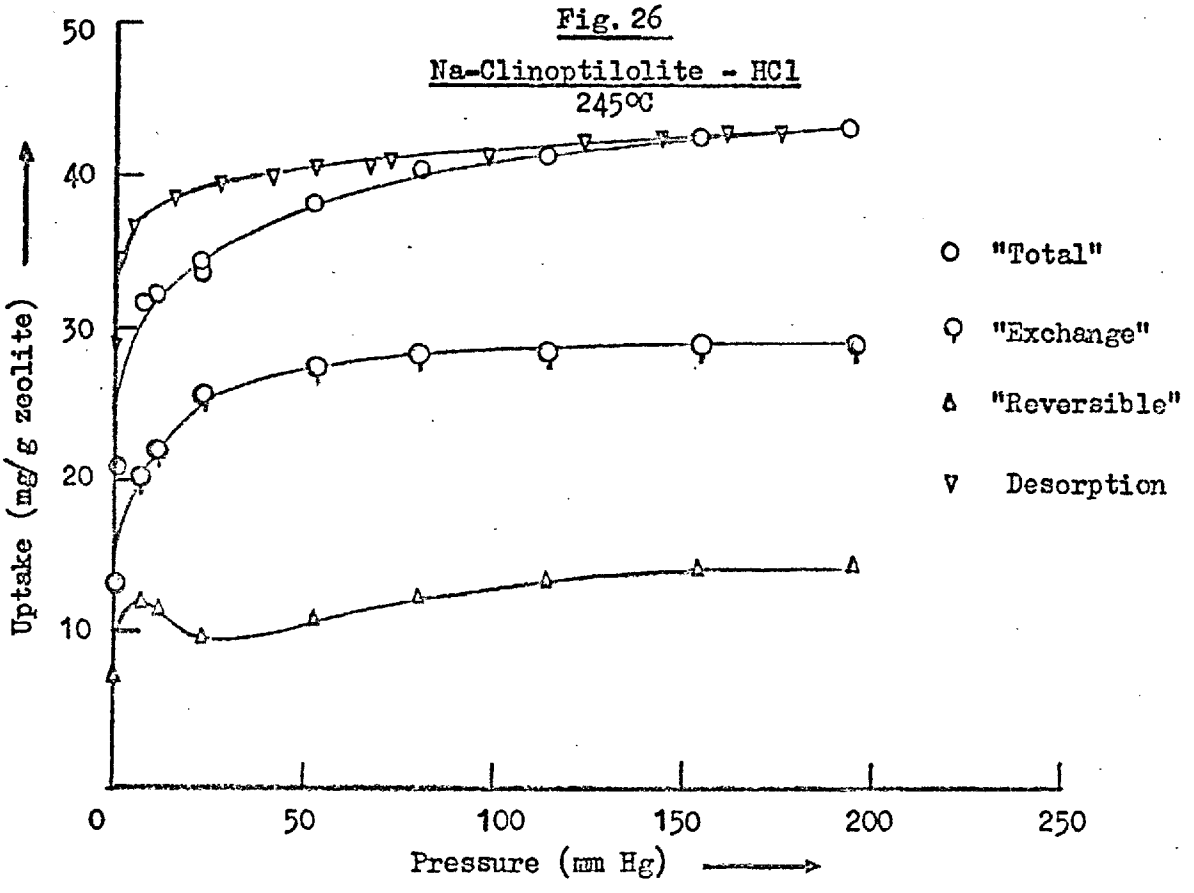


Fig. 27

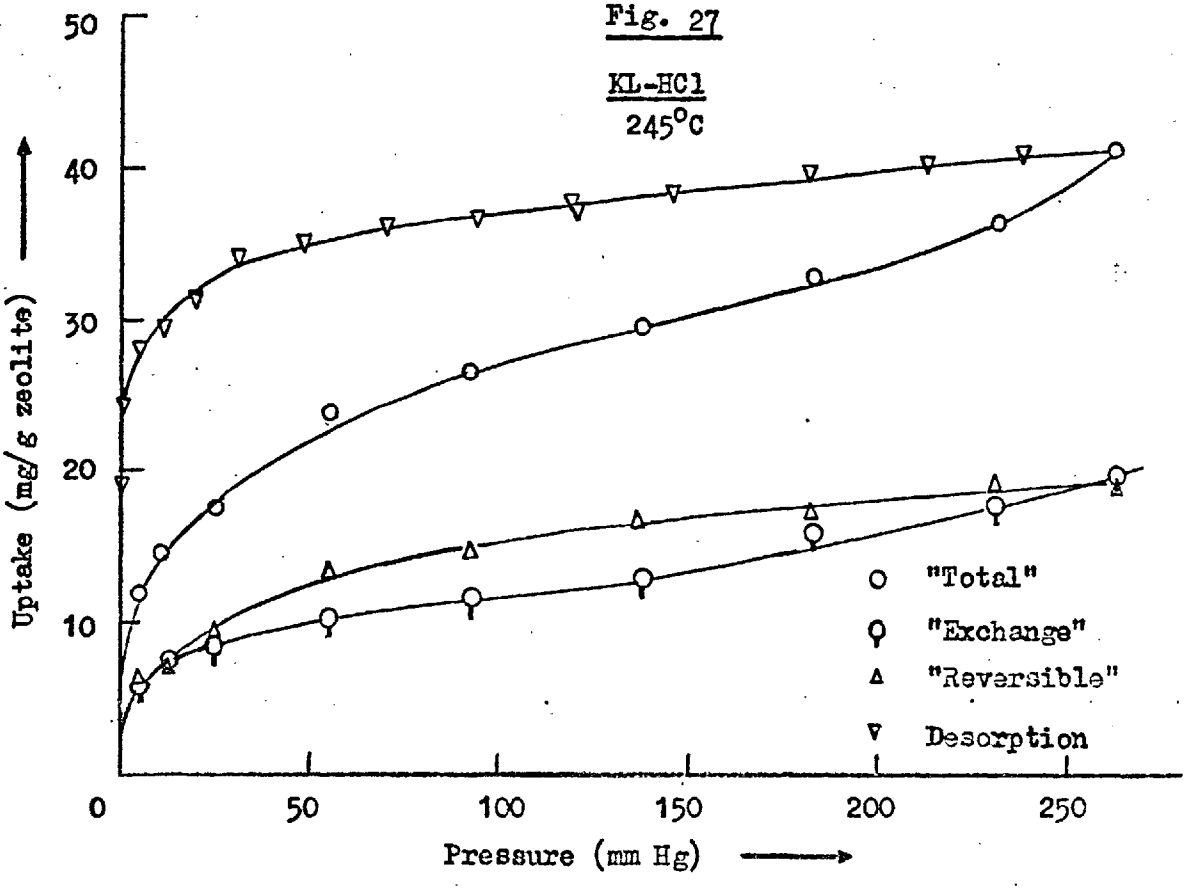
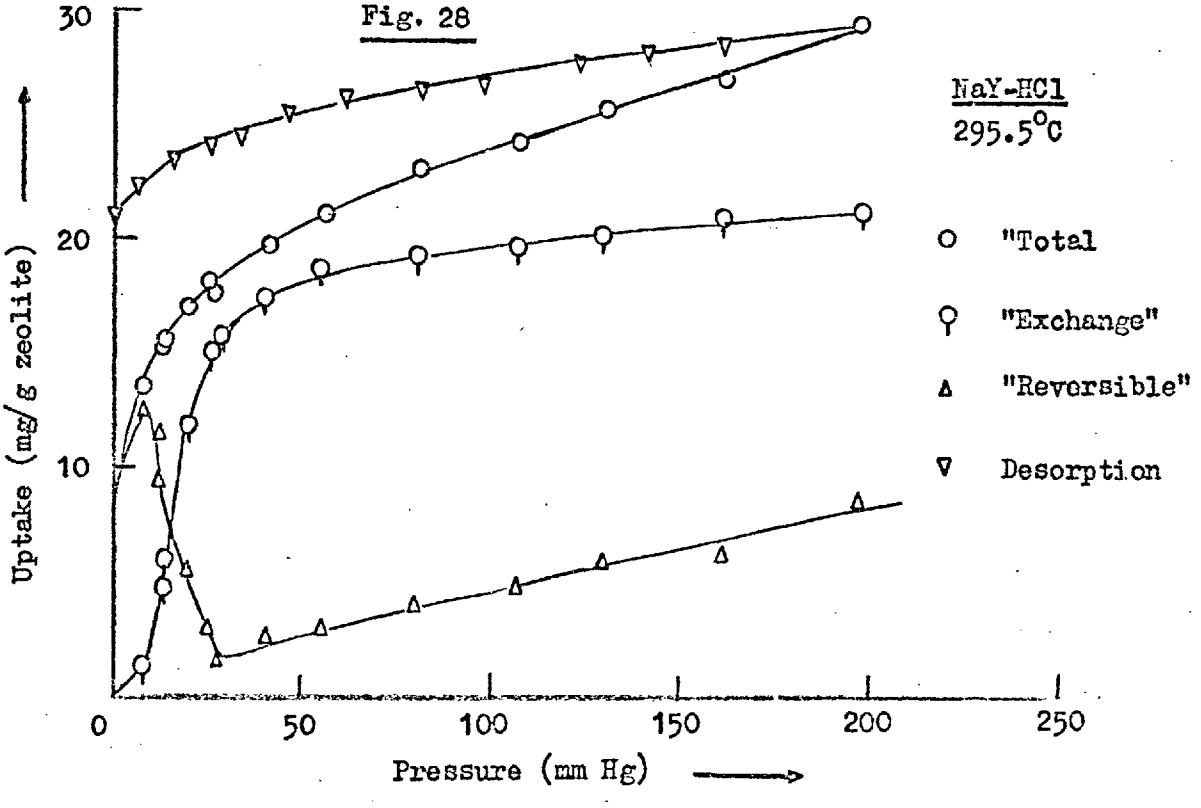

KL-HCl
245°C
Uptake (mg/g zeolite)
Pressure (mm Hg)
"Total"
"Exchange"
"Reversible"
Desorption
0
50
100
150
200
250
10
20
30
40
50

Fig. 28


NaY-HCl
295.5°C
Uptake (mg/g zeolite)
Pressure (mm Hg)
"Total
"Exchange"
"Reversible"
Desorption
0
50
100
150
200
250
10
20
30

two factors have opposite effects. Increase of hydrogen chloride pressure results in increase of sorption. But increase of sorption results in increase of ion-exchange and therefore modification of the sorptive properties of the zeolite which, as has already been mentioned, results in decrease of sorption. Thus the net effeot of the increase of hydrogen chloride pressure to the "reversible" uptake will be the difference of these two effects and will depend upon the shape of the "exchange" isotherm, which is oharacteristic for the zeolite. From fig. 28 , in which the data obtained for hydrogen chloride on NaY at 295.5°C have been plotted, it can be seen that the "exchange" isotherm is sigmoid in shape. The "reversible" isotherm shows a maximum at a pressure of ca 9 mm Hg and a minimum at a pressure of 30 mm Hg. At these pressures the amounts of exchange are 6.5% and 75% of the attainable exohange, respectively. At a pressure of 30 mm Hg the amount of exchange is 11.5 times higher than that at 9 mm Hg which is very low. Therefore the effect of this difference on the "reversible" isotherm is very clearly shown by a maximum and a minimum. In the case of Na-clinoptilolite the "exchange" isotherm resembles a type I isotherm (in Brunauer's classification) and is rectangular. The amounts of exchange at pressures of 7 mm Hg and 30 mm Hg are 69% and 89% of the attainable exchange. The maximum and minimum in the "reversible" isotherm are not as sharp as in NaY. In KL and Na-Zeolon the "exchange" isotherms lie below the "reversible" ones, and do not show maxima and minima. The "exchange" and "total" isotherms obtained for the four systems at 246°C are compared in figs. 29 and 30. At the examined pressure range the affinity sequence shown by the four zeolites for the "total" and "exchange" sorption of hydrogen chloride is almost the same. The sequence for the "total" sorption is:

$$\text{Na-clinoptilolite} \gtrsim \text{Na-Zeolon} \gtrsim \text{NaY} \gtrsim \text{KL}$$

and for the "exchange":

Fig. 29

"Exchange" isotherms at 245°C

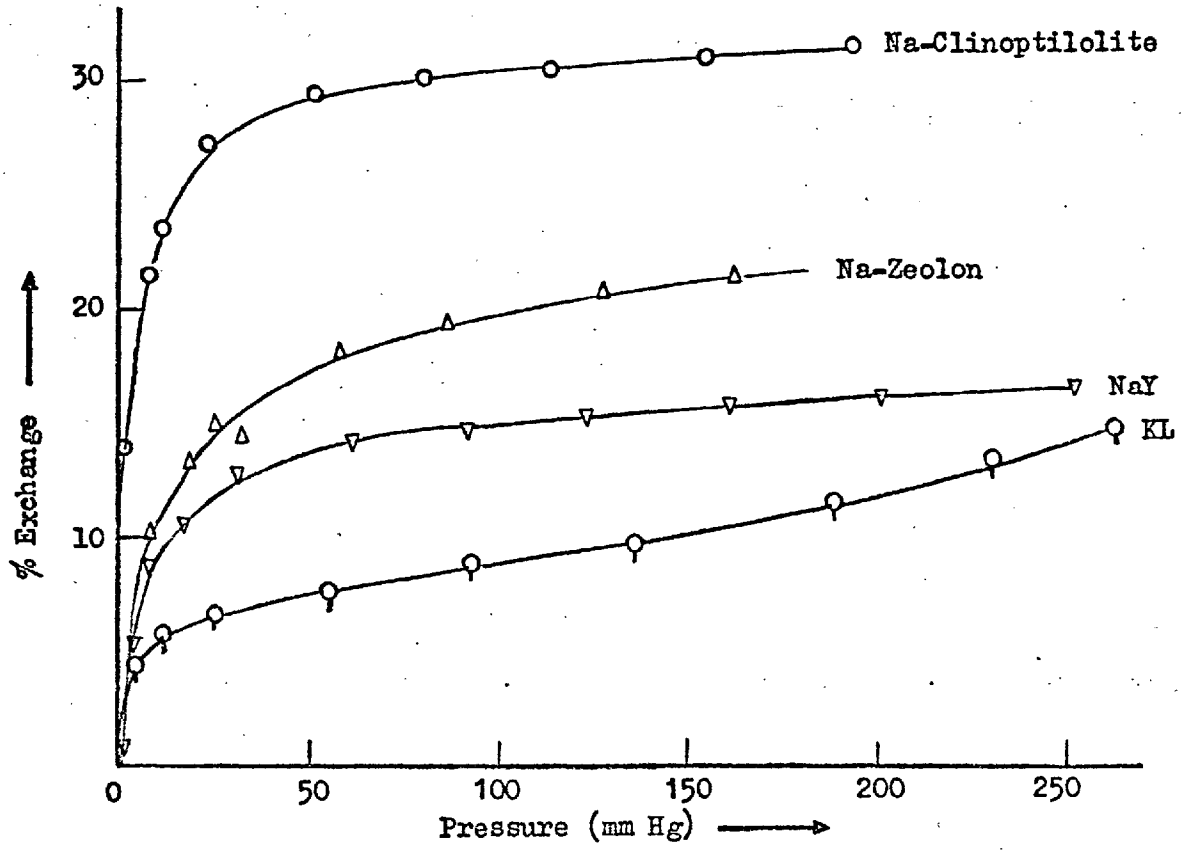
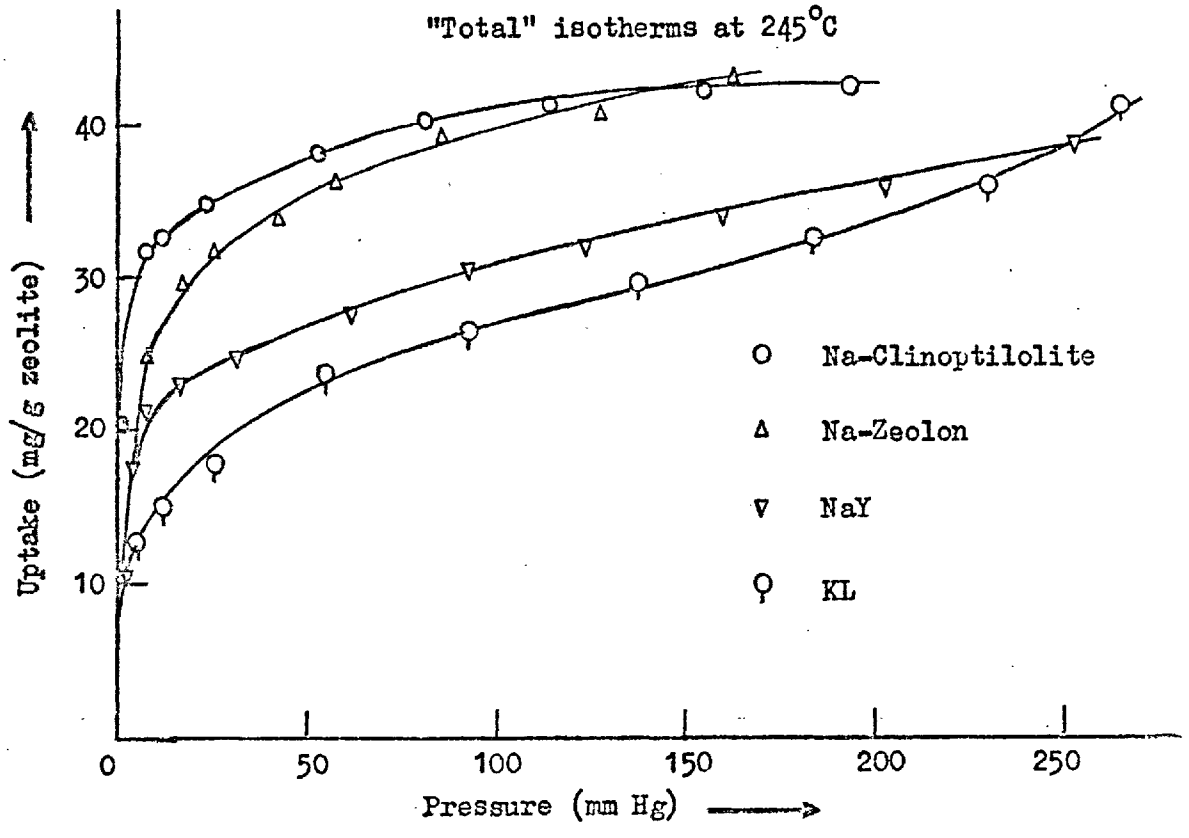


Fig. 30

"Total" isotherms at 245°C



Na-clinoptilolite > Na-Zeolon > NaY > KL.

The fact that the distribution of sodium chloride (or potassium chloride in the case of KL) inside and outside the crystals is not known adds another factor to those determining the "total" sorption, i.e. structure of zeolite and affinity of zeolite for the exchange reaction with hydrogen chloride. The affinity for the "reversible" sorption changes with pressure. For a pressure of 10 mm Hg it is:

Na-Zeolon > KL > Na-clinoptilolite > NaY.

"Exchange" isotherms for two of the four systems examined are shown in figs.31 & 32 . They resemble those obtained when the cations of a zeolite are exchanged in salt solutions[24]. The shapes of these isotherms vary with the system examined. From them it can be seen that complete exchange does not take place which means that, at least under these conditions, hydrogen chloride cannot be used for preparation of 100 per cent decationated zeolites. The maximum amounts of exchange in the four zeolites examined are given in Table 2.

Table 2

Ion-exchange in zeolites during the sorption of anhydrous hydrogen chloride

(Temperature 245°)

Zeolite	HCl pressure (cm Hg)	Exchange	% Exchange
Na-clinoptilolite	19.4	Na^+ by H^+	31.8
Na-Zeolon	16.3	Na^+ by H^+	21.3
NaY	19.7	Na^+ by H^+	14.4
KL	26.4	K^+ by H^+	14.9

Fig. 31

NaY-HCl

"Exchange" isotherms

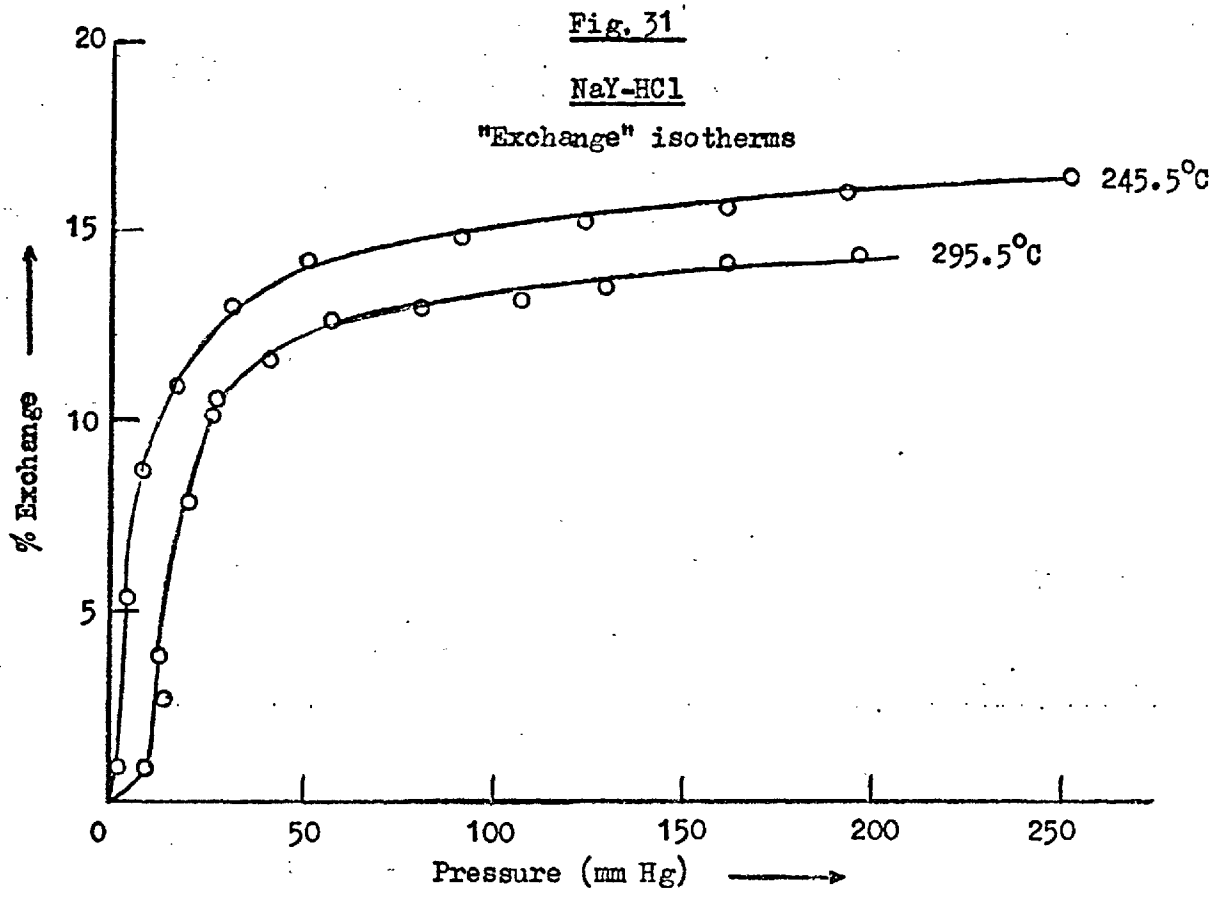
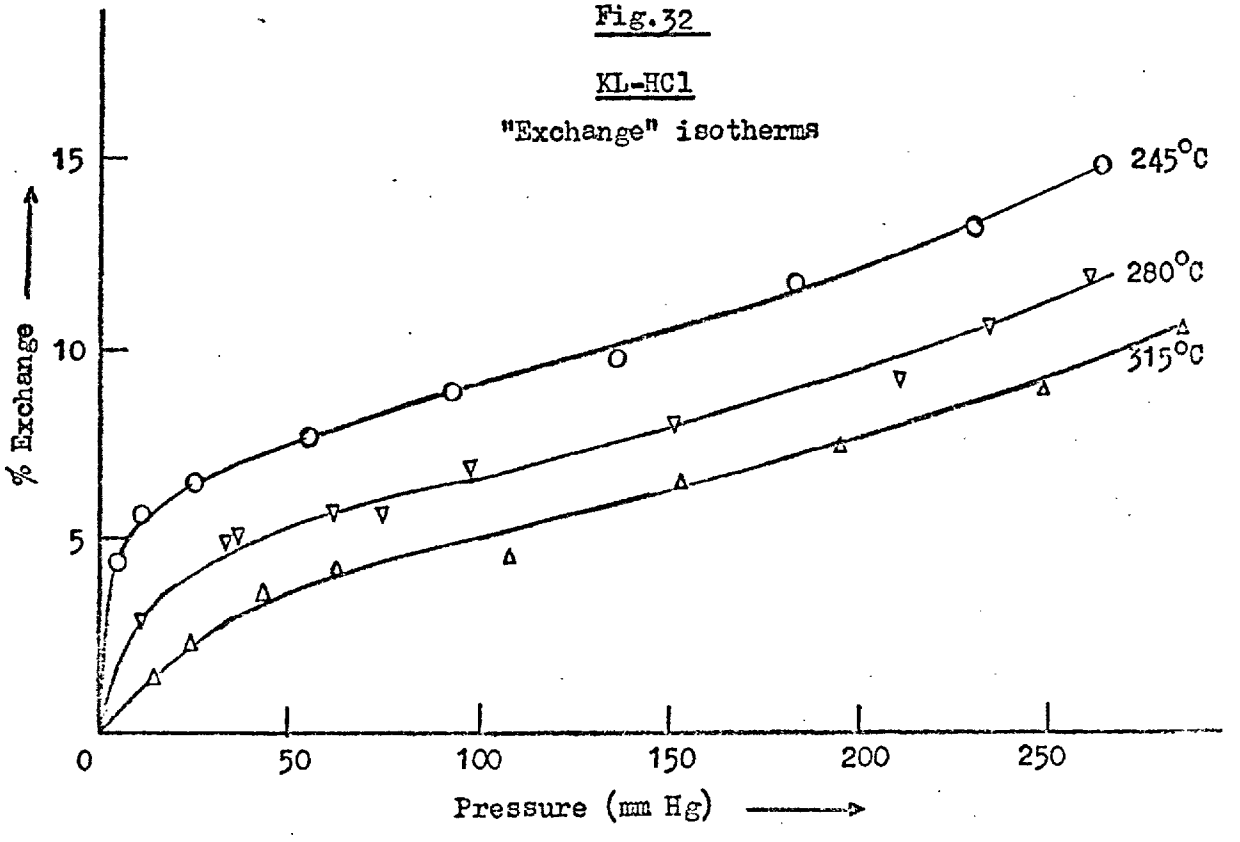


Fig. 32

KL-HCl

"Exchange" isotherms



Plots of % exchange vs "total" or "reversible" uptakes have different shapes for every system. The temperature coefficient in the curve of % exchange vs "total" uptake for KL (fig. 33) over the temperature range 245-315°C was very small. Plots of % exchange vs "total" and "reversible" uptakes for the system hydrogen chloride-KL at three temperatures are shown in figs. 33 and 34.

Fig. 33

KL-HCl

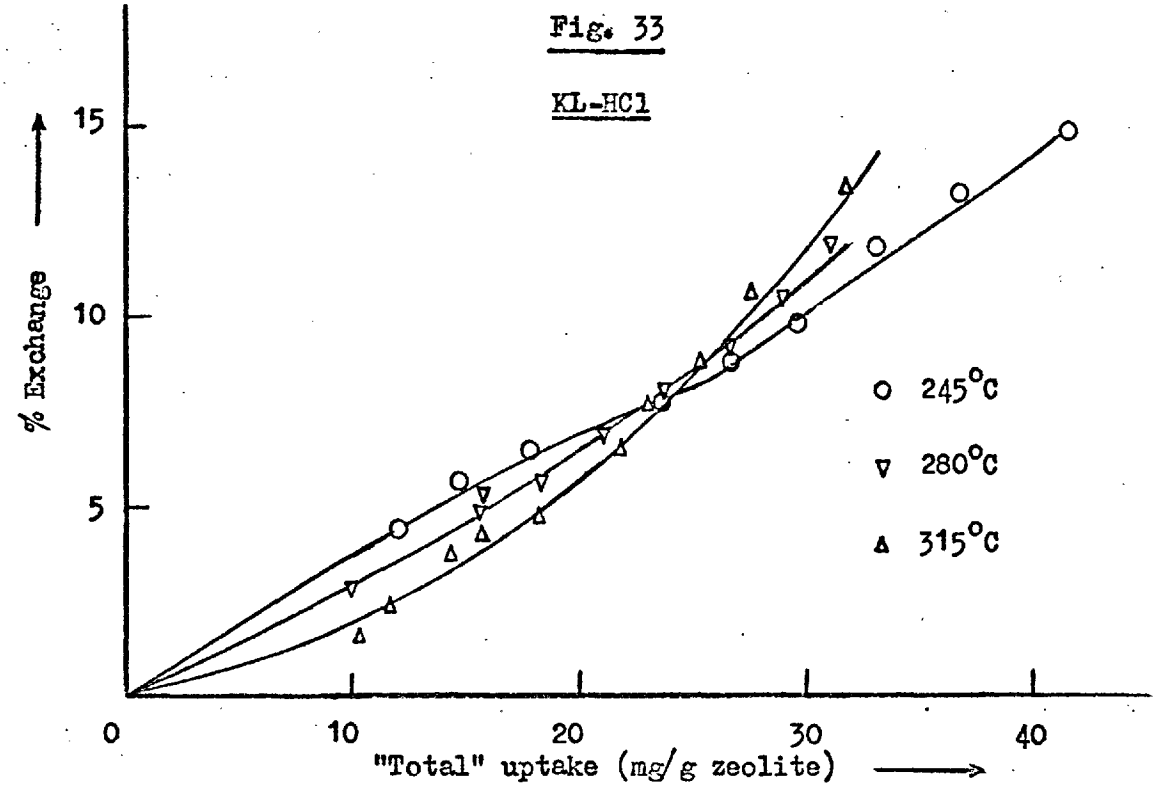
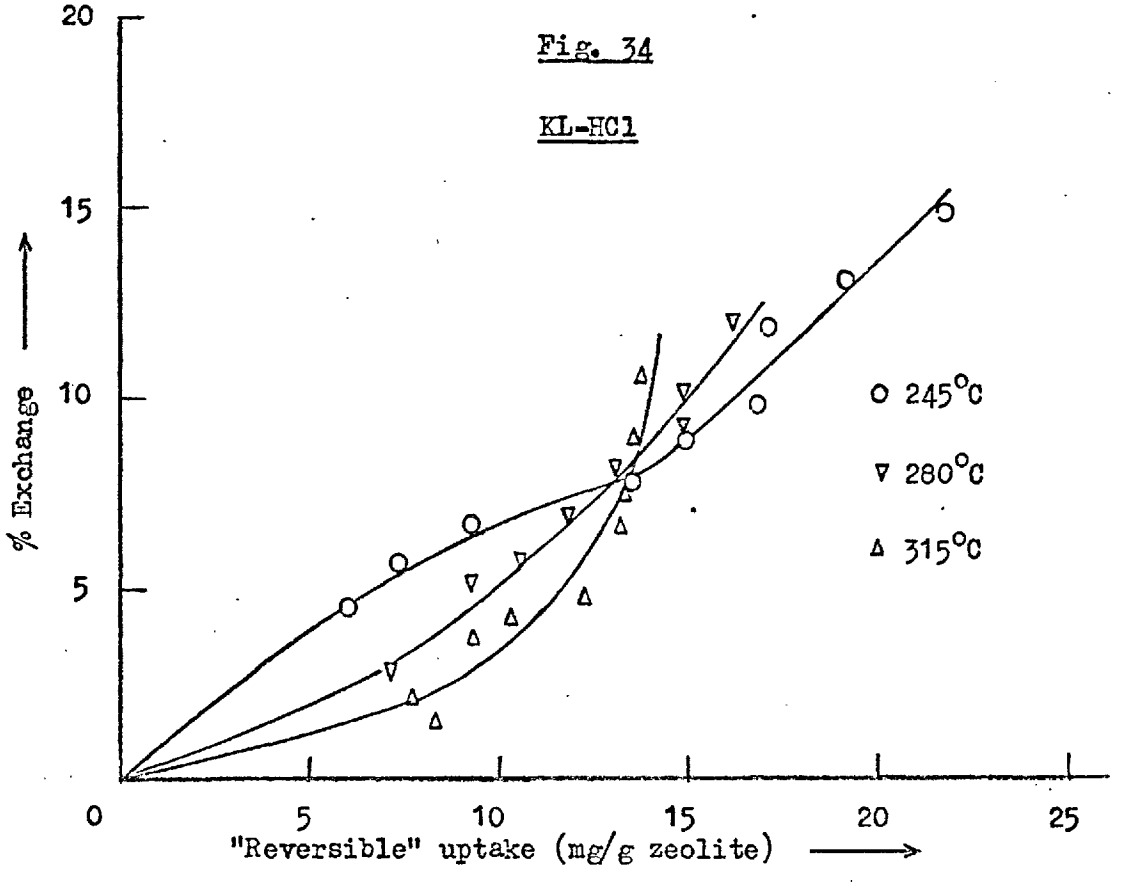


Fig. 34

KL-HCl



2. ION-EXCHANGE AND DECATIONATION EXPERIMENTS

2.1 Introduction

In attempts to prepare stable hydrogen forms of the synthetic zeolites L and Y, several methods were used. The basic procedures and the principles upon which these methods are based have been given in the Introduction (p. 25). More details regarding the methods employed will be given here because they are necessary for the discussion of the experimental results. As the structure and properties of the zeolites L and Y are different, different methods were used for the preparation of their decationated forms and the experimental results will be discussed in separate paragraphs. Since the aim of these experiments was to prepare a stable 100% hydrogen zeolite and find the exact conditions for this preparation, the intermediate and the final products were analysed and X-rayed. By "stable" we mean stable on heating to ca 400°C.

2.2 Decationated products from NaY

Four different methods were employed for the preparation of decationated Y zeolites. The details of these methods are given as follows.

Method 1 (97). This method comprised four steps.

(a) 10 g of NaY were treated with a 20% solution of ammonium sulphate for 15 minutes at 100°C with continuous stirring. The zeolite was filtered and treated in a similar way with a 7.5% solution of ammonium sulphate, filtered and washed free from sulphates (Ba^{++} test).

(b) The zeolite was heated at 560°C for 3 hours.

(c) The zeolite was then twice treated with a 20% solution of ammonium sulphate for 1 hour at 100°C, filtered and washed free from sulphates.

(d) The zeolite was heated at 440°C for 24 hours.

Method 2. The same procedure was followed but instead of using solutions of ammonium sulphate, solutions of ammonium chloride to which some 1:1 ammonia had been added were employed. The pH of the solution during the exchange was 9 to avoid possible hydrolysis of the zeolite.

Method 3 (via vapour phase). A quantity of ca 3 g of NaY was put in a glass tube and the tube was sealed to another glass tube containing ca 2 g of ammonium chloride. The system was outgassed (ammonium chloride at 90°C and NaY at 350°C) sealed and heated at 300°C for ca 24 hours. The zeolite was washed free from chlorides and heated at 420°C for 20 hours. This procedure was repeated twice.

Method 4. NaY was treated with a 20% solution of ammonium chloride (containing some ammonia) at 100°C for two hours, twice. It was then washed free from chlorides and heated at 245°C in a stream of air. The treatment with ammonium chloride solution was repeated and the zeolite was heated at 245°C. Finally, the zeolite was exchanged twice more, washed and heated in a stream of oxygen at different temperatures.

In Table 3, the ammonium forms and the decationated products obtained from zeolite Y with their cationic compositions and properties are given. The amount of exchange in Table 3 (a) was calculated from the amount of Na_2O contained in the ammonium form. The amount of decationation in all tables was calculated as the difference of the cation content (i.e. Na, K and NH_4^+) from the total cation capacity. The SiO_2 to Al_2O_3 ratio of the initial NaY was 4.78. The per cent of Na_2O and of NH_3 were calculated for the dehydrated zeolite. The amount of decomposition was found by X-ray powder photography using α-Al_2O_3 as internal standard (see p. 72). The amount of decomposition calculated by this method is not very accurate because the alteration of the reflection lines of HY (compared with those of NaY) could be partly due to the exchange or

removal of cations. For an accurate treatment, HY 100% crystalline should be employed as a comparison standard (100%). Since we did not have such a standard and since no particular stress was put on the amount of decomposition, NaY was used instead. The decationated products obtained by method 4 are listed in Table 4.

From the results of Tables 3 and 4 certain conclusions can be drawn regarding the nature of the decationated Y zeolites. It was not possible to prepare a fully decationated stable Y zeolite or a stable decationated Y zeolite with very low sodium content. The maximum degree of decationation that would be obtained without any change of the X-ray pattern (and presumably of the structure and properties of the zeolite) was between 66 and 75%, corresponding with a Na_2O content of 4.47 - 3.29%. The temperature necessary for removal of the ammonia from the zeolite (or for the "decationation step") was between 300-350°C, as found by ammonia analysis. It has been observed that it is not possible to exchange all the cations of NaY by NH_4^+ at 25°C(98). 32% Na^+ remains in the structure. This is the reason why, after NaY was exchanged twice with NH_4Cl, it was heated to 540°C. This heating has been reported(97) to be necessary for the re-distribution of the residual sodium ions on the most energetic sites. This re-distribution could be attained by heating the zeolite to 250°C only as can be seen from Table 4.

The decationated Y zeolite prepared by method 1 was used for sorption experiments of hydrogen chloride ammonia and ammonium chloride. Further decomposition of the zeolite was found after the sorption experiments of ammonia and ammonium chloride. This is discussed in the following chapter. Although the decationated zeolites prepared by the methods previously referred to may be good for catalysis experiments, they were not the most desirable sorbents for experiments on the sorption of ammonium chloride.

Table 3

(a) Ammonium zeolites prepared from NaY

Method	Treatment	composition and stability		
		% Na_2O	% exchange	X-ray pattern
1.	4 equil. with $(NH_4)_2SO_4$ soln. at 100°C.	0.26	98	similar to NaY
2.	4 equil. with $NH_4Cl + NH_3$ soln. at 100°C	0.26	98	"
3.	via vapour phase			
	1st exchange	8.0	38.5	"
	2nd exchange	5.5	58.2	"
	3rd exchange	2.5	81.0	"

Table 3 (continued)

(b) Decationated products from NaY

Method	Max. temp. of heating NH_4Y	% Na_2O	% NH_3	% decation-nation	X-ray pattern
1.	(b) 540°C (d) 440°C	0.26	0.0	98	*decomp.
2.	(b) 540°C (d) 440°C	0.26	0.0	98	"
3.					
1st exchange	420°C	8.0	0.0	38.5	similar to NaY
2nd exchange	430°C	5.5	0.0	58.2	"
3rd exchange	420°C	2.5	0.0	81	*decomp.

*decomp. = decomposition ca 20%

Table 4

Decationated products from NaY obtained by method 4

Treatment	Heated	Heating time (h)	Heating temp. (°C)	% NH_3	% Na_2O	% decat-ionation	X-ray pattern
(1) Twice equil. with NH_4Cl+NH_3 at 100°C	in air	16	245	3.5	2.5	35.84	similar to NaY
(2) Product (1) was treated as in (1)	in air	44	245	3.4	0.33	53.7	"
(3) Product (2) was treated as in (1)	in dry air	18	245	3.16	0.14	58.0	"
	"	46	245	2.7	0.14	65	"
	in oxygen	18	245	2.57	0.14	66	"
	"	16	295	1.87	0.14	75	*decomp.
	"	21	350	0.61	0.14	91	"
	under low vac.	21	350	0.60	0.14	92	"

*decomp. = decomposition ca 20%

Preparation of decationated Y zeolites has been reported previously[22,44,52,97,99]. Different investigators have used decationated Y zeolites with degrees of decationation varying between 70 and 90% and SiO_2 to Al_2O_3 ratio 4.5 - 6.0. The crystallinity of these decationated zeolites was reported to have been "highly retained" after heating to 400°C. McDaniel and Maher [97] reported the preparation of an ultra-stable form of zeolite Y with very low sodium content. They observed a loss of crystallinity of 20% of this sample as compared to an unstabilized decationated sample prepared by method 1. They did not define the critical requirements for its formation nor did they account for its composition. Kerr [95] considered a reaction occurring in hydrogen zeolite Y between its chemical water and the aluminium atoms to result in increase of its thermal stability.

It has been found [40] that dehydroxylation of decationated Y zeolites occurs at temperatures above 450°C and results in loss of their stability. Some of the decationated zeolites Y obtained by the methods 1-4 seem to be less stable than those previously reported, although a close comparison is not possible since the initial samples of NaY used were different. However, the poor stability of these zeolites may be connected with the occurrence of dehydroxylation at temperatures lower than 450°C. This suggestion was partly confirmed by thermogravimetric analysis of HY prepared by method 1. A rise in the % weight loss vs temperature curve for HY corresponding to ca 2.8% and starting at 450°C would be expected. The corresponding curve for HY (method 1) showed a rise of ca 1.5%.

2.3 Preparation of decationated zeolites from Linde L

Two methods were used for preparation of decationated zeolite L. The first involved the preparation of the ammonium form and the second consisted of treatment of the zeolite with dilute solutions of hydrochloric acid. The ammonium form of zeolite L was

prepared by shaking the zeolite with a 20% solution of ammonium chloride (containing 1:1 ammonia), at 100°C for one hour. Two such treatments resulted in 84% exchange of K^+ and Na^+ by ammonium ions as calculated from the Na and K analyses. More similar treatments had no effect on the amount of exchange.

This amount of exchange implies that at least those cations on sites D, C and B [20] have been replaced by ammonium ions. Those that have not been exchanged are presumably the cations (K,Na) of the sites A, i.e. the cations positioned in the hexagonal prisms. Part of the NH_4L so prepared was heated at 350°C for 24 hours and then shaken with NH_4Cl solution twice at 100°C as previously. No increase of the amount of exchange was found which suggests that the re-distribution of cations after heating that takes place in NaY does not take place in L at 350°C.

The 84% exchanged NH_4L thus obtained was subsequently heated under different conditions in order to remove the NH_3 and obtain the decationated form. The exact conditions and the products obtained are listed in Table 5. The per cent decationation was calculated in the same way as in zeolite Y (see p.104). From these results it can be seen that the critical degree of decationation for a stable product is between 54% and 74%. An amount of 60% decationation accounts numerically for the cations on sites C and D without ruling out the possibility of decationation of sites B instead of sites C. Increase of decationation results in collapse of the crystal structure.

Comparison of the results obtained for Y and L zeolites shows that ammonia can be removed more easily from Y than from L. A temperature as high as 450-500°C is necessary for the decationation step in L compared with 300-350°C in Y. Zhdanov and Novikov[100] reported the preparation of ammonium and decationated forms of synthetic erionite, the structure of which is related to L. The

Table 5

Decationated products from Linde L

NH_4L treatment			cation composition and stability of decationated product				
Heating temp.(°C)	Heated	Heating time(h)	% K_2O	% Na_2O	% NH_3	% decat-ionation	X-ray pattern
350	air	24	2.55	0.11	4.34	19.0	similar to Linde L
350	air	24	2.55	0.11	4.78	12.0	"
380	air	79	2.55	0.11	3.3	34.0	"
350	oxygen	20	2.55	0.11	2.82	41.0	"
395	vacuum	24	2.55	0.11	2.09	53.0	"
450	vacuum	24	2.55	0.11	0.47	74.0	*decomp.
450	oxygen	24	2.55	0.11	0.0	84.0	"
570	air	24	2.55	0.11	0.0	84.0	"
	Linde L		16.0	0.7			
	NH_4L				6.6		
0.05 NL			10.20	0.10	-	37	similar to original L
0.1 NL			7.40	0.10	-	54	

*decomp. = Replacement and weakening most of the lines compared with Linde L.
50% decomposition calculated by the internal standard method.

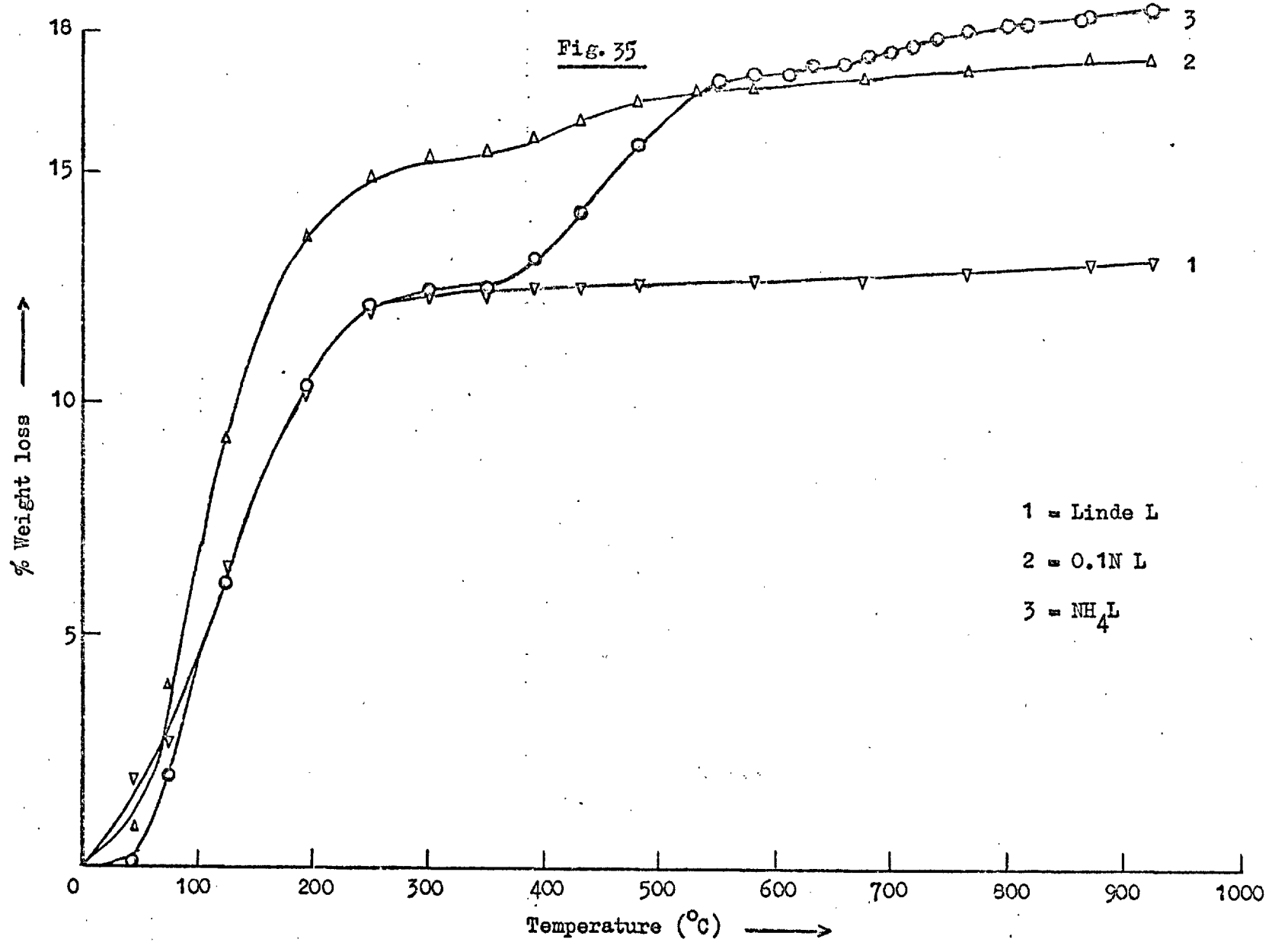
temperature necessary for complete removal of ammonia under evacuation from the ammonium erionite was 500°C which can be compared with 450°C for zeolite L. Also, heating at higher temperature is necessary to burn out the ammonia[25] in L than in Y. At 350°C after prolonged heating in air and oxygen, only 41% of the ammonium has been burnt out (of the 84% ammonium present) which corresponds in number to the ammonium ions of site D (of the main channel). A higher temperature (450°C) is necessary to burn out the ammonium ions positioned in the cancrinite cages and the "midway" cavities between them. A possible reason could be that there is not enough room for oxygen molecules to enter these cages which thus screen the NH_4^+ ions.

Samples of Linde L were refluxed with 0.05 N and 0.1 N solutions of hydrochloric acid[94] for 3.5 hours at 100°C. After treatment, the zeolite was filtered and washed free from chlorides. Their X-ray patterns were similar to that of the initial zeolite. Their stability was examined by outgassing them at 350°C for 24 hours under high vacuum. No change was observed in their X-ray patterns. During the treatment with hydrochloric acid, aluminium was removed from the zeolitic framework (Alizarin S test in the filtrate). The cationic compositions of the decationated and partly dealuminated samples of L (marked 0.05 NL and 0.1 NL) are given at the end of Table 5.

Additional information concerning the properties of some of the products prepared from Linde L were obtained by thermogravimetric analysis. In fig. 35 the per cent weight loss vs temperature curves for 0.1 NL, NH_4L and original L are plotted. The larger weight loss at temperatures between 100°C and 300°C from 0.1 NL (curve 2) than from NH_4L or Linde L is attributed to its higher water content and partly to the hydroxyls of the zeolitic framework formed because of its partial dealumination. The second shoulder of this curve at 400-500°C corresponds to the loss of water from the hydroxyls

due to decationation. This behaviour is similar to that of other decationated zeolites. Barrer and Peterson[73] found that the water loss due to the hydroxyls in H-Zeolon took place at temperatures between 600°C and 900°C. Zhdanov and Nivikov[100] reported that the water loss under evacuation in dealuminated synthetic erionite occurs at temperatures between 450°C and 550°C. In curve 3 the second rise at temperatures between 350°C and 500°C was attributed mainly to the loss of ammonia due to the decomposition of ammonium ions, and the third to the completion of the loss of ammonia and loss of hydroxyls. However, calculations based on the ammonia content showed that a considerable part of the hydroxyls must have been eliminated as water at lower temperatures. This is in agreement with the results of Table 5 and also curve 2.

Fig. 35


18
15
10
5
0
100
200
300
400
500
600
700
800
900
1000
% Weight loss
Temperature (°C)
1
2
3
1 = Linde L
2 = 0.1N L
3 = NH4L

3. AMMONIA-ZEOLITE SORPTION COMPLEXES

3.1 Experimental isotherms

Isotherms were obtained at intervals of 20°C or 30°C between 190°C and 320°C for ammonia sorbed on the synthetic zeolites H-Zeolon, NaY and KL; in addition, one isotherm was taken at room temperature (22.5°C) for ammonia sorbed on KL and another one at 245.5°C on HY.

Reversible and reproducible isotherms were obtained in all cases except for that of ammonia on HY which showed hysteresis; therefore, the HY-NH_3 data are excluded from comparison and will be discussed separately at the end of this chapter.

Equilibrium in sorption and desorption was established in ca 30 minutes. An hour to an hour and a half was, however, allowed between readings. Outgassing of the samples between the runs had no effect on the recorded isotherms. Comparison of the X-ray powder photographs of H-Zeolon, NaY and KL taken before and after the sorption experiments also showed that no change had occurred in their structures. The isotherms recorded for the three systems, i.e. H-Zeolon, NaY and KL, are shown in figs. 36, 37 and 38. All the isotherms obtained belong to type I of Brunauer's classification. The isotherms obtained for ammonia on H-Zeolon are the most rectangular of them all and removal of the sorbed ammonia on H-Zeolon at very low pressures ($p < 0.01$mmHg) could only be attained by evacuation. These facts show that ammonia is strongly sorbed on H-Zeolon or possibly chemisorbed. In other words, a reaction of ammonia with H-Zeolon to form the ammonium form of the zeolite may take place. Complete conversion of H-Zeolon to NH_4-Zeolon corresponds to an uptake of ca 38 mg/g.

Fig. 36

H-Zeolon - NH_3 isotherms

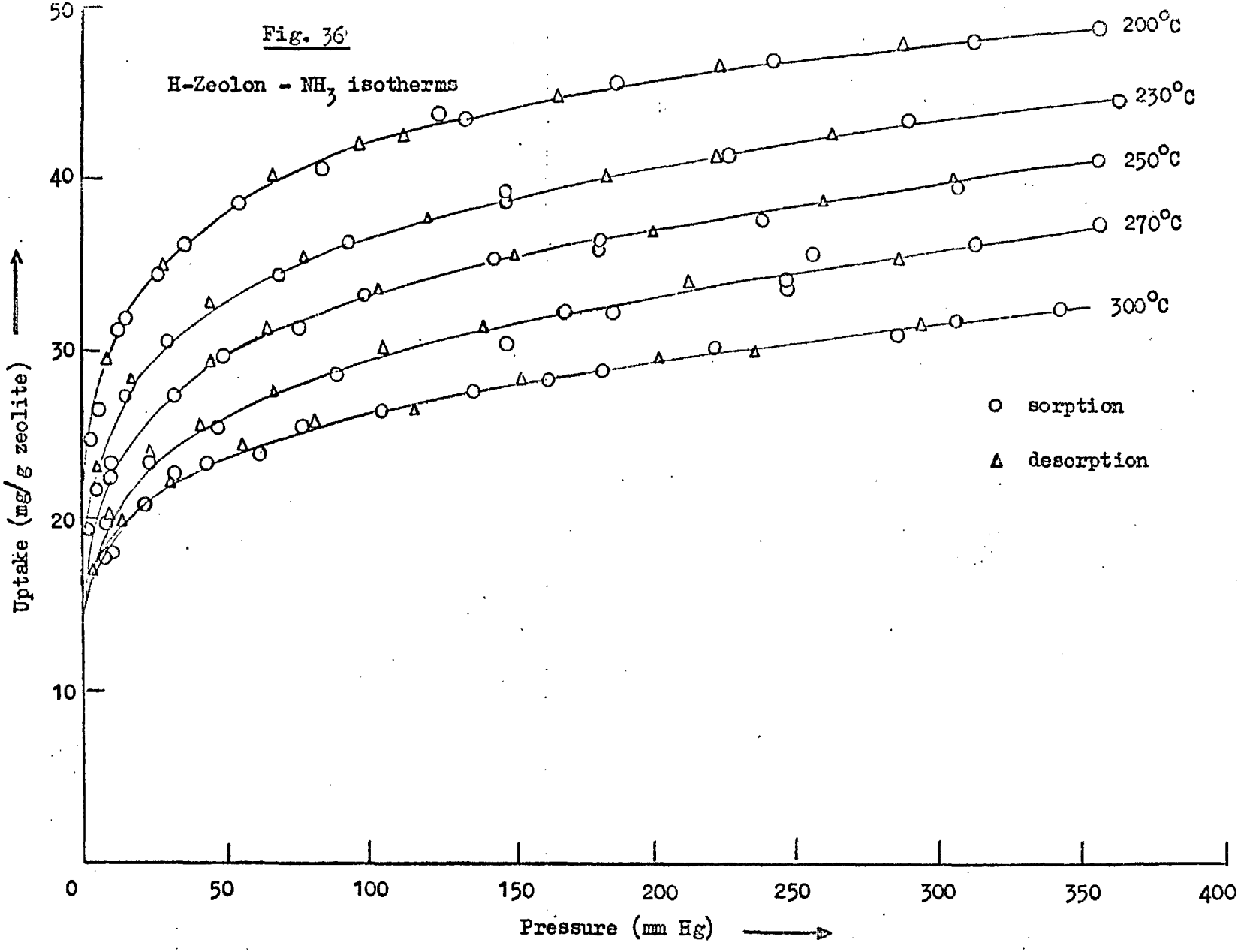


Fig. 37

NaY-NH_3 isotherms

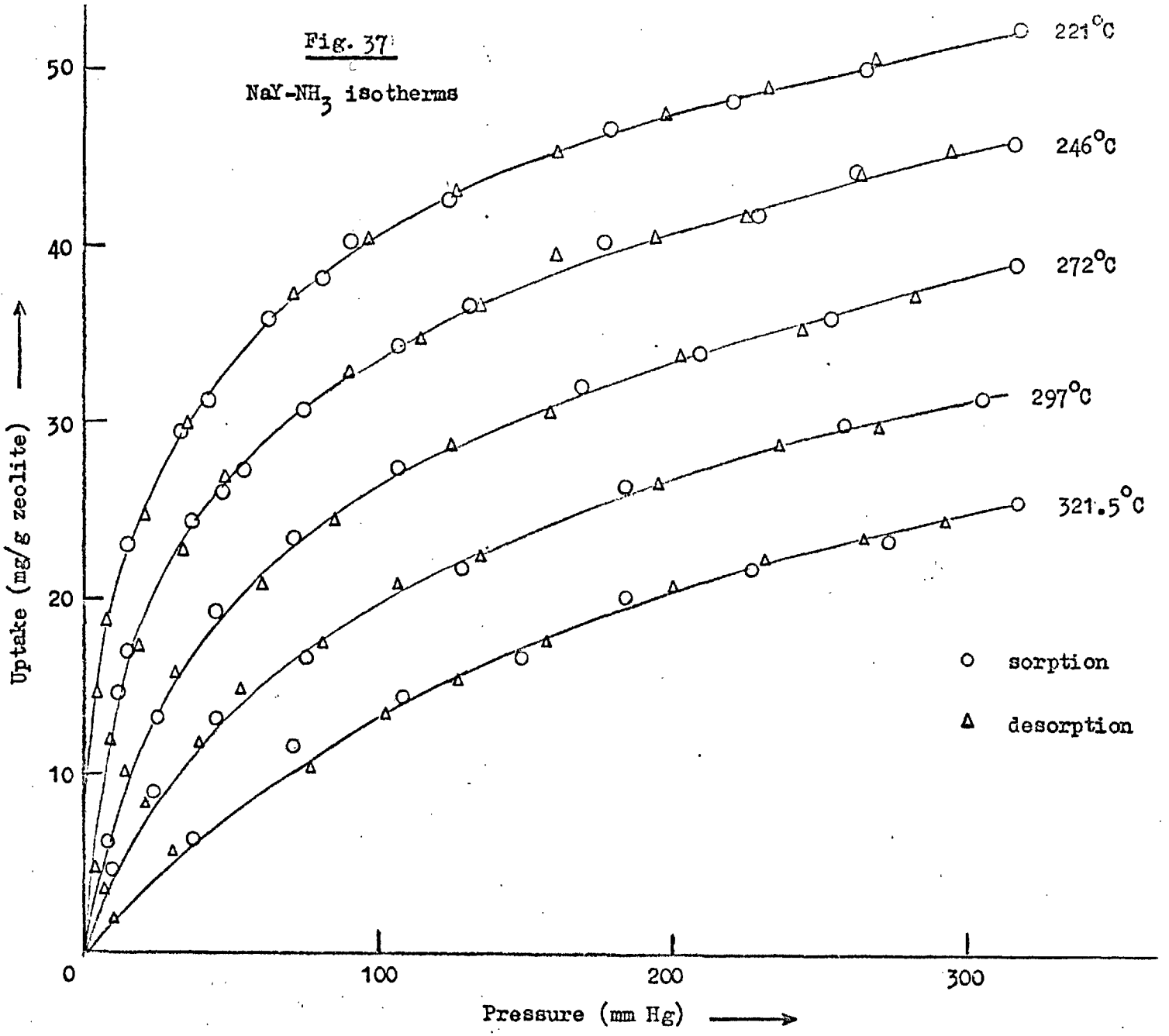
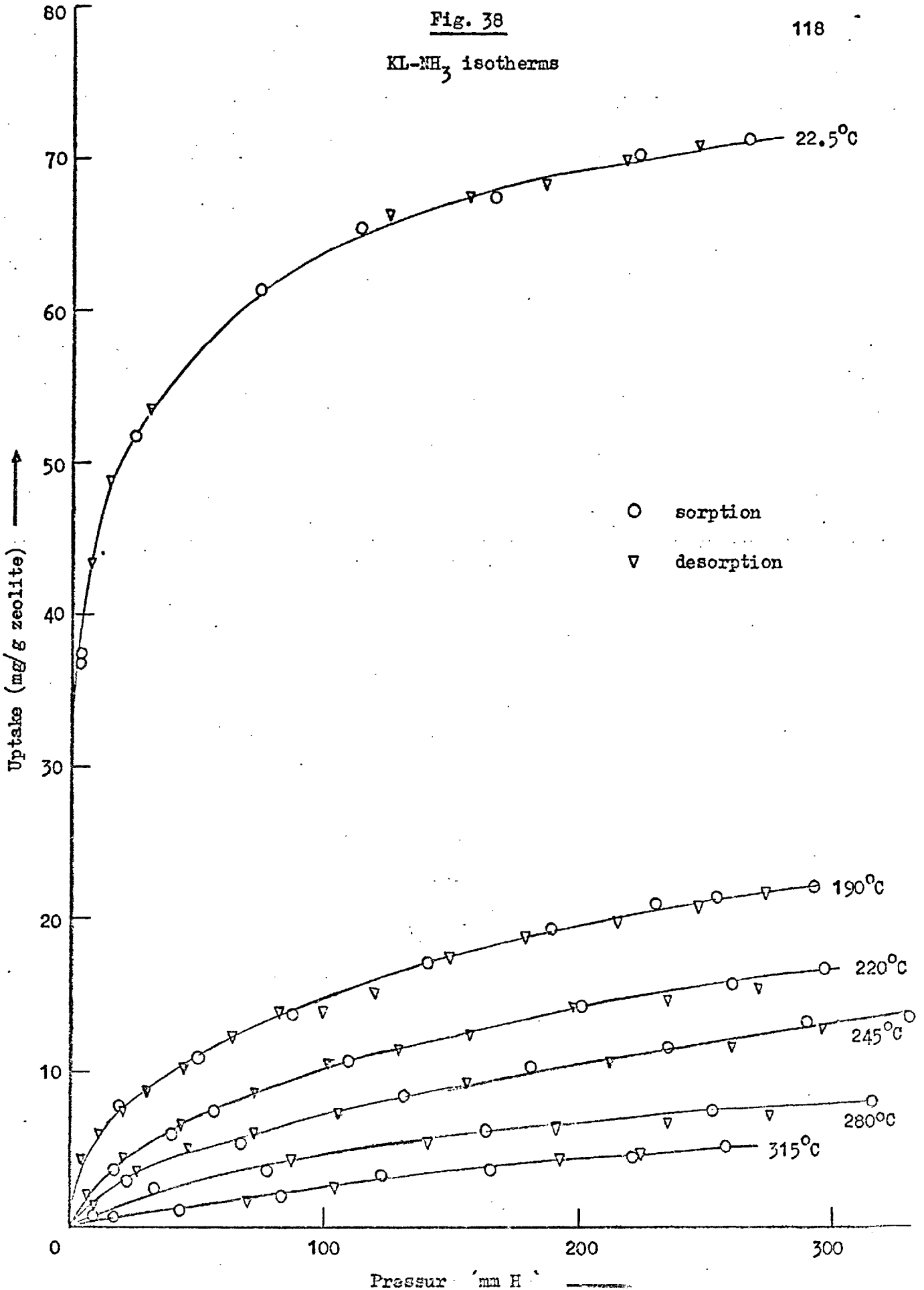


Fig. 38

KL-NH_3 isotherms



The isotherms can be used to calculate the thermodynamic quantities for the sorbed phase by applying general thermodynamic arguments (Ch.2, Pt.I). Some of the thermodynamic quantities have been calculated and are discussed in the following paragraphs. An empirical virial equation was also used to describe the sorption isotherms; the activity coefficients of sorbed ammonia at different temperatures and uptakes were calculated and compared with their values calculated from different isotherm models.

3.2 Thermodynamic properties of the sorbed phase

Isosteric heat of sorption

Isosteric heats of sorption were determined from the experimental isotherm data for H-Zeolon, NaY and KL using the Clapeyron-Clausius equation in its integrated form:

$$-\Delta\bar{H}_1 = q_{st} = -2.303R \left(\frac{T_1 T_2}{T_1 - T_2}\right) \log \frac{p_2}{p_1}$$

The isosteric heat for a given amount sorbed was calculated from the plot of log p vs uptake from all possible pairs of isotherms and the average was taken. In some cases, plots of log p vs $1/T$ were also used. There was no evidence of a temperature coefficient in $\Delta\bar{H}_1$, unless it was in the limits of experimental error. Because of the low uptakes and the difficulties in keeping constant temperature to within reasonable accuracy (see p.75) the deviations in the values of isosteric heats were rather high for all three systems, ranging from 3 to 10 per cent of the mean value.

In all systems studied, the isosteric heats decreased with increasing uptake because of the heterogeneity of the surface of the sorbents. The plots of isosteric heats against the uptake are shown in figs. 39-41. Since the isotherm families recorded cover the range of temperatures between 190°C and 320°C, the calculated

Fig. 39

H-Zeolon - NH_3

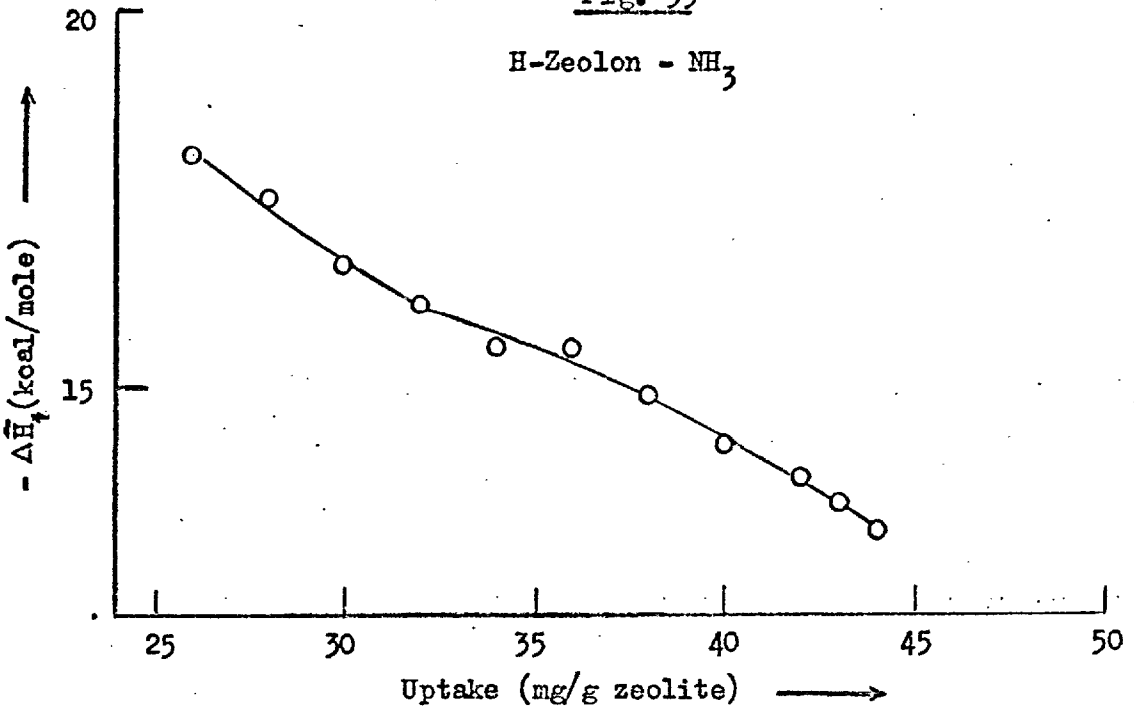


Fig. 40

NaY -- NH_3

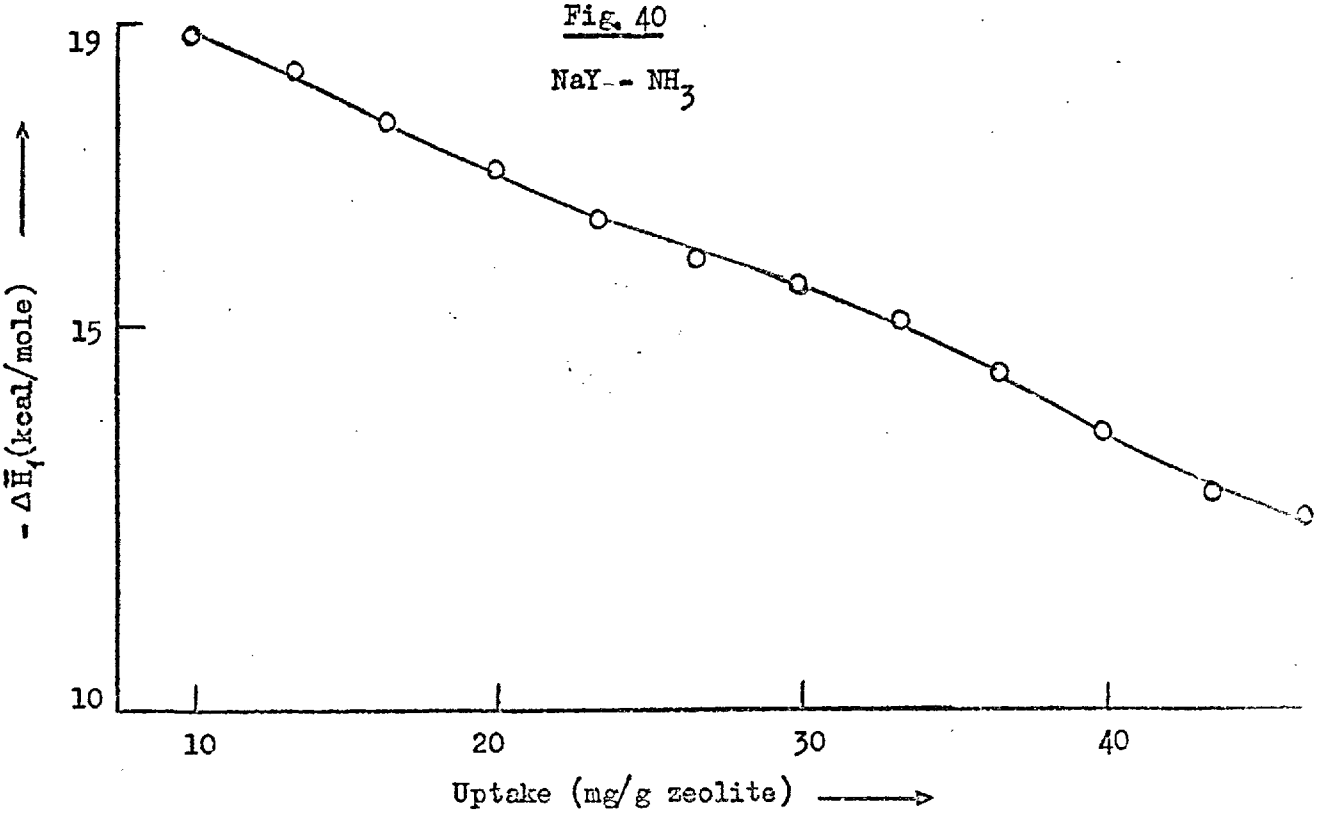


Fig. 41

KL - NH_3

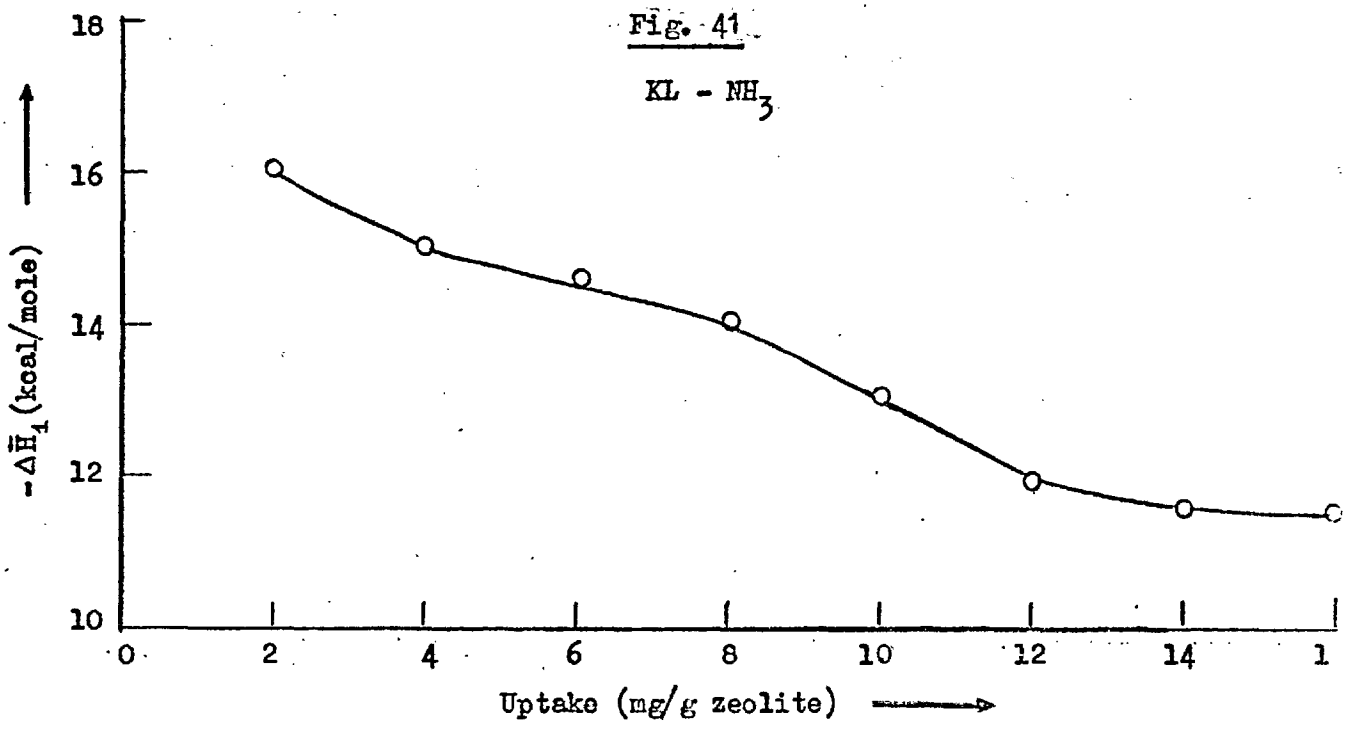
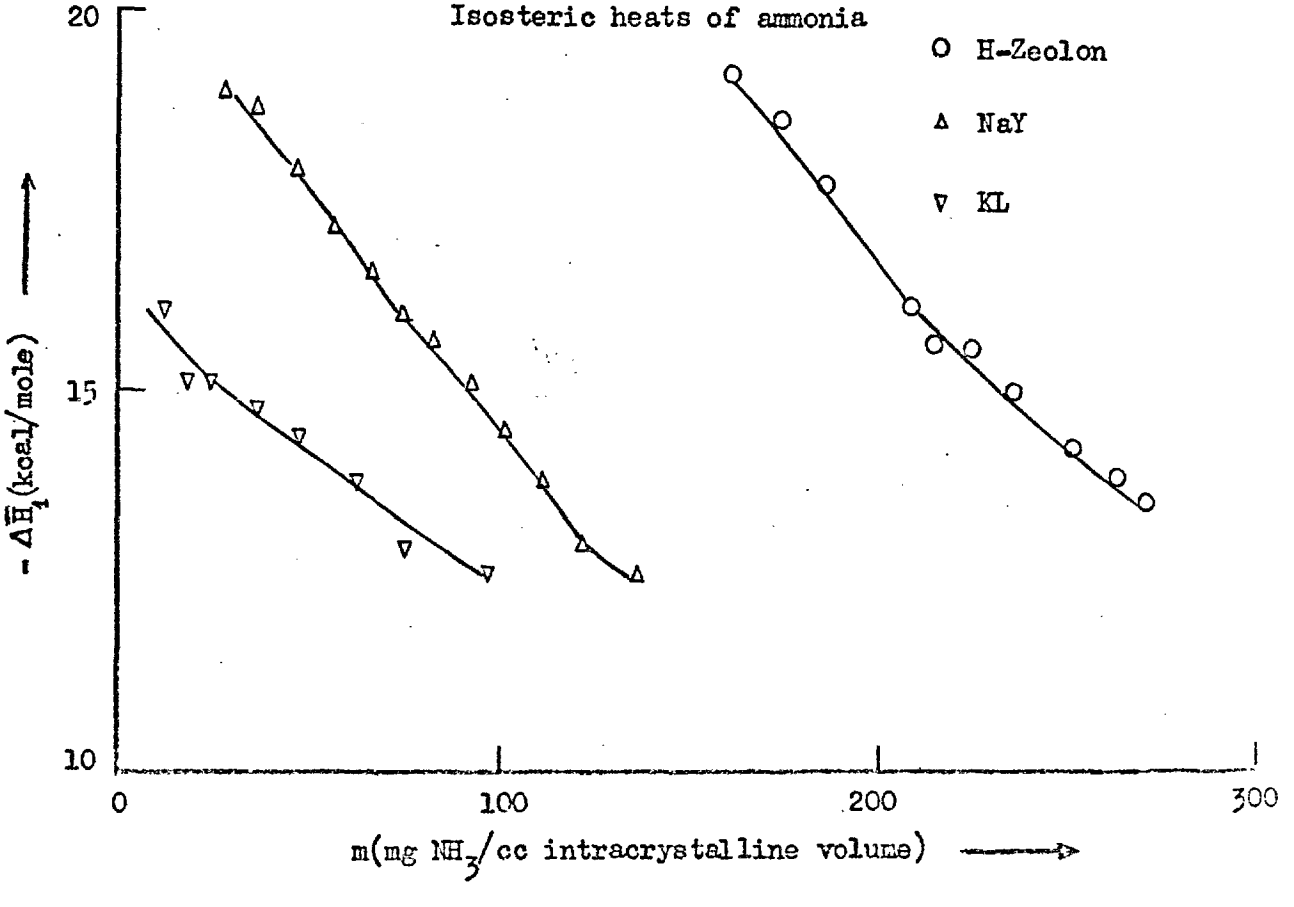


Fig. 42

Isosteric heats of ammonia



isosteric heats cover a short range of surface coverage. Therefore, the information that can be obtained from the isosteric heats should be considered to be qualitative rather than quantitative. The values of saturation capacities at these high temperatures (as calculated from the plot of $\frac{x}{p}$ vs p, where x is the uptake at equilibrium pressure p) are not accurate and θ, the fraction of the total available surface covered, cannot be used for plotting and comparing the isosteric heats for different zeolites. This difficulty was overcome by expressing the uptake in mg of ammonia per cc of intracrystalline volume of sorbent (m); the intracrystalline volume was calculated from the water content of the zeolites at room temperature. The plots of isosteric heats against m for the three systems are shown in fig.42. Although these graphs do not cover a wide range of m, it can be said that the isosteric heats for H-Zeolon are the highest and those for KL the lowest. In fig.43 the isosteric heats of ammonia sorbed on a sample of ca 70% HY as obtained by Benson et al[44] are compared with those obtained for H-Zeolon and NaY. The sorption of ammonia on decationated Y zeolite was studied by IR spectroscopy[28] It was found that ammonium Y was reconstituted when ammonia was sorbed at temperatures 200-300°C. This fact and the similarity of the plots of the isosteric heats for H-Zeolon and HY in fig. 43 support the suggestion that at least part of the sorbed ammonia on H-Zeolon is chemisorbed. The rest is physically adsorbed on two distinct sorption sites[73].

The isosteric heats for NaY-NH_3 were compared with those for NaX-NH_3 obtained by Barrer and Gibbons[38]. For low uptakes the isosteric heats on NaY were higher than on NaX; for higher uptakes the isosteric heats on NaY were lower than on NaX. Since the cation density in NaY is lower than in NaX, the isosteric heats of sorption of ammonia on NaY should be expected to be lower than on NaX at low uptakes. A possible explanation for this apparent discrepancy

is the cation deficiency in the sample of NaY used since the isosteric heat of ammonia on HY[44] is much larger than on NaY.

Integral heats of sorption

Integral heats of sorption $\Delta\tilde{H}_1$ can be obtained as functions of the amount sorbed by graphical integration according to the relations:

$$\Delta\tilde{H}_1 = \frac{1}{n_1}\int_0^{n_1} \Delta\bar{H}_1 dn_1 \qquad (46)$$

$$\Delta\tilde{H}_1 = \frac{1}{n_1-n_2}\int_{n_2}^{n_1} \Delta\bar{H}_1 dn_1 \qquad (47)$$

where n denotes the number of moles sorbed. For integration of equation (46) extrapolation of $\Delta\bar{H}_1$ vs coverage to zero sorption is necessary. Where this becomes inaccurate, equation (47) may be used. Equation (46) was used to calculate integral heats of ammonia on NaY and KL. The extrapolated values of $-\Delta\bar{H}_1$ necessary for this integration were taken as 20 kcal/mole and 16.5kcal/mole respectively. No attempts were made to calculate integral heats for ammonia sorbed on H-Zeolon since either equation (46) or (47) would lead to inaccurate results. The calculated values of integral heats of ammonia on NaY and KL for different uptakes (m) are given in table 6 . From the results of this table it can be seen that the values of the integral heats greatly exceed the latent heat of vaporisation of liquid ammonia which is 5.56 kcal/mole at 239.7°K. This may be interpreted to mean that there are substantial forces in the crystal without counterpart in the liquid.

Table 6

Integral heats of sorption of ammonia

	$-\Delta\tilde{H}_1$ (kcal/mole)	
Zeolite	NaY	KL
uptake (m)		
20		16.0
30	19.4	15.7
40	19.2	15.4
60	18.7	15.0
80	18.0	14.5
100	17.5	14.2
120	16.8	
140	16.3	

Differential entropy of the sorbate and half standard entropy of sorption

The differential molar entropies for ammonia adsorbed on the various sorbents examined were calculated from the isosteric heats of sorption using the equation:

$$\bar{S}_1 = \tilde{S}^o_g + R\ln\frac{p^o}{p} + \frac{\Delta\bar{H}_1}{T} \qquad (13)$$

where p^o is the pressure at standard state (1 atm), p in mmHg and $\Delta\bar{H}_1$ in cal/mole. The standard entropy of gaseous ammonia ($\tilde{S}^o_g$) was obtained from the data of Din[102]. The differential molar entropies for ammonia adsorbed on H-Zeolon, NaY and KL are shown in figs. 44, 45 and 46 respectively. The dotted parts in the entropy curves were calculated from the half standard differential entropies defined as

Fig. 43

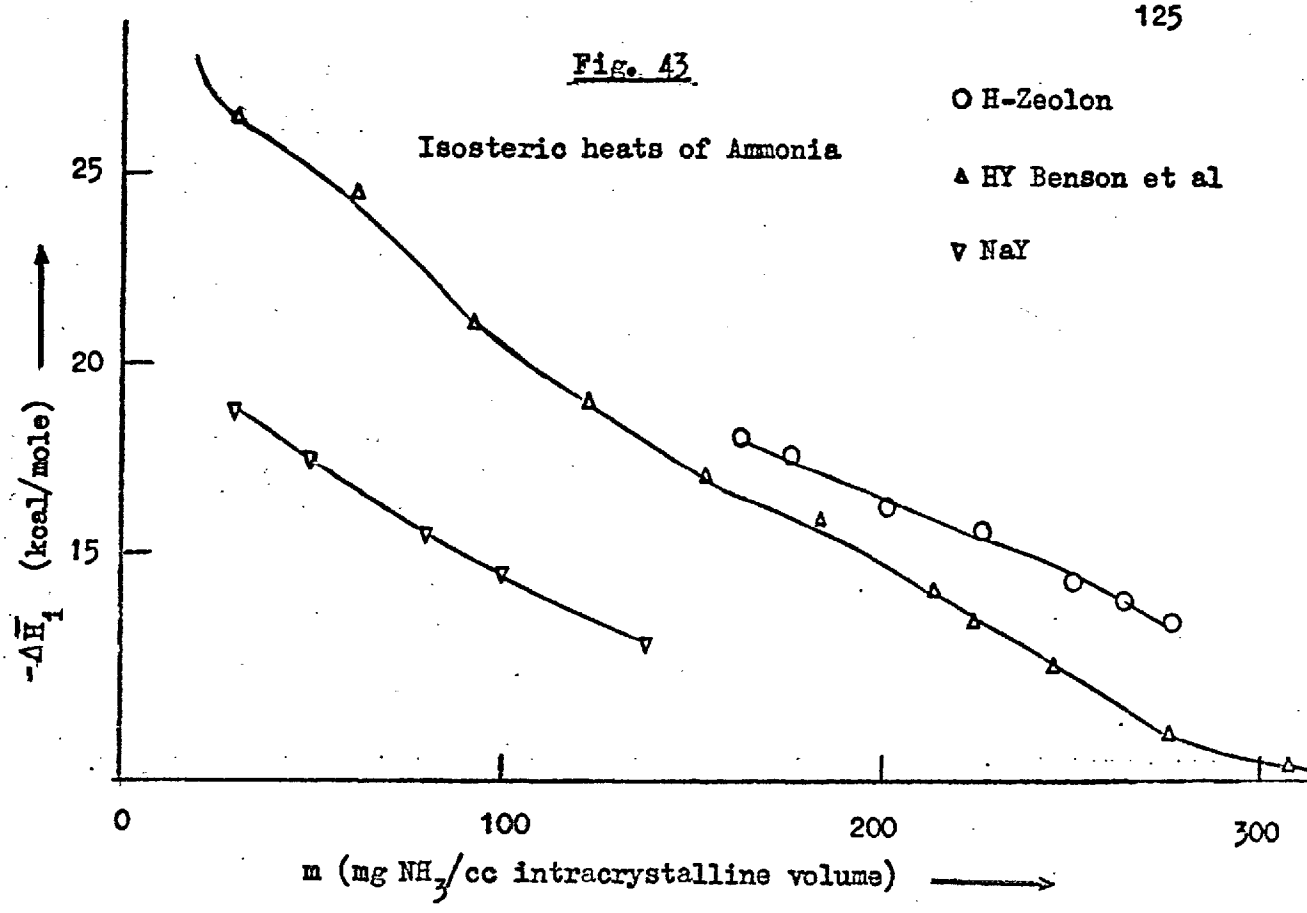

Isosteric heats of Ammonia
O H-Zeolon
▲ HY Benson et al
▽ NaY
25
20
15
$-\Delta\bar{H}_1$ (kcal/mole)
0
100
200
300
m (mg NH_3/cc intracrystalline volume)

Fig. 44

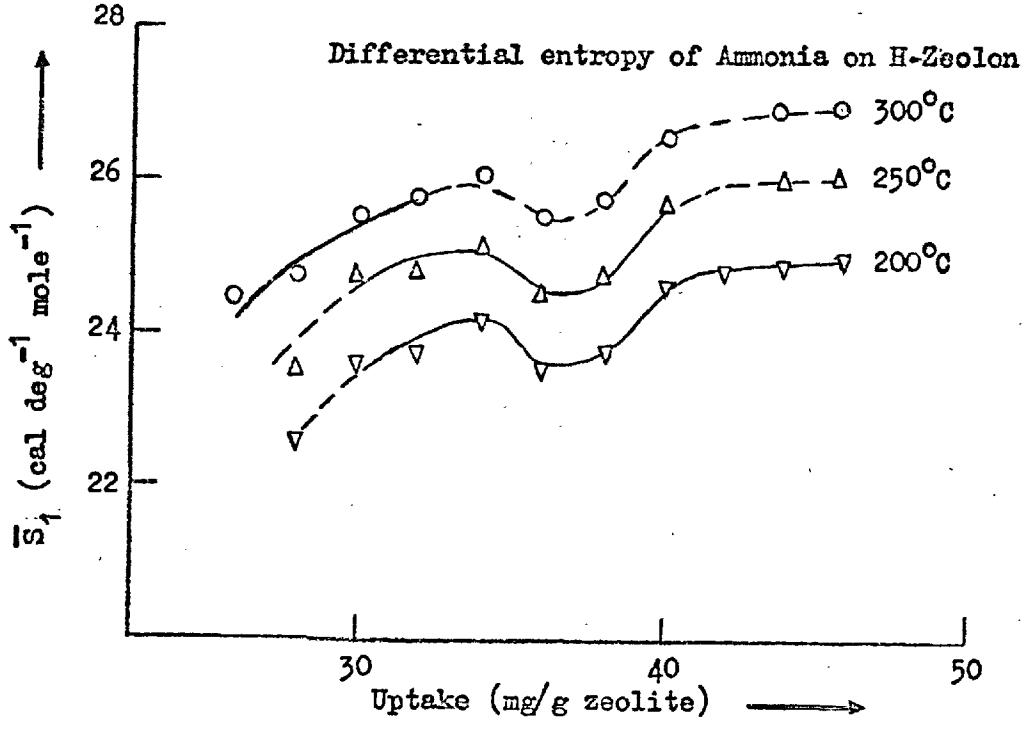

Differential entropy of Ammonia on H-Zeolon
300°C
250°C
200°C
28
26
24
22
$\bar{S}_1$ (cal deg^{-1} $mole^{-1}$)
30
40
50
Uptake (mg/g zeolite)

Fig. 45

Differential Entropy of Ammonia in NaY

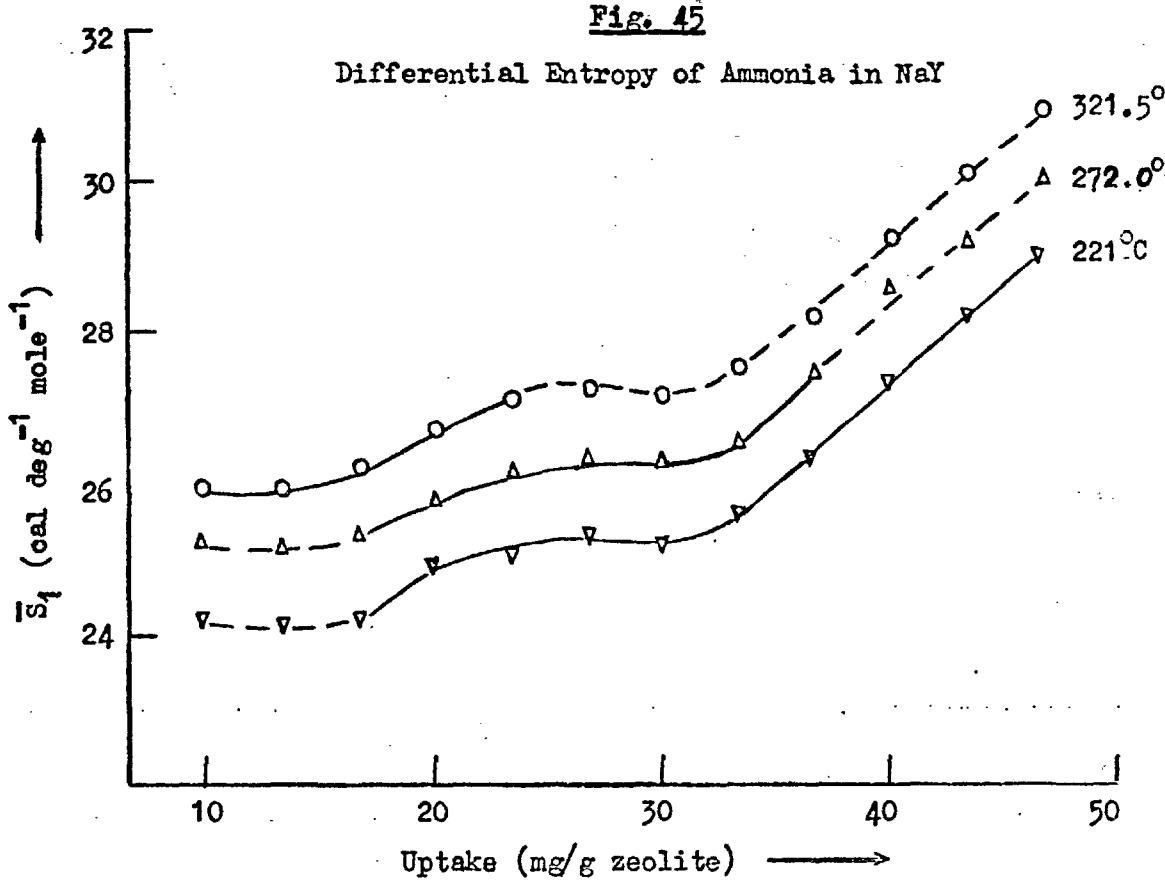
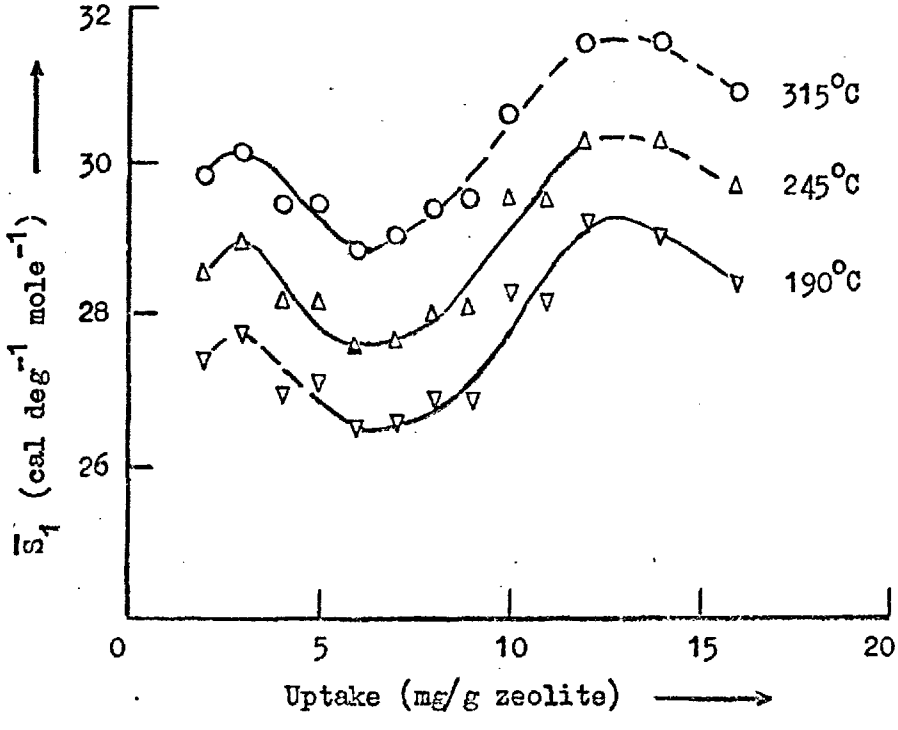


Fig. 46

Differential Entropy of Ammonia in KL



$$\Delta \bar{S}_1 = \tilde{S}^o_g - \bar{S}_1 \qquad (14)$$

and obtained from

$$\Delta \bar{S}_1 = -\frac{\Delta \bar{H}_1}{T} + R \ln \frac{p}{p^o} \qquad (14a)$$

where p^o and p have the same meaning as in (13). The half standard entropy of sorption should be independent of temperature[62]. This behaviour is well established by the data of table 7 . The differential entropy plots in figs. 44,45 and 46 show that the sorbents exhibit heterogeneity. The plots for KL show two maxima. In the H-Zeolon curves there is one well defined maximum and a second one is also probable. The differential entropy curves for NaY show a maximum and then increase with increasing uptake. Differential entropy should eventually decrease with increasing uptake. The apparent anomaly in the NaY curve is due to the small range of uptakes examined. A more detailed study should involve isotherm measurements at lower temperatures, extending the uptake range.

Table 7

Half standard entropies of sorption of ammonia

(a) H-Zeolon					
	$\Delta \bar{S}_1$ (cal deg^{-1} $mole^{-1}$)				
Temperature (^oK)	473	503	523	543	573
Uptake (mg/g)					
28		27.63	27.38	27.40	27.37
36	26.63	26.74	26.61	26.66	
38	26.28	26.32	26.32	26.31	
40	25.50	25.53	25.46		
44	25.25	25.15			

Table 7 (continued)

(b) NaY					
	$\Delta\bar{S}_1$ (cal deg^{-1} mole^{-1})				
Temperature (^{o}K)	494	519	545	570	594.5
Uptake (mg/g)					
13.30				26.22	26.68
23.27	25.52	25.38	25.48	25.54	25.43
29.92	25.41	25.31	25.35	25.38	
36.57	24.26	24.28	24.38		
39.90	23.34	23.33			
43.22	22.41	22.44			

(c) KL					
	$\Delta\bar{S}_1$ (cal deg^{-1} mole^{-1})				
Temperature (^{o}K)	463	493	518	553	588
Uptake (mg/g)					
2.0		22.65	22.52	22.54	22.58
6.0	23.50	23.64	23.57	23.62	
7.0	23.38	23.60	23.42	23.40	
10.0	21.59	21.39	21.70		
12.0	20.76	20.24	20.84		
14.0	20.89	20.83			
16.0	21.48	21.34			

3.3 Selectivity and affinity

A quantitative measure of the affinity of a sorbate for a certain sorbent is the decrease in chemical potential when the gas is transferred reversibly and isothermally from the gas phase at a standard pressure p^o (equal to 1 atm) into an infinite amount of the sorbent-sorbate mixture over which the equilibrium pressure is p. If we assume that the behaviour of the gas is not far from the ideal, this free energy change is given by:

$$\Delta\mu = RT\ln\frac{p}{p^o} \qquad (46)$$

Equation (46) was used to calculate changes of free energy at different uptakes for the systems examined. The plots of $-\Delta\mu$ vs uptake are given for three temperatures in figs. 47, 48 and 49. In order to make comparison possible, the change in chemical potential was plotted against the amount sorbed expressed in mg of ammonia per cc of intracrystalline volume of sorbent (n). The free energy changes vs uptake for H-Zeolon, NaY and KL at 246°C are shown in fig. 50 ; the curve for H-Zeolon has been calculated from the isotherm taken at 250°C, but since $\Delta\mu$ increases with decreasing temperature and the curve for H-Zeolon lies well above the others such a comparison is permissible. The affinity for ammonia shown by H-Zeolon is quite outstanding. The affinity sequence for ammonia at 246°C is:

$$\text{H-Zeolon} > \text{NaY} \gg \text{KL} .$$

This exceptional affinity for ammonia shown by H-Zeolon is believed to be due to chemisorption of ammonia on H-Zeolon to form the ammonium form of the zeolite.

Fig. 47

H-Zeolon - NH_3

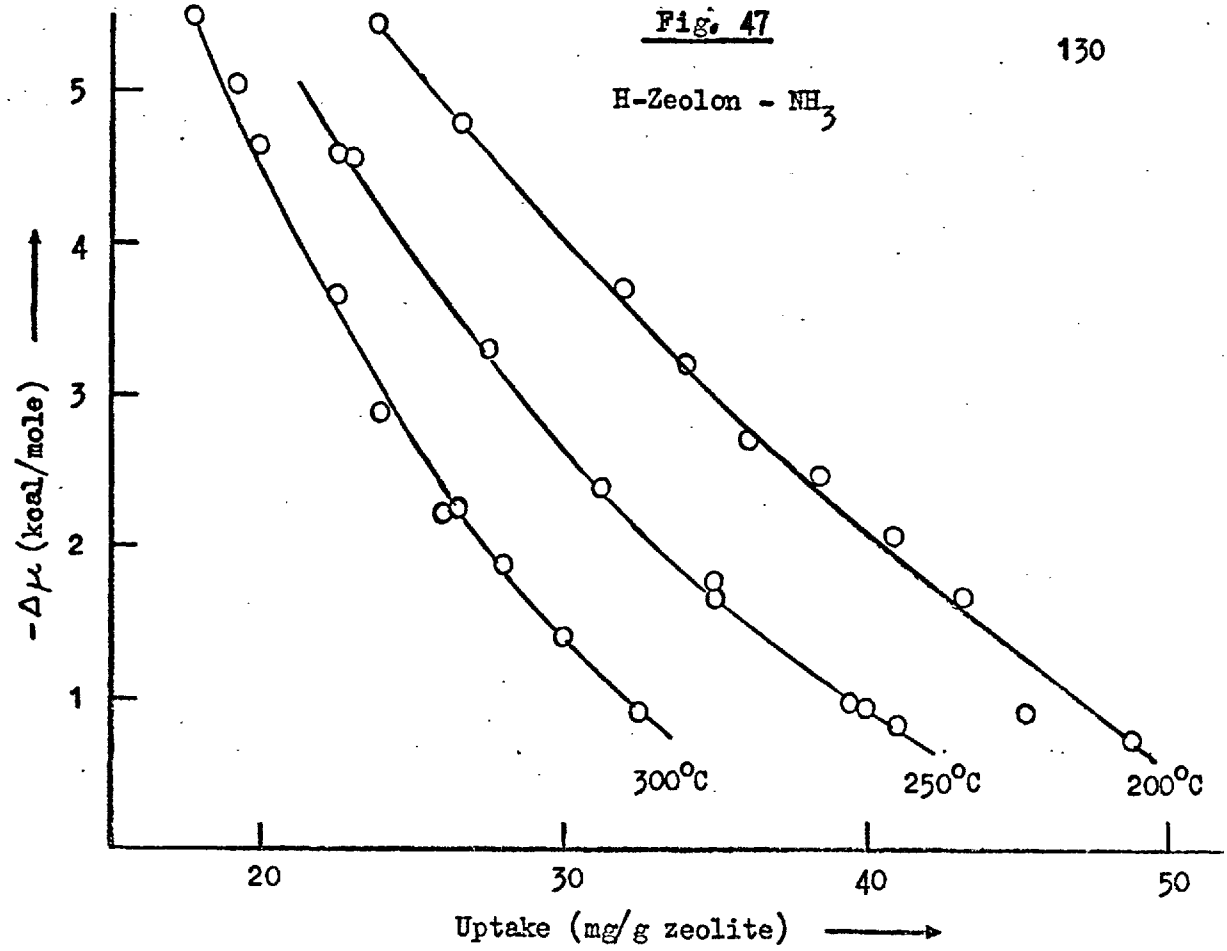


Fig. 48

NaY - NH_3

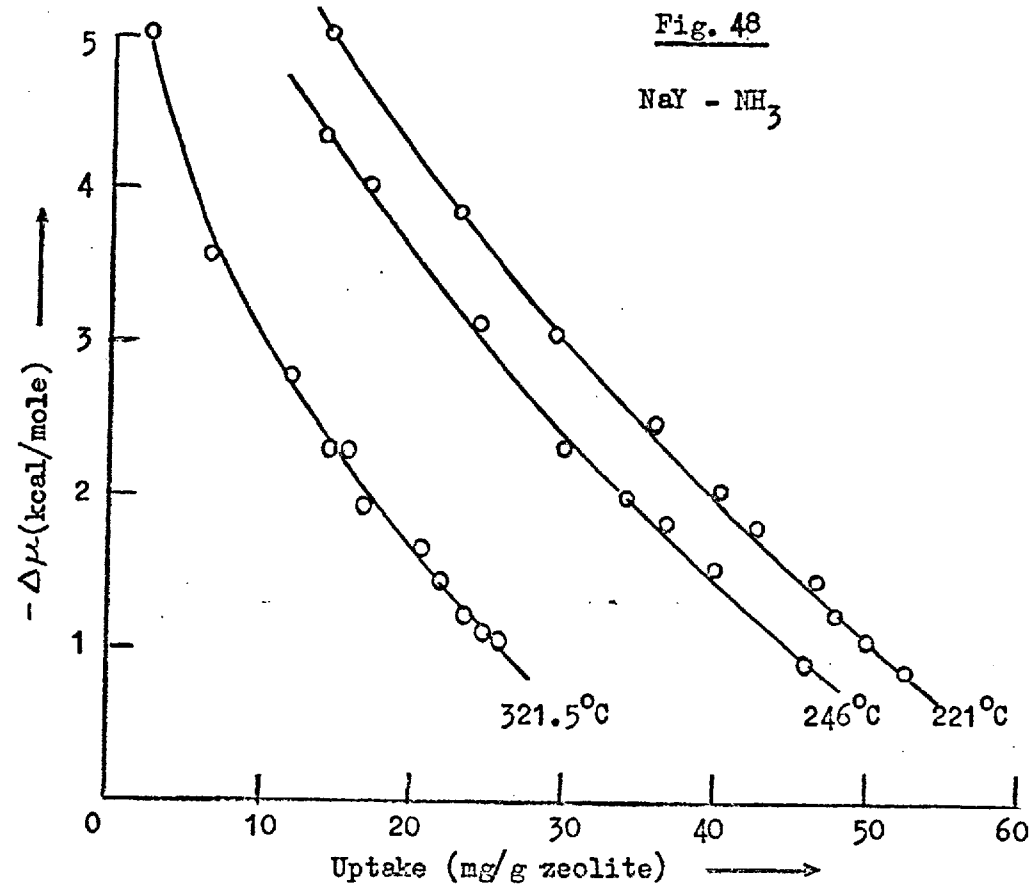


Fig. 49

KL-- NH_3

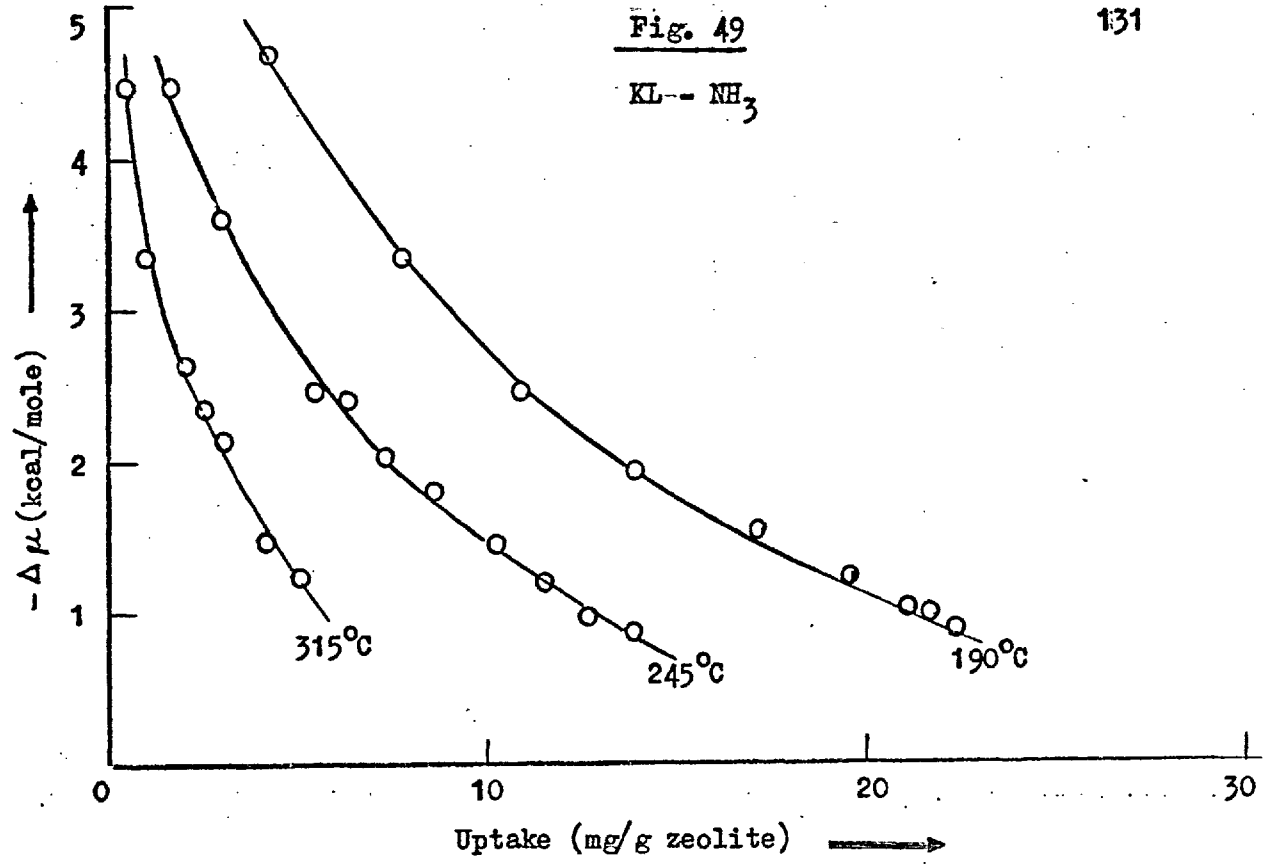
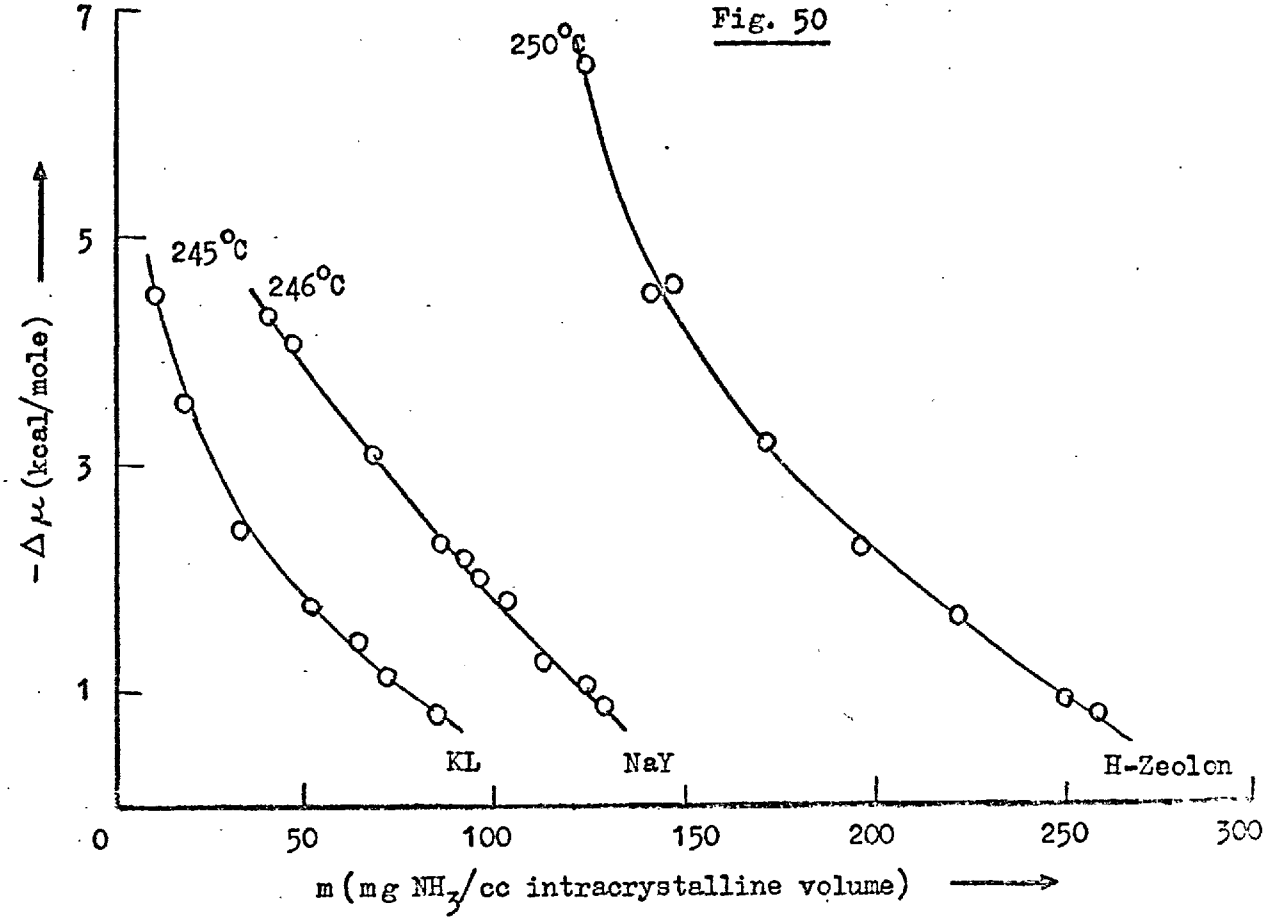


Fig. 50



3.4 Empirical isotherm equations

The results obtained for the systems NaY-NH_3 and KL-NH_3 were used to evaluate the virial coefficients and calculate the thermodynamic properties of the sorbed phase in its standard state. Also, activity coefficients for the sorbed phase were evaluated from the experimental data; activity coefficients calculated from isotherm models were compared with the former.

Evaluation of virial coefficients

Equation (35) can be written

$$\ln K = \ln\frac{c_s}{p} + 2A_1c_s + \frac{3}{2}A_2c_s^2 + \frac{4}{3}A_3c_s^3 + \ldots\ldots \qquad (47)$$

where c_s is the uptake expressed in moles of ammonia per litre of dehydrated zeolite (or per litre of zeolite-sorbate mixture) and p the equilibrium pressure in atmospheres. From the plot of $\ln\frac{c_s}{p}$ vs c_s, lnK can be found; it is the value of $\ln\frac{c_s}{p}$ for $c_s=0$. Also coefficients A_1, A_2, ..., as many as are necessary to describe the curve $\ln\frac{c_s}{p} = f(c_s)$ obtained for each isotherm, can be evaluated.

In the case of ammonia sorbed on NaY the plots of $\ln\frac{c_s}{p}$ vs c_s were straight lines so lnK could easily be found by extrapolation. Since it was difficult to obtain reliable results in the low pressure part of the isotherm (or the low c_s part of the curve $\ln\frac{c_s}{p} = f(c_s)$) the constant K and the coefficients A_1, A_2, ... thus obtained will describe the part of the isotherm which was used to obtain the reliable part of the above mentioned curve. The shape of this curve determines the number of the coefficients needed. For the system NaY-NH_3 only one coefficient was needed to describe the isotherms at each temperature. Thus equation (47) becomes

$$\ln K = \ln\frac{c_s}{p} + 2A_1c_s$$

which is a straight line with intercept lnK and slope $2A_1$. The equation which describes the isotherm of ammonia on NaY has the form

$$\frac{c_s}{p} = K\exp(-2A_1c_s)$$

The shape of the curve $\ln\frac{c_s}{p} = f(c_s)$ changed with the temperature for the system KL-NH_3. At 315°C it was concave to the c_s-axis; at 280°C it was a straight line and at lower temperatures it was convex to the c_s-axis. More than one coefficient was necessary to describe most of the isotherms. They were found by solving systems of simultaneous equations.

No attempts were made to calculate K's and A's for the system H-Zeolon - NH_3 since the isotherms were very rectangular and it was not possible to obtain reliable points for the curve $\ln\frac{c_s}{p} = f(c_s)$ over a reasonable range of c_s. The values of K's and A's obtained for the systems NaY-NH_3 and KL-NH_3 are listed in Table 8. These values were used in equation (35) to reproduce the isotherms. The reproducibility was very good for both systems as one can see from figs. 51 and 52.

Calculation of thermodynamic properties at the standard state

If in equation (25) we replace a_s by $c_s\gamma_s$ and a_g by p, we have:

$$K = \left(\frac{c_s\gamma_s}{p}\right)_{eq} \qquad (48)$$

Equation (48) was used to calculate γ_s and a_s at different values of c_s. From the plot of a_s vs c_s the concentration for which a_s=1 was found. This was the concentration of the sorbed phase at the standard state. The values of lnK for different temperatures as calculated from the curve $\ln\frac{c_s}{p} = f(c_s)$ were used in the formulae (22)

Fig. 51

NaY - NH_3

Test of the Isotherm Equation

$$\frac{c_s}{p} = K\exp(-AC_s)$$

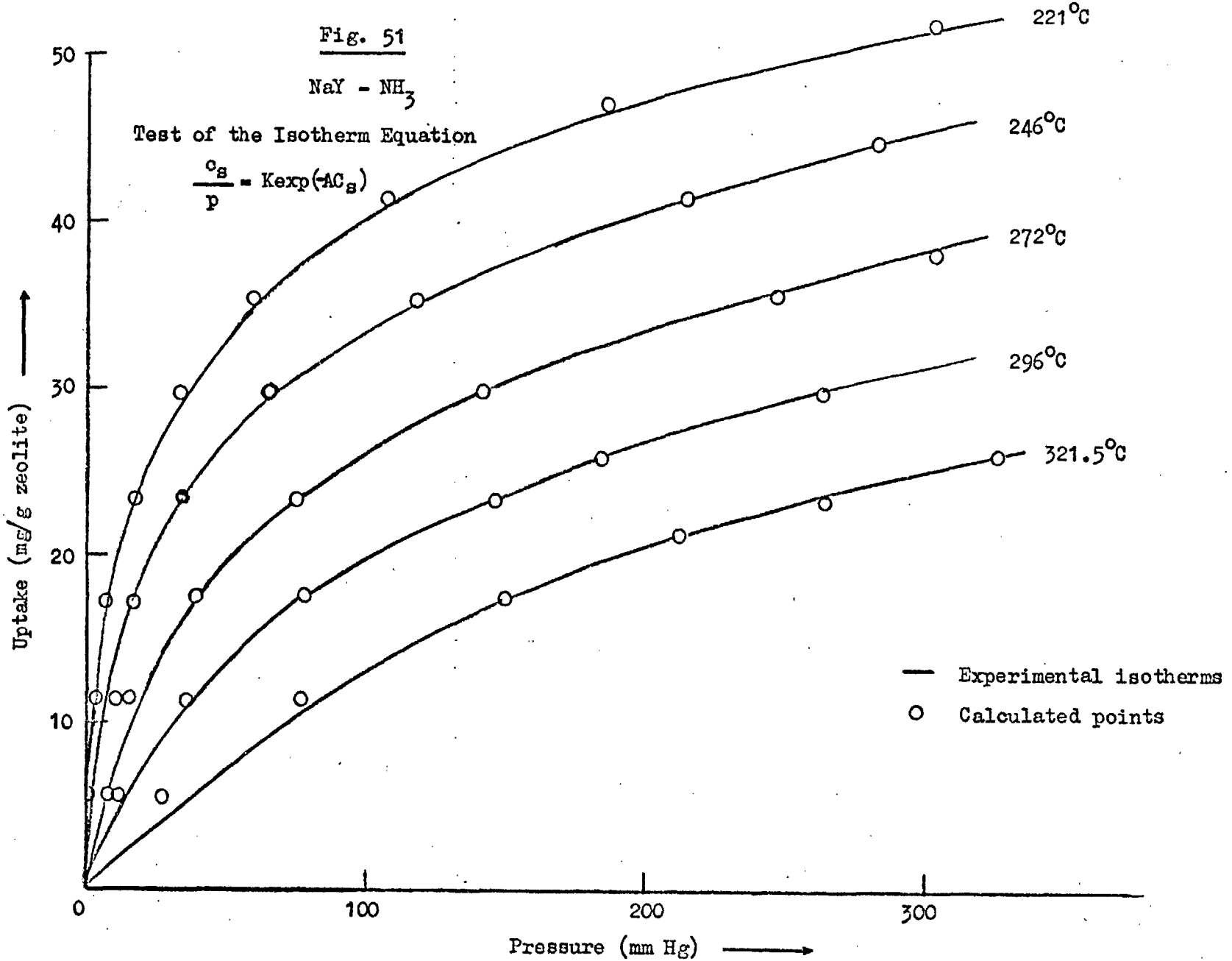


Fig. 52

KL - NH_3

Test of the isotherm equation

$$\frac{c_s}{p} = K \exp(-2A_1 c_s - \frac{3}{2} A_2 c_s^2)$$

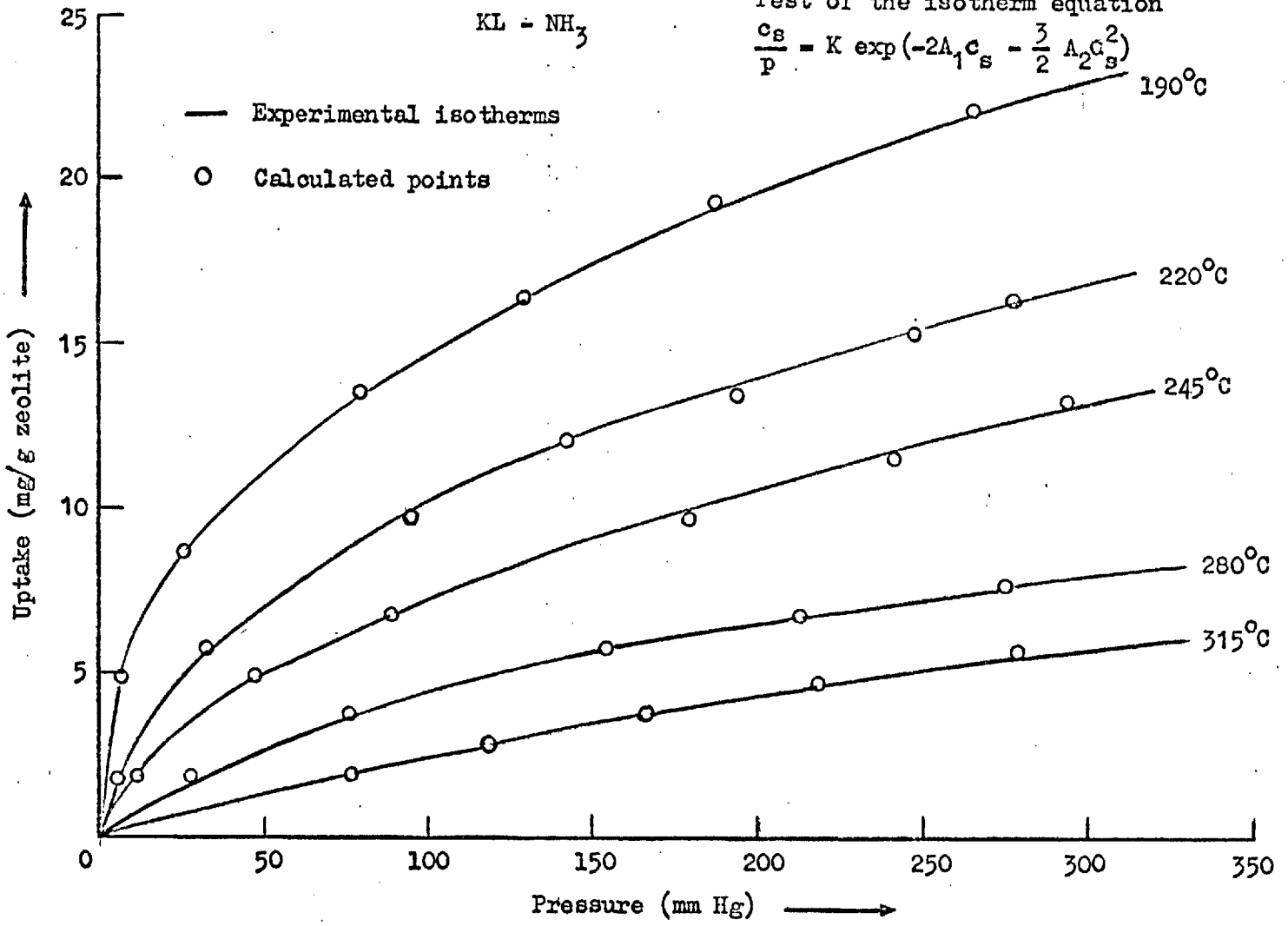


Table 8

Values of constants K and coefficients A

(a) NaY-NH_3

Temp.(°C)	lnK	K	A_1
221	6.30	537.0	+0.445
246	5.36	214.0	+0.400
272	4.53	92.0	+0.383
297	3.73	41.5	+0.350
321.5	2.84	17.1	+0.273

(b) KL-NH_3

Temp.(°C)	lnK	K	A_1	A_2
190	5.1	164.02	1.230	-0.308
220	3.86	47.42	1.169	-0.382
245	3.2	24.53	1.353	-0.638
280	2.0	7.38	+0.75	0.0
315	0.8	2.22	+0.23	0.05

and (23) for calculation of the values of ΔG_o, ΔH_o and ΔS_o, i.e. the free energy, enthalpy and entropy of sorbed ammonia at the standard state. ΔH_o was calculated from the slope of the plot lnK vs 1/T of figs. 53 and 54. The values of these thermodynamic quantities for the systems NaY-NH_3 are given in Table 9 .

Fig. 53

NaY - NH_3

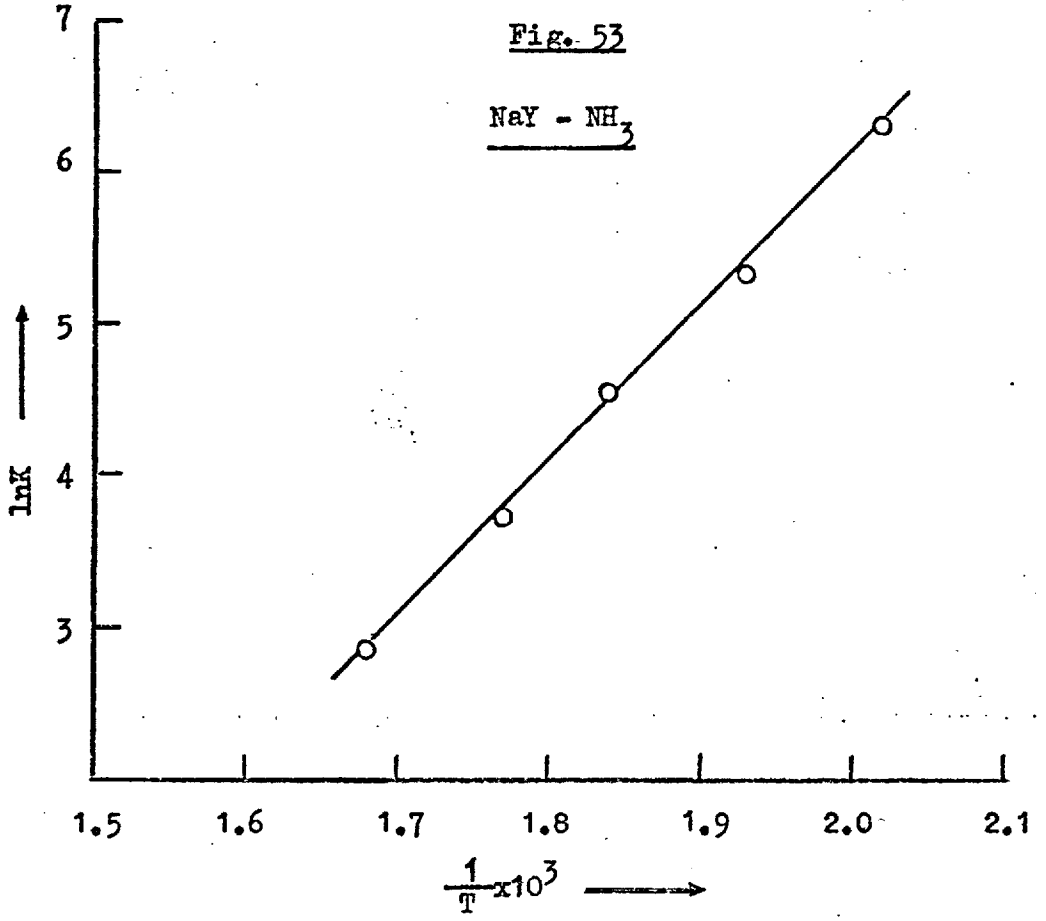


Fig. 54

KL - NH_3

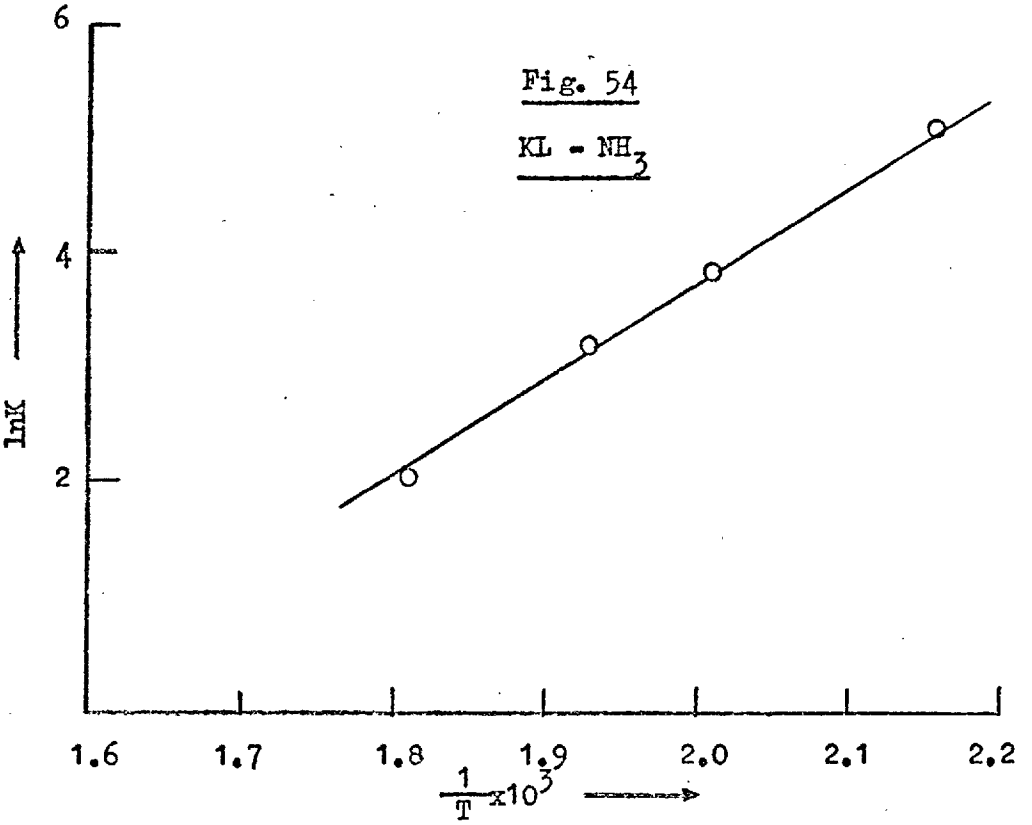


Table 9

Temperature (°C)	C_s (mole/l)	$-\Delta G_o$ (kcal/mole)	$-\Delta H_o$ (kcal/mole)	$-\Delta S_o$ (cal/mole^{-1}deg^{-1})
NaY-NH_3				
221	0.20	6.19	20.40	28.72
246	0.30	5.53		28.70
272	0.64	4.90		28.50
297	0.68	4.21		28.60
321.5	0.71	3.35		28.70
KL-NH_3				
190	0.34	4.70	16.50	25.50
220	0.40	3.78		25.80
245	0.40	3.28		25.60
280	0.49	2.19		25.90

3.5 Activity coefficients and correspondence with isotherm models

Equation (48) can be used for the calculation of the activity coefficients of the sorbed phase. Simple comparison of this equation with equilibrium constants as given by isotherm models (Ch.2, Part I) enable us to obtain expressions for the activity coefficients for every model. The expressions thus obtained and used in the following discussion are summarized in Table 10.

Table 10

Activity coefficients of the sorbed phase for different isotherm models

Isotherm	Equilibrium constant	Activity coefficient
Langmuir	$K = \frac{\theta}{p(1-\theta)}$	$\gamma_L = \frac{c_{sat}}{c_{sat}-c}$
Volmer	$K = \frac{\theta}{p(1-\theta)} \exp \frac{\theta}{(1-\theta)}$	$\gamma_V = \frac{c_{sat}}{c_{sat}-c} \exp\left(\frac{c}{c_{sat}-c}\right)$
Van der Waals	$K = \frac{\theta}{p(1-\theta)} \exp\left(\frac{\theta}{1-\theta} - \alpha\theta\right)$	$\gamma_{VW} = \frac{c_{sat}}{c_{sat}-c} \exp\left(\frac{c}{c_{sat}-c} - \alpha\frac{c}{c_{sat}}\right)$
Empirical	$K = \frac{c}{p} \exp(2A_1c + \ldots)$	$\gamma_E = \exp(2A_1c + \ldots)$

The values of c_{sat} used were obtained from the limiting slope of the plot $\frac{p}{x}$ vs p at every isotherm temperature. The value of α used in the Van der Waals isotherm model was calculated from the formula[64,72]

$$\alpha = \frac{a}{bkT}$$

where a and b are the three dimensional Van der Waals constants, k the Boltzman constant and T the absolute temperature. For the system KL-NH_3 since the calculated value for the Van der Waals constant gave very small values for the activity coefficient α was taken equal to 1. Since γ tends to 1 as c_s tends to zero, the expression for γ obtained from Langmuir, Volmer and Van der Waals isotherms were multiplied by c_{sat}.

In figs. 55 &56 the values of γ calculated from the experimental results and for different isotherm models are plotted at 221°C for NaY-NH_3 and at 220°C for KL-NH_3, respectively. In general, the values of γ obtained from equation (48) and from the empirical expression were in very good agreement with each other. The values of γ, calculated from Volmer's isotherm, are closer to the experimental ones than those calculated from Langmuir's or Van der Waals'. Besides γ, other thermodynamic quantities (solution thermodynamics) can be used to test isotherm models. Figs. 55 and 56 show that γ is very sensitive to c_s and it might prove to be a useful test for isotherm models.

3.6 The sorption of ammonia on HY

One isotherm was taken at 245.5°C of ammonia on HY. The sample of HY was prepared as described on p.103 and it was found by X-ray powder photography to be 80% crystalline (NaY = 100%). The isotherm was irreversible and complete removal of sorbed ammonia was attained only after evacuation at 340°C. The zeolite was X-rayed after the end of the experiment and further decomposition was found (ca 60% crystalline).

Benson et al[44] obtained reversible isotherms of ammonia on a ca 70% decationated sample of zeolite Y; its SiO_2:Al_2O_3 ratio was 4.5 and it was prepared by heating the ammonium form at 390°C. Cattanach et al[40] studied the thermal decomposition of NH_4Y. Their sample contained 10% Na^+ (expressed as a percentage of exchangeable cations) and its SiO_2:Al_2O_3 ratio was 5.52. They found that if NH_4Y was heated to 450°C by allowing ammonia into the system the NH_4Y could be reconstituted. But the dehydroxylated-Y (that could be obtained by heating the NH_4Y above 450°C) was extremely unstable. All their attempts to reconstitute NH_4Y from the dehydroxylated form failed and resulted in complete loss of crystallinity.

Fig. 55

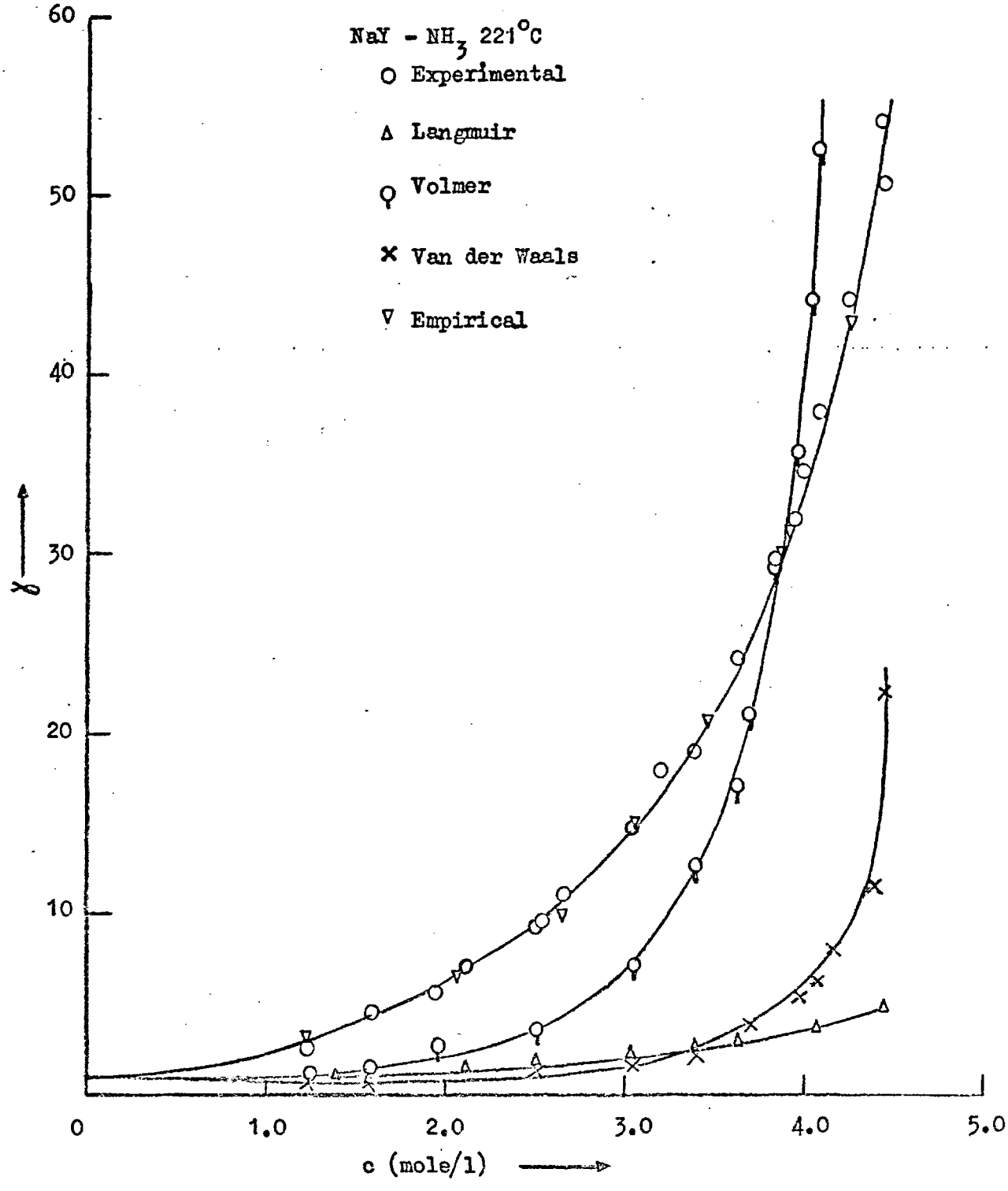

NaY - NH3 221°C
O Experimental
Δ Langmuir
Q Volmer
× Van der Waals
▽ Empirical
60
50
40
30
20
10
γ
0
1.0
2.0
3.0
4.0
5.0
c (mole/l)

Fig. 56

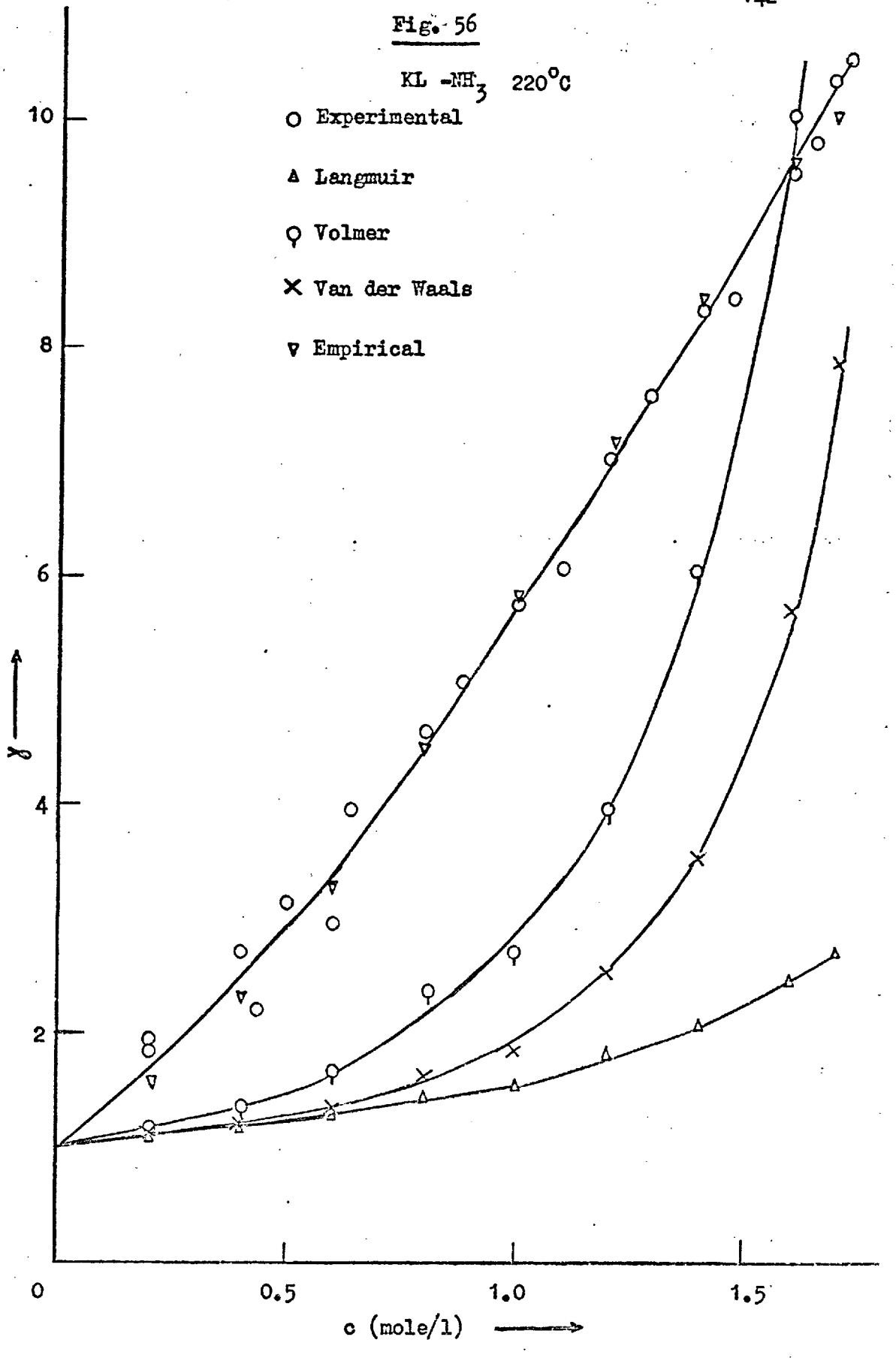
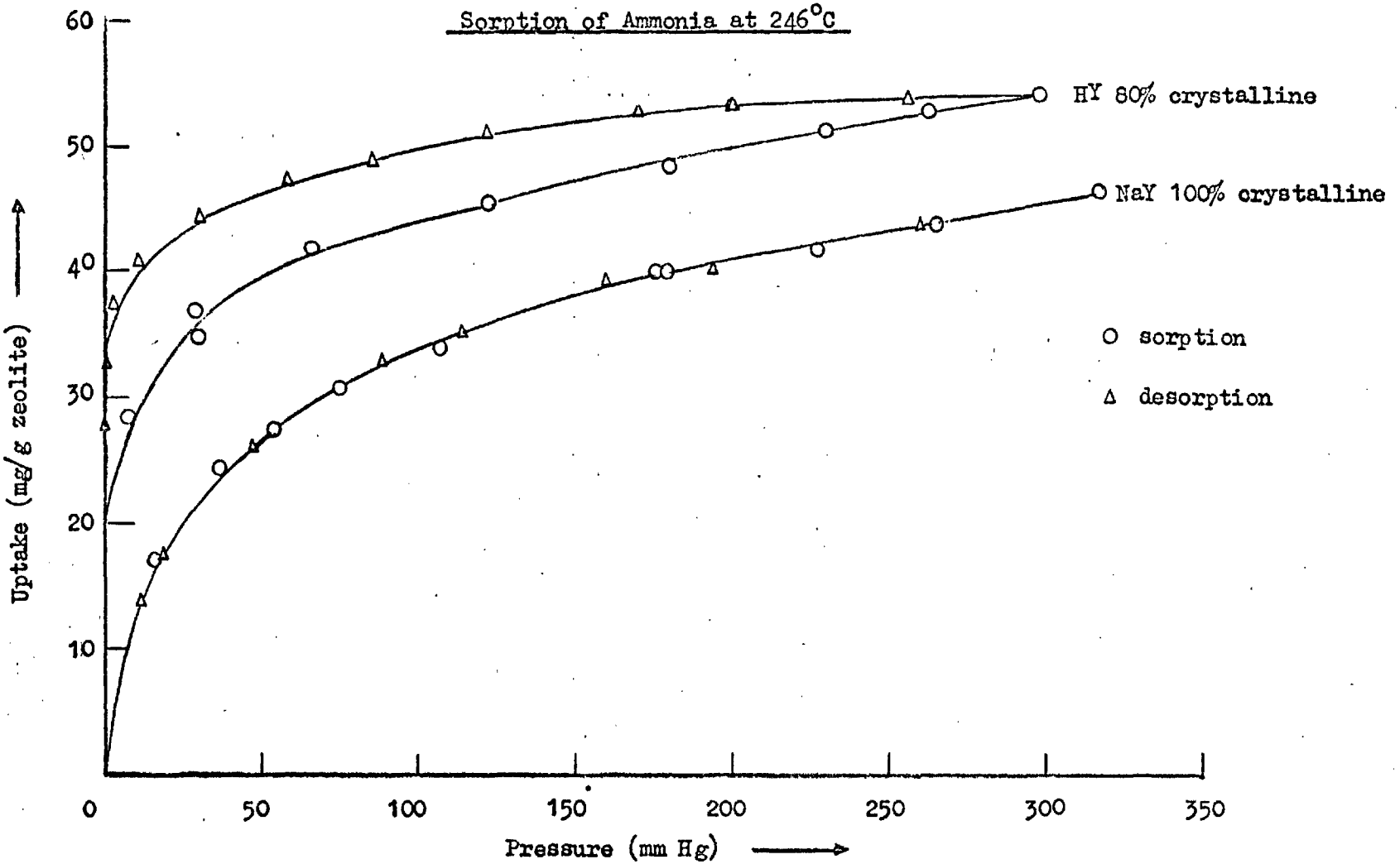

KL -NH3 220°C
Experimental
Langmuir
Volmer
Van der Waals
Empirical
10
8
6
4
2
γ
0
0.5
1.0
1.5
c (mole/l)

Fig. 57


Sorption of Ammonia at 246°C
HY 80% crystalline
NaY 100% crystalline
O sorption
Δ desorption
Uptake (mg/g zeolite)
Pressure (mm Hg)
60
50
40
30
20
10
0
50
100
150
200
250
300
350

The sample used in the present work was prepared by heating NH_4Y at 440°C; it contained 2% Na^+ and had a $SiO_2:Al_2O_3$ ratio of 4.78. A 20% loss of crystallinity was observed during decationation. This sample appears to be more sensitive than Cattanach's (Benson's being excluded from comparison because of its high Na^+ content[97]). Since the sample used in the present work was poorer in silica it is possible that this accounts for its poor stability. The $SiO_2:Al_2O_3$ ratio of the zeolites is believed to be one of the main factors of the stability of the decationated zeolites. The observed hysteresis is believed to be connected in part with the decomposition of the zeolite.

In fig. 57 the sorption isotherm of ammonia on HY is compared with that on NaY. Despite the difference in crystallinity of the samples, the sorption is higher in HY and the isotherm is more rectangular than in NaY. This experiment in connection with previous findings[28,40] suggests than ammonia sorption might prove to be a good test of the stability of decationated zeolites.

4. AMMONIUM CHLORIDE - ZEOLITE SORPTION COMPLEXES

4.1 H-Zeolon - ammonium chloride

Experimental isotherms

The sorption of ammonium chloride was studied in H-Zeolon at 230°C. Sorption and desorption were generally slow and their rates depended on the sorbate temperature. At sorbate temperatures higher than 200°C equilibrium was established in ca 10-15 hours but at lower temperatures in ca 40 hours. During this time pressure and uptake changed in the same way (i.e. both increased or decreased). The points measured between "equilibrium" points fit the isotherm. (By "equilibrium" we mean that pressure and uptake remained constant with time, for fixed sample and reservoir temperatures.) A residual uptake of 30 mg/g and a residual pressure of 6.5 mm Hg, which decreased extremely slowly with time, were found at the end of the desorption cycle. This pressure was due to condensable gases (presumably hydrogen chloride and ammonia) because it became negligible when the sorbate reservoir was put in liquid nitrogen. A decrease in uptake was also noticed. The residual uptake (and pressure) could be removed by raising the sample temperature to 350°C. An explanation for this uptake and pressure is given on p.161.

The pressures (p) measured at uptakes less than the saturation uptake were higher than the vapour pressure of ammonium chloride (p_o) corresponding to the sorbate reservoir temperature. The ratio p/p_o is plotted against reservoir temperature and measured pressure in figs. 58 and 59, respectively. The value of p/p_o tends to 1 as the sorbate temperature approaches the sample temperature or as the pressure approaches the vapour pressure of ammonium chloride corresponding to the isotherm temperature (i.e. 24 mm Hg).

Fig. 58

H-Zeolon - NH_4Cl
230°C

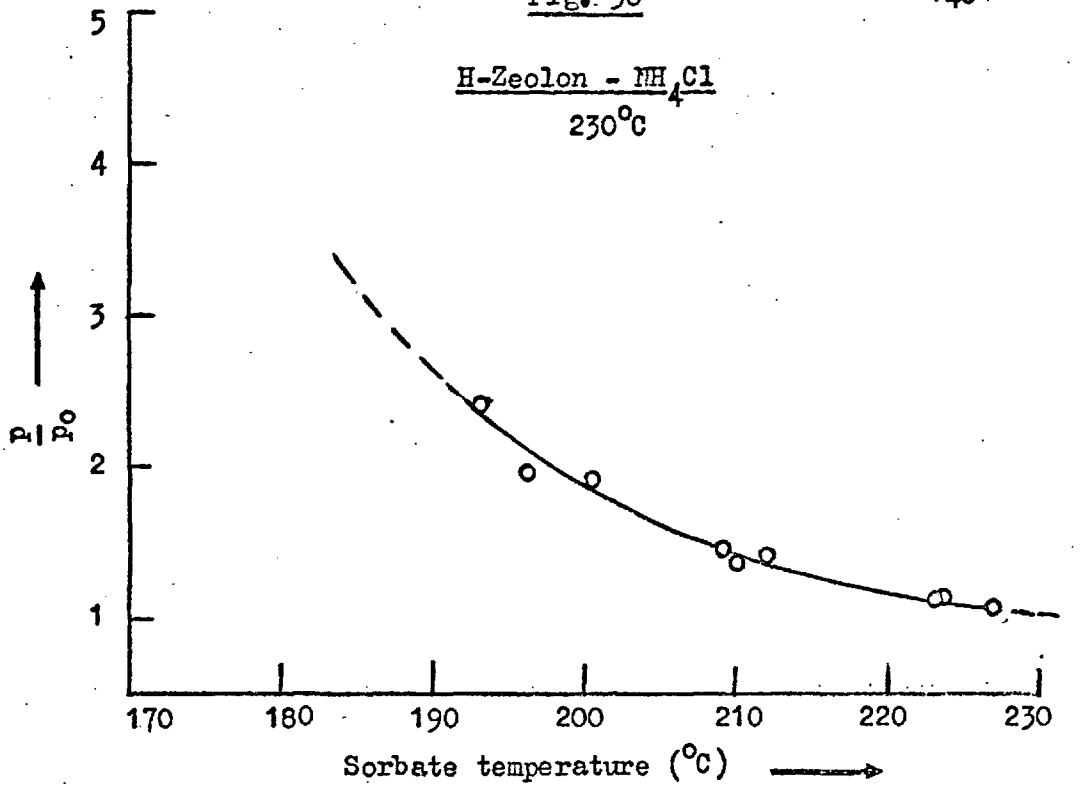
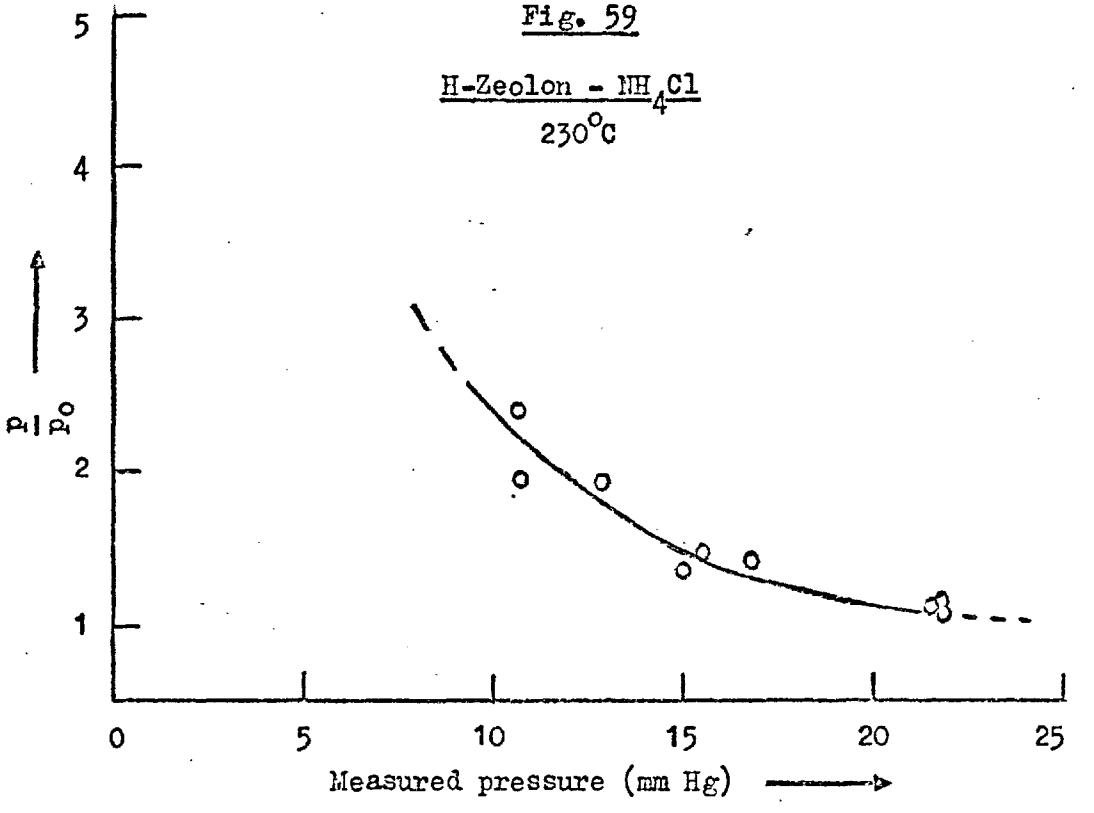


Fig. 59

H-Zeolon - NH_4Cl
230°C



The reproducibility of the isotherm was not good. When the sorption and desorption cycles were repeated on the same sample without opening the apparatus, the isotherm was very well reproduced. When different samples were used, or even the same sample with the apparatus being opened and then sealed and the zeolite subsequently outgassed, the initial isotherm could not be reproduced. However, the measured isotherms had the same shape (sigmoid) and the saturation uptake did not show significant change. A typical sorption isotherm of ammonium chloride vapour on H-Zeolon at 230°C, together with the isotherms of pure ammonia and pure hydrogen chloride measured at the same temperature, is shown in fig. 60 . The isotherms for the pure ammonia and pure hydrogen chloride have qualitatively the form of Langmuir's isotherm. The isotherm contour of ammonium chloride is that which typifies strong interaction corresponding with the steeply rising part of the isotherm. The strong interaction between ammonia and hydrogen chloride results in an increase in the amount sorbed from the mixture compared with that from the pure components at the same temperature.

Some theoretical considerations

Possible equilibria in the system ammonium chloride - H-Zeolon include:

$$NH_4Cl_{(s)} \rightleftharpoons NH_4Cl_{(g)} \rightleftharpoons NH_{3(g)} + HCl_{(g)} \qquad (49)$$

$$xHCl_{(g)} + yNH_{3(g)} + HZ \rightleftharpoons HZ.xHCl_{(a)}.yNH_{3(a)} \qquad (50)$$

with $y \geqslant x$

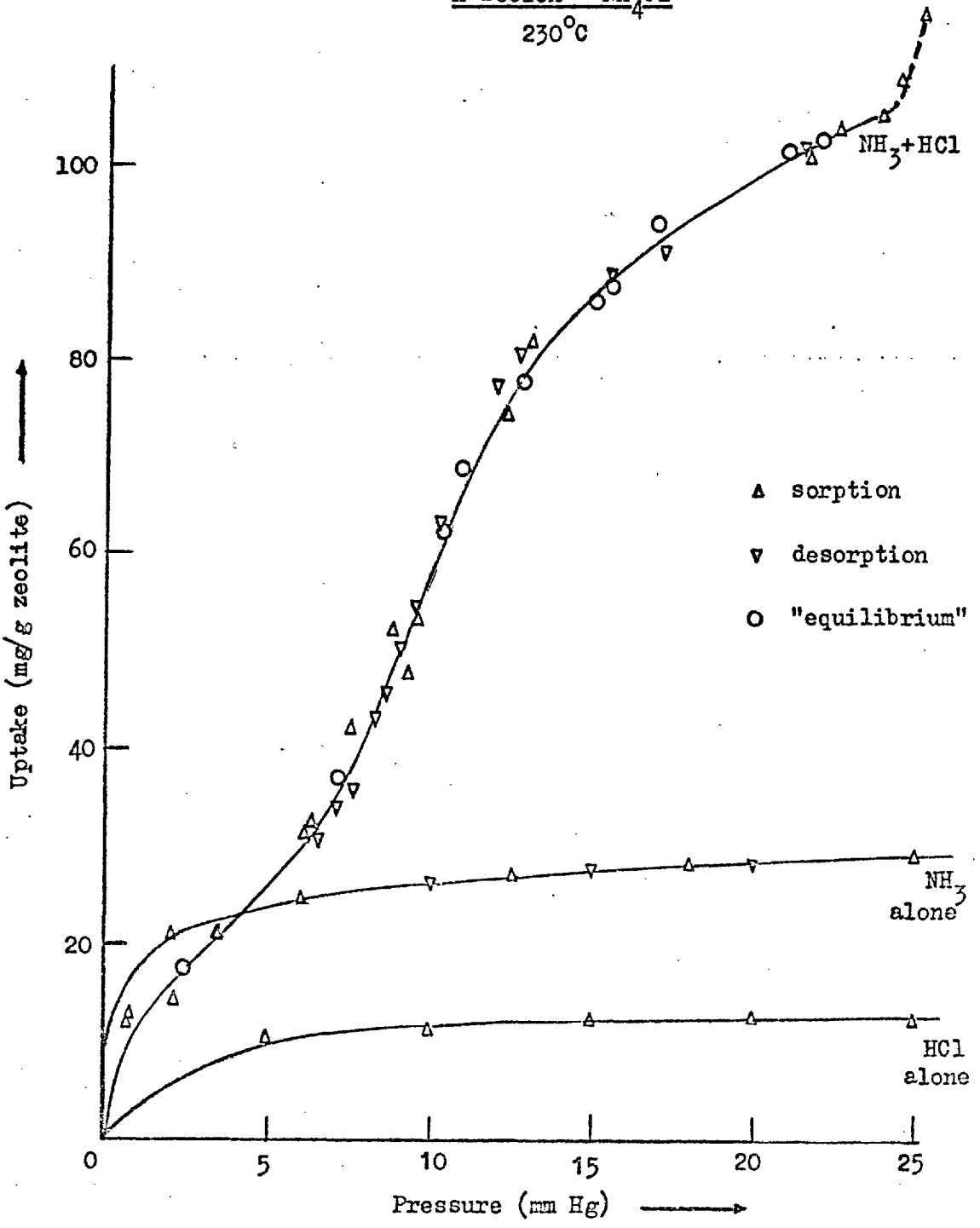
$$NH_{3(a)} + HCl_{(a)} \rightleftharpoons NH_4Cl_{(a)} \qquad (51)$$

$$NH_{3(a)} + HZ \rightleftharpoons NH_4Z \qquad (52)$$

Fig. 60

H-Zeolon - NH_4Cl

230°C



where "Z" denotes zeolite, "s" solid, "g" gas, and "a" adsorbed phase. Besides the reactions (49-52), another two, namely an ion-exchange reaction of the existing sodium ions in H-Zeolon (p.17) and a reaction of hydrogen chloride with the aluminium of the zeolite (p.86) will not be considered since it is believed that these reactions do not take place in this sorbent. Evidence for this was obtained from the following observations:

(a) No aluminium or sodium was found after washing the zeolite with distilled water after the end of the sorption experiment.

(b) No residual uptake was found after heating the zeolite at 350°C.

(c) The isotherms were reversible.

Therefore, two reactions are important during the sorption of ammonium chloride on H-Zeolon, reaction (51) and reaction (52). Reaction (51) represents the recombination of ammonium chloride from ammonia and hydrogen chloride in the zeolitic cavities, and explains the increase in sorption from the mixture compared with that of the pure components. This reaction results in removal of ammonia and hydrogen chloride from the vapour phase in equivalent amounts.

Reaction (52) represents the formation of ammonium-Zeolon. This reaction, which explains why ammonia is sorbed more than hydrogen chloride on H-Zeolon, results in removal of more ammonia than hydrogen chloride from the gas phase. Therefore, a disproportionation arises in the gas phase and the pressure becomes higher than the vapour pressure of ammonium chloride corresponding to the reservoir temperature.

That this disproportionation can take place in the gas phase can be shown theoretically. A method for analysis of these results can also be derived, based upon the law of conservation of mass and

the equation of ideal gases. The equilibrium

$$NH_4Cl_{(g)} \rightleftharpoons NH_3{}_{(g)} + HCl_{(g)} \qquad (49)$$

lies over to the right, and the equilibrium constant, K_1, is

$$K_1 = \frac{a_{NH_3}\, a_{HCl}}{a_{NH_4Cl}}$$

where a denotes activity. The activities can be replaced by pressures and, since K_1 is very large, p_{NH_4Cl} is very small and in the presence of solid ammonium chloride is a constant k which rises with the temperature. Thus from

$$K = K_1 k = p_{NH_3} \cdot p_{HCl} \qquad (53)$$

and also p

$$p\text{-}k(T) = p_{NH_3} + p_{HCl} \qquad (54)$$

where p is the total pressure, we obtain

$$\begin{aligned} p\text{-}k(T) &= \frac{K}{p_{HCl}} + p_{HCl} \\ p\text{-}k(T) &= \frac{K}{p_{NH_3}} + p_{NH_3} \end{aligned} \qquad (55)$$

Since hydrogen chloride is less strongly sorbed than ammonia, the partial pressure of ammonia (p_{NH_3}) must be lower than that of hydrogen chloride. When equations (55) are solved, the possible roots are:

$$\begin{aligned} p_1 = p_{HCl} &= \tfrac{1}{2}\left[(p\text{-}k) + \sqrt{(p\text{-}k)^2 - 4K} \right] \\ p_2 = p_{NH_3} &= \tfrac{1}{2}\left[(p\text{-}k) - \sqrt{(p\text{-}k)^2 - 4K} \right] \end{aligned} \qquad (56)$$

with

$$\frac{p_{HCl}}{p_{NH_3}} = \frac{1 + \sqrt{1 - \frac{4K}{(p-k)^2}}}{1 - \sqrt{1 - \frac{4K}{(p-k)^2}}} \tag{57}$$

Thus, as p increases sufficiently $\frac{p_{HCl}}{p_{NH_3}}$ tends to 1 but for smaller values of p this ratio is greater than 1. No real roots are possible for equations (55) when $\frac{4K}{(p-k)^2} \geqslant 1$. In equation (53) it is known that k is very small [33], the pressure p being approximately

$$p = p_{NH_3} + p_{HCl} \tag{58}$$

In absence of sorbent:

$$K_1 k = p^o_{NH_3} \cdot p^o_{HCl} = K \tag{59}$$

and

$$p = p^o_{NH_3} + p^o_{HCl} \tag{60}$$

also

$$p^o_{NH_3} = p^o_{HCl} \tag{61}$$

thus

$$p^o_{NH_3} = \sqrt{K} = p^o_{HCl} \tag{62}$$

and

$$\tfrac{1}{2}(p_o - k) = p^o_{NH_3} = p^o_{HCl} \tag{63}$$

and

$$p_o = 2\sqrt{K} \tag{64}$$

where p_o is the pressure of the pure ammonium chloride at the temperature

of the solid ammonium chloride. With equation (64) or the exact relation

$$(p_o - k) = 2\sqrt{K} \tag{65}$$

equations (56) and (57) become:

$$p_{HCl} = \tfrac{1}{2}(p-k)\left[1 + \sqrt{1 - \left(\frac{p_o-k}{p-k}\right)^2}\right]$$

$$p_{NH_3} = \tfrac{1}{2}(p-k)\left[1 - \sqrt{1 - \left(\frac{p_o-k}{p-k}\right)^2}\right] \tag{66}$$

and

$$\frac{p_{HCl}}{p_{NH_3}} = \frac{1 + \sqrt{1 - \left(\frac{p_o-k}{p-k}\right)^2}}{1 - \sqrt{1 - \left(\frac{p_o-k}{p-k}\right)^2}} \tag{67}$$

or since k is very small

$$p_{HCl} = \tfrac{1}{2}\left[p + \sqrt{p^2-p_o^2}\right]$$

$$p_{NH_3} = \tfrac{1}{2}\left[p - \sqrt{p^2-p_o^2}\right] \tag{68}$$

In the absence of the zeolite and with the solid ammonium chloride in the reservoir at the same temperature as before, p_o is known from the vapour pressure vs temperature curve. The equilibrium pressure p in the presence of zeolite is measured. Thus partial pressures p_1 and p_2 can be found from equations (68) . One also notes from

equations (66) that p must be greater than p_0 for real values of p_1 and p_2. As the amount of zeolite is reduced to zero, p tends to p_0 and $p_1 = p_2 = \frac{1}{2}p_0$. Thus, the difference between p and p_0 depends upon the amount of zeolite present and the difference in selectivity in sorption of ammonia and hydrogen chloride; if these were equally sorbed, p would always be p_0 and $p_1 = p_2 = \frac{1}{2}p_0$ whatever the amount of the zeolite. The presence of the zeolite results in a perturbation of the ammonium chloride solid-vapour system in the way indicated; the extent of this perturbation varies with the amount of the zeolite. From the experimental results it cannot be proved that this was the only factor affecting the reproducibility of the isotherms since, as has already been mentioned, the isotherm could not be reproduced using the same sample and weight when the system was opened and the sample outgassed again.

The partial uptakes of hydrogen chloride and ammonia can be calculated from the total uptake in the following way. Let n_1^g and n_2^g represent the numbers of moles of hydrogen chloride and ammonia in the gas phase. The total volume of the apparatus can be regarded as the sum of volumes V_i at temperatures T_i where T_i varies with V_i. Then n_1^g and n_2^g are given by:

$$n_1^g = \frac{p_1}{R} \sum_i \frac{\Delta V_i}{T_i}$$
$$n_2^g = \frac{p_2}{R} \sum_i \frac{\Delta V_i}{T_i} \qquad (69)$$

with

$$\frac{n_1^g}{n_2^g} = \frac{p_1}{p_2} \qquad (70)$$

Also evaporation of ammonium chloride yields ammonia and hydrogen

chloride in equal amounts

$$n_1^g + n_1 = n_2^g + n_2 \tag{71}$$

where n_1 and n_2 represent the moles of adsorbed hydrogen chloride and ammonia, thus

$$n_1^g - n_2^g = n_2 - n_1 = (p_1 - p_2)\frac{1}{R}\sum_i \frac{\Delta V_i}{T_i} = F\,(p_1 - p_2) \tag{72}$$

where $F = \frac{1}{R}\sum_i \frac{\Delta V_i}{T_i}$ and can in principle be evaluated from the constants of the apparatus.

Further,

$$w = 17n_2 + 36.45n_1 \tag{73}$$

where w is the total weight sorbed. Solving equations (72) and (73) for n_1 and n_2 (and also for $w_1 = 17n_1$ and $w_2 = 36.45n_2$) one has:

$$\begin{aligned} n_1 &= n_{HCl} = \frac{w}{53.45} - \frac{17}{53.45} F\,(p_1 - p_2) \\ n_2 &= n_{NH_3} = \frac{w}{53.45} + \frac{36.45}{53.45} F\,(p_1 - p_2) \end{aligned} \tag{74}$$

From equations (68) we obtain:

$$p_1 - p_2 = \sqrt{p^2 - p_o^2} \tag{75}$$

and so,

$$\begin{aligned} n_1 &= \frac{w}{53.45} - \frac{17}{53.45} F\sqrt{p^2 - p_o^2} \\ n_2 &= \frac{w}{53.45} + \frac{36.45}{53.45} F\sqrt{p^2 - p_o^2} \end{aligned} \tag{76}$$

From equations (76) and (68) the partial isotherms n_1 vs p_1 and n_2 vs p_2 can be found. In the steeply rising region of the isotherm of the mixture where ammonia and hydrogen chloride are associating strongly, presumably in the 1:1 proportion of ammonium chloride, n_1 and n_2 will be approaching one another and so $p-p_o$ will be becoming less and p_1 and p_2 will also be approaching to each other and $\frac{1}{2}p_o$.

Calculation of the partial isotherms from the isotherm of the mixture

Equations (68) and (76) were used to calculate the partial isotherms of ammonia and hydrogen chloride from the experimental isotherm of the mixture. The application of the above argument to the experimental results involves the accurate measurement of two more variables, besides those already measured, namely the sum $\sum_i \frac{\Delta V_i}{T_i}$ and the sorbate temperature. The sum $\sum_i \frac{\Delta V_i}{T_i}$ can be measured with satisfactory accuracy (by allowing a known amount of argon to expand to a known volume, p. 71) as it is shown in Table 11.

Table 11

Change of factor F with reservoir temperature

Sample Temperature (°C)	Reservoir Temperature (°C)	$V_{app.}$ (cc)	$\sum_i \frac{\Delta V_i}{T_i}$ (cc/deg)	$Fx10^{-5}$ (mole/mm Hg)
230	132	1196	2.426	3.890
"	164	1199	2.410	3.865
"	193	1203	2.404	3.856
"	210	1206	2.412	3.868
"	223	1207	2.402	3.852
"	230	1209	2.396	3.843

The knowledge of the exact sorbate temperature determining the equilibrium is very important since it is used to obtain p_o from the vapour pressure-temperature curve of ammonium chloride (fig. 9). This temperature could not be accurately measured under the experimental conditions used. The error in its measurement was $\pm$ 1-2°C. However, for temperatures lower than 230°C, the temperature coefficient of the vapour pressure of ammonium chloride is not very big so that reasonable accuracy can be obtained. The partial isotherms of ammonia and hydrogen chloride as calculated from the formulae (68) and (76) are shown in fig. 61 together with the isotherm of the mixture. In figs. 62 and 63 they are compared with the isotherms of pure ammonia and pure hydrogen chloride. The effect of the presence of both gases on their sorption is very well shown by comparison of the partial isotherms with the isotherms of the pure components.

The change of the composition of the mixture is illustrated in figs. 64 and 65 . In fig. 64 the ratio of partial pressures $\frac{p_1}{p_2}$ is plotted against total pressure. The value of this ratio decreases with increasing pressure and tends to 1 as p approaches the saturation pressure. In fig. 65 the ratios $\frac{n_1}{n_2}$ and $\frac{n_2}{n_1}$ are plotted against the total uptake. Both ratios tend to 1 - from values lower and greater than 1, respectively - as the total uptake approaches the saturation uptake.

Difficulties in estimating θ_1 and θ_2 (where θ_1 is the fraction of the total available surface covered by ammonia and θ_2 by hydrogen chloride) prevent us from testing isotherm models.

Additional evidence for the disproportionation was obtained by another experiment, similar to the sorption experiment. The apparatus shown in fig. 66 was used. H-Zeolon was put in Z and ammonium chloride in A. Both were outgassed under high vacuum for

Fig. 61

H-Zeolon - NH_4Cl

230°C

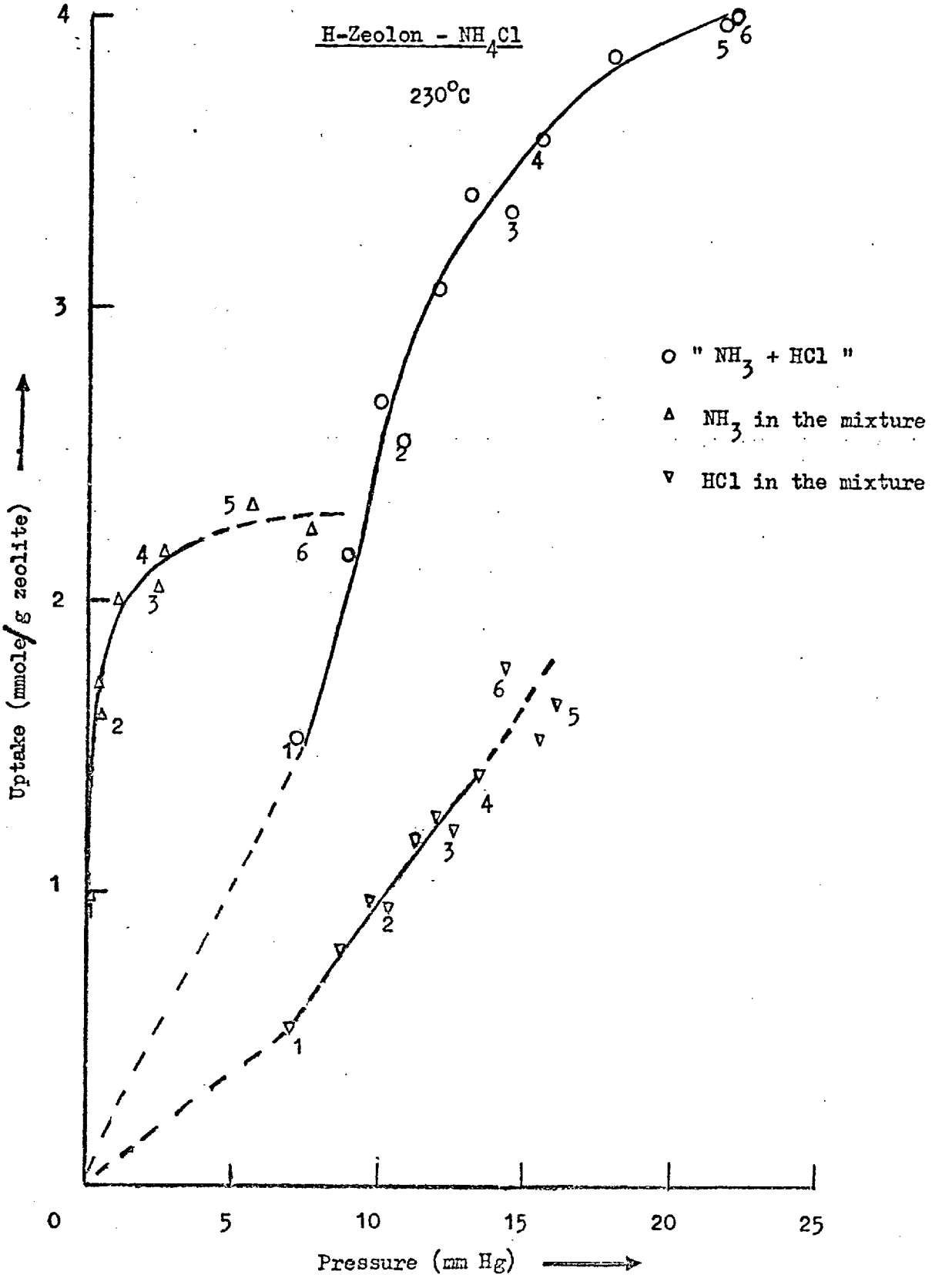


Fig. 62

H-Zeolon - NH_4Cl
230°C

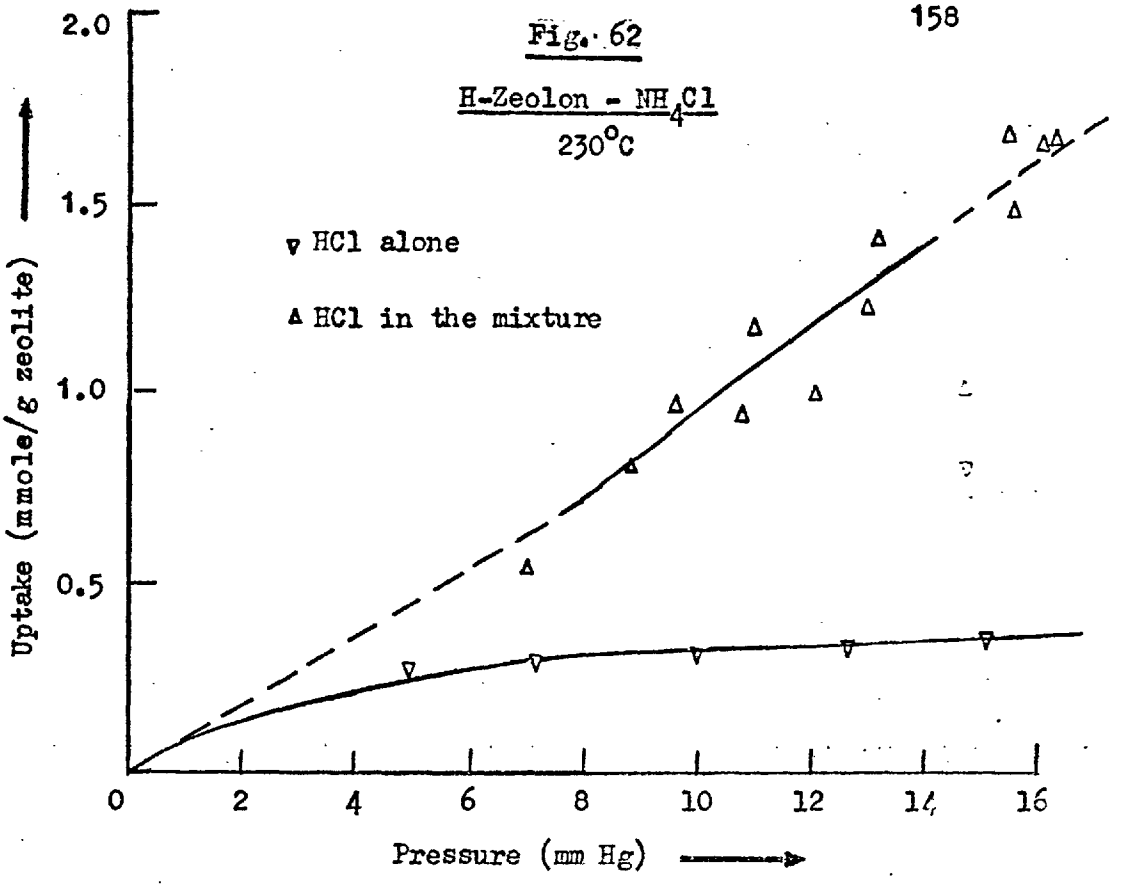


Fig. 63

H-Zeolon - NH_4Cl
230°C

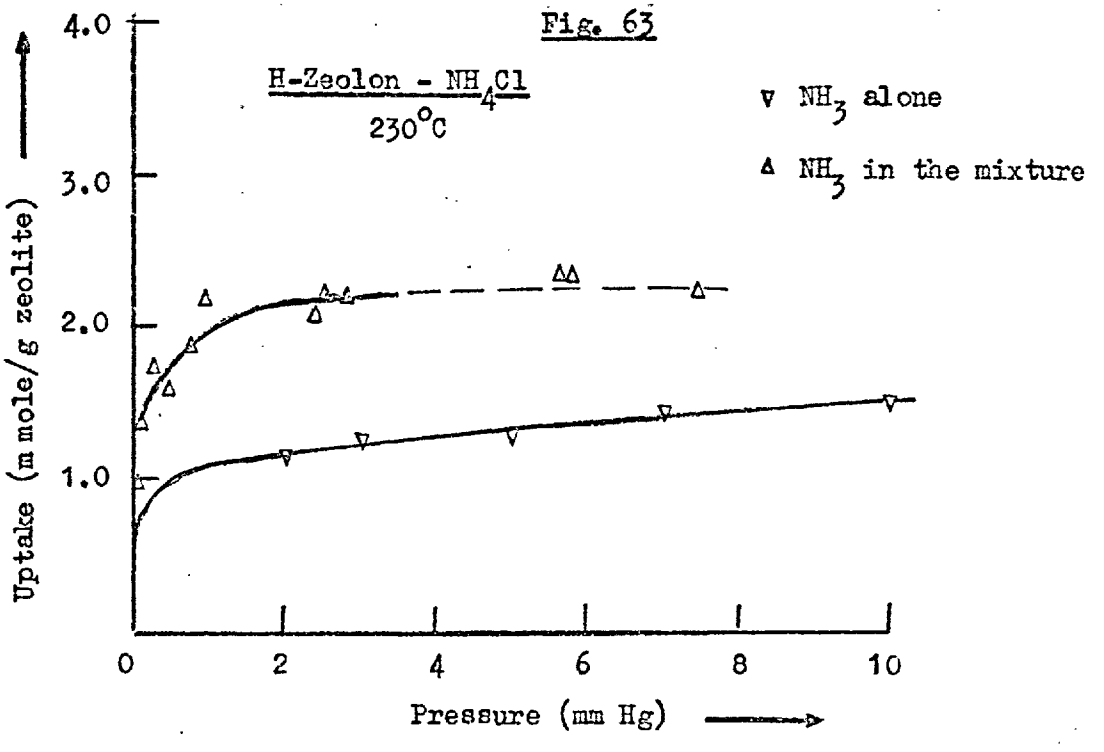


Fig. 64

H-Zeolon - NH_4Cl

230°C

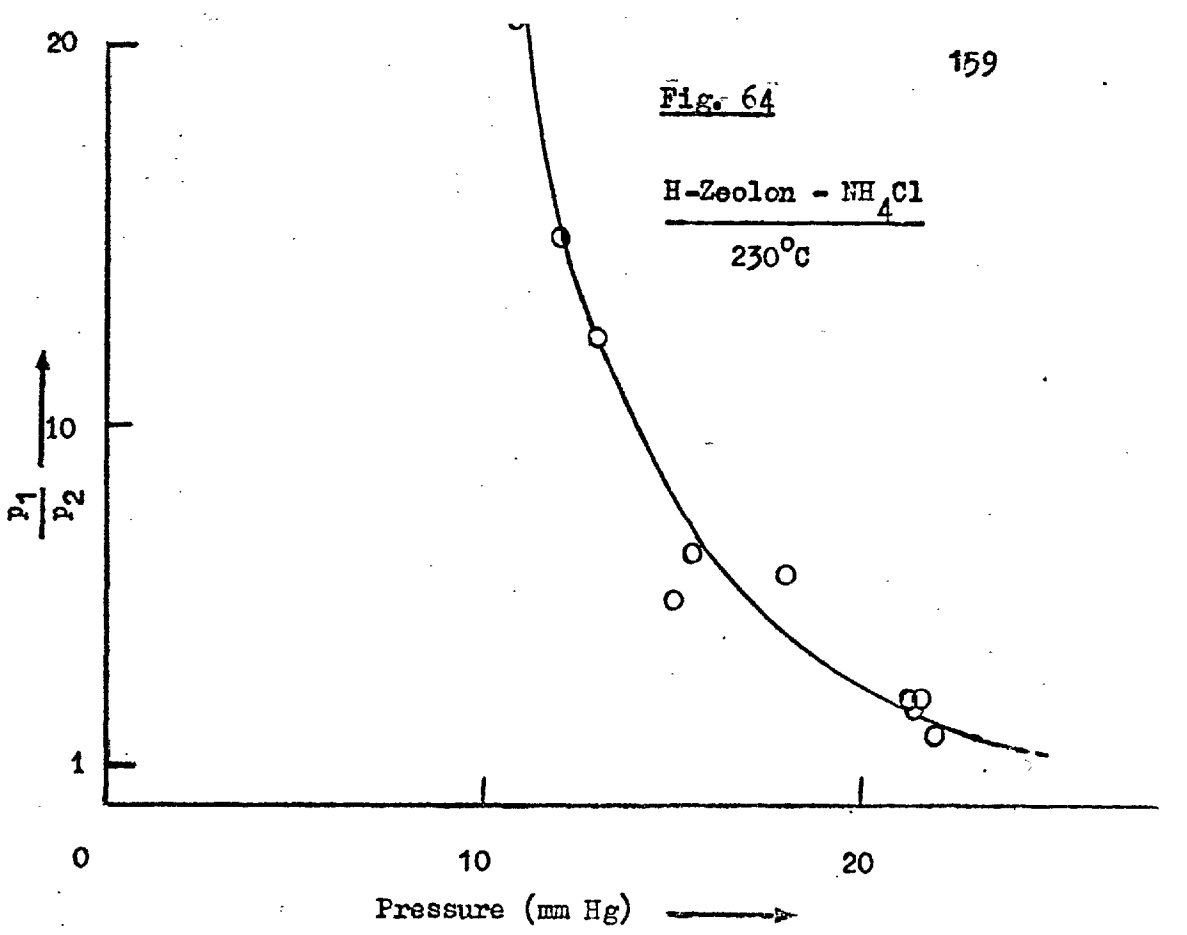


Fig. 65

H-Zeolon - NH_4Cl

230°C

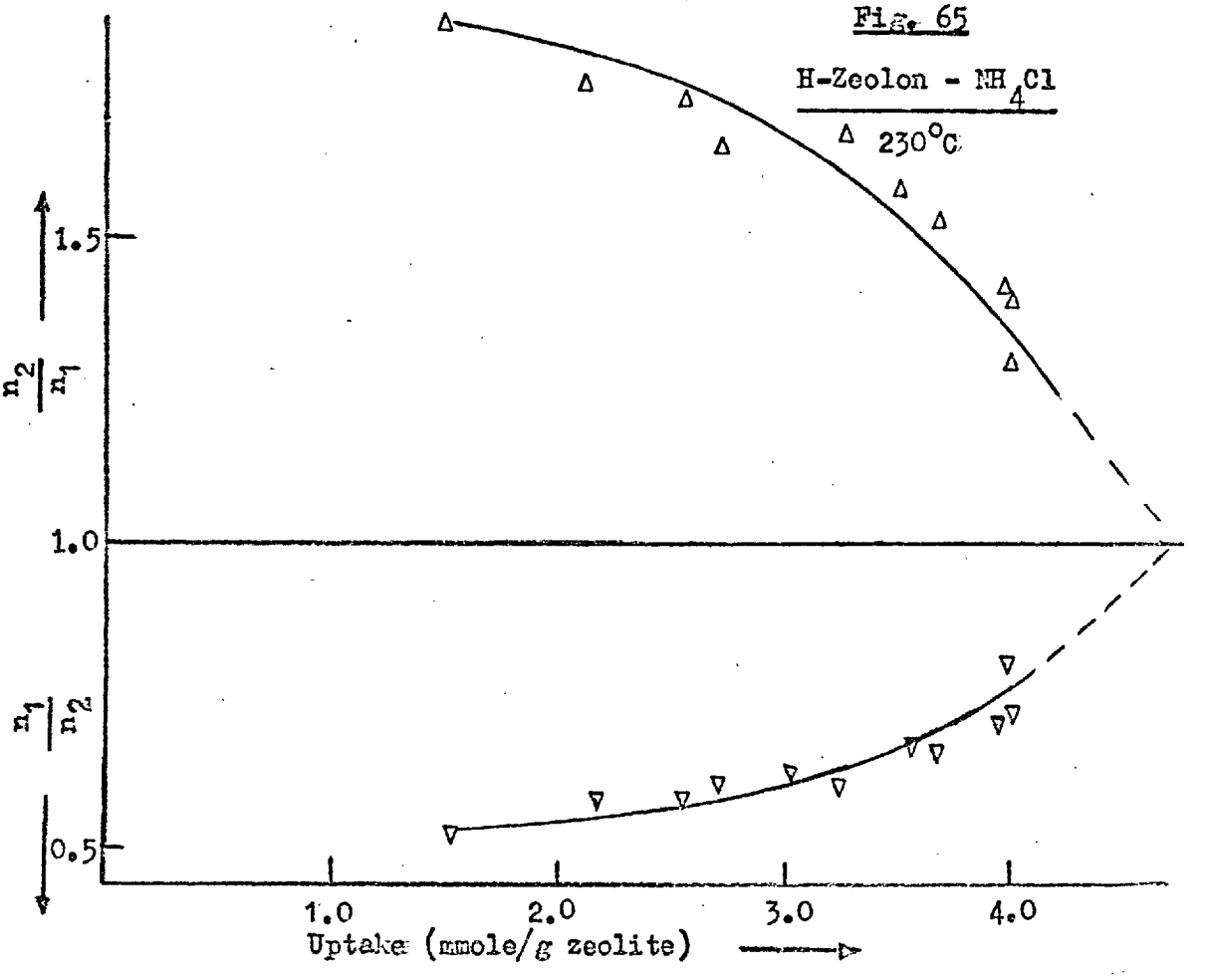
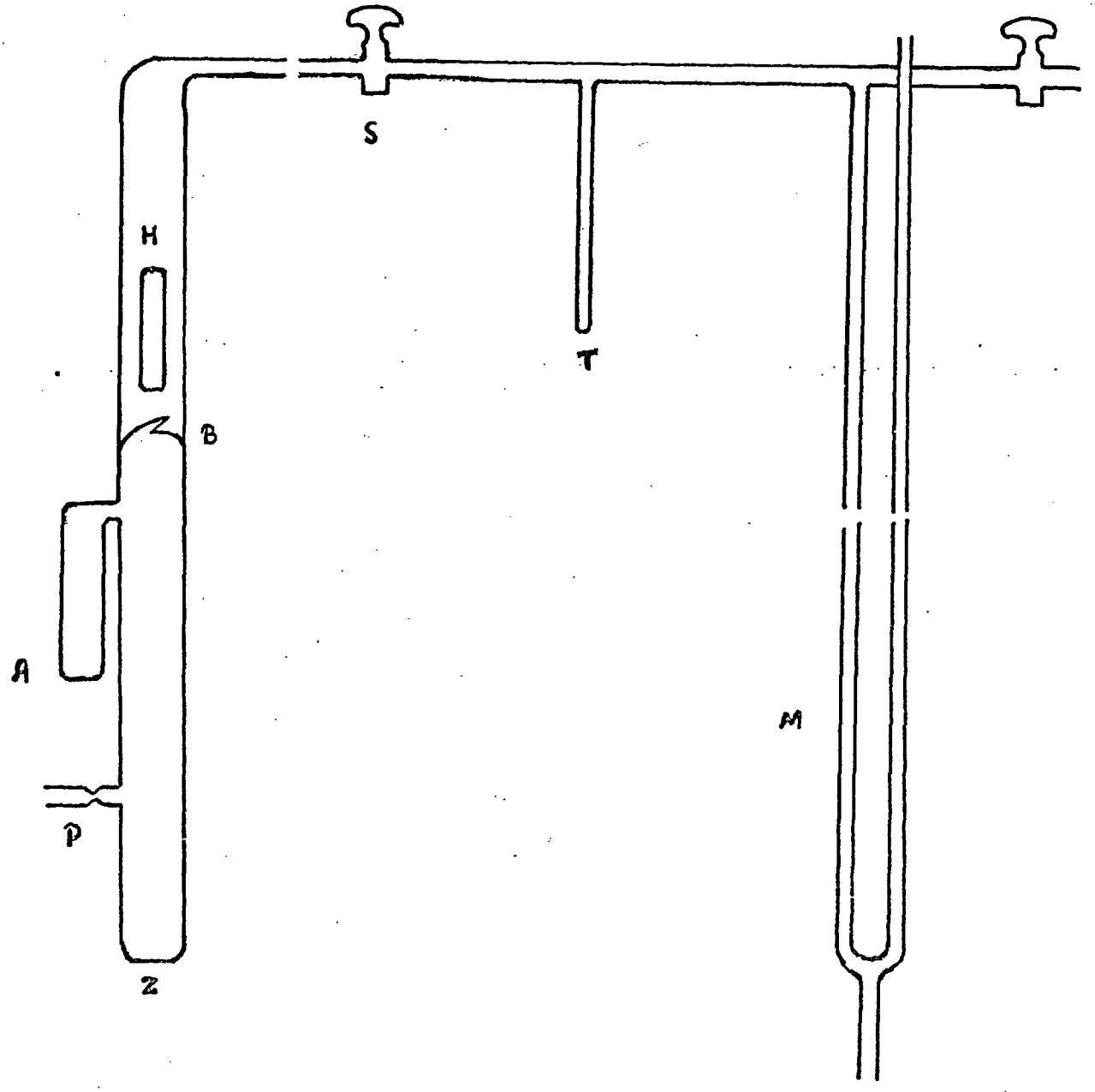


Fig. 66

Apparatus used in the study of the system H-Zeolon - NH_4Cl



two days, the zeolite at 350°C and the ammonium chloride at 90°C. The reaction tube was sealed at P and the apparatus was heated by means of a round electric furnace at 230°C for two days. The furnace was then lowered so it could heat the zeolite only, and the break seal at B was broken with the magnetic hammer H. The pressure, which was measured by means of the mercury manometer M, was due to condensable gases because it became negligible when the trap T was put in liquid nitrogen. This pressure decreased slowly with time and became almost zero after about a month (fig. 67). This was explained because of the disproportionation in the gas phase and the slow desorption of ammonia from H-Zeolon (or slow decomposition of ammonium-Zeolon). Ammonia is desorbed very slowly from H-Zeolon and in the presence of hydrogen chloride (which is believed to be the main constituent of the gas phase) reacts with the hydrogen chloride to form solid ammonium chloride. This results in a decrease in pressure. This process is controlled by the desorption of ammonia from H-Zeolon (or the decomposition of ammonium-Zeolon) and should obey a first order reaction equation. If we call p_1 the pressure at time t_1 and p_2 the pressure at time t_2 then the plot of

$$\Delta t = t_2 - t_1 = \frac{2.303}{k} \log \frac{p_1}{p_2}$$

should be a straight line with intercept $\frac{2.303}{k}$. This plot is shown in fig. 68 . From this figure, the reaction constant k was found to be equal to 1.94×10^{-6} sec^{-1}. The results of this experiment are in agreement with the observed residual uptake and pressure (p. 145) after the desorption of ammonium chloride from H-Zeolon. From the partial isotherms the constitution of the sorbed and gas phases was found at p = 6.5 mm Hg. From fig. 61 we find that the total uptake at p = 6.5 mm Hg is 1.26 mmole/g, and from fig. 65 that for n = 1.26 mmole/g, $\frac{n_1}{n_2} = 0.52$. Therefore,

Fig. 67

The slow condensation of NH_4Cl in the presence of H-Zeolon

230°C

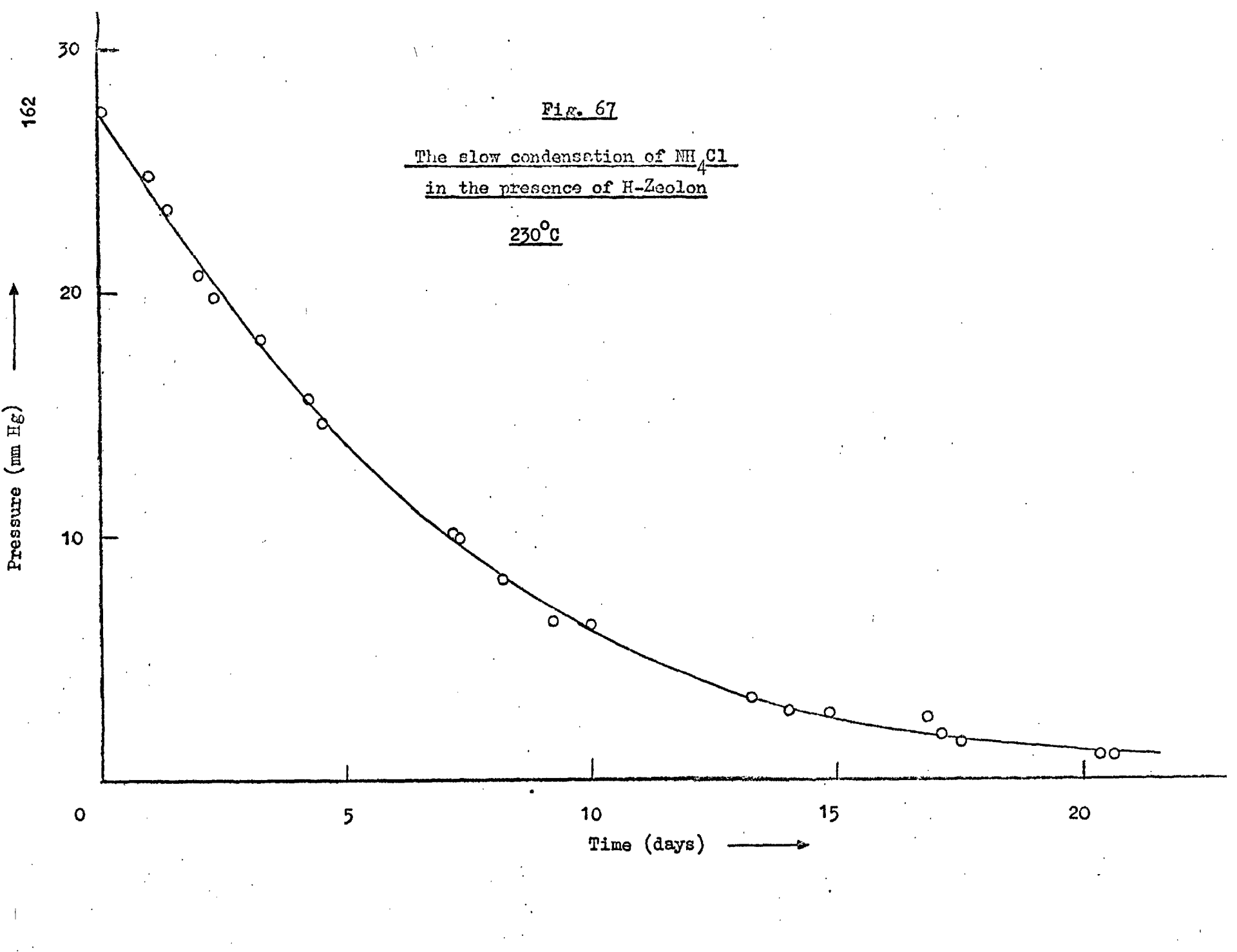
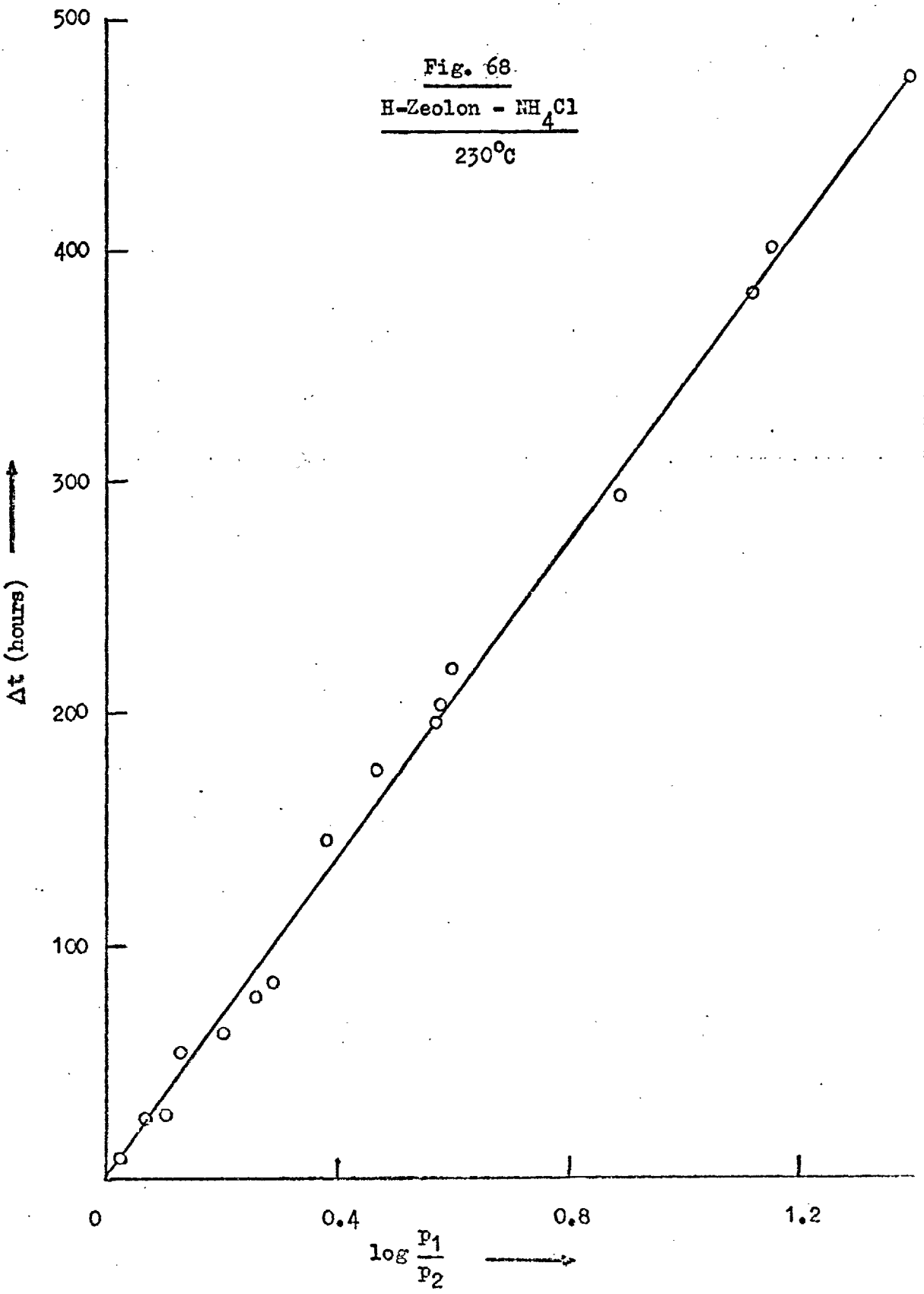


Fig. 68

H-Zeolon - NH_4Cl

230°C



$$\frac{n_1}{n_2} = 0.52, \quad n_1 + n_2 = 1.26$$

which yields

$$n_2 = n_{NH_3} = 0.83 \text{ mmole/g} \quad p_2 = 0.2 \text{ mm Hg}$$

and $$n_1 = n_{HCl} = 0.43 \text{ mmole/g} \quad p_1 = 6.3 \text{ mm Hg}$$

At this partial pressure of ammonia the desorption is very slow. (This is in agreement with observations on the desorption of pure ammonia from H-Zeolon at this pressure.) By raising the sample temperature the equilibrium position changes and ammonia is more easily desorbed. The uptake also decreased when the reservoir was put in liquid nitrogen, because hydrogen chloride froze and its partial pressure decreased and therefore some hydrogen chloride was desorbed.

Description of the sorbed phase by a virial equation

For the sorption of a mixture of two gases 1 and 2 in a non-swelling zeolite crystal the change of the chemical potential of the sorbent when c_1 and c_2 moles of the constituents 1 and 2 per unit volume (litre) of the crystal have been sorbed is given by[63]:

$$\Delta \mu_z = \mu_z - \mu_z^o = V_m \left[(p_1+p_2) - RT \int_0^{p_1} \frac{c_1}{p_1} dp_1 - RT \int_0^{p_2} \frac{c_2}{p_2} dp_2 \right] \quad (77)$$

where p_1 and p_2 are the partial pressures corresponding to c_1 and c_2 and V_m the molecular volume of the lattice-forming unit (taken by Barrer that containing two atoms of oxygen).

Also, if the sorbate-zeolite mixed phase is treated as a solution, the osmotic pressure π is given by [101]:

$$\Delta \mu_z = -\pi V_m \quad (78)$$

Thus

$$\pi = -(p_1+p_2) + RT\int_0^{p_1} \frac{c_1}{p_1}\, dp_1 + RT\int_0^{p_2} \frac{c_2}{p_2}\, dp_2 \qquad (79)$$

and π is independent of the choice of lattice-forming unit. If π is to be in atm then p_1+p_2 is in atm, R in cc-atm per mole per deg. In general, the term (p_1+p_2) is negligible in comparison with the integrals and unless p_1+p_2 is very large it can be omitted:

$$\pi = RT\int_0^{p_1} \frac{c_1}{p_1}\, dp_1 + RT\int_0^{p_2} \frac{c_2}{p_2}\, dp_2 \qquad (80)$$

For the isotherm of the mixture the osmotic virial equation truncated at the same point is (as eq. 82) thus:

$$\frac{\pi}{RT} = (c_1+c_2) + c_1^2 A_{11} + c_2^2 A_{22} + 2c_1c_2A_{12} \ldots\ldots \qquad (81)$$

where the equation has been terminated to include only the coefficients A_{11} and A_{22} and the cross-coefficient A_{12}. For the isotherms of the pure components

$$\frac{\pi_1}{RT} = c_1+c_1^2 A_{11}+ \ldots$$

$$\frac{\pi_2}{RT} = c_2+c_2^2 A_{22}+ \ldots \qquad (82)$$

A_{11} and A_{22} should be obtainable from the isotherms for the pure components and, hence, from the isotherm of the mixture, A_{12} could follow. From equations (80) and (81) follows that:

$$c_1+c_2+c_1^2A_{11}+c_2^2A_{22}+2c_1c_2A_{12}+\ldots = \int_0^{p_1} \frac{c_1}{p_1}\, dp_1 + \int_0^{p_2} \frac{c_2}{p_2}\, dp_2 \qquad (83)$$

Equation (83) defines the isotherm.

In the present case A_{22} (for hydrogen chloride) could not be obtained because the isotherm of pure hydrogen chloride was irreversible. An accurate value for A_{11} (for ammonia) could not also be obtained (see p. 133). Therefore, three values of c_1 and c_2, and p_1 and p_2 were used in equation (83) to obtain the coefficients A_{11}, A_{22} and A_{12}. The values of c_1 and c_2 were chosen in such a way that they covered the whole range of c's. However, different sets of c's gave different values for the coefficients. These values could differ from each other considerably but their ratio was almost constant. Some of the sets of values of A_{11}, A_{22} and A_{12}, when used to calculate the ratio $\frac{\pi}{RT(c_1+c_2)}$, gave satisfactory results. In fig. 69 this ratio is plotted against (c_1+c_2) from the experimental data. The calculated points, using the following values of the virial coefficients:

$$A_{11} = 29.46, \quad A_{22} = 11.39, \quad A_{12} = -18.14,$$

are in good agreement with the experimental points.

The opposite sign of the coefficient A_{12} to those of A_{11} and A_{22} shows that the effect of the cross-coefficient A_{12} is acting in the opposite way to that of A_{11} and A_{22}. These latter contribute curvature in the sense of a Type I isotherm in Brunauer's classification, whereas the cross-coefficient causes the isotherm in the middle range of uptake to inflect upwards, and to become of Type IV or V (fig. 60).

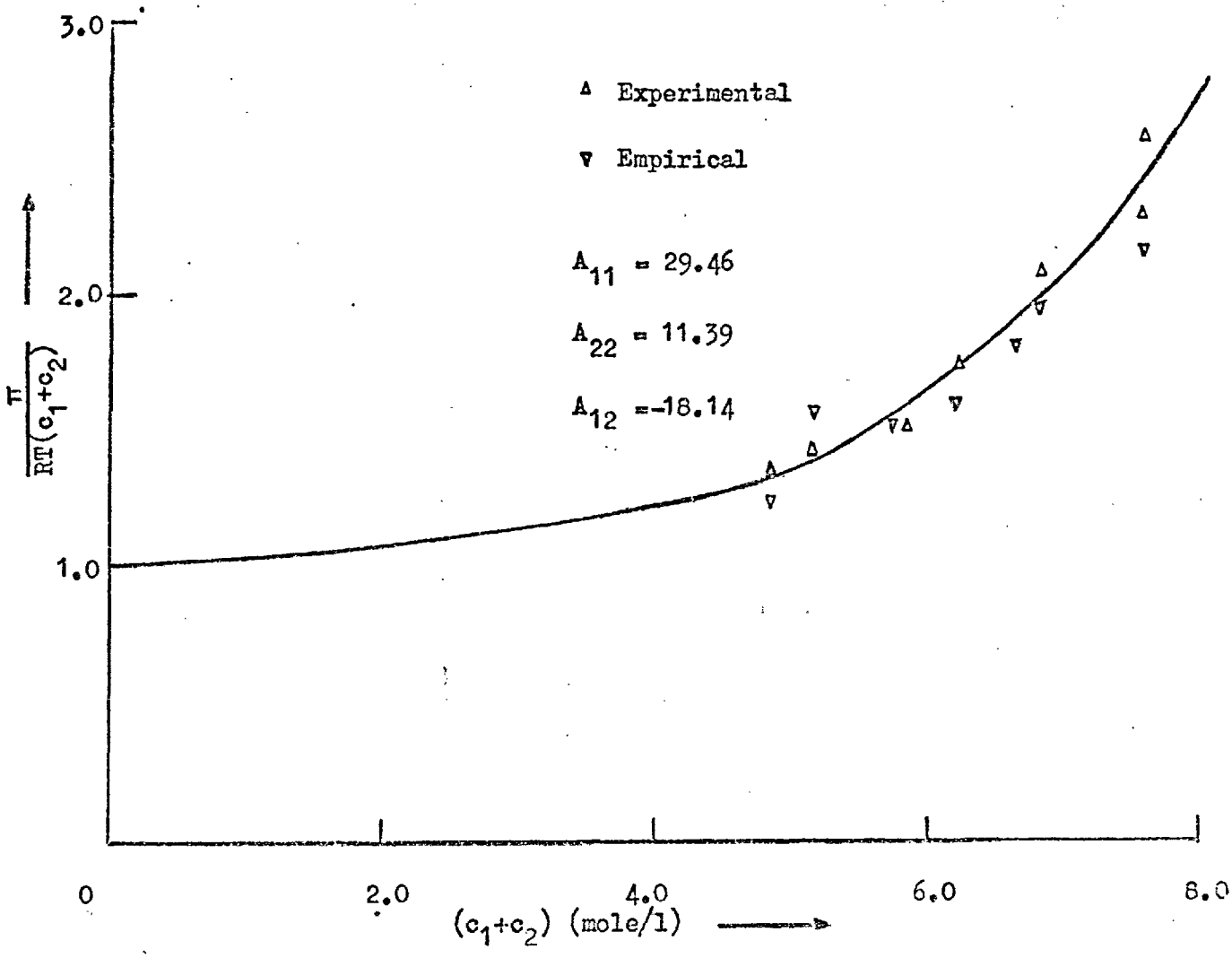
4.2 HY - ammonium chloride

The sorption of ammonium chloride in HY (prepared by method 1 of p. 103, and ca 80% crystalline) was studied at 246°C. Equilibrium in sorption was established in about 24 hours and in desorption in about 8 hours, but at low pressures (or low reservoir temperatures) desorption was very slow and when the sorbate reservoir was at room temperature, pressure and uptake decreased slowly for 12 days to a residual uptake and almost zero pressure. The pressures measured at

Fig. 69

H-Zeolon - NH_4Cl

230°C



uptakes lower than the saturation uptake were again higher than the vapour pressure of ammonium chloride corresponding to the sorbate temperature. As this temperature increased, the difference between the measured pressure and the vapour pressure of ammonium chloride, corresponding to the sorbate temperature, decreased. A disproportionation, therefore, existed in the gas phase as in the system ammonium chloride - H-Zeolon, and can be attributed to the same reasons (see p. 149).

The isotherm in HY at 246°C of the dissociation products, NH_3 + HCl, from vapourised NH_4Cl is recorded in fig. 70 , together with the sorption branches of the isotherms of pure ammonia and pure hydrogen chloride measured at the same temperature. The isotherm of the mixture is similar in shape to that of ammonium chloride in H-Zeolon. It was, however, irreversible and a residual uptake of 32.0 mg/g corresponding to a pressure of 0.14 mm Hg was found after the end of the desorption cycle. The zeolite was X-rayed after the end of the experiment and a further decomposition of about 20% was found (60% crystalline). Decomposition of HY was also observed when ammonia was sorbed (p. 140) but no change in crystallinity was found after the sorption of hydrogen chloride. Therefore, the decomposition of HY must be connected with the sorption of ammonia.

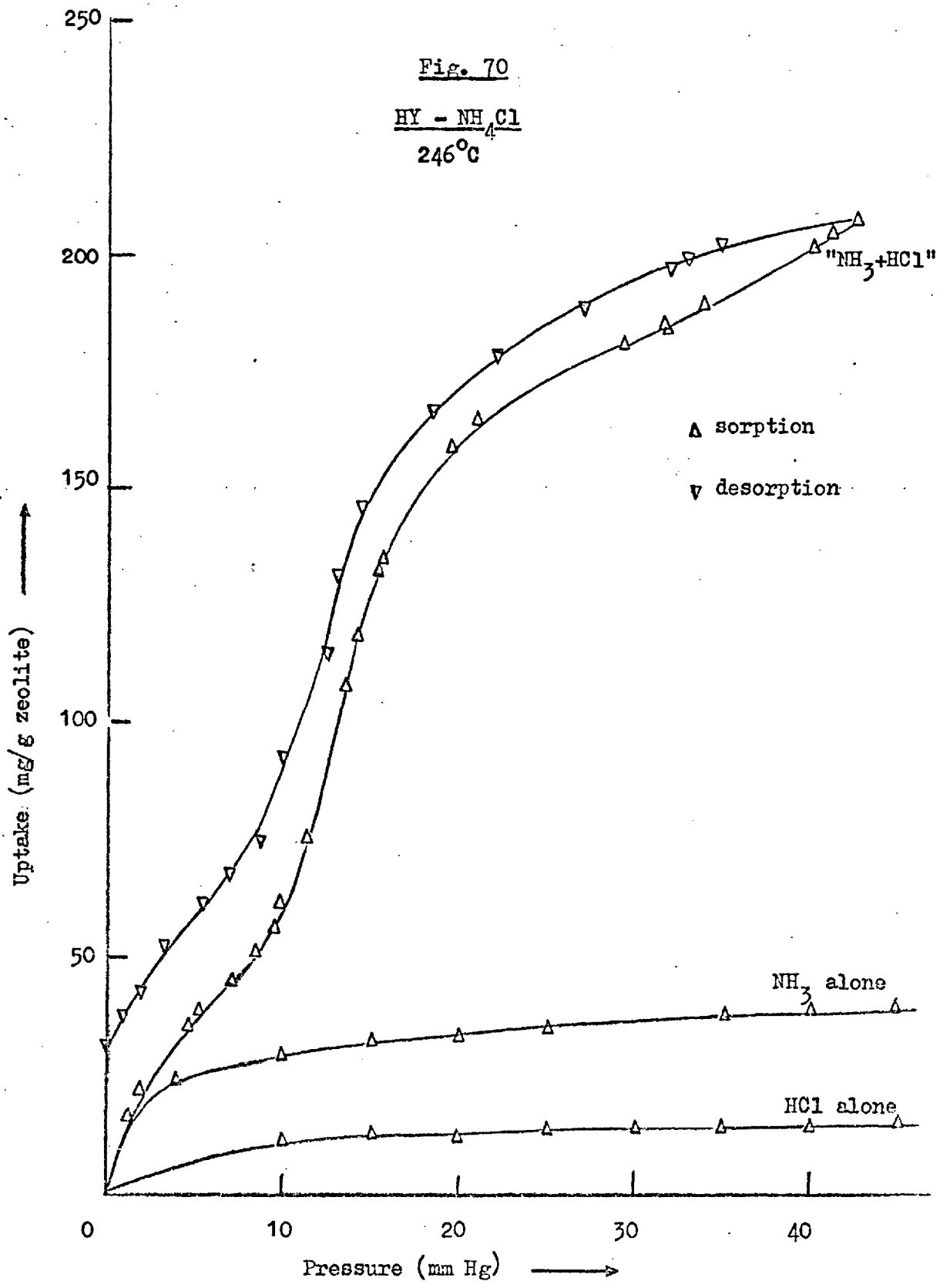
A reaction of hydrogen chloride with the aluminium of the framework is possible (p. 86). Aluminium was found in the filtrate when the ammonium chloride-treated zeolite was washed with distilled water and filtered. The hysteresis is believed to be connected with the decomposition of the zeolite and the reaction of hydrogen chloride with the aluminium of the zeolitic framework.

The residual uptake can be explained in terms of the reaction of hydrogen chloride with the zeolite. If a certain quantity of hydrogen chloride is irreversibly fixed on the zeolite, an equivalent

Fig. 70

HY - NH_4Cl

246°C



amount of ammonia must either remain in the zeolite or in the gas phase when the sorbate reservoir is at room temperature. This is because ammonia and hydrogen chloride react in the 1:1 proportion to form solid ammonium chloride during desorption. Since the residual uptake corresponds to a pressure of 0.14 mm Hg, this amount of ammonia must be in the zeolite. In an ammonium chloride uptake of 32.0 mg/g there is an ammonia uptake of 10.30 mg/g. From the isotherm of pure ammonia on HY (fig. 57) we find that an uptake of 10.30 mg/g corresponds to a pressure of ca 0.0 mm Hg which is in good agreement with the observed pressure of 0.14 mm Hg.

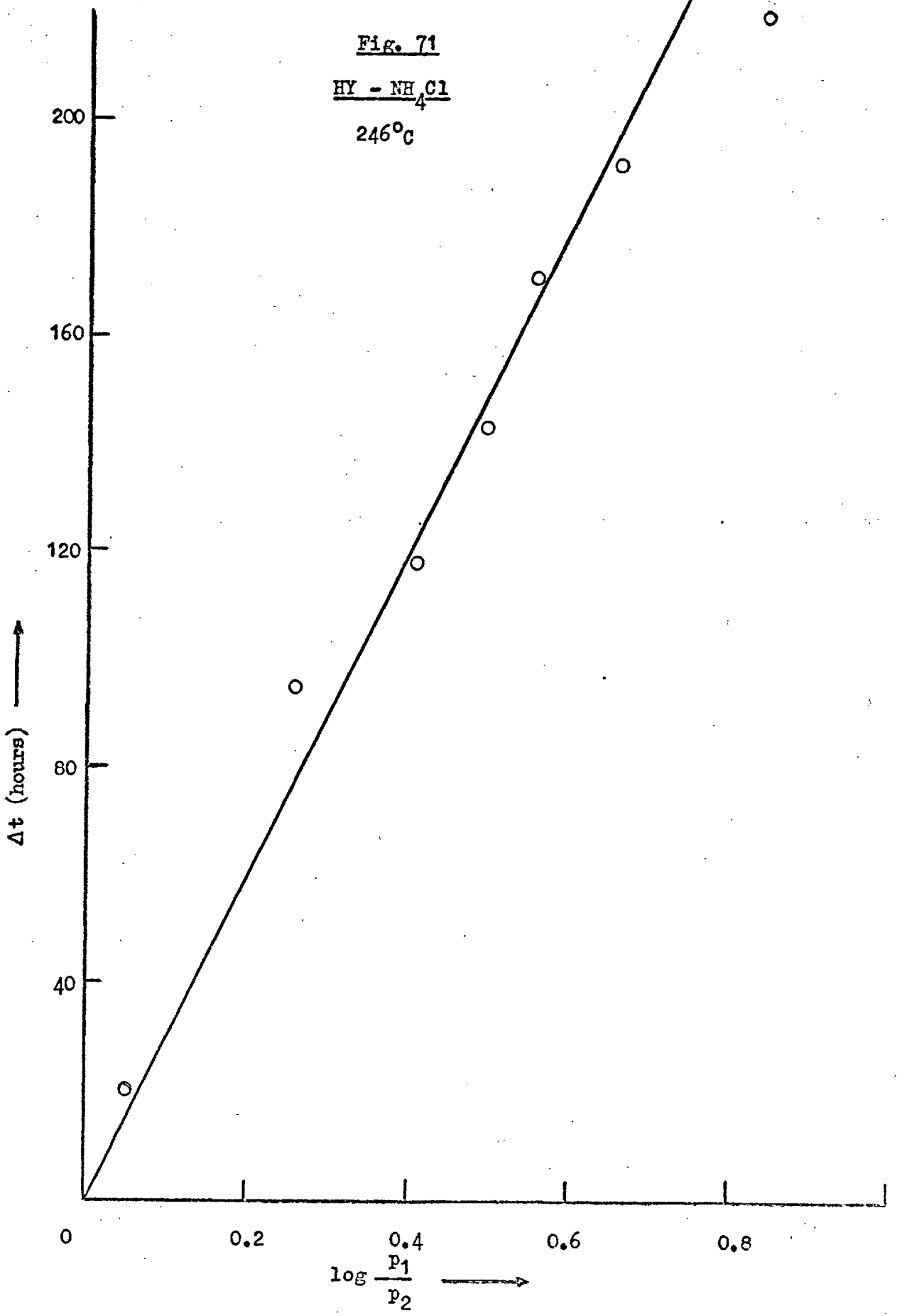
The slow desorption when the sorbate reservoir was at room temperature was attributed to the disproportionation in the gas phase and the slow decomposition of ammonium-Y (or the slow desorption of ammonia from HY). Applying the same arguments as in the case of H-Zeolon (p. 161), we expect the plot of Δt against $\log \frac{p_1}{p_2}$ to be a straight line. This plot is shown in fig. 71. The first order reaction constant was calculated from the slope of the straight line (fig. 71). It was found to be 2.13×10^{-6} sec^{-1}.

In conclusion, the sorption of "ammonium chloride" vapour in HY seems to be similar to that in H-Zeolon, controlled by the recombination reaction of NH_3 and HCl to form ammonium chloride in the zeolitic cavities, and also the stronger sorption of ammonia compared with that of hydrogen chloride. In the particular sample used in this experiment, additional reactions can take place and also partial decomposition of the zeolite occurred. Therefore, an accurate analysis of the isotherm of the mixture and calculation of the partial isotherms of ammonia and hydrogen chloride is not possible.

Fig. 71

HY - NH_4Cl

246°C



4.3 KL - ammonium chloride

The sorption of ammonium chloride in KL was studied for the temperature range 245-315°C. Four isotherms were measured at temperatures 245°C, 262.5°C, 280°C and 315°C. All isotherms were reversible and reproducible. Equilibrium in sorption and desorption was established in about 8 hours, except for desorption at very low pressures which took longer but no more than two days (depending on the isotherm temperature). The measured pressures were equal to the vapour pressure of ammonium chloride corresponding to the sorbate reservoir temperature except at low pressures, where a disproportionation existed in the gas phase, which decreased with pressure and finally disappeared at a certain pressure. Since the temperature coefficient of the vapour pressure increases with temperature and because of the experimental difficulties in measuring the exact temperature of the sorbate that determined the equilibrium (p. 156), this pressure could not be accurately measured, especially at high isotherm temperatures. It was found to increase with isotherm temperature from ca 8.0 mm Hg (for 245°C) to ca 50 mm Hg (for 315°C) and approximately corresponded to the end of the steeply rising part of the isotherms.

A small residual uptake was observed after desorption, which could be removed by raising the sample temperature to 350°C. No change in position or intensity of lines in the X-ray powder photograph of the zeolite was observed after the end of the experiment. In figs. 72 and 73 the measured isotherms of ammonium chloride together with the isotherms of pure ammonia and pure hydrogen chloride are shown at temperatures of 245°C and 315°C, respectively. In fig. 74 the four isotherms of ammonium chloride in KL are shown.

Possible equilibria in the system ammonium chloride-KL include:

$$NH_4Cl_{(s)} \rightleftharpoons NH_4Cl_{(g)} \rightleftharpoons NH_{3(g)} + HCl_{(g)} \qquad (49)$$

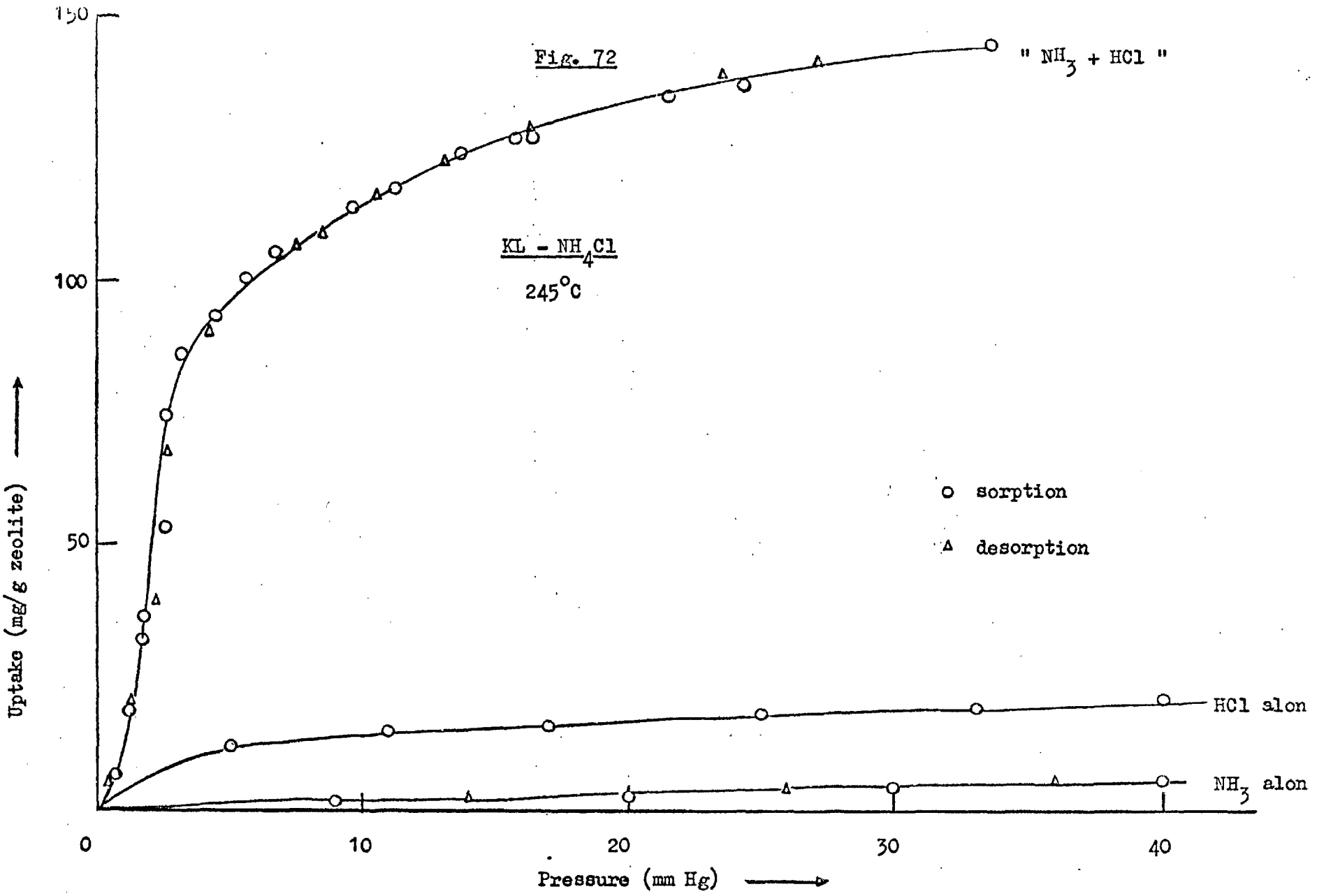

Fig. 72
" NH_3 + HCl "
KL - NH_4Cl
245°C
o sorption
Δ desorption
HCl alon
NH_3 alon
Uptake (mg/g zeolite)
Pressure (mm Hg)
150
100
50
0
10
20
30
40

Fig. 73

KL - NH_4Cl

315°C

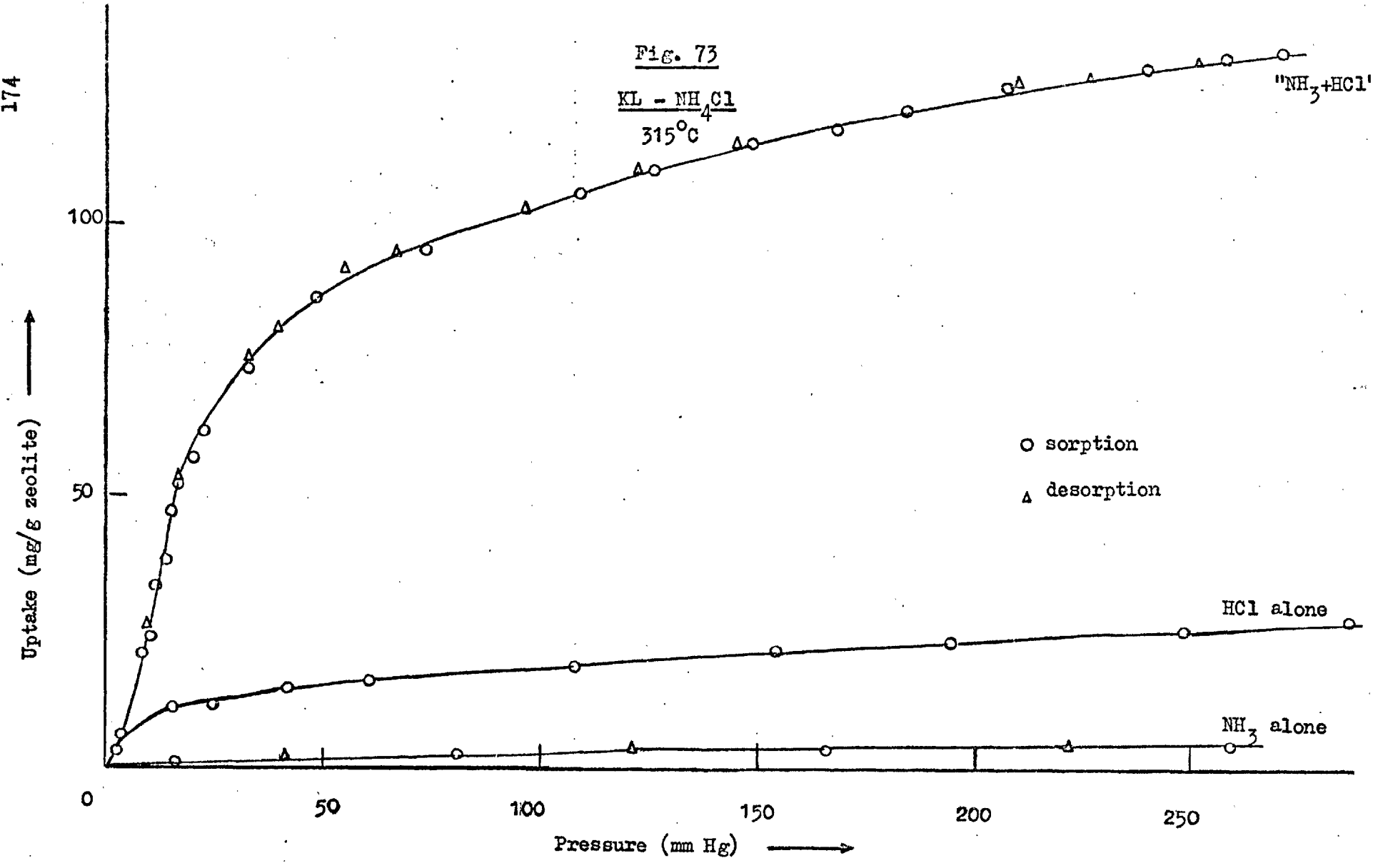
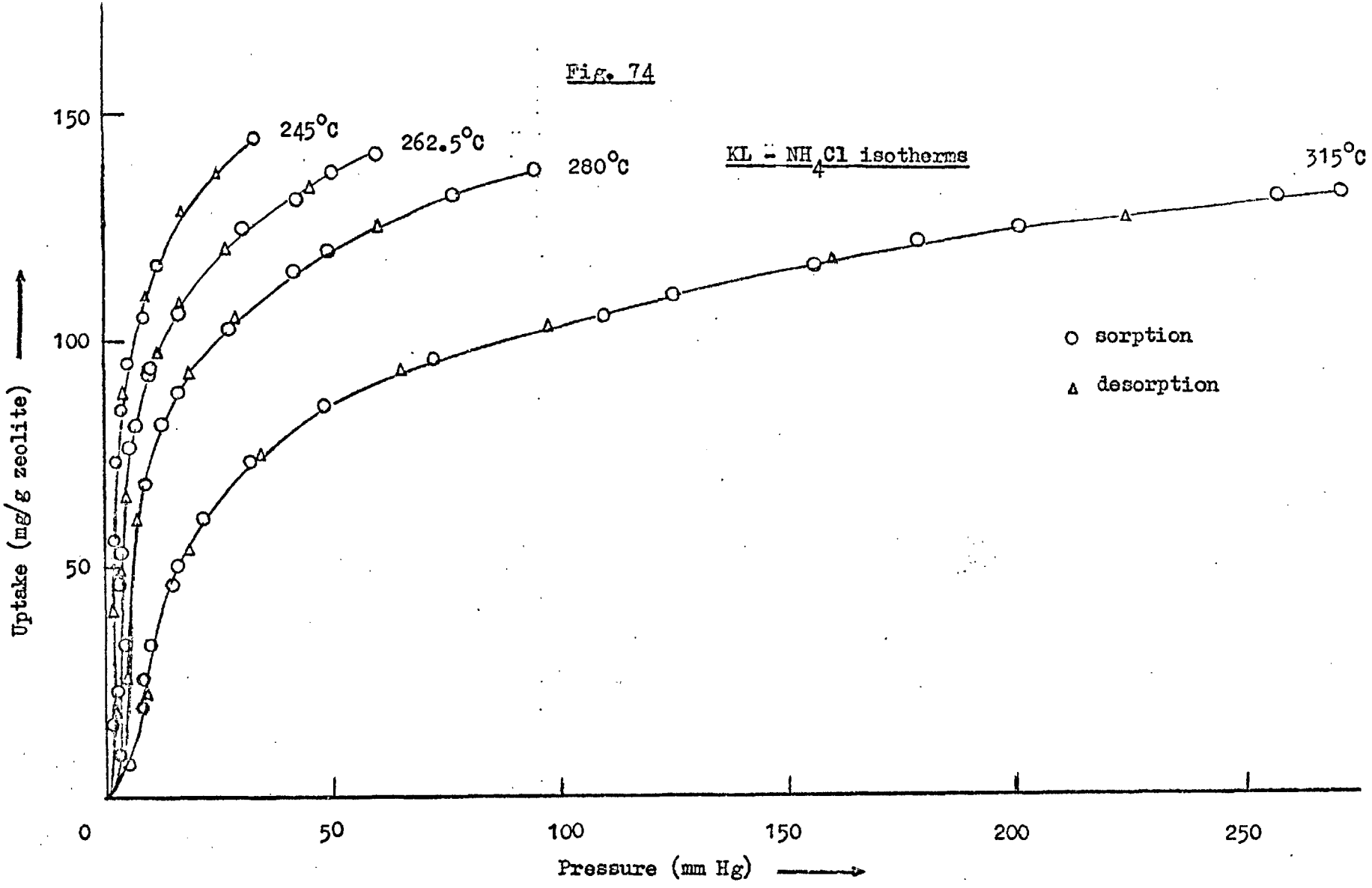


Fig. 74


KL - NH4Cl isotherms
245°C
262.5°C
280°C
315°C
sorption
desorption
Uptake (mg/g zeolite)
Pressure (mm Hg)
0
50
100
150
200
250
50
100
150

$$xHCl_{(g)} + yNH_{3(g)} + KL \rightleftharpoons KL.xHCl_{(a)}.yNH_{3(a)} \qquad (84)$$

with $x \geqslant y$

$$HCl_{(a)} + NH_{3(a)} \rightleftharpoons NH_4Cl_{(a)} \qquad (51)$$

$$mHCl_{(a)} + KL \rightleftharpoons (K_{1-m}H_m)L + mKCl_{(i,o)} \qquad (85)$$

$$mNH_{3(a)} + (K_{1-m}H_m)L \rightleftharpoons [K_{1-m}(NH_4)_m]L \qquad (86)$$

where $0.81 \geqslant m \ll x$ and i,o denotes inside or outside the crystals.

The unequal sorption of ammonia and hydrogen chloride at low pressures was attributed to the greater affinity of KL for hydrogen chloride than for ammonia, as can be seen from the isotherms of the pure gases. At high enough pressures the two gases are sorbed in the 1:1 proportion of ammonium chloride, and the whole process can be considered as the sorption of "ammonium chloride" vapour with possible exchange of some K^+ by NH_4^+. Complete exchange corresponds to an uptake of 181.5 mg/g. As the maximum uptake was 148 mg/g, the maximum exchange that could have taken place (corresponding to this uptake) was 81.5%. Since the ammonium chloride sorbed in KL could be completely desorbed, either no exchange takes place or, if it does, the potassium chloride produced remains in the crystals and the reactions (85) and (86) are reversible.

Reaction (51) explains the increase in sorption from the mixture as compared with the sorption of the pure components.

The isosteric heat of sorption was calculated from the experimental isotherms using the Clausius - Clapeyron integrated relation (p. 37). The part of the isotherms where there was no disproportionation was used for this calculation. This heat near saturation, for an uptake of 130 mg/g, was equal to -22.50 kcal/mole (vapour). The heat of condensation of ammonium chloride is -21.07 kcal/mole (vapour)[103].

Calculation of the partial isotherms

For the part of the isotherms where ammonia and hydrogen chloride are equally sorbed, the partial isotherms can be calculated as follows.

Since there is no disproportionation in the gas phase, the partial pressures of both gases should be the same and equal to one half of the measured pressure. Therefore:

$$p_1 = p_2 = \tfrac{1}{2}p \qquad (87)$$

where p_1 and p_2 are the partial pressures of ammonia and hydrogen chloride respectively and p is the measured pressure. Ammonia and hydrogen chloride are sorbed in 1:1 ratio. Therefore, if w_1 and w_2 are their partial uptakes (in mg/g) and w the total uptake (in mg/g) the following relations should apply:

$$\left.\begin{aligned} w &= w_1 + w_2 \\ \frac{w_1}{w_2} &= \frac{17}{36.45} \end{aligned}\right\} \qquad (88)$$

Equations (88) give $w_1 = \frac{w}{3.14}$ and $w_2 = \frac{w}{1.46}$ (89)

The relations (87) and (89) can be used to calculate the partial isotherms of ammonia and hydrogen chloride for the part of the isotherm where both gases are equally sorbed.

For the part of the isotherm where there is disproportionation in the gas phase, formulae similar to those derived for the system ammonium chloride - H-Zeolon (p. 154) can be obtained. Following the same argument and considering that hydrogen chloride is more strongly sorbed than ammonia, we obtain:

$$\left.\begin{aligned} p_1 &= \tfrac{1}{2}\left[p + \sqrt{p^2 - p_o^2} \right] \\ p_2 &= \tfrac{1}{2}\left[p - \sqrt{p^2 - p_o^2} \right] \end{aligned}\right\} \qquad (90)$$

and

$$w_1 = 17\left[\frac{w}{53.45} - \frac{36.45}{53.45} F\sqrt{p^2 - p_o^2}\right]$$

$$w_2 = 36.45\left[\frac{w}{53.45} + \frac{17}{53.45} F\sqrt{p^2 - p_o^2}\right] \qquad (91)$$

where the symbols F, w, p and p_o have the same meaning as in the system ammonium chloride-H-Zeolon.

In figs. 75 and 76 the partial isotherms of ammonia and hydrogen chloride, as calculated from the 245°C and 315°C isotherms of ammonium chloride on KL, are shown. For low pressures the partial isotherm of hydrogen chloride lies above that of ammonia but at high pressures the two isotherms become identical.

4.4 NaY-ammonium chloride

The sorption of "ammonium chloride" vapour was studied on NaY at 246°C. For pressures lower than 10 mm Hg, equilibrium in sorption was established in ca 24 hours. For higher pressures, sorption was rapid and it took ca 6 hours to reach equilibrium. The plot of uptake vs time, in sorption, for uptakes less than 250 mg/g showed a maximum. This maximum can be explained in terms of the exchange reaction (95), p. 182. The exchange of Na^+ by NH_4^+ results in a decrease in the dipole-field interaction and therefore a decrease in sorption. Plots of uptake vs time (in sorption) at different ammonium chloride pressures are shown in fig. 77. Equilibrium in desorption was attained in ca 6 hours.

The measured pressures were equal to the vapour pressure of ammonium chloride corresponding to the reservoir temperature, which means that there was no disproportionation. Therefore, ammonia and hydrogen chloride are sorbed on NaY approximately in the 1:1 proportion.

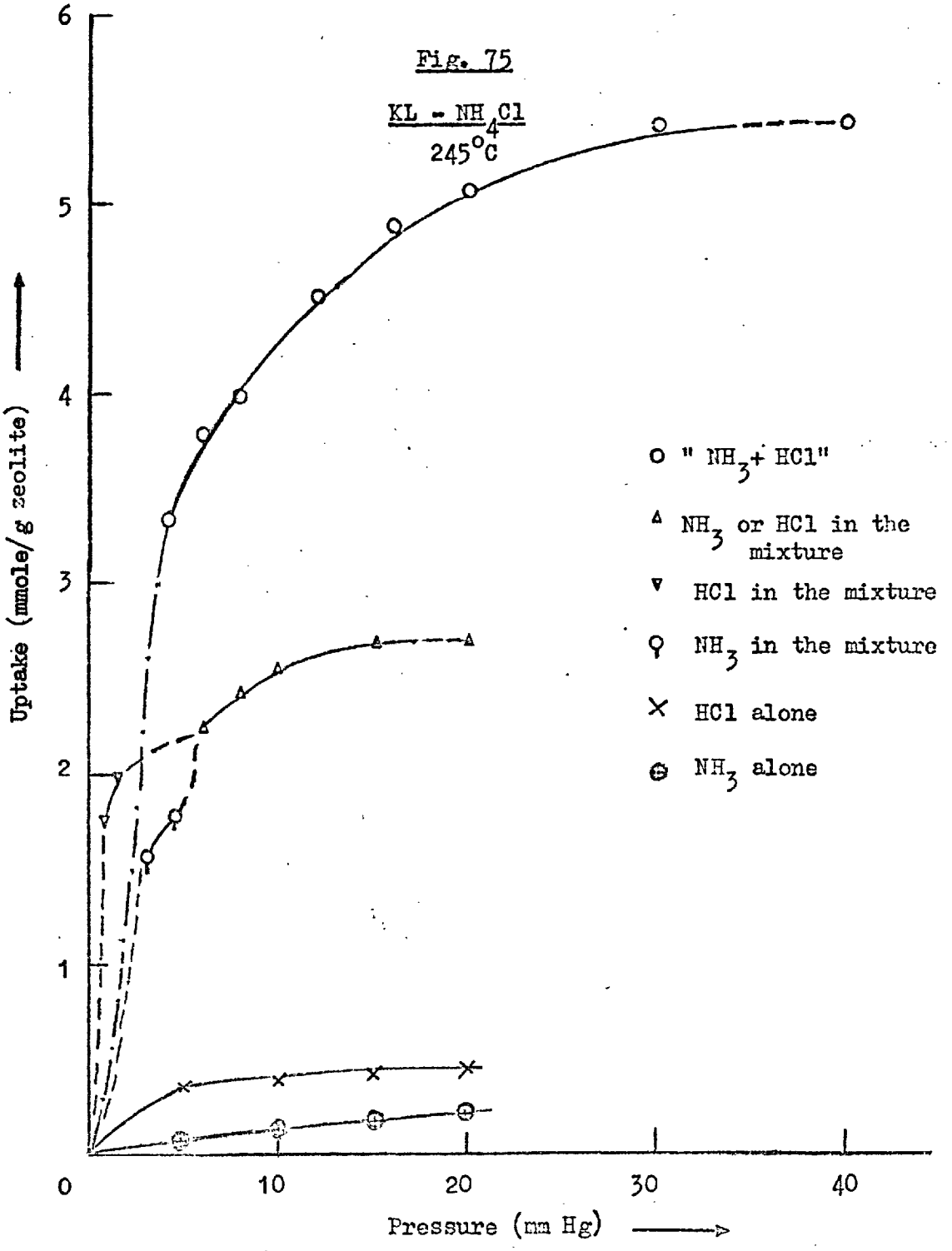

Fig. 75
KL - NH_4Cl
245°C
Uptake (mmole/g zeolite)
Pressure (mm Hg)
0
10
20
30
40
1
2
3
4
5
6
" NH_3+ HCl"
NH_3 or HCl in the mixture
HCl in the mixture
NH_3 in the mixture
HCl alone
NH_3 alone

Fig. 76

KL - NH_4Cl

315°C

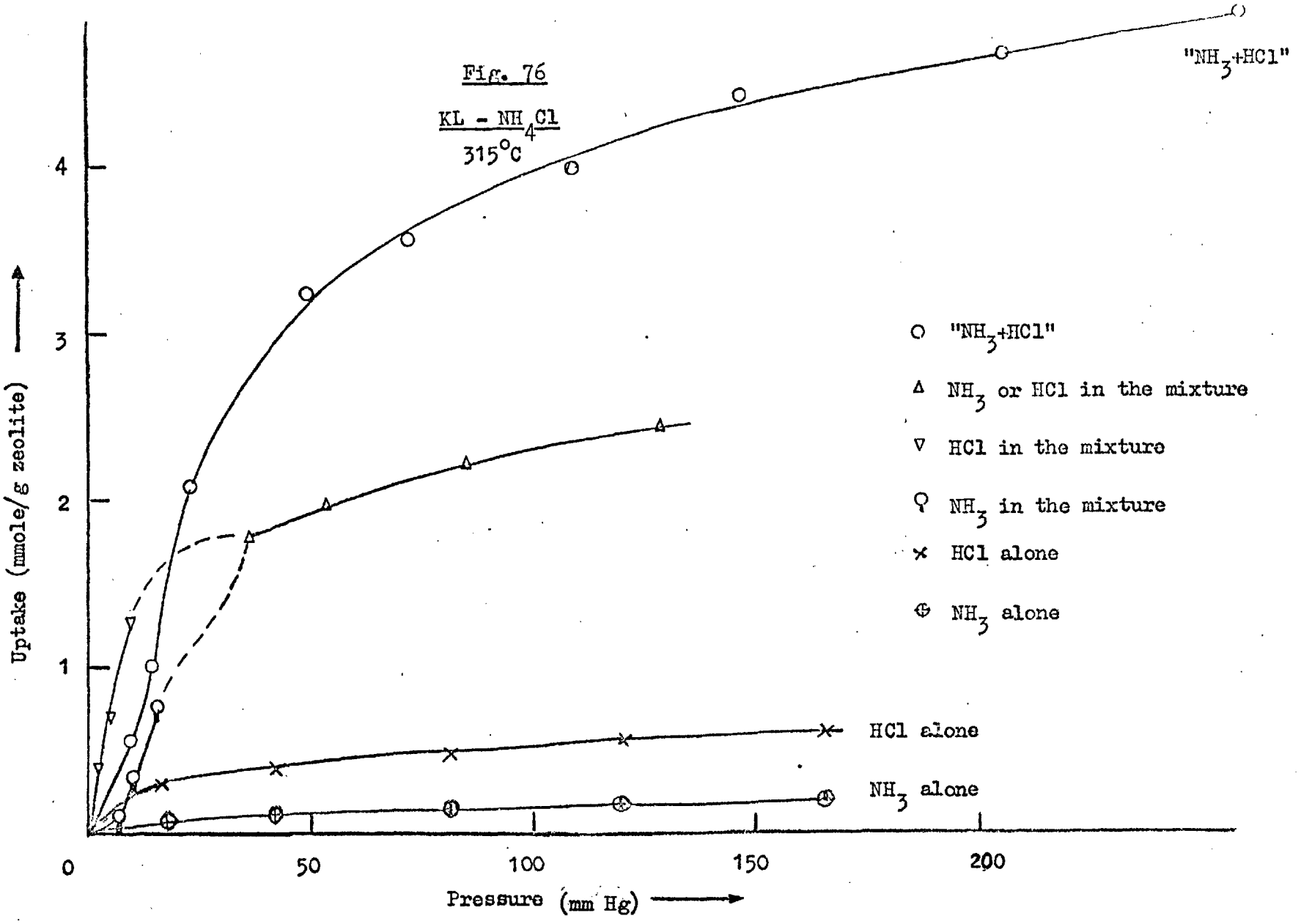
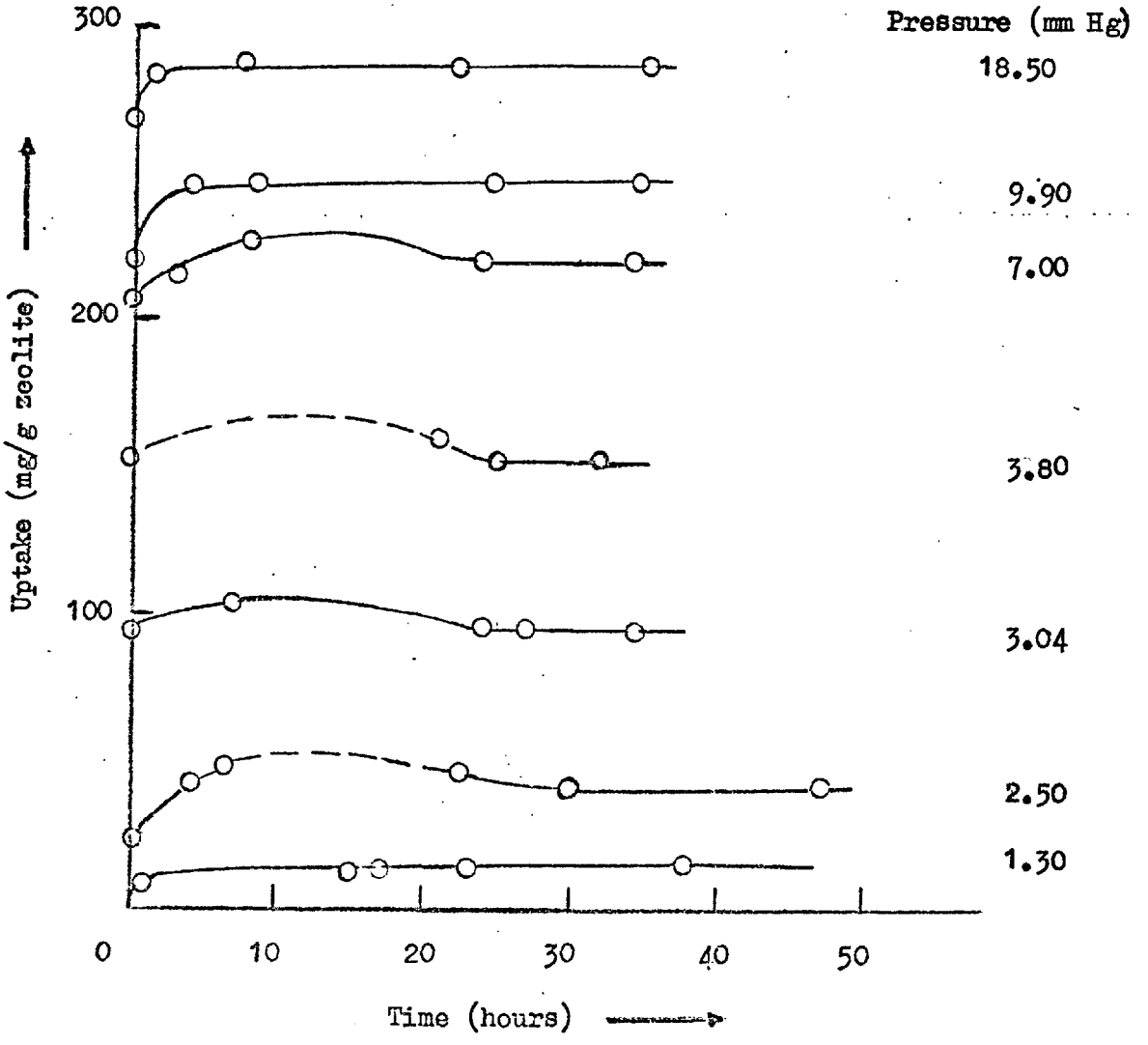


Fig. 77

NaY - NH_4Cl

246°C



The isotherm was, however, irreversible and a residual uptake of 35 mg/g was found at the end of the desorption cycle corresponding to a pressure of ca 0.0 mm Hg. The isotherm was repeated on the same sample. The second isotherm lay above the first and was also irreversible. The residual uptake after the second desorption cycle was 39 mg/g, at a pressure of ca 0.0 mm Hg. The isotherm is shown in fig. 78 , together with the isotherms of pure ammonia and hydrogen chloride, at the same temperature. A very large increase in sorption of the mixture is shown compared with the sorption of the pure components.

Possible equilibria in the system NaY-ammonium chloride include

$$NH_4Cl_{(s)} \rightleftharpoons NH_4Cl_{(g)} \rightleftharpoons NH_3(g) + HCl_{(g)} \qquad (49)$$

$$xHCl_{(g)} + yNH_3(g) + NaY \rightleftharpoons NaY.xHCl_{(a)}.yNH_3(a) \qquad (92)$$

with $x \simeq y$

$$mHCl_{(a)} + NaY \rightleftharpoons (Na_{1-m}, H_m)\,Y + mNaCl_{(i,o)} \qquad (93)$$

$$mNH_3(a) + (Na_{1-m}, H_m)\,Y \rightleftharpoons \left[Na_{1-m}, (NH_4)_m\right] Y \qquad (94)$$

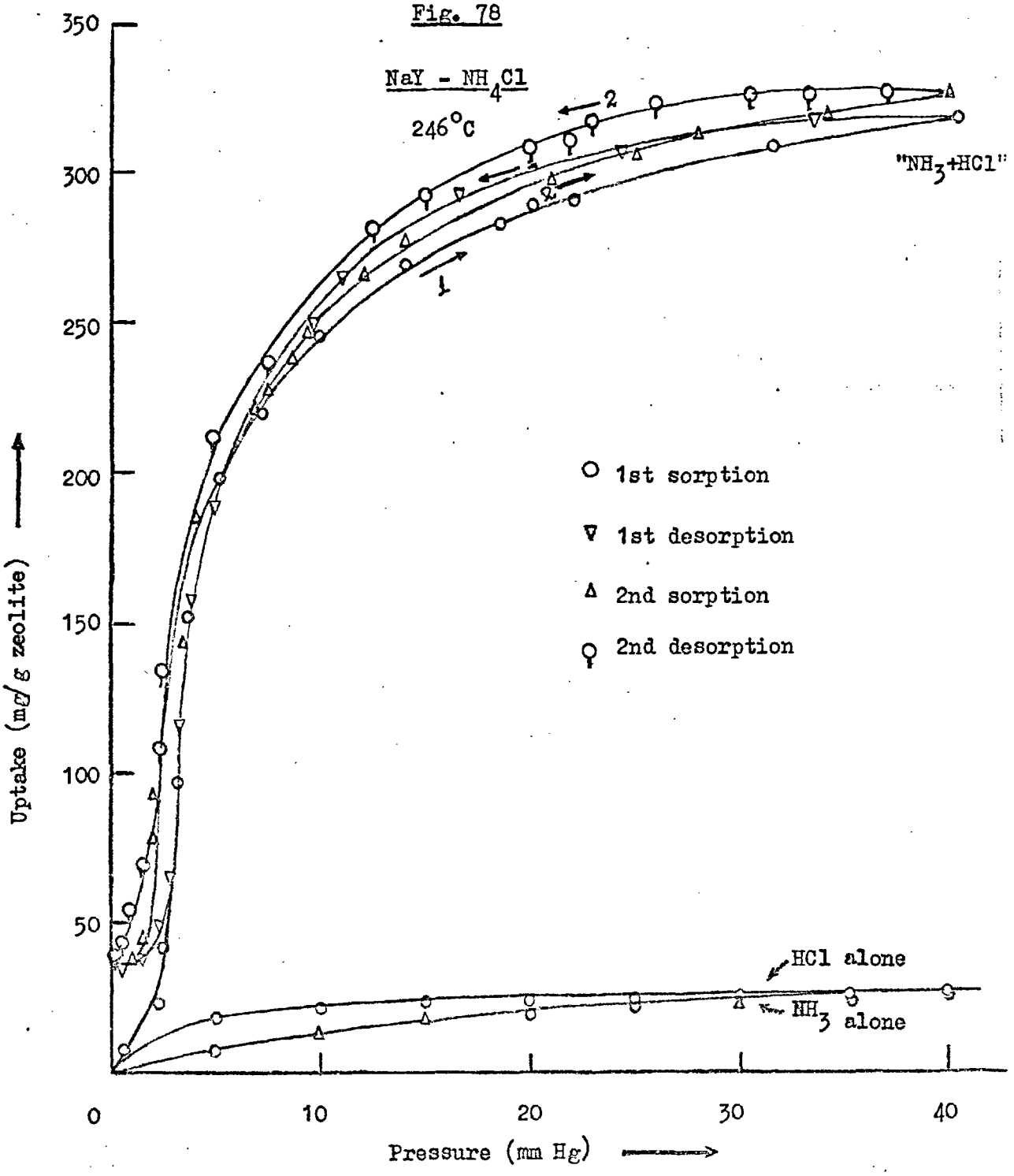
$$NH_3(a) + HCl_{(a)} \rightleftharpoons NH_4Cl_{(a)} \qquad (51)$$

where $1 \geqslant m \leqslant x$ and (i,o) denotes inside or outside the crystal. Reactions (93) and (94) can be added so that their net effect can be represented by:

$$mHCl_{(a)} + mNH_3(a) + NaY \rightleftharpoons \left[Na_{1-m}, (NH_4)_m\right] Y + mNaCl_{(i,o)} \qquad (95)$$

Reactions (51) and (95) are the main reactions taking place during the sorption of ammonium chloride. Since in both reactions ammonia

Fig. 78


NaY - NH4Cl
246°C
"NH3+HCl"
1
2
1st sorption
1st desorption
2nd sorption
2nd desorption
HCl alone
NH3 alone
Uptake (mg/g zeolite)
Pressure (mm Hg)
350
300
250
200
150
100
50
0
10
20
30
40

and hydrogen chloride react in the 1:1 ratio, equal amounts of both gases are removed from the gas phase. This explains why no disproportionation was observed in the gas phase. Therefore, this case could be considered as sorption of "ammonium chloride" vapour with possible exchange of Na^+ by NH_4^+ and the overall process can be written as:

$$nNH_4Cl_{(g)} + NaY \rightleftharpoons \left[Na_{1-m},(NH_4)_m\right] Y_{,}(n-m)NH_4Cl_{(a)} + mNaCl_{(i,o)} \qquad (96)$$

where $1 \geqslant m < n \leqslant 1.5$.

Complete exchange of the sodium ions by ammonium ions corresponds to an uptake of 217 mg/g. As the maximum uptake was 325 mg/g, it is possible that all the sodium ions were replaced by ammonium ions during the sorption of ammonium chloride. The observed hysteresis and residual uptake are attributed to the exchange reaction (95). A residual uptake of 35 mg/g corresponds to 16.2% exchange and 39.0 mg/g to 17.9%. The zeolite, after the end of the experiment, was washed with water and filtered. The amount of sodium estimated in the filtrate was in good agreement with the residual uptake. The zeolite was also X-rayed after the end of the experiment. No sodium chloride lines were observed in the X-ray photograph.

Using the formulae (87) and (89) as derived in Section 3 of this chapter, the partial isotherms of ammonia and hydrogen chloride can be calculated from the sorption part of the isotherm of the mixture. These partial isotherms are compared with the isotherms of the pure gases in figs. 79 and 80. Inspection of the isotherms of pure ammonia and pure hydrogen chloride shows that at low pressures both gases are equally sorbed on NaY. This explains why no disproportionation was observed even at low pressures.

If complete exchange of Na^+ by NH_4^+ takes place, the sodium chloride produced or most of it must remain in the crystal cavities. Two explanations can be given for the residual uptake:

Fig. 79

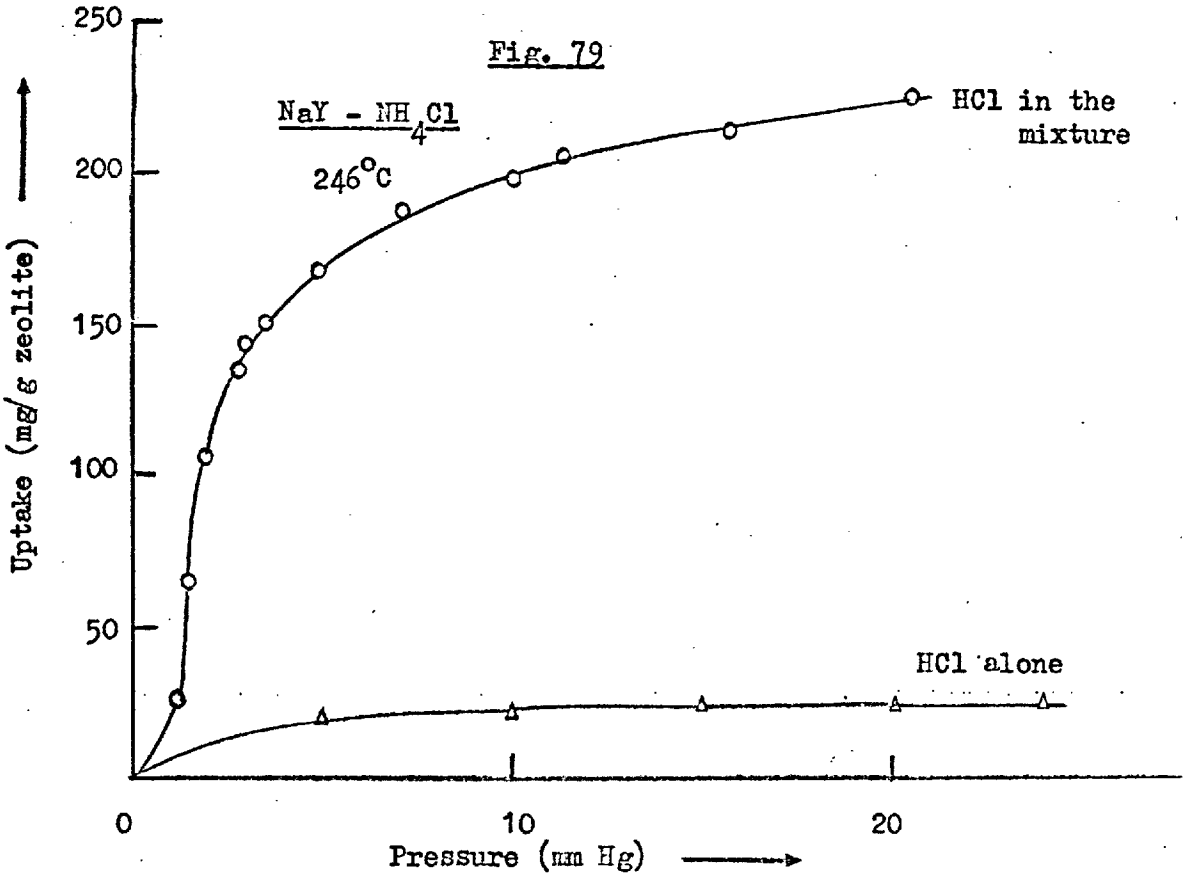
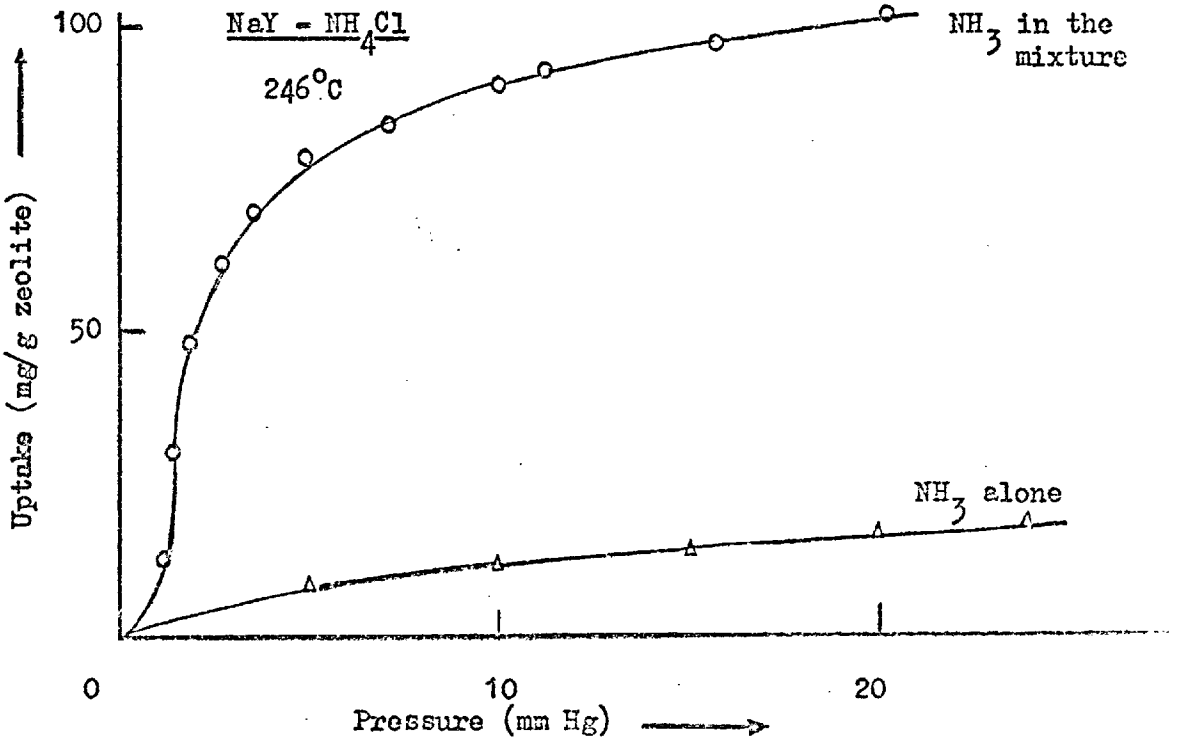

NaY - NH4Cl
246°C
HCl in the mixture
HCl alone
Uptake (mg/g zeolite)
250
200
150
100
50
0
10
20
Pressure (mm Hg)

Fig. 80


NaY - NH4Cl
246°C
NH3 in the mixture
NH3 alone
Uptake (mg/g zeolite)
100
50
0
10
20
Pressure (mm Hg)

(i) Part of the sodium chloride (corresponding to this uptake) migrates out of the crystals, or

(ii) the reverse reaction (95) is very slow.

4.5 Comparison of the sorption of ammonium chloride in different zeolites

From the results obtained on the sorption of ammonium chloride in the different zeolites certain conclusions can be drawn.

There is evidence that in all cases examined, a reaction between ammonia and hydrogen chloride took place in the zeolitic cavities to form ammonium chloride. The shape of the recorded isotherms (type IV or V in Brunauer's classification) typifies sorption in a finite sorption volume with strong interaction between the sorbed molecules. In the present case the strong interaction is expected between ammonia-hydrogen chloride rather than ammonia-ammonia or hydrogen chloride-hydrogen chloride pairs. The sorption from the mixture was always higher than from the pure components. Thus the presence of both gases results in an increase in their sorption. In this respect, the systems examined show some similarities with other sorption complexes formed at high temperatures. Barrer and Whiteman[104] found that in the sorption of sulphur and phosphorus in NaX the interaction of sulphur with sulphur and of phosphorus with phosphorus was also sufficient to give isotherms of types IV or V in Brunauer's classification.

The sorption of the pure components affects the sorption from the mixture to an extent depending on the nature of the zeolite (or the nature of the complex between ammonia or hydrogen chloride and the zeolite). Three different cases of sorption from the pure components were found:

(a) ammonia and hydrogen chloride were equally sorbed (NaY at low pressures);

(b) ammonia is sorbed more strongly than hydrogen chloride (H-Zeolon, HY);

(c) hydrogen chloride is sorbed more strongly than ammonia (KL).

In the above cases (b) and (c) where one of the gases is sorbed more strongly than the other, a disproportionation can arise in the gas phase (and therefore in the sorbed phase). This disproportionation decreases with the pressure (or the sorbate temperature) and can become equal to zero at a certain pressure. This shows that a competition exists between the recombination reaction and that responsible for the disproportionation. As the pressure increases, the recombination reaction becomes the most predominant reaction.

During the sorption of ammonium chloride in an ion-exchanged zeolite, an exchange reaction of the cations by ammonium ions can simultaneously take place. This is actually the Clark-Steiger method (p. 10) of preparation of ammonium zeolites. In view of the results of the present work and considering the decomposition of ammonium chloride in the gaseous phase, the reactions taking place during the preparation of an ammonium zeolite by the Clark-Steiger method should be:

$$mHCl_{(a)} + MZ \rightleftharpoons (M_{1-m}, H_m)\,Z + mMCl_{(i,o)} \qquad (97)$$

$$mNH_{3(a)} + (M_{1-m}, H_m)\,Z \rightleftharpoons \left[M_{1-m}, (NH_4)_m\right] Z \qquad (98)$$

where $m \ll 1$ i,o denotes that the salt MCl is formed inside or outside the zeolite Z and M is monovalent cation.

Since both zeolite and ammonium chloride are heated at the same temperature, hydrogen chloride and ammonia are in excess. Therefore, according to the law of mass action, the equilibrium is shifted to the right and a high degree of exchange is obtained.

5. SUMMARY OF RESULTS AND CONCLUSIONS

A comparative study has been made of the sorption of the gases ammonia, hydrogen chloride and "ammonium chloride" vapour in certain synthetic and natural zeolites at temperatures between 200°C and 350°C.

The stability of a number of silicates (in their Na- or K-form and with different silica content) when exposed to anhydrous hydrogen chloride at temperatures between 20°C and 600°C was found to be mainly dependent on their SiO_2:Al_2O_3 ratio. The silicates that have a SiO_2:Al_2O_3 ratio higher than 5 sorb hydrogen chloride without decomposing but in those for which SiO_2:$Al_2O_3 < 5$, a decomposition - which usually increases with temperature - takes place during the sorption of hydrogen chloride. However, since in certain silicates the silica content can vary considerably, the value 5 is an approximate borderline between the silicates that sorb hydrogen chloride with and without decomposing. When hydrogen chloride is sorbed in an ion-exchanged zeolite, part of it is physically sorbed and the rest reacts with the zeolite. The reaction that takes place is an exchange reaction of the cations of the zeolite by protons. This reaction followed by dehydroxylation was considered to explain the decomposition of silica-poor zeolites.

The sorption isotherms of hydrogen chloride in four ion-exchanged zeolites (with SiO_2:$Al_2O_3 > 5$) showed a hysteresis loop open along the entire length of the isotherms. A considerable residual uptake was also observed after prolonged outgassing at 350°C. The irreversibility and the residual uptake were due to the ion-exchange reaction. Under the experimental conditions used (temperature 240-350°C and hydrogen chloride pressure 0-25 cm Hg) the sorption of hydrogen chloride gas cannot be used for preparation of 100% decationated zeolites. The salt produced from the ion-

exchange reaction can either remain molecularly dispersed in the crystal cavities or migrate out of the crystals. The isotherms of hydrogen chloride in H-Zeolon and HY at temperatures around 250°C were irreversible. The irreversibility was due to the ion-exchange reaction (since in both zeolites the decationation was not complete) and a reaction of hydrogen chloride with the aluminium of the zeolite.

A sample of Linde L with SiO_2:Al_2O_3 equal to 6 was used for preparation of a decationated form using conventional decationation techniques. Decationation to a degree higher than 54% resulted in partial collapse of the crystal structure. Decationated L zeolites were also prepared by refluxing Linde L with 0.05N and 0.1N solutions of hydrochloric acid. These treatments lead to decationation of 37 and 54% and partial dealumination. The samples after being outgassed under high vacuum for 24 hours at 350°C gave X-ray powder photographs similar to that of Linde L.

Sorption isotherms of ammonia in NaY, KL, H-Zeolon and HY were measured at temperatures between 190°C and 320°C. All isotherms belonged to type I in Brunauer's classification and were reversible except that in HY. Calculation of the thermodynamic properties of sorption (i.e. isosteric heats and differential entropies) for NaY, KL and H-Zeolon showed that the internal surface of these zeolites was energetically heterogeneous to ammonia. The irreversible sorption of ammonia in HY was attributed in part to the decomposition of the zeolite which occurred during the sorption experiment. An interesting result from these experiments was the greater affinity of the hydrogen zeolite for ammonia compared with that of ion-exchanged zeolites. This was attributed to a reaction of ammonia with the hydrogen zeolites to form the ammonium-zeolites. Empirical isotherm equations were used to describe the state of the sorbed ammonia in NaY and KL and the thermodynamic properties of the sorbed phase were calculated at the standard state. The activity coefficients of the sorbed phase were also calculated and used as a test of isotherm models.

The sorption of "ammonium chloride" vapour was studied at temperatures between 230°C and 315°C in H-Zeolon, HY, NaY and KL. Since ammonium chloride is completely dissociated in the vapour phase, the sorption of "ammonium chloride" vapour can be better described as the sorption from the mixture of its dissociation products, i.e. ammonia and hydrogen chloride. The isotherms obtained for all systems typify strong sorbate-sorbate interaction in a finite volume. In all cases the sorption was dominated by the reaction of the sorbed ammonia and hydrogen chloride to form ammonium chloride in the zeolitic cavities. The sorption of the pure components can influence the sorption from the mixture. If both gases, i.e. ammonia and hydrogen chloride, are equally sorbed, as e.g. in NaY at low pressures, the sorption of the mixture can be considered as the sorption of "ammonium chloride" vapour. But if one of the gases is more strongly sorbed than the other, as e.g. in H-Zeolon and HY where ammonia is more strongly sorbed than hydrogen chloride, a disproportionation in the gas and sorbed phases arises. As the pressure increases, the disproportionation decreases implying that a competition exists between the recombination reaction of ammonia and hydrogen chloride to form ammonium chloride and that responsible for the disproportionation. In an ion-exchanged zeolite an exchange of the cations of the zeolite by ammonium ions can also take place. This can cause irreversibility of the isotherms.

The isotherms recorded in H-Zeolon were reversible. They could only be reproduced under certain conditions. Sorption and desorption were very slow at low pressures. The slow desorption of ammonium chloride from H-Zeolon and HY at low pressures was due to the slow decomposition of ammonium-zeolite in the presence of hydrogen chloride governed by a first order process. The sorption of ammonium chloride in HY was similar to that in H-Zeolon but it was irreversible and a residual uptake was found after the end of

the experiment. The irreversibility and the residual uptake were due to a reaction of hydrogen chloride with the zeolite. Irreversible isotherms and residual uptake were also observed in NaY due to the ion-exchange reaction of sodium ions by ammonium ions.

The isotherms of ammonium chloride in Kl were reversible and reproducible. Disproportionation was observed at low pressures. The isosteric heat of sorption calculated near saturation was found to be 22.50 kcal/mole of vapour.

A method of analysis of the isotherms when disproportionation took place was developed and the partial isotherms of ammonia and hydrogen chloride were calculated. The sorption from the mixture was always higher than that from the pure components due to the recombination reaction of ammonia and hydrogen chloride to form ammonium chloride in the crystals.

Considering the dissociation of ammonium chloride in the gas phase and the results of the present work, it appears that the Clark-Steiger method of exchange of the cations of a zeolite by ammonium ions (when the outgassed zeolite is heated with ammonium chloride at ca 300°C) takes place through the formation of the hydrogen form of the zeolite and its subsequent reaction with ammonia.

REFERENCES

1. Barrer, R.M., Ann.Reps.Chem.Soc., 41, 31 (1944); Brit.Chem. Eng., 4, 267 (1959).
2. Clark, F.W. and Steiger, G., Amer.J.Sci., 13, 27 (1902); Z.anorg.Chem., 29, 338 (1902).
3. Breck, D.W., Eversole, W.G., Milton, R.M., Reed, T.B., Thomas, T.L., J.A.C.S., 78, 5963 (1956).
4. Barrer, R.M., Endeavour, XXIII, No. 90, 122-30 (1964).
5. Breck, D.W., J. of Chem.Educ., 41, 678-89 (1964).
6. Löwenstein, W., Amer.Miner., 39, 42 (1954).
7. Barrer, R.M. and Meier, W.M., Trans.Far.Soc., 54, 1074 (1958).
8. Meier, W.M., Molecular Sieve Conference, London, April 1967.
9. Taylor, W.H., "The Feldspars" in Crystal Structure of Minerals edited by L. Bragg, London (1965).
10. Meier, W.M., Z.Kristallogr., 115 439 (1961).
11. Zoltai, T. and Buerger, M.J., Z.Kristallogr., 114, 1 (1960).
12. Murphy, E.V.T., private communication.
13. Reed, T.B. and Breck, D.W., J.A.C.S., 78, 5972 (1956).
14. Szymanski, H.A., Stamires, D.N. and Lynch, G.R., J.Opt.Soc.Amer., 50, 1323 (1960).
15. Dent, L.S. and Smith, J.V., Nature, 181, 1794 (1958).
16. Mason, B. and Sand, L.B., Amer.Mineralogist, 45, 341 (1960).
17. Mumpton, F.A., Amer.Mineralogist, 45, 351 (1960).
18. Merkle, A.B. and Slaughter, M., Amer.Mineralogist, 52, 273 (1967).
19. Breck, D.W. and Acara, N.A., U.S. Patent No. 711, 565 (1958).
20. Barrer, R.M. and Villiger, H., in the press.
21. Jarchow, O., Z.Kristallogr., 112, 407-21 (1965).
22. Rabo, J.A. et al, Actes Deuxième Congrès Intern. Catalyse (Paris, 1960).
23. Bennett, J.M. and Gard, J.A., Nature, 214, 1005-6 (1967).
24. Barrer, R.M. Proc.Chem.Soc., 99 (1958).
25. Barrer, R.M., Nature, 164, 112 (1949).
26. Hall, W.K., Chem.Eng.Progr.Symp.Ser., 63, 73 (1967).

27. Lingme, B.V. and Hall, W.K., Trans.Far.Soc., 62, 3229 (1966).

28. Uytterhoeven, J.V., Christner, L.G. and Hall, W.K., J.Phys.Chem., 69, 2117 (1965).

29. Yates, D.J.C., Chem.Eng.Prog.Symp.Ser., 63, 57 (1967).

30. Rodebush, W.H. and Michalek, J.C., J.A.C.S., 71, 748 (1929).

31. Smith, A. and Lombart, R.H., J.A.C.S., 37, 38 (1915).

32. Smits, A., Rec.Trav.Chim., 42, 826-9 (1928).

33. Stephenson, C.C., J.Chem.Phys., 12, 318 (1944).

34. Spingler, H., Z.Phys.Chem., B52, 90-116 (1942).

35. Mellor, J.W., Comprehensive Treatise on Inorganic and Theoretical Chemistry, Longmans (London).

36. Landolt-Börnstein, Physikalisch-chemische tabellen, Springer Verlag (Berlin).

37. Barrer, R.M. and Ibbitson, D.A., Trans.Far.Soc., 40, 195 (1944).

38. Barrer, R.M. and Gibbons, R.M., Trans.Far.Soc., 59, 2569 (1963).

39. Kiselev, A.V., Lygin, V.I. and Titova, T.I., Zh.fiz.Kh., 38, 2730 (1964).

40. Cattanach, J., Wu, E. and Venuto, P.B., in the press.

41. Felden, M., J.Chim.Phys., 57, 430-3 (1960).

42. Stone, F.S. and Whalley, L., J.Catalysis, 8, 173-82 (1967).

43. Pohl, K. and Rebentisch, G., Z.Chem., 5, 396-7 (1965).

44. Benson, J.E., Ushiba, K. and Boudart, M., J.Catalysis, 9, 91 (1967).

45. Reyerson, L.H. and Bemmels, C., J.Phys.Chem., 46, 35-42 (1942).

46. Murata, K.J., Amer.Mineralogist, 28, 546 (1943).

47. Barrer, R.M. and White, E.A., J.Chem.Soc., 1561 (1952).

48. Barrer, R.M. and Brook, D.W., Trans.Far.Soc., 49, 940-8 (1953).

49. Bering, B.P., Serpinskii, V.V. and Smirnova, S.T., Izv.Akad. Nauk,SSSR,Ser.Khim., 12, 2603-10 (1967).

50. Angell, C.L. and Schaffer, P.C., J.Phys.Chem., 69, 3473 (1965).

51. Hughes, T.R. and White, H.M., J. Phys. Chem., 71, 2192 (1967)

52. Stamires, D.N. and Turkevich, J., J.A.C.S., 86, 749 (1964).

53. Barrer, R.M., J.Chem.Soc., 2342 (1950).

54. Brunauer, S., Emmett, P.H. and Teller, E., J.A.C.S., 60, 3098, (1938).

55. Amberg, C.H., Spencer, W.B. and Beebe, R.A., Can.J.Chem., 33, 305 (1955).

56. Hill, T.L., J.Chem.Phys., 17, 520 (1949).

57. Hill, T.L., J.Chem.Phys., 18, 246 (1950).

58. Hill, T.L., Trans.Far.Soc., 47, 376 (1951).

59. Everett, D.H., Trans.Far.Soc., 46, 942 (1950); ibid, 46, 957 (1950).

60. Hill, T.L., Adv. in Catalysis, 4, 212 (1952).

61. Everett, D.H., Proc.Chem.Soc., London, 38 (1957).

62. Barrer, R.M. and Sutherland, J.W., Proc.Roy.Soc., A237, 439 (1956).

63. Barrer, R.M., J.Phys.Chem.Solids, 16, 84-89 (1960).

64. Garden, L.A., Kington, G.L. and Laing, W., Proc.Roy.Soc., A234, 24 (1956).

65. Barrer, R.M. and Wasilewski, S., Trans.Far.Soc., 57, 1153 (1961).

66. Barrer, R.M. and Coughlan, B., Molecular Sieve Conference, Soc.Chem.Ind., London (1967).

67. Langmuir, I., J.A.C.S., 40, 1361 (1918).

68. Fowler, R.H., Proc.Camb.Phil.Soc., 31, 260 (1936).

69. Young, D.H. and Crowell, A.D., Physical Adsorption of Gases, Butterworths (1962).

70. Lacher, R., Proc.Roy.Soc., A161, 525 (1937).

71. Volmer, M., Z.phys.Chem., 115, 253 (1925).

72. Hill, T.L., J.Chem.Phys., 14, 44 (1946).

73. Barrer, R.M. and Peterson, D.L., Proc.Roy.Soc., A280, 466 (1964).

74. Barrer, R.M., J. Colloid and Interface Science, 21, 415 (1966).

75. Dubinin, M.M., Quart. Rev.Chem.Soc., 9, 101 (1955).

76. Gregg, S.J. and Sing, K.S.W., Adsorption Surface Area and Porosity, Academic Press, London (1967).

77. Barrer, R.M., Report to the Xth Solvay Council, Brussels, 27 (1956).

78. Everett, D.H. and Whitton, N.I., Trans.Far.Soc., 48, 749 (1952).

79. Everett, D.H., The Solid Gas Interface, Vol.2, Ed. E.A. Flood, E. Arnold, London (1967).

80. Barrer, R.M. and Wasilewski, S.,J.Sci.Instr., 37, 432 (1960).

81. Taniguchi, H. and Janz, G.J., Anal.Chem., 28, 287 (1956).

82. Whiteman, J.L., Ph.D. thesis, London Univ. (1965).

83. Bockris, J. O'M., White, J.L. and Mackenzie, J.D., Physico-chemical Measurements at High Temperatures, Butterworths, London (1959), p.22.

84. Edwards, J.W., Ph.D. thesis, London Univ. (1959).

85. Platinum Resistance Thermometry, Handbook, Johnson and Matthey (1958).

86. Roeser, W.F. and Wensel, H.T., Temperature, its Measurement and Control in Science and Industry, Vol. I, Reinhold (1941), p. 284.

87. Handbook of Chemistry and Physics, 45th Ed., Chem. Rubber Co., (1965), p. E.48.

88. Nielsen, K.L., Methods in Numerical Analysis, MacMillan (1956).

89. Vogel, A.I., Quantitative Inorg-Analysis, Longmans (1958), p.588.

90. Treadwell and Hall, Analytical Chemistry, Vol.II, Wiley and Sons (1930), p.422.

91. Ma, T.S. and Zuagaga, G., Industrial Eng. Chem. (Anal.), 14, 280 (1942).

92. Bennett, H. and Hawley, W.G., Methods of Silicate Analysis, British Ceramic Ass. (1958), p. 87-90.

93. Azároff, L.V. and Buerger, M.J., The Powder Method, McGraw Hill (1958), p.280.

94. Barrer, R.M. and Makki, M.B., Can.J. of Chem., 42, 1481 (1964).

95. Kerr, G.T., J.Phys.Chem., 71, 4155 (1967).

96. Barrer, R.M. and Wasilewski, S., private communication.

97. McDaniel, C.V. and Maher, P.K., Molecular Sieve Conference, Soc.Chem.Ind., London, April (1967).

98. Sherry, H.S., J.Phys.Chem., 70, 1158 (1966).

99. Ward, J.W., J.Catalysis, 9, 225 (1967).

100. Zhdanov, S.P. and Novikov, B.G., Dokl.Akad.Nauk SSSR, 166, 1107 (1966).

101. Barrer, R.M. and Gibbons, R.M., Trans.Far.Soc., 59, 2875 (1963).

102. Din, F., Thermodynamic Functions of Gases, Vol. 1, Butterworths, London (1965).

103. J.A.N.A.F., Thermochemical tables Addendum (1966).

104. Barrer, R.M. and Whiteman, J.L., J.Chem.Soc., 13 (1967).

P A R T I I I

APPENDIX

ISOTHERM DATA

For all systems:

p = Pressure in mm Hg

x = Uptake in mg of sorbate per g of dehydrated zeolite

For systems 3 - 6:

x^* = Residual uptake after evacuation for 24-30 hours (see p.92)

For system 11:

t = Sorbate reservoir temperature ^{o}C

"Equilibrium points" see p.145

Sorption systems referred to in Part III

1. H-Zeolon - HCl
2. HY - HCl
3. Na-Zeolon - HCl
4. Na-clinoptilolite - HCl
5. NaY - HCl
6. KL - HCl
7. H-Zeolon - NH_3
8. NaY - NH_3
9. HY - NH_3
10. KL - NH_3
11. H-Zeolon - NH_4Cl
12. HY - NH_4Cl
13. NaY - NH_4Cl
14. KL - NH_4Cl

1. H-Zeolon - HCl

230°C

p	x
sorption	
3.95	8.20
11.15	10.14
15.75	11.91
50.02	14.28
49.60	15.15
80.44	16.00
123.23	16.94
161.66	18.43
199.39	19.20
258.23	20.20
27.0	13.90
56.33	15.36
106.83	17.10
148.40	18.10
205.0	19.40
250.0	20.04
desorption	
222.21	20.13
160.73	19.76
133.61	19.13
96.17	17.89
67.10	17.30
3.53	11.81
27.55	15.35
10.96	14.11
210.38	20.16
150.69	20.08
103.65	18.44
18.76	14.51
46.87	16.61
0.60	10.33
0.00	9.60

294°C

sorption	
4.0	7.20
9.40	9.09
21.31	10.87
38.08	11.47
57.81	12.71
6.15	8.33
17.51	9.87
80.88	13.00
116.30	14.25
144.40	15.08
196.10	16.00
207.29	16.20
desorption	
187.71	16.09
155.49	15.74
124.13	15.24
91.01	14.97
66.75	14.55
48.35	13.66
33.28	12.94
19.21	12.24
5.12	10.00
1.45	9.51

2. HY - HCl

245.5°C

p	x
sorption	
5.10	10.10
21.10	12.00
39.85	14.54
66.99	16.48
89.45	18.43
117.96	19.66
154.28	21.06
201.07	23.39
desorption	
165.50	23.20
143.16	23.10
116.31	22.90
86.51	21.85
62.51	21.66
46.90	21.66
38.01	20.91
24.61	20.20
15.45	19.45
5.96	19.35
3.72	18.37
1.40	17.05
0.00	12.50

3. Na-Zeolon - HCl

245°C

p	x	x*
sorption		
17.60	29.40	12.10
25.00	31.64	13.50
42.72	33.71	12.84
57.70	36.20	16.37
85.80	39.00	17.50
127.19	40.98	18.77
162.61	43.88	19.20
164.89	43.48	19.50
8.00	24.72	9.20
desorption		
149.00	43.00	
135.04	42.55	
115.36	42.30	
86.57	40.54	
71.47	39.01	
55.37	37.64	
44.68	37.51	
31.60	36.21	
22.08	35.15	
12.37	33.60	
4.88	30.64	
0.00	23.75	
101.87	41.04	

4. Na-clinoptilolite - HCl

245°C

p	x	x*
sorption		
0.08	20.33	13.00
7.50	31.76	20.00
10.13	32.60	21.72
23.00	34.80	25.37
52.00	38.10	27.40
80.00	40.29	28.00
113.80	41.20	28.47
154.00	42.36	29.00
193.80	42.70	29.50
desorption		
172.61	42.60	
161.37	42.47	
143.26	42.47	
122.59	42.45	
98.28	41.20	
72.59	41.10	
67.20	40.60	
52.46	40.40	
40.90	39.87	
27.84	39.29	
14.49	38.63	
7.56	38.19	
1.00	34.75	

5. NaY - HCl

245.5°C

p	x	x*
sorption		
1.40	10.30	1.30
3.35	17.48	7.77
7.00	21.10	12.81
16.00	23.00	16.00
31.00	24.91	19.14
61.00	27.72	21.00
91.00	30.65	22.00
123.00	32.15	22.64
160.58	33.96	23.33
202.91	36.62	23.90
252.90	39.02	24.36

295.5°C

sorption		
8.30	13.76	1.28
12.20	15.20	5.60
20.00	17.20	11.80
25.85	18.11	15.00
13.50	15.80	4.10
26.80	17.50	15.90
40.80	19.80	17.30
56.61	21.30	18.67
80.12	23.21	19.20
107.34	24.30	19.45
129.67	25.47	20.00
160.82	27.01	21.00
196.90	29.85	21.20

p	x	x*
desorption		
5.94	22.49	
162.10	28.40	
140.01	28.22	
124.78	27.97	
96.04	26.82	
94.58	27.00	
81.29	26.40	
62.55	26.27	
46.87	25.35	
34.66	24.63	
26.16	24.00	
15.88	23.46	

6. KL - HCl

245°C

sorption		
4.87	12.06	5.80
11.25	14.90	7.58
24.96	17.92	8.56
55.21	23.78	10.25
92.43	26.63	11.72
136.62	29.81	12.96
183.90	32.83	15.72
230.26	36.49	17.44
263.89	41.56	19.65
desorption		
238.06	41.39	
212.23	40.32	
181.71	39.76	

p	x	x^*
144.99	38.69	
119.71	38.00	
120.00	37.00	
94.15	37.14	
70.59	36.49	
48.32	35.19	
31.27	34.29	
20.53	31.53	
11.16	29.73	
4.40	28.50	
0.00	24.71	

280°C

sorption

11.08	10.83	3.78
34.00	15.32	5.90
37.05	15.96	6.82
60.67	18.29	7.54
74.63	20.31	7.41
98.97	21.14	9.18
151.85	23.57	10.53
210.93	26.87	12.03
234.31	28.93	14.00

desorption

206.74	28.93	
173.29	28.50	
147.95	28.34	
121.51	27.43	
102.58	26.91	
79.07	25.56	
64.14	24.56	
46.29	23.94	
29.37	23.08	
18.60	22.00	
12.66	20.87	
7.52	19.86	
3.00	19.00	
0.00	16.46	

315°C

sorption

15.00	10.37	2.06
24.26	11.48	3.70
43.31	14.24	4.90
62.50	15.91	5.54
108.92	18.05	5.94
153.90	21.86	8.56
195.40	23.12	9.96
249.08	25.11	11.70
286.27	27.54	13.84

desorption

246.34	27.25
238.77	27.18
206.29	26.35
152.38	26.47
117.67	26.56
100.35	25.95
77.69	25.26
66.39	24.71
56.91	23.78

p	x	p	x	p	x
41.52	23.52	77.15	25.45	6.10	19.30
29.84	22.76	189.19	28.92	257.51	35.63
22.16	21.52	306.34	31.72	144.43	32.29
12.33	20.14	93.99	26.26	34.69	25.06
6.54	19.24	43.40	23.29	17.01	22.26
0.00	13.84	163.35	28.62	5.87	19.60
		60.95	23.85		

7. H-Zeolon - NH_3

300°C

p	x
6.10	17.80
8.68	19.07
30.55	22.40
60.95	23.04
105.43	26.30
137.50	27.64
182.49	28.85
221.96	30.01
284.72	30.97
293.84	31.34
236.55	30.17
202.66	29.69
154.10	28.10
116.61	26.42
81.36	25.73
30.64	22.60
56.54	24.01
13.14	20.23
3.03	17.00
20.57	21.01
342.95	32.43

270°C

p	x
8.41	20.38
23.11	23.43
47.43	25.34
89.62	28.50
149.83	30.45
185.80	32.42
246.20	34.52
313.46	36.40
356.40	37.45
287.39	35.74
213.95	34.04
141.66	31.65
104.97	30.13
66.00	27.59
23.63	23.80
7.13	20.40
41.11	25.75
86.55	28.92
118.98	30.83
169.51	32.23

250°C

p	x
1.34	19.73
9.60	23.48
31.68	27.41
49.44	29.76
74.93	31.28
99.26	33.20
144.29	35.28
239.40	37.95
307.00	39.71
356.58	41.33
306.60	40.12
260.46	38.91
150.79	35.42
104.66	33.77
64.06	31.35
47.34	29.25
9.40	22.52
181.00	36.14

230°C

p	x
4.00	21.78

p	x
13.13	27.40
68.11	34.14
29.65	30.46
148.20	38.64
226.35	41.36
289.54	43.28
253.26	42.45
364.13	44.22
264.13	42.32
223.44	41.31
184.24	40.14
122.36	37.82
78.59	35.40
44.74	32.70
17.53	28.21
5.19	23.17
93.23	36.35

200°C

4.75	26.70
14.99	31.92
26.00	34.44
12.53	31.22
2.30	23.58
18.07	32.56
36.11	36.34
55.79	38.62
83.78	40.52
86.14	40.96
134.93	43.34
188.14	45.33
242.72	46.90
313.27	47.85
357.08	48.80
288.44	47.82
224.37	46.47
167.66	44.44
113.95	42.67
97.10	42.04
66.08	40.07
27.60	34.90
24.88	34.58
124.63	43.61
64.34	39.38
9.29	29.52

8. NaY - NH_3

321.5°C

36.66	6.56
71.05	11.71
108.25	14.52
148.68	16.87
184.18	20.26
227.59	21.72
273.06	23.25
317.40	25.75
293.09	24.39
264.70	23.42
230.82	22.68
199.18	20.83
156.54	17.93
127.42	15.58
101.90	13.80
77.48	12.36
55.36	8.41
30.44	6.14
10.63	2.18

297°C

9.26	4.80
23.05	9.20
44.79	13.34
76.34	16.87
129.14	21.79
184.32	26.15
258.29	29.77
305.05	31.32
270.44	29.60
236.45	28.27
195.28	26.38
134.90	22.57
107.55	21.10
81.49	17.68
52.70	15.00
38.70	12.04
21.03	8.74
7.55	3.83

p	x
272°C	
5.91	6.18
25.22	13.34
44.36	19.27
71.31	23.52
107.50	27.63
168.58	32.21
209.38	33.96
263.12	36.00
317.00	39.00
282.04	37.18
203.05	33.84
159.73	30.57
125.79	28.13
85.40	24.58
61.34	20.85
31.49	16.15
14.19	10.69
246°C	
15.50	17.00
36.15	24.52
54.39	27.28
74.74	30.73
107.44	34.33
131.51	36.79
176.87	40.20
224.84	41.94
261.72	44.47
316.74	46.00
294.91	45.46
263.71	44.19
225.29	41.38
194.21	40.54
160.63	39.85
134.68	36.75
114.47	34.81
89.63	33.00
47.93	27.00
34.78	22.69
19.10	17.63
9.56	12.19
3.75	4.86
11.07	14.78
47.52	26.64
221°C	
4.28	14.61
33.29	29.54
63.57	36.00
91.38	40.32
124.20	42.88
178.90	46.80
219.71	48.32
264.64	50.08
317.80	52.56
15.00	23.15
268.42	50.88
196.11	47.28
161.05	45.27
127.20	43.45
96.47	40.25
71.07	37.37
33.63	29.71
21.11	24.90
9.93	18.76
41.71	31.21
80.52	37.78
232.32	48.96

9. HY - NH_3

245.5°C

sorption

7.57	28.52
29.03	37.01
66.29	41.83
96.02	44.03
122.52	45.69
180.40	48.69
229.26	51.44
261.98	52.98
296.67	54.25

desorption

256.85	53.84

p	x
200.36	52.40
172.36	52.34
122.42	51.28
86.00	48.87
59.05	47.14
31.38	44.40
11.68	40.99
3.70	37.45
1.24	32.88
0.00	27.50
0.00	15.20

10. KL - NH_3

315°C

17.16	0.46
43.00	1.09
80.76	2.15
122.75	3.17
165.77	3.65
221.88	4.36
259.72	5.23
224.73	4.61
193.80	4.17
104.18	2.58
70.07	1.46

280°C

8.04	0.68
33.54	2.42
76.83	3.55
163.53	6.18
252.65	7.69
314.85	8.08
275.00	7.12
235.41	6.58
190.99	6.24
140.74	5.30
87.68	4.59

245°C

22.73	3.00
67.43	5.45
131.23	8.64
181.12	10.27
236.50	11.50
289.71	13.21
330.48	13.82
296.16	12.70
260.00	11.90
212.07	10.86
156.99	9.20
106.63	7.37
72.88	6.40
47.21	5.37
26.04	3.94
9.40	1.62

220°C

15.82	4.29
40.05	6.04
17.46	3.58
57.49	7.40
109.55	10.81
201.59	14.31
260.18	15.89
296.85	16.93
270.46	15.58
237.44	14.71
197.19	13.51
157.52	12.33
129.85	11.44
100.93	10.81
72.90	8.58
44.44	6.83
21.60	4.42
6.58	2.09

190°C

19.57	7.87
50.67	10.99
87.24	13.88
140.30	17.10
189.32	19.60
229.25	21.18
255.77	21.73
292.49	22.29
273.44	21.98
247.32	20.85
215.35	19.85
179.16	18.99

p	x
148.63	17.72
118.34	15.15
98.45	13.88
81.00	13.43
63.76	12.55
44.70	10.36
31.12	9.25
20.62	7.69
10.93	6.04
4.66	4.25

22.5°C

3.02	36.87
3.66	37.30
8.08	43.38
18.50	49.60
25.61	51.50
73.90	61.39
112.35,	55.35
166.00	68.92
223.41	70.17
266.44	71.26
245.91	70.86
217.64	69.93
186.27	68.38
156.11	67.45
124.00	66.36
30.80	53.87
15.38	48.66
3.24	36.41

11. H-Zeolon - NH_4Cl

230°C

sorption

p	x
0.63	11.98
0.75	12.46
2.13	13.83
3.50	20.90
6.08	30.79
7.14	36.57
7.54	41.32
8.82	57.88
10.16	62.45
10.84	69.65
15.00	85.43
22.00	103.02
22.33	102.80
8.08	38.40
9.33	47.61
9.67	51.94
13.10	82.00
12.92	78.44
21.46	101.29
8.76	46.15
12.30	73.93
17.31	90.84
16.91	93.78
23.86	103.15
24.39	109.02
25.14	114.96

desorption

p	x
21.48	101.56
9.07	50.37
8.37	42.73
7.98	39.29
7.10	36.47
6.52	30.11
12.70	80.68
12.00	77.41
10.15	62.88
9.87	59.68
8.76	46.15
15.58	88.76

"Equilibrium points"

p	x	t
7.14	36.57	164
10.14	62.45	193
10.84	69.65	196
12.96	78.44	200.5
15.00	85.43	210
15.58	88.76	209.5
16.91	93.78	212
21.47	101.30	223
21,46	101.29	223
22.00	103.20	227

12. HY - NH_4Cl

246°C

p	x
sorption	
1.18	16.90
1.55	22.85
4.68	35.95
5.10	37.69
6.99	42.50
7.69	44.76
8.83	53.95
9.32	58.59
9.83	61.50
11.37	74.10
13.76	107.35
14.33	118.42
15.33	133.78
15.40	137.00
19.53	159.53
20.77	165.75
29.79	180.22
31.79	182.92
32.85	187.00
33.15	189.60
40.73	202.72
41.40	206.70
desorption	
34.88	203.07
32.97	198.90
32.17	194.93
27.0	186.12
22.04	178.85
18.39	168.95
17.75	166.50
14.87	145.94
13.13	130.88
12.50	115.40
10.05	93.23
8.38	77.45
7.10	67.55
5.50	62.09
5.12	61.59
3.97	56.75
3.45	53.13
2.16	43.60
1.48	39.95
1.26	38.66
1.1	37.27
0.84	36.18
0.57	35.09
0.15	33.92
0.14	32.00

13. NaY - NH_4Cl 246°C

p	x
1st run	
sorption	
0.60	7.99
1.30	13.74
2.48	40.52
3.03	96.36
3.80	152.74
5.25	197.32
6.47	215.86
7.00	220.0
7.12	228.88
9.62	244.66
9.9	245.0
13.65	266.71
14.20	269.34
17.55	282.30
18.45	282.70
20.00	288.60
21.64	290.17
22.50	299.70
31.50	308.41
40.50	318.00
desorption	
33.5	317.20
23.95	304.80
17.32	292.78
16.68	292.00
11.23	265.44
10.11	258.40
9.70	249.71
5.26	188.75
4.00	155.72
3.45	115.46
2.22	50.80
2.10	48.00
1.65	41.20

p	x
1.60	38.71
1.19	36.87
0.79	35.46
0.40	35.40
2nd run	
sorption	
1.30	42.94
1.97	92.20
3.30	142.67
4.12	184.22
6.94	220.00
7.51	225.31
8.40	236.86
9.38	247.53
9.29	249.91
10.30	210.13
12.17	265.25
12.94	274.44
14.00	276.60
20.94	296.29
25.34	305.68
28.45	312.78
29.70	315.45
31.55	315.27
33.71	319.30
37.88	323.66
39.76	326.00

p	x
desorption	
36.81	326.00
34.51	326.79
30.57	325.77
26.48	322.40
23.03	316.81
22.0	310.35
21.37	311.32
20.0	308.50
17.29	300.95
18.98	303.46
15.03	292.09
12.57	281.90
7.87	245.51
7.44	234.90
5.06	212.39
2.40	134.64
1.55	69.32
1.06	54.40
0.96	41.48
0.61	39.36
0.50	38.84
0.20	38.91

14. KL - NH_4Cl

245°C

p	x
sorption	
0.50	7.47
1.10	19.37
3.19	86.10
4.55	93.64
5.80	100.00
6.86	105.48
9.73	113.70
11.40	117.50
13.81	125.00
14.54	125.30
15.92	126.72
16.73	128.66
21.62	133.82
23.55	136.50
24.41	137.62
33.65	144.66
1.35	32.50
1.55	36.24
2.51	74.32
desorption	
27.27	140.20
23.78	139.69
18.60	133.52
16.70	129.00
13.34	122.67
12.03	119.40

p	x
10.46	116.95
8.55	108.28
7.36	105.99
4.39	89.22
2.20	39.86
1.23	21.40
1.17	14.70
0.20	5.86
2.90	67.04
262.5°C	
sorption	
1.04	9.80
1.66	18.07
2.65	46.96
3.19	53.15
6.11	82.00
10.01	94.20
17.67	108.40
27.82	121.70
27.60	120.77
43.59	131.50
60.82	140.95
desorption	
42.39	129.90
46.55	133.36
37.00	129.22
18.67	108.00
10.65	98.25
8.20	91.89
3.70	65.40

p	x
2.64	49.79
2.00	24.26
1.15	5.13
280°C	
sorption	
1.96	9.13
4.57	33.83
7.41	61.60
8.86	69.22
10.11	72.96
15.23	89.11
16.01	88.67
21.04	94.55
28.64	103.24
34.05	108.11
42.50	115.57
49.35	118.88
59.29	122.62
69.20	127.49
77.05	132.50
89.80	135.20
102.73	138.69
113.75	144.32
1.58	6.75
3.2	16.72
6.36	52.78
desorption	
92.47	138.00
85.70	135.82
72.15	131.44

p	x
68.12	129.38
62.05	127.38
53.80	124.00
49.07	120.88
39.41	112.00
32.63	107.37
29.84	105.40
25.41	101.06
17.76	93.30
12.37	81.17
10.11	73.22
8.05	61.28
4.25	23.20
0.30	2.67
315°C	
sorption	
2.24	2.54
15.40	53.49
9.5	26.33
7.1	20.29
1.19	5.13
10.07	24.11
13.23	33.00
15.10	37.10
17.44	46.08
20.00	56.69
23.00	61.40
32.30	73.58
49.31	86.44
73.19	95.49

p	x
109.35	105.96
125.79	110.49
149.73	115.63
168.31	118.27
184.16	121.71
206.51	126.11
224.00	127.49
257.85	131.38
272.23	130.85
desorption	
253.33	130.83
224.60	127.80
210.87	127.30
145.41	115.12
122.81	111.62
98.30	103.90
67.88	95.55
35.30	75.83
17.21	52.31
15.01	47.25
8.00	23.30
160.50	118.20
55.10	92.00
40.08	81.65